UAB
Universitat Autònoma de Barcelona

Evaluation of BET proteins and LSD1 as epigenetic targets for peripheral nerve injury treatment

Georgina Palomés Borrajo

Evaluation of BET proteins and LSD1 as epigenetic targets for peripheral nerve injury treatment

Academic dissertation

To obtain the degree of PhD in Neuroscience by the Universitat Autònoma de Barcelona

January 2024

PhD Candidate

Georgina Palomés Borrajo

Thesis Supervisor

Dr. Clara Penas Pérez

Dr. Xavier Navarro Acebes

Academic Tutor

Dr. Xavier Navarro Acebes

Group of Neuroplasticity and Regeneration

Department of Cell Biology, Physiology, and Immunology

Institute of Neurosciences (INc)

This work was financially supported by:

- The Universitat Autònoma de Barcelona by means of Personal Investigador en Formación (PIF) grant to Georgina Palomés Borrajo.
- The grant PID2019-108496RA-I00 from Ministerio de Ciencia e Innovación and Agencia Estatal de Investigación of Spain.
- Centro de Investigación Biomédica en Red sobre Enfermedades Neurodegenerativas CIBERNED (CB06/05/1105).
- TERCEL (RD16/0011/0014) funds from the Instituto de Salud Carlos III of Spain, co-funded by European Union (ERDF/ESF, “Investing in your future”).

A la meva iaia,

Et trobaré a faltar.

Index

Index

Abbreviations **1**

Summary **7**

Introduction **11**

1. Peripheral nerve injury 13
2. Peripheral nerve regeneration 16
3. Neuropathic pain 30
4. Epigenetic interventions to improve functional outcome after nerve injury 39

Hypotheses **53**

Objectives **57**

Experimental design **61**

Scientific contributions **73**

Results **77**

Chapter 1 79

Chapter 2 95

Chapter 3 113

Chapter 4 139

Discussion **167**

Conclusions **183**

References **187**

Acknowledgements **219**

Abbreviations

Abbreviations

ATF3: Activating transcription factor 3

AMPA receptor: α-amino-3-hydroxy-5-methyl-4-isoxazolepropionic acid receptor

ASIC: Acid-sensing ion channel

BDNF: Brain-derived neurotrophic factor

BET proteins: Bromodomain and extraterminal domain proteins

BRD4: Bromodomain Containing 4

BMDM: Bone marrow-derived macrophages

C/EBPs: CCAAT-enhancer-binding proteins

CAMKII: calcium/calmodulin-dependent protein kinase II

ChIP: Chromatin immunoprecipitation

CCI: Chronic constriction injury

CDK9: Cyclin-dependent kinase 9

CGRP: Calcitonin gene related peptide

CHD4: Chromodomain Helicase DNA Binding Protein 4

CHD8: Chromodomain Helicase DNA Binding Protein 8

COX-2: Cyclooxygenase-2

CNS: Central nervous system

CREB: cAMP-response element binding protein

CTNF: Ciliary neurotrophic factor

DAMPS: Danger-associated molecular patterns

DNA: Deoxyribonucleic acid

DRG: Dorsal root ganglion

ECM: Extracellular matrix

ERK: Extracellular-signal-regulated kinase

FGF: Fibroblast growth factor

GABA: Gamma-aminobutyric acid

GAP-43: Growth associated protein 43

GDNF: Glial cell line-derived neurotrophic factor

GFAP: Glial fibrillary acidic protein

GM-CSF: Granulocyte-macrophage colony-stimulating factor

HCN: Hyperpolarization-activated cyclic nucleotide–gated

H3K4: Histone 3 lysine 4

H3K9: Histone 3 lysine 9

HDACi: Histone deacetylase inhibitor

Hsp27: Heat shock protein 27

IB4: Isolectin B4

IEG: Immediate early gene

IL-: Interleukin-

JAK: Janus kinase

JNK: c-Jun N-terminal kinase

kDa: Kilodalton

KO: Knockout

LIF: Leukemia inhibitory factor

lncRNA: Long non-coding RNAs

LPC: Lysophosphotidylcholine

LSD1: Lysine-specific histone demethylase 1A

LTP: Long-term potentiation

MAG: Myelin-associated glycoprotein

MAP2: Microtubule-associated protein 2

MAPK: Mitogen-activated protein kinase

MBP: Myelin basic protein

MCP-1: Chemokine monocyte chemoattractant protein-1

M-CSF: Macrophage colony-stimulating factor

mGluR: Metabotropic glutamate receptor

mTOR: Mammalian target of rapamycin

MTT:3-(4,5-Dimethylthiazol-2-yl)-2,5-diphenyltetrazolium Bromide

NCAM: Neural cell adhesion molecule

NF-Kβ: Nuclear factor kappa-light-chain-enhancer of activated B cells

NFAT: Nuclear factor of activated T cells

NGF: Nerve growth factor

NK-1: Neurokinin 1

miRNA MicroRNA

NMDA receptor: N-methyl-D-aspartate receptor

NT-3: Neurotrophin-3

Oct-6: Octamer-binding factor 6

p38: p38 mitogen-activated protein kinases

p53: Tumor protein p53

PLA-2: Phospholipase A2

PGE2: Prostaglandin E2

PI3K/Akt: Phosphoinositide-3-kinase/ Protein kinase B

PKA: Protein kinase A

PKC: Protein kinase C

PNI: Peripheral nerve injury

PNS: Peripheral nervous system

PSNL: Partial sciatic nerve ligation

pTEFb: Positive transcription elongation factor b

qPCR: Quantitative polymerase chain reaction

RAGs: Regeneration-associated genes

RNA: Ribonucleic acid

SARM1: Sterile alpha and Toll/interleukin-1 receptor motif-containing protein 1

SCG-10: Superior cervical ganglia neural-specific 10 protein

siRNA: Small interfering RNA

SNI: Spared nerve injury

SNL: Spinal nerve ligation

Sox11: SRY-Box transcription factor 11

STAT: Signal transducer and activator of transcription

TLR: Toll-like receptor

TNF-α: Tumor necrosis factor-α

TRPA: Transient receptor potential ankyrin channel

TRPM: Transient receptor potential melastatin channel

TRPV: Transient receptor potential vanilloid channel

VEGF: Vascular endothelial growth factor

Summary

Summary

Traumatic injury to the peripheral nerve promotes the disconnection between axons and target organs, leading to serious functional defects in motor, sensory or autonomic systems. In addition, subjects that suffer from nerve injury may also experience secondary problems, like neuropathic pain, which further decreases their quality of life. Currently, there are no effective therapies to promote nerve regeneration or ameliorate neuropathic pain after nerve injury. This situation subjugates patients to prolonged periods of rehabilitation, as well as to high medical expenses, that must be covered either by the subject or by the public healthcare system. For these reasons, the development of new strategies to treat peripheral nerve injuries is needed. Since epigenetic research has promoted the development of novel treatments for distinct neuropathological diseases, we aimed to unravel the potential therapeutic effects of two epigenetic targets "BET proteins" and "LSD1" after nerve injury.

We discovered that inhibition of BET proteins using JQ1 had promising effects on the amelioration of neuropathic pain in a mouse model of spared nerve injury (SNI). In this regard, JQ1 was able to reduce mechanical hyperalgesia trough the modulation of ion channel expression and the inflammatory environment. We also determined that conditioned media from BET-inhibited macrophages increased neurite outgrowth in DRG explants through the activation of the STAT6 pathway *in vitro.* However, BET inhibition using JQ1 did not improve motor and sensory reinnervation *in vivo* after sciatic crush injury. Provided that BET proteins were closely linked to inflammatory events; we proceed to assess the role of the BET protein family member BRD4 in the transcription of anti-inflammatory cytokines. We deciphered that, under physiological conditions, BRD4 forms a repressor complex with CHD4 on the IL-13 promoter, preventing its transcription. Then, upon BET-inhibition both repressor proteins were released from this genetic region, facilitating anti-inflammatory cytokine expression.

Regarding LSD1, we determined that global LSD1 inhibition using RN-1 at 500 nM in DRG explants increased neurite number *in vitro*. Additionally, early administration of RN-1 in crush-injured mice promoted the expression of certain regeneration associated genes (RAGs) and led to immunosuppression. Although long-term treatment with RN-1 did not affect Wallerian degeneration, it did not improve motor and cutaneous reinnervation after sciatic nerve crush.

In conclusion, this thesis provides insights onto the use of BET proteins and LSD1 as therapeutic targets to improve the functional outcome after peripheral nerve injury.

Introduction

1. Peripheral nerve injury

1.1 Incidence

Peripheral nerve injuries (PNI) affect around 5 million people annually worldwide, with an average of 300.000 cases per year in Europe (Lackington, Ryan, & O'Brien, 2017). A recent study conducted on European trauma patients with lower limb injuries showed that 1.8% of the subjects suffered from deficits due to nerve injury (Huckhagel et al., 2018). Common causes are vehicle accidents, work accidents and iatrogenic injuries among others (Lien et al., 2020).

From a physiological standpoint, nerve injuries result in the disconnection between the neuronal soma and the distal axon stump, leading to the degeneration of the distal fibers, and to the loss of contact between the neuron and the target organ. This results in total or partial deficits in motor, sensory and autonomic functions in the territory supplied by the injured nerve. Although peripheral nerve axons can regrow to some extent, the regenerative process is usually slow and incomplete (Navarro, Geuna, Grothe, & Haastert-Talini, 2018). Consequently, patients with nerve injuries undergo long periods of denervation and may suffer lifelong functional deficits. In addition, nerve injuries can arise secondary problems like neuropathic pain, often described by patients as a tingling, burning or electrical-like sensation (Gibson, 2007). Altogether, loss of function and neuropathic pain negatively impact the psychological well-being of patients and their quality of life.

Besides, nerve injuries impose a high economic burden for the subject and the public healthcare system. A study conducted in Germany estimated that rehabilitation costs for upper extremity nerve injuries summed around 5.840€, the sick leave an average of 17.600€ and if the patient received a disability pension the expenses would account for a total of 102.167€ in a lifetime (Bergmeister et al., 2020). Thus, provided that current treatments offer limited enhancement of functional outcome and limited amelioration of pain, there is a need for the development of novel strategies to improve functional recovery after nerve injury. These advancements would not only benefit the health of the patients but would also result in a reduction of medical expenses required.

1.2 Classifications of nerve injury

In 1942 Seddon proposed a classification of nerve injuries dividing them in three main types:

1) *Neurapraxia*: is the mildest form of nerve damage, characterized by a blockage of impulse conduction without disruption of the axon or the perineurium. Patients with neurapraxia experience paresthesia and loss of function. However, since axons do not degenerate, recovery from the conduction block occurs in a few weeks without the initiation of a regenerative process (see Figure 1).
2) *Axonotmesis*: is the disruption of the axons due to a compression or contusion, but without affecting the surrounding connective layers. In axonotmesis, the distal stump undergoes the process of Wallerian degeneration and recovery will require spontaneous regeneration.
3) *Neurotmesis*: is the most severe form of injury, where there is a total disruption of the nerve, including the axons as well as the connective layers. Recovery does not occur significantly without surgical repair (Kaya & Sarikcioglu, 2015; Seddon, 1942).

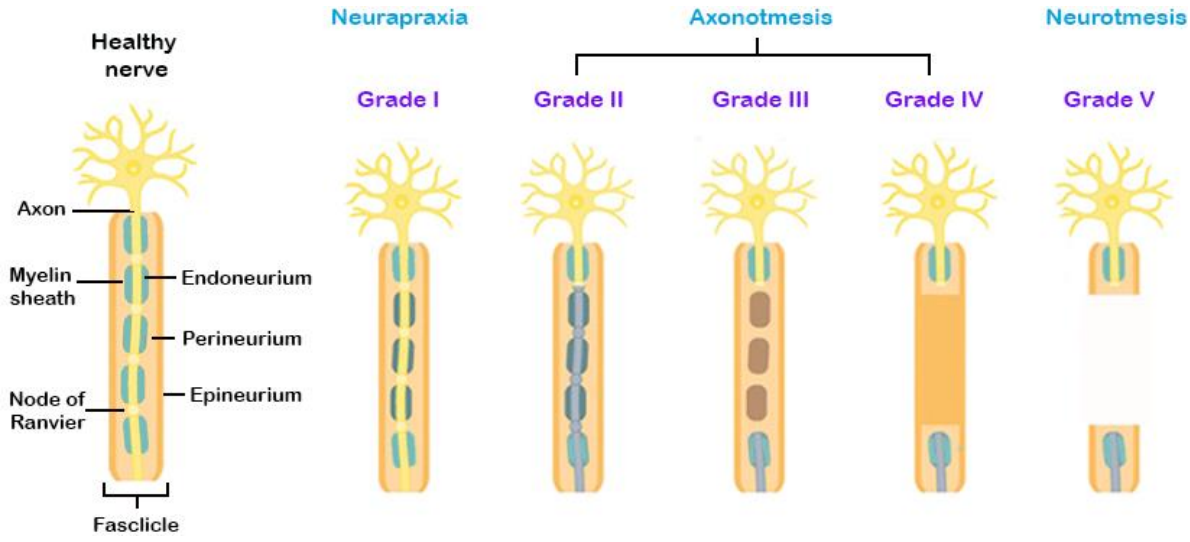

Figure 1: Nerve injury classifications by Seddon (blue) and Sunderland (purple), where the left image represents a healthy nerve with its different structural units. Modified from (Lopes et al., 2023).

Although Seddon's classification provided a nomenclature and protocol to help clinicians classify nerve injuries, it also raised criticism (Sunderland, 1951). Consequently, in 1951 Sunderland proposed a new classification with five degrees of nerve injury. Sunderland first- and fifth-degree injuries correspond to neurapraxia and neurotmesis of Seddon's

classification, respectively. Additionally, Sunderland subdivided the axonotmesis in three degrees to solve the variability that patients with axonotmesis had on their prognosis, depending on factors like intraneural hemorrhage and the discontinuity of endoneurial tubules and perineural layer (see Figure 1). Currently, both classifications are used in the clinics, being Seddon's more used by electrophysiologists and Sunderland's preferred by surgeons (Chhabra, Ahlawat, Belzberg, & Andreseik, 2014).

1.3 Animal models of traumatic nerve injuries

In vivo animal models have been developed to investigate molecular and cellular processes involved in degeneration and regeneration of the peripheral nerve and to assess new therapeutic procedures. Rodents are the most used species in nerve injury studies due to their similar nerve distribution to humans and their affordability in terms of housing and maintenance (Menorca, Fussell, & Elfar, 2013). Among rodents, rats are the most frequently used species for studying nerve regeneration, followed by mice. Rats are preferred as a model due to their larger size, which allows the induction of bigger nerve gaps for repair studies. However, mouse models have the advantage of having a greater availability of transgenic strains and a wider variety of antibodies, which facilitates the study of molecular cues in this specie (A. Li, Pereira, Hill, Vukcevich, & Wang, 2022; Ronchi et al., 2019).

The sciatic nerve is the most widely used nerve for studying nerve regeneration. Another utilized nerve is the femoral, which allows to examine separately the muscular and cutaneous branches (Menorca et al., 2013). Models of upper limb nerve injuries are also of interest because of their potential clinical applications. In this case, the median nerve is preferred for upper extremity studies (A. Li et al., 2022).

When it comes to surgical procedures, the most common types of injuries applied are:

Crush injury: consists in compressing the nerve with forceps until the continuity of the axons inside the nerve is broken, while preserving the epineurium and perineurium integrity.

Transection and suture repair: implies the disruption of the whole nerve by cutting it and then suturing the ends together using a thread or binding them with fibrin glue. The transection procedure is more severe than axonal crush, since it implies the destruction of the connective tissue of the nerve (A. Li et al., 2022).

Transection and graft or tube repair: is the most severe form of nerve injury, that results after the generation of a nerve gap that cannot be united by suturing. In this type of nerve damage, a nerve graft or a synthetic conduit are used to bridge the gap between nerve stumps. Larger mammals may be used as an animal model after this type of lesion, as their size is more similar to humans (Angius et al., 2012; Muheremu & Ao, 2015).

Comparative experimental studies have analyzed the outcome of sciatic nerve injuries of mice and rats that underwent both crush and transection and suture injuries (Navarro, Verdu, & Buti, 1994; B. B. Wang et al., 2023). The degenerative process was similar in both cases, but the crush injury allowed faster recovery of motor, sensory and sympathetic functions. There was 4-5 days difference in mice and 7 days difference in rats, considering the time required for reinnervation when comparing the two injury models. Additionally, the levels of functional recovery progressively decreased with the severity of the lesion, affecting more the larger nerve fibers. After all types of nerve injury, small nerve fibers (sympathetic and nociceptive) regenerated at a slightly faster rate and achieved a higher degree of reinnervation than large myelinated fibers (motor and mechanosensory) (Navarro et al 1994). Based on these results, researchers suggested that crush injury may be used for shorter studies involving gene expression, growth factors, inflammation, or pharmacological research. On the other hand, transection injury is a more suitable option for studying repair strategies using nerve graphs or determining the reinnervation of the regrowing axons (B. B. Wang et al., 2023). To note, the higher rate of recovery after crush injuries may mask small differences when comparing treatments than more severe types of nerve damage.

2. Peripheral nerve regeneration

After injuries that cause rupture of peripheral nerve fibers, axons and myelin sheaths distal to the lesion site are degraded by a process named Wallerian degeneration. The degenerative end products are eliminated by the cooperative action of Schwann cells and infiltrating macrophages, generating a distal microenvironment that is favorable for the axonal regrowth of surviving neurons. Additionally, cell bodies undergo a retrograde neuronal reaction, that promotes the metabolic and phenotypic changes necessary for the elongation of the sectioned axons.

2.1 Wallerian degeneration

In the Peripheral Nervous System (PNS), Wallerian degeneration is orchestrated by the release of chemokines and cytokines secreted by Schwann cells and macrophages, leading to the division of the process in an early pro-inflammatory phase and a late anti-inflammatory phase.

2.1.1. Early pro-inflammatory phase

Minutes after PNI, neurons raise the concentration of intracellular calcium, promoting the activation of the Sterile alpha and Toll/interleukin-1 receptor motif-containing protein 1 (SARM1) pathway, which is responsible for facilitating axonal disruption. This mechanism triggers the proteolytic activity of the calcium-dependent enzyme calpain, leading to complete axonal degeneration (DeFrancesco-Lisowitz, Lindborg, Niemi, & Zigmond, 2015; Metwally, Zhao, & Zhang, 2021).

Axonal breakdown results in the release of danger-associated molecular patterns (DAMPs), which are detected by Schwann cells through Toll-like receptors (TLRs). As a result, this promotes the secretion of pro-inflammatory cytokines and chemokines by Schwann cells. Furthermore, the loss of axonal contact induces Schwann cell dedifferentiation, triggering their transition from a myelinating to a repair-like phenotype (DeFrancesco-Lisowitz et al., 2015; Fornaro, Marcus, Rattin, & Goral, 2021; Jessen & Mirsky, 2016). Specifically, the repair phenotype is characterized by an increased expression of the transcription factor c-Jun, a regulator of phenotype transition, and by the inhibition of myelin synthesis. For instance, there is a reduction in the transcription of myelin components, such as MBP, MAG and P0, after nerve injury (Fornaro et al., 2021; Jessen & Mirsky, 2016)

Within a few hours following nerve damage, Schwann cells increase the transcription of the pro-inflammatory mediators TNF-α, IL-1α and IL-1β. Meanwhile, fibroblasts secrete IL-6 and GM-CSF early after injury (Rotshenker, 2011). Concomitantly the secretion of a variety of chemokines increases, particularly MCP-1 is released by Schwann cells hours after the impact in the damaged area and a day after injury in distal regions of the nerve (Martini, Fischer, Lopez-Vales, & David, 2008; Rotshenker, 2011). This chemokine plays a dual role by recruiting circulating macrophages, and by promoting debris clearance (P. Chen, Piao, & Bonaldo, 2015; Martini et al., 2008). In this regard, MCP-1 along with other pro-inflammatory cytokines such

as TNF-α and IL-1β, stimulates the expression of distinct members of the phospholipase A2 (PLA2) family. Importantly, PLA2 hydrolysis leads to the synthesis of lysophosphotidylcholine (LPC), which has myelinolytic activity. Moreover, LPC also triggers complement system activation and acts as an "eat me" signal for macrophages, promoting phagocytosis (Martini et al., 2008).

Both resident and hematogenous macrophages actively participate on Wallerian degeneration (Boissonnas et al., 2020; P. Chen et al., 2015). In fact, resident macrophages have been found to contribute to axonal regrowth, whereas recruited macrophages are most responsible for efficient myelin stripping and clearance (Boissonnas et al., 2020). Macrophage recruitment starts between day 2 and 3 after injury, peaking at 7 days. This pattern coincides with the secretion peaks of the pro-inflammatory cytokine IL-6, being the first peak at day 2 and the second peak at day 7 after injury. Paradoxically, while macrophages raise in number within the nerve, there is a decrease in the secretion of the pro-inflammatory cytokines TNF-α and IL-1β (Rotshenker, 2011). Notably, other immune cells are involved in the development of Wallerian degeneration, such as T cells and neutrophils, which are also recruited in the injured nerve (P. Chen et al., 2015).

To conclude, the early phase of Wallerian degeneration is characterized by the synthesis of the inflammatory mediators MCP-1, TNFα, IL-1α, IL-1β, GM-CSF and IL-6. The marked pro-inflammatory environment promotes the recruitment of phagocytic cells, which engulf the myelin debris that prevents further axonal regeneration. The second phase of Wallerian degeneration is characterized by the enhanced production of IL-6, IL-4, IL-10 and GM-CSF and a decreased secretion of TNFα and IL-1β. Consequently, enhancing the anti-inflammatory influence in the environment surrounding the injury (Rotshenker, 2011) (Figure 2).

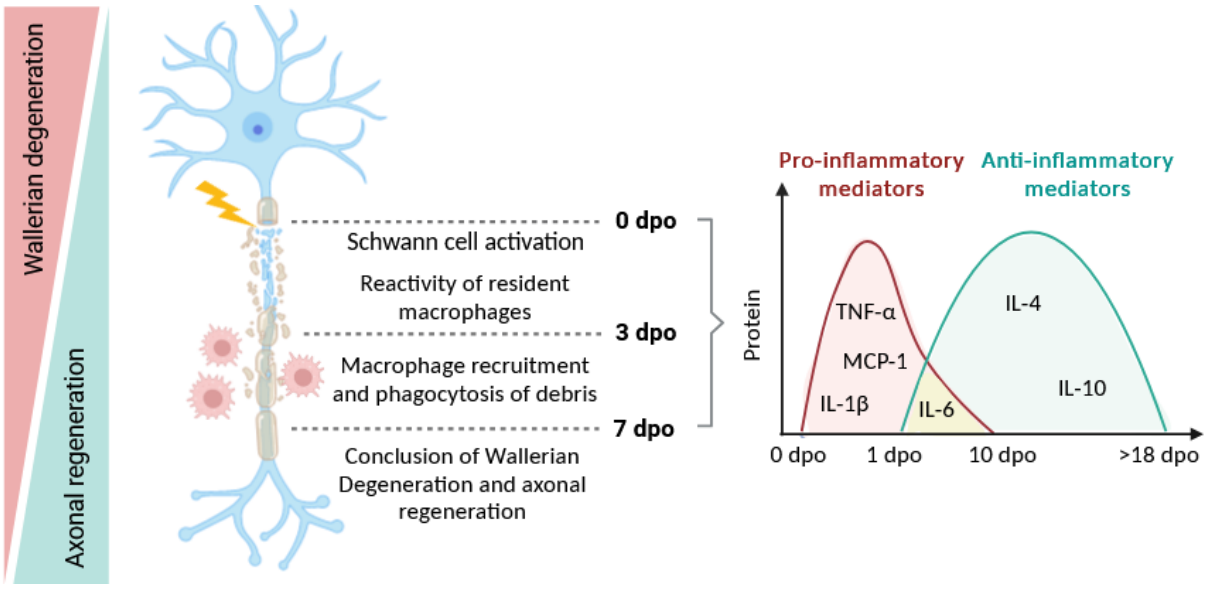

Figure 2: Critical time-points of the development of Wallerian degeneration and dynamics of the inflammatory environment following nerve injury. Created with BioRender.

2.1.2. Late anti-inflammatory phase

Recruited macrophages are characterized by the secretion of both IL-6 and IL-10 cytokines. In fact, the detection of IL-10 peaks at day 7, coinciding with the highest rate of macrophage infiltration. IL-10 has an important role orchestrating the conclusion of Wallerian degeneration, because it downregulates the expression of pro-inflammatory cytokines leading to the resolution of the degenerative process (Martini et al., 2008; Rotshenker, 2011).

Other anti-inflammatory cytokines also participate after PNI. For instance, in human samples IL-4 immunohistochemical staining has been detected after nerve injury (Daines, Schellhardt, & Wood, 2021; Deprez et al., 2001; M. R. Wells, S. P. Racis, & Vaidya, 1992). Hence, pro-inflammatory M1 macrophages adopt an M2 phenotype favoring tissue remodeling and regeneration in the last stage of Wallerian degeneration (DeFrancesco-Lisowitz et al., 2015). In conclusion, the anti-inflammatory phase has a crucial role in promoting the resolution of the degenerative process.

It is important to note that both, pro- and anti-inflammatory phases of Wallerian Degeneration, are necessary for proper myelin clearance. For instance, TLR2- and TLR4-deficient mice have a compromised expression of the pro-inflammatory mediators IL-1β and MCP-1, which further decreased macrophage recruitment and functional outcome after

sciatic nerve crush (Boivin et al., 2007). In addition, neutralization of MCP-1 and IL-1β suppressed macrophage response and myelin clearance in mice that underwent sciatic transection (Perrin, Lacroix, Aviles-Trigueros, & David, 2005). Considering the role of anti-inflammatory cytokines, the administration of IL-4, IL-10 and IL-13 have been found to facilitate axonal regeneration in models of traumatic nerve and spinal cord injuries (Ali et al., 2020; Atkins et al., 2007; Van Broeckhoven et al., 2022). Altogether, these findings suggest that an advancement of the anti-inflammatory phase of Wallerian degeneration, without compromising the development of the pro-inflammatory phase, may improve outcome after nerve injury.

2.2. Neuronal response

2.2.1. Retrograde reaction and chromatolysis

In parallel to the course of Wallerian degeneration, proximal regions of the affected nerve trunk can also undergo limited retrograde axonal degeneration.

Moreover, several signals act on the neuronal soma to initiate and maintain the regenerative response (Hanz & Fainzilber, 2006). The first signal to reach the neuronal body after axonal injury is a burst of action potentials generated at the lesion site, due to the inflow of Ca^{2+} and Na^{+}. Later, the suppression of retrograde transport of neurotrophic factors and the arrival of activated proteins at the lesion, termed "positive injury signals", induce the expression of immediate early genes (IEG) in the neuronal soma. As a result, this promotes the expression of genes involved in cell survival and axonal growth (for reviews see (Navarro, Vivo, & Valero-Cabre, 2007; Raivich & Makwana, 2007)). In addition, the neuronal soma undergoes a phenotypical response after injury, that represents a shift from a transmission state towards a regenerative state. Specifically, the cell body is subjected to a physiological mechanism known as chromatolysis. This process consists in the loss of cytoplasmic Nissl staining, due to the dissolution of the endoplasmic reticulum, rich in aggregated ribosomes.

To note, nerve injury can induce cell death of the affected neurons, depending on the distance between the axonal lesion and the neuronal soma. If the damage is close to the neuronal body, cells are more susceptible to die (Navarro et al., 2007). This relation between the damage site and cell death has been mainly observed in motor neurons. Contrary, sensory neurons can experience cell death up to 40% regardless of the injury location and the age of

the subject (Daines et al., 2021). Despite the neuronal origin, damage produces transcriptional reprogramming in surviving neurons, which is essential to promote regeneration.

2.2.2 Transcriptional reprogramming

Injured neurons change their transcriptional profile by reducing the synthesis of proteins used for neurotransmission and increasing the expression of structural proteins that facilitate axonal rebuilding. The switch from a neurotransmission to a regenerative state is characterized by the expression of Regeneration Associated Genes (RAGs), leading to the expression of inflammatory mediators, neurotrophic factors, and cytoskeletal elements to support nerve regeneration.

The synthesis of RAGs after axotomy is triggered by the activation of signaling pathways that promote the translocation of transcription factors to the neuronal nucleus. Well-known signaling pathways associated with nerve regeneration include MAPK (ERK, p38, JNK), mTOR, Ras and PI3/Akt among others. For example, growth factors, such as NT3, NGF, and FGF12, activate the MAPK/ERK pathway, leading to the translocation of ERK into the nucleus, which promotes regeneration (R. Li et al., 2020). The JNK/c-JUN, PI3/Akt and p38 pathways have also been suggested to trigger axonal regeneration (Allodi, Udina, & Navarro, 2012; Patodia & Raivich, 2012). Additionally, mTOR is involved in protein synthesis regulation. Overexpression of mTOR increases the levels of the growth-associated protein GAP43. However, prolonged overexpression of mTOR reduces the accuracy of target reinnervation (Abe, Borson, Gambello, Wang, & Cavalli, 2010; Allodi et al., 2012).

Regarding transcription factors, a total of 26 families are implicated in regeneration after PNI, including c-Jun, ATF3, CREB, STAT3, C/EBPs, p53, Oct-6, NF-KB, Sox 11 and NFATs (Michaelevski et al., 2010; Patodia & Raivich, 2012). For instance, STAT3 induces GAP43 expression. This phenomenon can be prevented with JAK inhibition, indicating that JAK/STAT3 pathway may be involved in neurite outgrowth (Patodia & Raivich, 2012). Further, Sox11 is implicated in the transcription of β-III tubulin and MAP2 which are genes associated with axonal growth (Bergsland, Werme, Malewicz, Perlmann, & Muhr, 2006).

2.3 Nerve regeneration

The process of neuronal reprogramming occurs in parallel to the progression of Wallerian degeneration and is reversed when neurons reach a target organ. It is important to note, that

the formation of the neural growth cone begins after the resolution of Wallerian degeneration. Thus, slowing of the degenerative process can be a limiting factor for the outcome after injury (Menorca et al., 2013).

Growth cones emerge from the severed axons and grow if they find a favorable terrain. When growth cones cannot reach the distal degenerating nerve, they twist in the proximal stump forming a neuroma. In contrast, when the regenerating axonal tips gain the distal nerve, they elongate within the endoneurial tubules in association with the Schwann cells and the basal lamina. The rate of axonal regeneration is initially very slow but reaches a constant value of about 1-3 mm/day. In addition, the advancing growth cone is guided by gradients of neurotrophic and neurotropic factors mainly produced by reactive Schwann cells and the ECM within the degenerated nerve (for reviews see Allodi et al., 2012). The regenerating axons follow the distal nerve to eventually reach target tissues in the periphery.

During axonal elongation several sprouts appear from an original axon, resulting in an excess of axons in the distal nerve (Witzel, Rohde, & Brushart, 2005). This situation is temporary, as axonal surplus is eliminated by neuronal pruning when reinnervation is mismatched (T. Brushart, Gerber, Kessens, Chen, & Royall, 1998; T. M. Brushart, 1988). Axons that regenerate through erroneous distal pathways to targets that cannot reinnervate, such as motor axons to the skin or cutaneous axons to muscle, tend to withdraw and may be eliminated. Despite regeneration may be successful, the normal nerve structure and function are not completely restituted. In fact, after nerve injury and repair, the diameter and conduction velocity of regenerated axons remains below normal.

2.3.1 Growth cone and associated proteins

After axotomy, there is an immediate raise on the production of cytoskeletal proteins such as actin, tubulin, and the growth cone component GAP43. These proteins are anterogradely transported to the distal process (Menorca et al., 2013; Wale Sulaiman & Gordon, 2013), and are essential for axonal elongation (see Figure 4).

GAP43 plays an important role in the growth cone consolidation. It is a located in the growth cone's inner plasma membrane, facilitating its interaction with actin and subsequently leading to filopodia constitution (Denny, 2006). It has been described that GAP43 can be subjected to post-translational modifications, which are of utmost importance in the modulation of the

growth cone dynamics. Specifically, phosphorylated GAP43 is necessary to stabilize actin filaments, while unphosphorylated GAP43 inhibits growth cone progression by attracting capping proteins that attenuate actin polymerization (Chung, Shum, & Caraveo, 2020). The phosphorylated forms of GAP43 at S96 or T172 were described as specific markers for regenerating axons (A. Kawasaki et al., 2018; Okada et al., 2021).

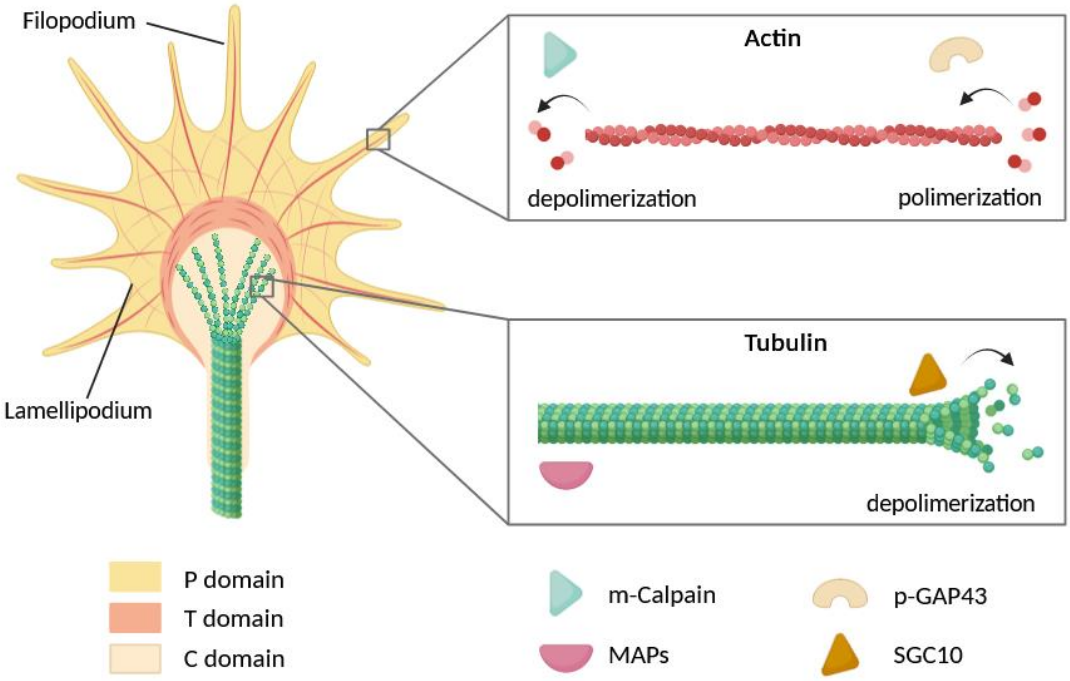

Figure 4: The growth cone structure is divided in three domains. The P-domain enables the exploration of the microenvironment. It is formed by filopodia (long bundled actin filaments) and lamellipodia (mesh-like actin networks). Microtubules form the central C-domain, that serves as the structural foundation of the growth cone and the T-zone is a transition area rich in myosin (Allodi et al., 2012; Lowery & Van Vactor, 2009). Along with cytoskeletal elements, microtubule associated proteins regulate of growth cone dynamics by promoting active polymerization (p-GAP43), stabilization (MAPs) and depolymerization (m-Calpain and SGC10). Elaborated using BioRender.

Superior cervical ganglion 10 (SCG10) is a microtubule-associated protein, whose expression is also increased after nerve injury (Sanchez-Huertas & Herrera, 2021; Shin, Geisler, & DiAntonio, 2014). This protein has been identified as an axonal regeneration marker, as it is detected in the growth cone. Particularly, it is preferentially expressed by growing sensory neurons rather than motor neurons (Shin et al., 2014). From a functional standpoint, SGC10 belongs to the family of stathmins, which bind to tubulin dimers to withdraw them from microtube endings (Sanchez-Huertas & Herrera, 2021). Paradoxically, the expression of cytoskeleton destabilizing proteins is necessary to allow rearrangements on the microtubule network that facilitate growth cone elongation. In fact, SGC10 downregulation, leads to

microtubule overstabilization and neurite growth suppression (Morii, Shiraishi-Yamaguchi, & Mori, 2006).

While the production of cytoskeletal proteins is increased after injury, the structural protein neurofilament which maintains axon diameter, is temporally downregulated (Menorca et al., 2013). In addition to cytoskeleton-related proteins, neuroprotectants such as heat-shock protein (HSP27) are upregulated to promote neuronal survival.

2.3.2 Regenerative environment in the distal nerve

Following injury, Schwann cells, fibroblasts and macrophages secrete protein mediators that act as chemoattractant or chemorepulsive signals that guide the growth cone (DeFrancesco-Lisowitz et al., 2015; Rotshenker, 2011). This crosstalk between the environment and the growing axon is essential for determining the regenerative outcome.

Specifically, there is an increase on the expression of the neurotrophic factors BDNF and GDNF in the distal stump of neurons, while CNTF is reduced after nerve damage (Menorca et al., 2013). However, there are some differences between sensory and motor neurons when considering the transcription of neurotrophic factors following injury. In fact, while both neuronal subtypes upregulate the expression of BDNF and FGF, NGF is specifically increased in sensory neurons (Allodi et al., 2012). Importantly, besides their role on axonal guidance, most neurotrophic factors also favor neuroprotection.

In addition to neurotrophic factors, cytokines and chemokines also play a role shaping the regenerative milieu. Proper regulation of the inflammatory events is crucial to achieve a permissive environment for nerve regeneration. Following injury, pro-inflammatory cytokine secretion is necessary for efficient macrophage recruitment and debris clearance. However, recent evidence indicates that chronic inflammation hinders the nerve regenerative capacity (Buttner et al., 2018), whereas exogenous treatment with anti-inflammatory cytokines improves nerve regeneration (Ali et al., 2020; Atkins et al., 2007). As discussed in previous subchapters, orchestrating a rapid resolution of Wallerian degeneration by facilitating the transition from the pro-inflammatory phase towards the anti-inflammatory phase could promote a favorable environment for the formation of the growth cone, leading to axonal growth. In fact, evidence supports that anti-inflammatory mediators play a critical role in

nerve regeneration. Thus, recent findings regarding the role of the anti-inflammatory cytokines IL-4, IL-10 and IL-13 are discussed below.

Interleukin 4

IL-4 is a 13 kDa protein secreted mainly by T cells, B cells, macrophages, and mast cells. Additionally, stromal cells such as fibroblasts are also known to be a source of IL-4 (Daines et al., 2021; Vidal, Lemmens, Dooley, & Hendrix, 2013). The IL-4 receptor system exhibits some complexity as it relies on two transmembrane subunits for functioning. The first subunit is the IL-4Rα chain, which has high affinity for the IL-4 ligand. The second transmembrane subunit can either be IL-13Rα1 or the common γ chain (Daines et al., 2021).

A recent study revealed that macrophages and neuronal subsets are targets for IL-4 after a nerve crush, whereas Schwann cells expressed limited amounts of IL-4 receptor (Pan et al., 2022).

Following nerve injury, the cytokine IL-4 is downregulated in the ipsilateral DRG, while pro-inflammatory mediators are upregulated, probably facilitating macrophage recruitment to promote regeneration (Uceyler, Tscharke, & Sommer, 2007). Although limited literature has focused on unravelling the impact of IL-4 as a potential treatment after neve injury, studies conducted *in vivo* and *in vitro* have shown promising results when assessing its effects on axonal regeneration. An *in vivo* study observed that IL-4 administration promoted facial motor neuron survival through the STAT6 pathway (Deboy et al., 2006). Additionally, nerve repair models that used conduits containing IL-4 obtained greater axon regeneration than cytokine-free conduits (Ali et al., 2020). In fact, IL-4KO mice subjected to crush injury exhibited delayed axonal regeneration and lower reinnervation of the neuromuscular-junction compared to wild-type animals, whereas IL-4 treatment on crush-injured wild-type mice produced an increased early neurite extension. However, no significant effects were detected in functional recovery (Pan et al., 2022). *In vitro* studies using DRG cultures have shown enhanced neurite outgrowth under IL-4 treatment or when combining IL-4 with neurotrophins (Golz et al., 2006; Vidal et al., 2013).

Interleukin 10

IL-10 is an 18kDa cytokine primarily produced by monocytes and macrophages (Vidal et al., 2013). It has a pivotal role in regulating cytokine production and is indispensable for the

proper development of Wallerian degeneration. The importance of IL-10 after nerve injury was proven in a study conducted with IL-10 null mice. The researchers observed that lack of IL-10 resulted in altered macrophage infiltration and poor motor and sensory recovery in mice subjected to crush injury. Additionally, IL-10 KO mice failed to downregulate pro-inflammatory cytokine transcription after phagocytosis *in vitro* (Siqueira Mietto et al., 2015). Moreover, treatment with IL-10 has shown beneficial effects on nerve regeneration in mice with transection injury, as it reduced collagen scarring and improved electrophysiological recordings (Atkins et al., 2007). Positive effects of IL-10 have been assessed in vitro, where it increased neurite outgrowth and improved synapse formation in a glucose-deprived cortical culture via JAK/STAT3 pathway (H. Chen et al., 2016).

Interleukin 13

IL-13 is a 12 kDa protein produced mainly by T cells, mast cells, eosinophils, and basophils (Kelly-Welch, M. Hanson, & D. Keegan, 2005; Vidal et al., 2013). The IL-13 receptor is formed by two transmembrane proteins and shares a common heterodimeric structure with IL-4, consisting of IL-13Rα1 and IL-4Rα1 chains. IL-13 also has another receptor subtype that consists of the interaction between IL-13Rα1 and IL-13Rα2 chains. The signal transduction through the heterodimer shared by IL-13 and IL-4 leads to the activation of JAK/STAT signaling, with STAT6 as a final target. However, the IL-13Rα1- IL-13Rα2 heterodimer can suppress the signaling mediated by the IL-13/IL-4 receptor. Importantly, the STAT6 pathway has already been associated with neuroprotection and nerve regeneration (Deboy et al., 2006). Although there is a lack of studies investigating the role of IL-13 after nerve injury, its potential effects on STAT6 as a downstream target suggest that it could have favorable effects on the regenerative outcome. Additionally, a study conducted in spinal cord injured mouse that had reprogrammed macrophages with high secretion of IL-13 reported increased neuroprotection and improved motor function (Van Broeckhoven et al., 2022).

2.3.3 Cells that participate in the regenerative environment

Schwann cells

Non-neuronal cells are also subjected to transcriptional reprogramming after nerve injury. In the case of Schwann cells, the loss of contact with neurons promotes a phenotype switch that alters their original function. Specifically, within 24 to 48 hours after axotomy the axonal

cytoskeleton is disintegrated, leading to the detachment of the myelin sheath due to the loss of contact between the neuron and the Schwann cell. This detachment is triggered by the activation of the receptor tyrosine kinase ErbB2 (S. B. Han et al., 2017; Navarro et al., 2007). Activated ErbB2 signals through Erk and Akt pathways, which stimulate Schwann cell proliferation (S. B. Han et al., 2017). However, other studies suggest that other mechanisms may be also involved (Atanasoski et al., 2006). The highest rate of Schwann cell proliferation is 3 days after injury, and this process continues for 2 to 3 weeks when Schwann cells triplicate their number in the distal nerve (Navarro et al., 2007; Salonen, Aho, Roytta, & Peltonen, 1988). The increased population of Schwann cells align into Bünger bands, which will provide support and guidance for axonal regeneration (Navarro et al., 2007).

Apart from proliferation, loss of contact with neurons triggers dedifferentiation. In fact, Schwann cells adopt a phenotype that reassembles progenitor cells before transforming towards a regeneration-supportive phenotype (Fornaro et al., 2021). During the first stage of dedifferentiation, Schwann cells downregulate the expression of genes associated with their myelinating function. For instance, there is a reduced expression of enzymes that regulate cholesterol synthesis, membrane associated proteins such as myelin-associated glycoprotein (MAG), and myelin structural proteins such as P0 and myelin basic protein (MBP). On the other hand, there is an upregulation of genes that are found in immature Schwann cells such as L1, NCAM, p75NTR and glial fibrillary acidic protein (GFAP) (Jessen & Mirsky, 2008; Jessen, Mirsky, & Lloyd, 2015). Then, Schwann cells undergo a second stage of differentiation that transforms them into regeneration-supportive Schwann cells. This involves an upregulation of neurotrophic factors and adhesion molecules such as GDNF, BDNF, NGF, VEGF, bFGF, pleiotrophin and NCAM, which promote neuronal survival and axonal elongation (Jessen et al., 2015; Klimovich, Rubina, Sysoeva, & Semina, 2021; Wale Sulaiman & Gordon, 2013). Schwann cells present in the neural distal stump raise the expression of pro-inflammatory cytokines and chemokines that would contribute to the development of Wallerian degeneration and promote macrophage recruitment. Specifically, as seen in previous subchapters, Schwann cells increase the secretion of TNF-α, LIF, MCP-1, IL-1α and IL-1β (Jessen et al., 2015). Finally, there is an initiation of a cell-intrinsic process that promotes myelin breakdown, facilitating further myelin clearance.

Macrophages as regulators of degeneration and regeneration

Macrophages are pleiotropic cells that perform a wide variety of functions related to homeostasis, phagocytosis, inflammation, and tissue repair. These cells can be divided between infiltrating and resident macrophages considering their ontology. Resident macrophages originate from the yolk sac or the fetal liver and enter peripheral tissues during embryonic development. Their population is maintained mainly by local proliferation and are independent from blood-monocytes (Italiani & Boraschi, 2014; Zigmond & Echevarria, 2019). In PNS, resident macrophages are distributed along the nerves and ganglia. In fact, in human adult samples of sensory ganglia, sympathetic ganglia and the associated nerve roots, resident macrophages accounted between a 5 and 20% of the total amount of cells (Esiri & Reading, 1989). In contrast, infiltrating or hematogenous macrophages originate from the bone-marrow and migrate towards peripheral tissues under local recruitment. They can infiltrate in the peripheral nerve under different phenomena that disrupts homeostasis, such as peripheral neuropathies, infection, and nerve injury (Msheik, El Massry, Rovini, Billet, & Desmouliere, 2022). In a study conducted in rats with sciatic nerve injury, it was observed that the populations of resident and hematogenous macrophages were proportional until day 3. However, from day 4 to 14 after injury, the number of infiltrated macrophages increased until quadruplicating the population of resident endoneurial macrophages (Mueller et al., 2003). This differences on the population numbers suggested that both macrophage subtypes could have different roles in the regenerative process. In fact, evidence points that resident macrophages may contribute to ECM and microenvironment maintenance being indispensable for nerve regeneration. Whereas infiltrating macrophages intervene in phagocytosis and the resolution of Wallerian degeneration (Boissonnas et al., 2020).

In addition to the classification based on their origin, macrophages have also been classified according to their phenotype under activation. In the 1990's, it was described that INFγ and LPS had different effects on macrophage gene expression when compared to IL-4 (Stein. M, Keshav. S, Harris. N, & Gordon. S, 1992). Another categorization took into consideration macrophage metabolism, leading to the terminology of M1-M2 macrophages. In M2 macrophages, the arginine metabolism is shifted towards the production of ornithine, which is a precursor of polyamines and collagen. Contrary, M1 metabolism is shifted towards the production of NO and citrulline (Mills, Kincaid, Alt, Heilman, & Hill, 2000). In fact, NO inhibits

cell proliferation and can lead to cell death (Beltran, Mathur, Duchen, Erusalimsky, & Moncada, 2000; Murphy, 1999). This metabolic classification led to the description of M1 macrophages as killing cells and M2 macrophages as repairing cells. The resulting dichotomy of M1 and M2 macrophages is inspired in the Th1 and Th2 classification of T cells.

Finally, the metabolic classification also included the phenotype under activation, leading to multiple subdivisions that describe a wider range of macrophage profiles. M1 macrophages have been associated with inflammation, their role as antigen-presenting cells and the increased production of reactive-oxygen species (ROS) upon stimulation by pathogens or damage-associated molecular patterns (Zigmond & Echevarria, 2019). M2 macrophages have been subdivided into M2a, M2b, M2c and M2d. M2a are also known as alternative activated macrophages, and their phenotype is activated upon IL-4 or IL-13 stimulation. M2b macrophages are also known as regulatory macrophages and are activated upon Toll-Like-Receptor (TLR) or IL-1R agonists. M2b produce both pro- and anti-inflammatory cytokines, acting as an immunoregulator. M2c are activated by IL-10, which triggers a feedback that leads to the secretion of more IL-10 and IL-1β. This macrophage subtype is associated with anti-inflammatory phase resolution and wound healing. Finally, M2d macrophages are associated with angiogenesis and metastasis. This subtype is activated through TLR agonists and IL-6 (Lis-Lopez, Bauset, Seco-Cervera, & Cosin-Roger, 2021; Murray et al., 2014).

Currently, the classification of macrophages is controversial. For instance, advances on research have revealed that the differences on the metabolism between M1 and M2 macrophages are dependent on the mice strain. Specifically, the C57BL6/J mouse strain has a deletion on an arginine transporter, leading to alterations in metabolism and on M1/M2 classification (Sans-Fons et al., 2013). Additionally, inconsistencies arise when different protocols are used by researchers, as macrophages grown in M-CSF or GM-CSF display different phenotypes (Joshi et al., 2014). Thus, more research is required to successfully characterize macrophage phenotypes. To address this issue guidelines have been proposed (Murray et al., 2014). Although M1-M2 polarization is now considered a spectrum and further characterization is necessary, the concepts of M1 and M2 macrophages would be used in this thesis to simplify their implication on inflammatory events. Concretely, the term M1 would be used for pro-inflammatory macrophages and the M2 concept for anti-inflammatory macrophages.

3. Neuropathic pain

3.1 Definition and incidence

Neuropathic pain arises from neuronal damage and produces pain and sensations that are deviated from normal nociception (Cervero, 2009; Costigan, Scholz, & Woolf, 2009). Currently, the IASP has defined neuropathic pain as "pain caused by a lesion or disease of the somatosensory system" (Jensen et al., 2011). Specifically, neuropathic pain that is generated from PNS damage is referred as peripheral neuropathic pain. Peripheral neuropathic pain can be caused by several factors like chemical toxics, trauma, infection, metabolic diseases, or tumor invasion (Costigan et al., 2009). Patients with neuropathic pain may describe the sensation as burning, pricking, needle-like or freezing, that can be accompanied by an electric shock-like perception (Bouhassira et al., 2004; Costigan et al., 2009; Finnerup, Kuner, & Jensen, 2021). In addition to pain, paresthesia (abnormal sensations) and dysesthesia (unpleasant anomalous sensations) may appear. The sensory alterations and pain can be spontaneous or evoked (Finnerup et al., 2021). In fact, evoked pain can lead to the perception of allodynia (pain from a non-noxious stimulus) or hyperalgesia (exaggerated painful response to a stimulus that provokes pain).

While the persistence of pain can vary depending on several factors such as age, size of the damaged nerve or genetical background, epidemiological studies suggest that the prevalence of neuropathic pain is around 8.2– 6.9 % in European population (Bouhassira, Lanteri-Minet, Attal, Laurent, & Touboul, 2008; Torrance, Smith, Bennett, & Lee, 2006). Further, neuropathic pain supposes an economic burden to the patients or the states, as it includes surgical expenses, sick-leave, drugs, and non-surgical procedures. In Spain, the economic cost to the national healthcare system associated with neuropathic pain was above than 500 million euros in 2012 (Ruiz, Liedgens, & Obradovic, 2013). Thus, investing in the research on neuropathic pain is essential to improve the well-being of the patients and to reduce long-term economic investment on rehabilitative treatments.

3.2 Animal models

Injuries that result in damage to nerve fibers have become valuable techniques for generating and assessing neuropathic pain in animals. These injuries trigger self-protection behaviors and

exaggerated reactions to non-noxious stimuli. The following are some commonly used injury models in preclinical peripheral neuropathic pain research:

Axotomy: Transection or crush of the sciatic nerve is a frequently used procedure to induce neuropathic pain in rodents. However, animals can acquire self-mutilation behaviors and milder forms of PNI have been developed to solve this issue (Sousa, Lages, Pereira, & Slullitel, 2016).

Chronic Constriction Injury (CCI): In this surgical intervention four loose knots are tied around the sciatic nerve, causing swelling and strangulation. Animals that undergo CCI exhibit enhanced responses to thermal and mechanical algesimetry tests.

Spared Nerve Injury (SNI): This procedure involves the cut and ligation of tibial and peroneal branches of the sciatic nerve, while leaving the sural branch intact. In this injury, responsiveness to the stimulus is increased on the innervation territory of the intact sural nerve. Like in CCI, animals that undergo SNI react both to mechanical and heat stimuli (Casals-Diaz, Vivo, & Navarro, 2009; Sousa et al., 2016).

Spinal Nerve Ligation (SNL): Sometimes referred as spinal root ligation, this surgical intervention implies the loose ligation of L5 and L6. Animals subjected to SNL develop cold allodynia and thermal hyperalgesia.

Partial Sciatic Nerve Ligation (PSNL): In this procedure a suture is placed on one half to one third of the sciatic nerve and induces thermal and mechanical hypersensitivity (Korah et al., 2022; Sousa et al., 2016) (See Figure 5).

To note, axotomized animals display different behavior when compared to other neuropathic pain models, in which the sciatic nerve is only partially injured. In these neuropathic pain models, mice show increased hyperalgesia early after nerve damage. In contrast, after crush or section and repair injuries, there is a first stage of anesthesia generated by the complete denervation of the damaged nerve. Later, animals suffer from hyperalgesia as regenerating axons start reinnervating the skin. This phenomenon can be observed in the lateral side of the injured paw when analyzing thermal and mechanical stimuli. Contrary, the medial side of the hind paw develops hyperalgesia few days after axotomy. This occurs because the medial hind paw is partially innervated by the saphenous nerve, which remains intact after the sciatic nerve lesion (Casals-Diaz et al., 2009).

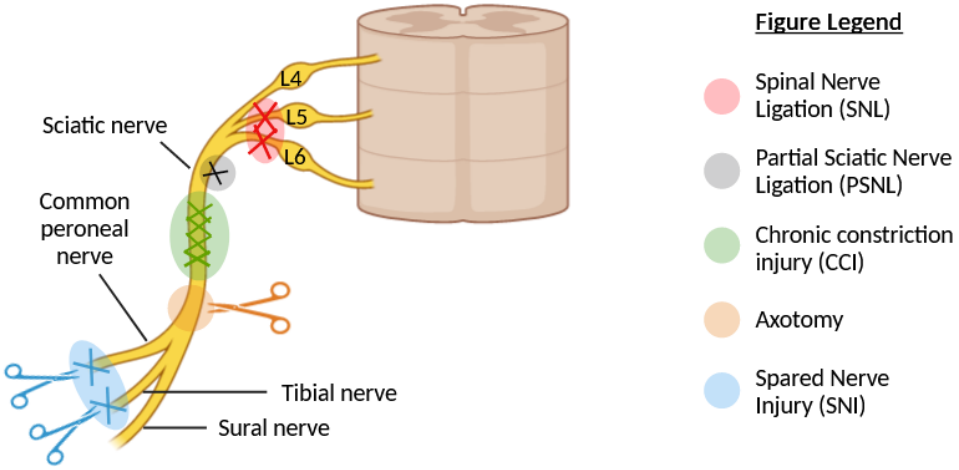

Figure 5: Summary of the most common injury models to study neuropathic pain in preclinical research. Scissors represent cut injuries, while crosses ligation of the nerve. Own elaboration using BioRender.

3.3 Physiopathology of neuropathic pain

In healthy subjects, painful stimuli is perceived by primary nociceptors, which are free nerve endings without specialized detection structures. Upon stimulation, primary nociceptive neurons synapse with second-order neurons and with interneurons in the dorsal horn of the spinal cord, through unmyelinated C axons or thinly myelinated Aδ fibers (Coutaux, Adam, Willer, & Le Bars, 2005; López-Álvarez, 2017).

Unmyelinated C fibers can be categorized as peptidergic (substance P and CGRP positive) or non-peptidergic (IB4 positive and rich in P2X3 purinergic receptors). Specifically, peptidergic fibers project to Rexed laminae I, while non-peptidergic neurons project to inner and outer laminae II of the dorsal horn (Casals-Diaz et al., 2009). Additionally, Aδ fibers are both neurofilament and CGRP positive and target to laminae I, IV and V of the dorsal horn (Coutaux et al., 2005; López-Álvarez, 2017). Painful information is then transmitted to the thalamus through the spinothalamic tract, and to the brainstem by the spinomesencephalic tract, to be later integrated in several areas of the brain (Boadas-Vaello et al., 2016).

Although nerve injury can lead to peripheral neuropathic pain that persists once the cause of damage has long occurred, it is important to note that neuropathic pain only becomes chronic in a minority of cases (Costigan et al., 2009). In this regard, under neuropathic pain conditions, functional dysregulation occurs both in first and second order neurons following nerve injury. First-order neurons undergo alterations in the expression of ion channels, receptors, and neurotransmitters, resulting in increased neuronal excitability and peripheral sensitization

(Boadas-Vaello et al., 2016; Finnerup et al., 2021). In addition, nerve injury leads to the generation of bursts of ectopic action potentials that overactivate second order neurons. At the spinal cord, second order neurons also suffer changes in receptors, neurotransmitters, and a reorganization of afferent projections (central remodeling). Additionally, second order neurons are also susceptible to alterations of inhibitory pathways, which may exacerbate the perception of pain (Boadas-Vaello et al., 2016). Altogether, these modifications in the spinal cord trigger a process known as central sensitization.

3.4 Excitability under neuropathic pain conditions

3.4.1 First-order neurons and peripheral sensitization

Peripheral sensitization occurs when nerves respond to the neuronal insult and to the local inflammatory mediators, through the release of molecules that contribute to increase neural excitability. Specifically, nerve damage reduces the threshold of nociceptors, raising the responsiveness of nociceptive fibers (Toth, 2013). Additionally, intact neurons in the vicinity undergo variations on the expression of receptors and ion channels and may also exhibit collateral axon growth (Costigan et al., 2009). Hence, these alterations together with the inflammatory events that occur after nerve injury, lead to an exacerbation of the excitability of first order sensory neurons (Ellis & Bennett, 2013).

Therefore, excitability results from the molecular changes that occur in neurons after nerve damage and from the influence of inflammation. The following subchapter will review the molecular mechanisms that promote excitability in primary afferents.

Alterations on ligand-gated channels and receptors

Following nerve injury, there is an upregulation of several receptors and channels, including ASICs, TRP channels and purinergic receptors (Boadas-Vaello et al., 2016).

TRP channels

The TRP channel family consists of TRPV1-4, TRPM8 and TRPA1, each with different response to temperature. TRPV1 is activated by protons (H+), capsaicin and heat over 43ºC, and is involved in neuropathic pain, since different types of nerve injury raise its expression (Facer et al., 2007; H. Y. Kim et al., 2008; Toth, 2013). Additionally, a study conducted in TRPV1 deficient mice reported diminished response to painful heat, suggesting that this channel is critical for injury-induced thermal hyperalgesia (Caterina et al., 2000). TRPM8 is associated

with cold hypersensitivity, and TRPA1 is sensitized by the secretion of bradykinin (Stucky et al., 2009). To note, activation of TRP channels leads to depolarization through calcium influx, further increasing neuronal excitability (Vangeel & Voets, 2019).

ASIC channels and Purinergic receptors

Injury and inflammation decrease the tissue pH leading to acidosis, which plays a significant role in hyperalgesia. ASIC channels are pH-detecting receptors, involved in nociception. Studies have described that spinal nerve ligation and spinal nerve injury lead to alterations on the regulation of ASICs. In spinal nerve ligation almost all ASICS are upregulated, whereas spinal nerve injury is associated with downregulation of ASIC1 (Poirot, Berta, Decosterd, & Kellenberger, 2006). In a model of cuff compression of the sciatic nerve, alterations of ASIC expression were found to occur in purinergic CGRP positive neurons (Papalampropoulou-Tsiridou, Labrecque, Godin, De Koninck, & Wang, 2020). In addition to pH alterations, injury leads to an increased secretion of purines such as ATP, which sensitize the purinergic receptors P2X3 and P3Y (Ellis & Bennett, 2013).

Alterations on the expression of voltage-gated ion channels

Neuropathic pain is characterized by alterations in the expression and function of voltage-gated ion channels. These changes have significant implications in neuronal excitability and the subsequent transmission of pain signals. Among the various ion channels involved, the upregulation of sodium channels and HCN channels, along with decreased activity of certain potassium channels, are recognized as key contributors to the development and maintenance of neuropathic pain. Further, alteration of the expression of other channels, such as calcium and chloride channels, has also been reported (Toth, 2013). The following sections will focus into the changes observed in sodium, potassium, and HCN channels, providing insights into their implication in neuropathic pain.

Sodium channels

Nav1.3 channel is expressed in embryonic neurons but faintly expressed in adult peripheral nerves. However, following nerve injury, the embryonic Nav1.3 channel is upregulated and promotes ectopic firing through increased axonal excitability (Bennett, Clark, Huang, Waxman, & Dib-Hajj, 2019). In fact, upregulation of Nav1.3 has been reported to accumulate on the distal process of injured and uninjured afferents increasing their excitability (Black et

al., 1999; Lindia, Kohler, Martin, & Abbadie, 2005). However, studies involving the silencing of Nav1.3 channel in mice reported contradictory results regarding its effects on the amelioration of pain (Minett et al., 2014; Nassar et al., 2006).

Nav 1.7 and Nav1.8 are voltage-gated sodium channels normally expressed in adult neurons (Bennett et al., 2019). Research findings show conflicting results on the role of these channels in the development of neuropathic pain in mice. For instance, individual or double knocking-out of Nav1.7 and Nav1.8 in mice led to the development of neuropathic pain in SNL (Nassar, Levato, Stirling, & Wood, 2005). However, the same research group observed that after CCI pain is attenuated when Nav1.7 is deleted in sensory neurons (Minett et al., 2014). Other studies on SNI proved that independent silencing of Nav1.7 and Nav 1.8 channels ameliorated pain in mice (Daou et al., 2016; Shields et al., 2018).

Potassium channels

DRG neurons display a wide variety of potassium channels that regulate the membrane potential, including delayed rectifiers (K_v1.1, 1.2), A-channels (K_v1.4, 3.3, 3.4, 4.1, 4.2, and 4.3), KCNQ channels (K_v7.2, 7.3, 7.4, and 7.5) and ATP-sensitive channels (K_{IR}6.2) among other subtypes (P. A. Smith, 2020).

Specifically, delayed rectifiers and KCNQ channels are associated with the development of pain. Delayed rectifiers maintain a sustained potassium ion efflux and are activated with delay following membrane depolarization (P. A. Smith, 2020). In the context of pain, the transcription of delayed rectifier channels decreases after nerve injury (Alles & Smith, 2021). In addition, the lack of Kv1.1 was demonstrated to be related to the development of mechanical allodynia (Hao et al., 2013). Also, Kv7.2 and 7.3, which are M channels product of KCNQ2/3 gene, play a crucial role in determining neuronal excitability and firing accommodation (Alles & Smith, 2021). Like delayed rectifiers, these channels activate upon depolarization but do not inactivate for minutes. Kv7.2 expression was found decreased after axotomy in the DRG, but it increased on fiber endings. This trafficking pattern seemed relevant for the behavioral development of pain, probably because it may facilitate excitability in the neuronal soma (Cisneros, Roza, Jackson, & López-García, 2015). Furthermore, mice lacking Kv7.2 expression exhibited increased neuronal excitability and pain-related behaviors (King, Lancaster, Salomon, Peles, & Scherer, 2014).

HCN channels

Hyperpolarization-activated and cyclic nucleotide-gated (HCN) channels work differently than classical voltage-gated channels. Specifically, HCN channels are closed during a depolarizing stimulus and open to membrane hyperpolarization, generating and inward current that regulates the membrane resting potential (Ramirez, Zuniga, Concha, & Zuniga, 2018). HCN channels have an enhanced activation and expression following nerve damage. Particularly, the increase of HCN1 and HCN2 subtypes appears critical for the generation of neuropathic pain (Chaplan et al., 2003; Emery, Young, Berrocoso, Chen, & McNaughton, 2011; Jiang et al., 2008).

3.4.2 Second-order neurons and central sensitization

Central sensitization refers to the enhanced responsiveness of the central nervous system to sensory inputs, resulting in an increased perception of pain. After peripheral nerve injury, there is a release of the excitatory neurotransmitter glutamate, as well as BDNF and neuropeptides (Substance P and CGRP), at the central synaptic terminals of primary afferents. These transmitters activate different receptors in the neurons of the dorsal horn, leading to enhanced excitability (Noguchi, 2006). Specifically, glutamate activates mGluR, AMPA and NMDA receptors. Substance P binds to the protein-coupled neurokinin 1 (NK1) receptor, and BDNF is detected by TrkB. Stimulation of mGluR and NK-1 receptors activate phospholipase C, which promotes calcium release from intracellular compartments. The increase of intracellular calcium levels can stimulate the activation of protein kinases, including PKC, PKA and CAMKII. In addition, TrkB receptor promotes the activation of the tyrosine kinase Scr, which along with the other kinases can phosphorylate AMPA and NMDA receptors. This phenomenon increases AMPA and NMDA receptor activity and promotes the recruitment of AMPA receptors to the post-synaptic membrane. Additionally, PKA and PKC lead to ERK activation, which subsequently triggers the inactivation of potassium channels. Moreover, post-synaptic increase of the Nav1.3 channel has also been detected in the dorsal horn of the spinal cord after PNI (Hains, Saab, Klein, Craner, & Waxman, 2004). Altogether, these changes favor excitability in the dorsal horn, amplifying pain perception (Noguchi, 2006; Toth, 2013) (see Figure 6).

While there is an increased activity of glutamate receptors, secondary neurons also become less responsive to the inhibitory regulation of GABA and Glycine due to changes in chloride

transporters (López-Álvarez et al 2015). In addition, injury-induced inflammation on central segments further raises excitability (Toth, 2013).

Neural plasticity also plays a role in central sensitization. Synaptic strengthening of nociceptive neurons occurs by long-term potentiation in the dorsal horn and the cingulate cortex (Ikeda, Heinke, Ruscheweyh, & Sandkuhler, 2003; Toyoda et al., 2009). Moreover, nerve injury can result in degeneration of C-fiber terminals in lamina II, mainly of non-peptidergic neurons (Casals-Diaz et al., 2009). This creates an opportunity for Aβ fibers to sprout into laminae I-II and establish contact with nociceptive neurons (Latremoliere & Woolf, 2009).

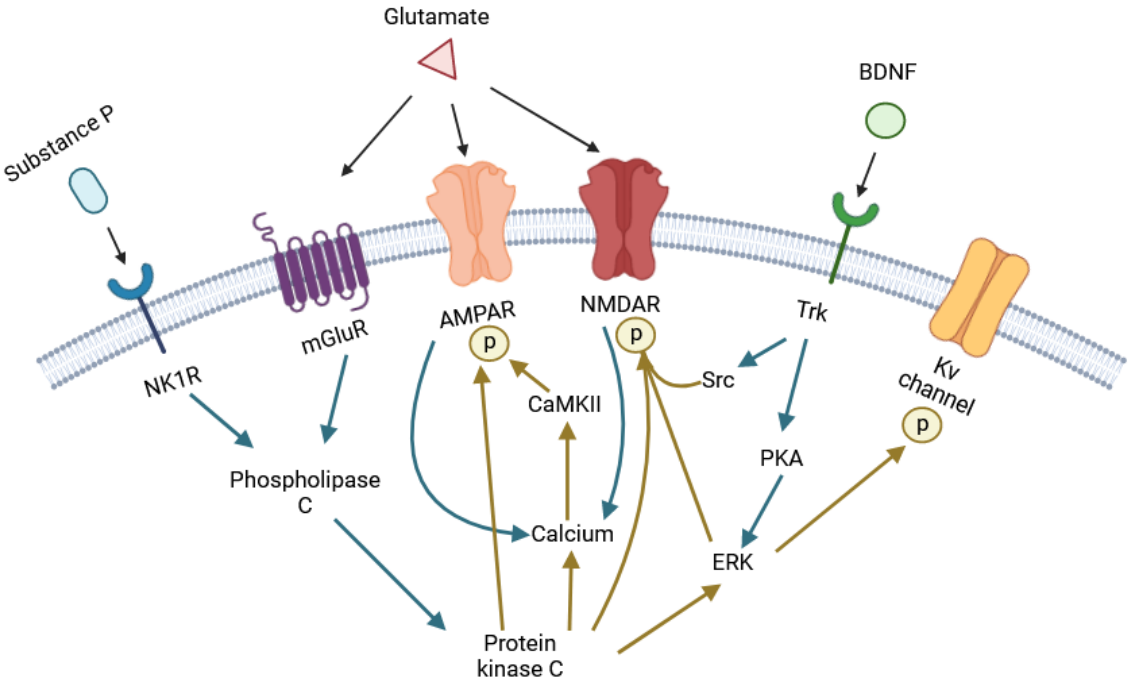

Figure 6: Molecular alterations in the dorsal horn of the spinal cord that are responsible for central sensitization. In blue are displayed the mechanisms that activate kinases and in yellow the consequences on the expression of glutamate receptors and ion channels. Modified from (Toth, 2013) using Biorender.

3.5 Inflammation and neuropathic pain

Injury to the somatosensory system initiates a cascade of inflammatory mechanisms, which can activate or sensitize nociceptors, triggering aberrant activity and leading to neuropathic pain both in the peripheral and in the central nervous system (Paul J. Austin & Moalem-Taylor, 2013).

3.5.1. Inflammation and peripheral sensitization

After injury, Schwann cells and macrophages secrete cytokines and growth factors that promote phenotypic changes in neurons (Ellis & Bennett, 2013; López-Álvarez, 2017; Toth, 2013). One example is COX-2, released by macrophages and Schwann cells after injury, which produces prostanglandin PGE2, that acts as a nociceptive sensitizer (Ma & Quirion, 2008; Toth, 2013). Moreover, nociceptive terminals release neuropeptides through the antidromic transmission of action potentials (Ellis & Bennett, 2013). For instance, the neuropeptide Substance P enhances the release of bradykinin, which sensitises nociceptors and increases the permeability of vasculature. Substance P also stimulates the secretion of histamine, a molecule associated with inflammation (Toth, 2013). CGRP also acts as a vasoactive peptide that promotes the recruitment of immune cells enhancing the inflammatory response. In this regard, pro-inflammatory cytokines, such as TNF-α, stimulate the p38-MAPK pathway, leading to increased sodium influx and subsequent neuronal depolarization (P. J. Austin & Moalem-Taylor, 2010).

3.5.2. Inflammation and central sensitization

Peripheral nerve injury leads to a transient alteration of the blood-spinal cord barrier integrity, facilitating the entry of infiltrating macrophages and T cells in the dorsal horn. These events further exacerbate the inflammatory environment inside the spinal cord (Clark, Old, & Malcangio, 2013).

Moreover, nerve injury triggers the activation of microglia and astrocytes. Activated microglia produce a wide range of neurotransmitters, cytokines, trophic factors, and reactive oxygen species (ROS) that can lead to neuronal sensitization. Importantly, microglial activity can produce neuronal death by generating high levels of ROS and by impairing glutamate uptake by glial cells. Astrocytes also undergo activation after injury and may play a role in the maintenance of neuropathic pain (Latremoliere & Woolf, 2009).

Notably, pro-inflammatory cytokines secreted by microglia and infiltrating cells are responsible for exacerbating neuronal excitability in the spinal cord. For instance, an *in vitro* path clamp study conducted in the dorsal horn of the spinal cord revealed that TNF-α and IL-1β enhanced AMPA and NMDA-induced excitatory currents. Conversely, IL-1β and IL-6 suppressed inhibitory currents in the dorsal horn (Y. Kawasaki, Zhang, Cheng, & Ji, 2008). Moreover, *In vivo* administration of TNF-α induced neuropathic pain behaviors, while genetic

impairment of IL-1β signaling reduced neuropathic pain in mice (Wagner & Myers, 1996; Wolf, Gabay, Tal, Yirmiya, & Shavit, 2006). Additionally, spinal downregulation of the pro-inflammatory cytokines IL-1β, TNF-α and IL-6 following LipoxinA_4 treatment prevented behavioral hypersensitivity following a chronic compression of the DRG (T. Sun et al., 2012). Although further investigation is needed to elucidate the mechanisms by which distinct cytokines influence excitability, the effects of TNF-α are relatively well-described. In fact, it has been reported that TNF-α decreased the expression of GLAST and EAAT2/GLT-1 glutamate transporters in astrocytes, impairing glutamate uptake (Korn, Magnus, & Jung, 2005; Sitcheran, Gupta, Fisher, & Baldwin, 2005). Consequently, increasing glutamate availability and triggering hyperexcitability in the spinal cord (P. J. Austin & Moalem-Taylor, 2010; Schafers & Sorkin, 2008).

Hence, inflammation and excitability are interconnected in the development of neuropathic pain. Specifically, the inflammatory reaction acts as a positive feedback mechanism triggering neuronal hyperexcitability. Thus, it is speculated that regulation of inflammation could alleviate neuropathic pain (Fonseca et al., 2019; Milligan, Penzkover, Soderquist, & Mahoney, 2012; Okutani, Yamanaka, Kobayashi, Okubo, & Noguchi, 2018).

4. Epigenetic interventions to improve functional outcome after nerve injury

4.1 Epigenetic modifications

Epigenetics studies the changes in gene expression that do not result from alterations in DNA sequence but by changing the structural arrangement of chromatin (Christopher, Kyle, & Katz, 2017; Hwang, Aromolaran, & Zukin, 2017). Epigenetic mechanisms use the DNA template to acquire stable programs, such as cell type identities, or to regulate gene expression in response to environmental alterations. The most well-known epigenetic mechanisms include DNA methylation, changes in nucleosome position, post-translational modifications, miRNA and lncRNAs.

4.1.1 DNA methylation

DNA can undergo methylation in some of their cytosine or adenosine nucleobases. Among these modifications, cytosine methylation is the most widespread DNA modification in

eukaryotes. The process of cytosine methylation is catalyzed by DNA methyltransferases (DNMTs), which facilitate the transference from S-adenosyl-L-methionine (SAM) to the fifth carbon of the cytosine, resulting in the production of 5-methylcytosine (Hwang et al., 2017).

Cytosine methylation in mammals takes place primarily on CpG islands, which are genomic regions rich in cytosine and guanine nucleotides. CpG islands are often found in gene promoters and in this situation, methylation is associated with gene repression. However, when cytosine methylation occurs in gene bodies is linked with active transcription. Nevertheless, neurons are an exception of this rule and methylation of cytosines and adenosines in neuronal cell bodies is associated with transcriptional repression (Christopher, Kyle, et al., 2017; Hwang et al., 2017). The establishment of CpG methylation is mediated de novo by DNMT3a and DNMT3b, whereas DNMT1 maintains the DNA methylation during replication on the daughter cells (Cheng, Song, Ming, & Weng, 2023). Outside of CpG islands methylation is recognized by MeCP2, which leads to gene repression in mature neurons (Cheng et al., 2023). Reversion of methylation generates several intermediates, with the initial intermediate of cytosine methylation (generated through hyrdroxymethylation) playing a role in gene activity. Aberrant patterns of DNA methylation and hyrdroxymethylation have been associated with different psychiatric disorders (Cheng et al., 2023).

4.1.2 Changes in nucleosome position

Canonical histones have variants that can replace the canonical form within nucleosomes. This substitution could erase or alter the pattern of post-translational modifications and have profound effects on nucleosome stability and positioning (Greer & Shi, 2012; Hwang et al., 2017). The alteration of histone variants has been found to have an impact on cognition (Hwang et al., 2017).

4.1.3 Post-translational histone modifications

Nucleosomes are considered the basic unit of chromatin. This structure is formed by histone octamers around which the DNA is wrapped. In turn, octamers are the result of combinations of the core histone proteins H2A, H2B, H3 and H4. Alterations in the structure of octamers can affect the exposure of chromatin, which influences future gene expression.

In this regard, histones can suffer post-translational modifications in their N-terminal tails, such as acetylation, methylation, phosphorylation and ubiquitylation among others. The post-

translational marks are added by a group of proteins named “writers” and deleted by enzymes named “erasers”. The resulting histone code can be recognized by a group of proteins known as “readers” that would detect the post-translational marks on distinct genomic regions (Christopher, Kyle, et al., 2017; Hwang et al., 2017). The most well-studied post-translational modifications include histone methylation and acetylation.

Histone acetylation

Histone acetylation relaxes the interaction between the DNA strands and the histones, leading to an open chromatin configuration that is easier to access for transcription. The attachment of acetyl groups to histones is performed by histone acetyltransferases (HATs), whereas histone deacetylases (HDACs) remove acetylated histone marks. These newly formed acetylations or deacetylations form a histone code which can be recognized by reader proteins that own specialized domains, examples of these are bromodomains and chromodomains (Wahane, Halawani, Zhou, & Zou, 2019). In the neurosciences, increased histone acetylation has been associated with memory consolidation and with the regulation of neuronal death after ischemia (Hwang et al., 2017). Well-known histone acetylation marks are displayed in the table below (Table 1).

Summary of common acetylation marks in histones

Histone modification	*Effects on gene expression*	*Location*	*Source*
H3K9ac	Activation	Promoters, enhancers	(Kumar et al., 2016)
H3K27ac	Activation	Enhancers, promoters	(Barral & Dejardin, 2023; Kumar et al., 2016)
H4K8ac	Activation	Promoters	(Z. Wang et al., 2008)
H4K16ac	Activation	Promoters, gene bodies	(Taylor, Eskeland, Hekimoglu-Balkan, Pradeepa, & Bickmore, 2013; Z. Wang et al., 2008)

Table 1: Common post-translational histone acetylation marks and their location.

Histone methylation

Alterations on histone methylation also affect the conformation of chromatin, although the effects in gene expression of this type of post-translational modification are more complex than acetylation. Histone methylation can occur in lysine, arginine and histidine residues. In this regard, lysine methylation has largely been studied, specifically in three distinct locations: histone 3 lysine 4 (H3K4), histone 3 lysine 9 (H3K9) and histone 3 lysine 27 (H3K27) (Greer & Shi, 2012). Notably, for each histone variant methylation is conducted by specific proteins.

H3K4 can be mono-, di- or trimethylated by MLL and SET family of writer proteins (Christopher, Kyle, et al., 2017). Each degree of methylation has a different outcome on gene expression. Hence, monomethylated H3K4 is found in enhancers and promoters at the 3' of active genes, facilitating gene transcription. H3K4me2 is usually found in gene bodies and enhancers that are linked with active genetic expression. Whereas H3K4me3 is found in promoters of both working and dormant genes (Greer & Shi, 2012). It is important to acknowledge that the same modifications can have opposing roles, such as repression and activation. This occurs with H3K4me2 and H3K4me3, that while they are usually linked to gene activation, they can also lead to gene repression. This phenomenon is probably mediated by readers that can recruit transcriptional machinery as well as repressor complexes. H3K4 methylation can be reversed by different demethylases: LSD1/KDM1A, LSD2/KDM1B, JARID1a/KDM5A and JARID1b/KDM5B, which facilitates the adaptation of gene expression under different conditions.

Contrarily to H3K4, di- and trimethylation of H3K9 promotes transcriptional repression. In H3K9, methylation is conducted by the methyltransferases SETDB1 and SUV39H1, while demethylation is executed by JHDM2A/KDM3A and LSD1. Finally, H3K27 usually undergoes trimethylation by PRC2 or EZH2, which can be erased by UTX/KDM6A and JMJ3/KDM6B. Specifically, trimethylation of H3K27 leads to genetic repression (Christopher, Kyle, et al., 2017; Greer & Shi, 2012) (Table 2).

Summary of common histone methylation marks			
Histone modification	*Effects on gene expression*	*Location*	*Source*
H3K4me1	Activation	Enhancers	(Barral & Dejardin, 2023; Greer & Shi, 2012)
H3K4me2	Activation/Repression	Gene bodies	(Greer & Shi, 2012)
H3K4me3	Activation or poised expression	Promoters	(Greer & Shi, 2012)
H3K9me2	Repression	Transposable elements, satellite repeats and gene bodies	(Padeken, Methot, & Gasser, 2022)
H3K9me3	Repression or poised expression	Enhancers, telomeres, transposable elements, gene bodies and satellite repeats	(Barral & Dejardin, 2023; Ninova, Fejes Toth, & Aravin, 2019; Padeken et al., 2022)
H3K27me3	Repression	Enhancers, promoters	(Barral & Dejardin, 2023)
H3K36me3	Activation	Gene bodies	(Z. Sun et al., 2020)

Table 2: Popular histone modifications and where to find them.

4.1.4 miRNA and lncRNA

Noncoding RNA can also serve as epigenetic regulators by recruiting other molecules that would catalyze alterations on the chromatin compaction. These transcripts vary in size, being miRNA composed by sequences under 25 nucleotides and lncRNA containing over 200 nucleotides. Particularly, lncRNA can act as a scaffold molecule. One example is the case of the HOTAIR transcript that binds both PRC2 and the LSD1-CoREST complex on H3K4me, resulting in gene repression (Tsai et al., 2010).

4.2 Epigenetic modifications involved in regeneration and neuropathic pain

Recent findings had started to elucidate the mechanisms that link epigenetic machinery with neuronal regeneration and pain. However, research still needs to fully unravel the epigenetic alterations that occur after nerve trauma. Hereof, understanding the

epigenetic mechanisms behind pain and regeneration is of utmost importance, as it has contributed to the development of new therapies to treat nerve injuries.

For instance, as histone acetylation promotes the expression of regeneration associated genes, facilitating axonal regeneration (Hutson et al., 2019; Puttagunta et al., 2014), histone deacetylase inhibitors (HDACi) have been used as a strategy to promote regeneration. Their application favored the conservation of histone marks, improving the outcome in studies conducted both *in vivo* and *in vitro* (Brugger et al., 2017; Finelli, Wong, & Zou, 2013).

In table 3 there is a list of post-translational modifications that occur after traumatic injuries of the nervous system , which have been linked with pain and regeneration.

Post-translational modifications linked with regeneration and pain

Enzyme	*Epigenetic modification*	*Gene expression*	*Altered genes/targets*	*Outcome and injury*	*Source*
PCAF	↑H3K9Ac	Activation	↑GAP43, Galanin and Bdnf	↑ Regeneration (nerve axotomy)	(Puttagunta et al., 2014)
CbP	↑H4K8Ac	Activation	Not described	↑ Regeneration (SCI)	(Hutson et al., 2019)
Unknown	↑H3K9me2	Repression	↓GAP43, Bdnf, SCG10 and Galanin	↓ Regeneration (nerve axotomy)	(Puttagunta et al., 2014)
REST	↓H3Ac and H4Ac	Repression	↓MOP, Nav1.8 and Kv4.3	↑Pain (PNL)	(Uchida, Ma, & Ueda, 2010; Uchida, Sasaki, Ma, & Ueda, 2010)
HDAC	↓H3Ac and H4Ac	Repression	↓ Gad65 and mGluR2	↑Pain (CCI)	(Penas & Navarro, 2018)
G9a	↑H3K9me2	Repression	↓ *Kcna4, Kcnd2, Kcnq2, Kcnma1*	↑Pain (SNL)	(Laumet et al., 2015)

Table 3: Summary of epigenetic modifications after traumatic injuries of the nervous system. In the table is displayed an enzyme, its effects on post-translational histone modifications, the genes or proteins altered and the outcome on regeneration and pain.

4.3 BET proteins as a target to reduce neuropathic pain and enhance nerve regeneration

The bromodomain and extra-terminal domain (BET) proteins are a family of epigenetic readers that bind to acetylated lysine residues found on both histone and non-histone proteins (Hajmirza et al., 2018). This protein family consists of four members BRD2, BRD3, BRD4 and BRDT. All BET proteins are localized within the nucleus. However, while the first three proteins are ubiquitously distributed in all cell types, BRDT is mainly located in germ cells (Morgado-Pascual, Rayego-Mateos, Tejedor, Suarez-Alvarez, & Ruiz-Ortega, 2019). Additionally, all members of the BET protein family share a common structure formed by two N-terminal bromodomains (BD1 and BD2) and an extra-terminal (ET) domain. Nevertheless, BRDT and BRD4 differ from the other members by owning a C-terminal domain (CTD) that promotes transcription elongator factor activity (Hajmirza et al., 2018; Liu, Yang, & Candelario-Jalil, 2021) (Figure 7).

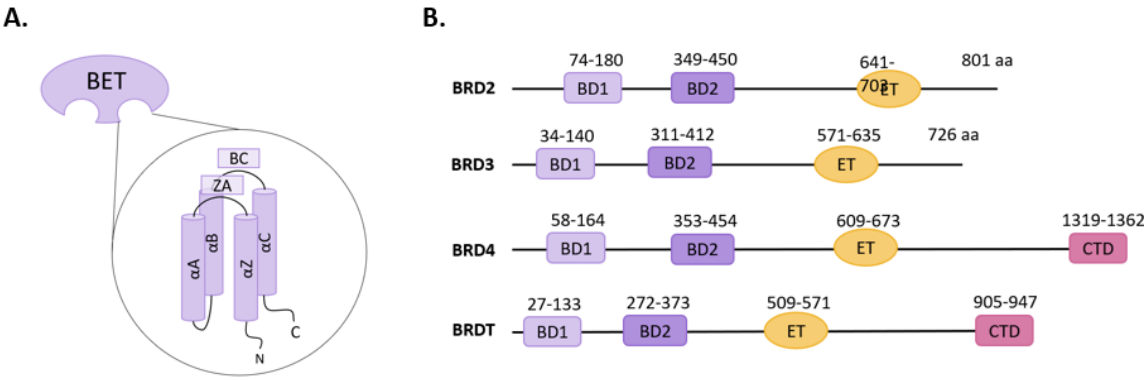

Figure 7: Structure of BET proteins. A) Conformation of the hydrophobic pockets BD1 and BD2. B) Subunits of the distinct bromodomain and extra-terminal domain family members. Modified from (Liu et al., 2021; Morgado-Pascual et al., 2019).

Concerning the structural domains of BET proteins, BD1 and BD2 are bromodomain modules conforming hydrophobic pockets that facilitate protein-protein interactions by binding to acetylated-lysine residues. Typically, bromodomain proteins recognize and bind to two acetylated-lysine marks, as their affinity with mono-acetylated lysine is weak (Filippakopoulos & Knapp, 2014; Hajmirza et al., 2018). These structural characteristics of the bromodomain pocket makes BET proteins an attractive target for drug development. Most BET inhibitors can bind both BD1 and BD2 domains, targeting all BET proteins. However, the affinity of these inhibitors is variable among the BET protein family members (Liu et al., 2021).

In general, the BD domain of BET proteins is typically involved in interacting with acetylated residues at gene promoters and enhancers, triggering the initiation of transcription. Additionally, the C-terminal ET domain has been described to establish protein-protein interactions, enabling BET proteins to recruit either activator or repressor complexes (Hajmirza et al., 2018).

4.3.1 BET protein-protein interactions and effects on gene expression

Most of the protein interactions studied in BET proteins have been focused on BRD4, which has provided insights into the mechanisms by which this epigenetic reader modulates gene expression. BRD4 participates in transcriptional elongation through its interaction with the pTEFb complex, which consists of the Cyclins T1 and T2 along with the protein CDK9. The kinase CDK9 inhibits negative regulators of RNA polymerase II and promotes transcriptional elongation through its phosphorylation (Figure 8B). The interaction between BRD4 and pTEFb complex occurs through the C-terminal region and the BD2 domain (Hajmirza et al., 2018; B. Huang, Yang, Zhou, Ozato, & Chen, 2009).

In addition, the ET domain of BRD4 is essential for mediating protein-protein interactions. In fact, the ET domain can interact with histone modifiers or chromatin remodelers, leading to structural changes in chromatin and the subsequent alterations in gene expression. Specifically, it has been reported that the ET domain of BRD4 has a high affinity with JMJD6, NSD3, CHD4, ATAD5 and GLTSCR1 (Figure 8A) (Rahman et al., 2011). In this regard, JMJD6 is an arginine demethylase, linked with carcinogenesis and the promotion of the immune response (K. Wang et al., 2022). ATAD5 functions as regulator of DNA repair (Giovannini et al., 2020). GLTSCR1 role is mostly unknown, but it has been observed to negatively regulate BRD4-induced elongation in cancer and it participates in SWI/NSF chromatin remodeler complexes (Alpsoy & Dykhuizen, 2018; F. Han et al., 2019). CHD4 belongs to the chromodomain helicase DNA-binding protein family, a group of ATP-dependent chromatin remodeling enzymes that modulate DNA accessibility. CHD4 interacts with the repressive complex NuRD and plays a role in hematopoietic cell differentiation, as well as in the proliferation and development of neural stem cells (Micucci, Sperry, & Martin, 2015; Nitarska et al., 2016). Lastly, NSD3 is a lysine methyltransferase targeting H3K36 and is associated to cancer progression. However, it has been described that a short isoform of NSD3 lacking the methyltransferase activity served as a link between CHD8 chromatin remodeler and BRD4 in leukemia cells (Shen et al.,

2015). Further, CHD8 has been reported to have both activator and repressor activities on gene expression (Hurley et al., 2021).

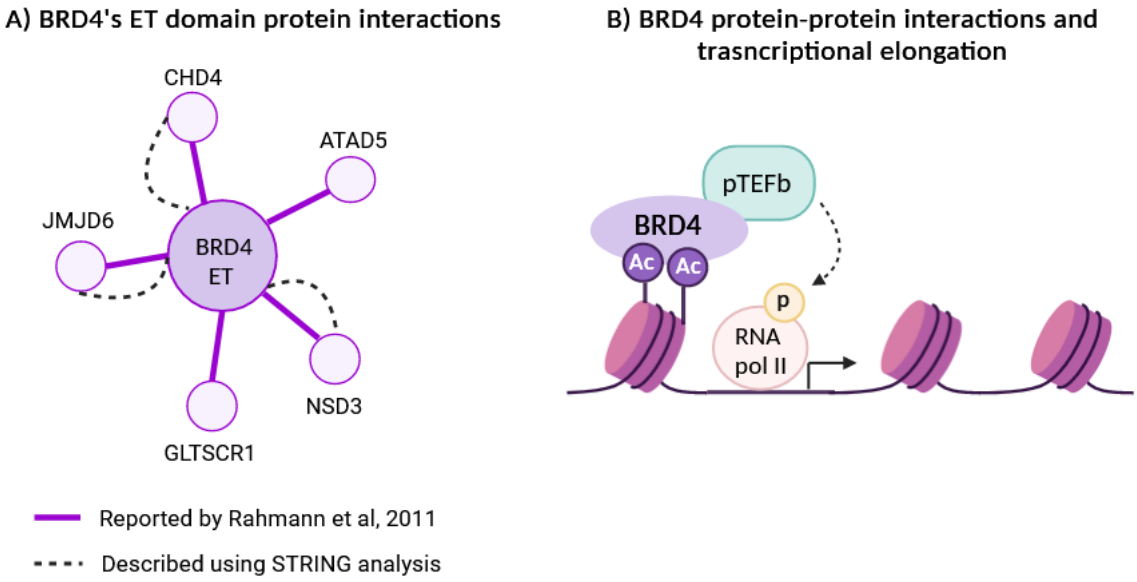

Figure 8: BRD4 relationship with other proteins. A) Interactions in the BRD4's ET domain described by Rahmann in human cell lines and the coincidences found using STRING analysis in mouse (highest confidence 0.9 and no more than 20 interactors as parameters) (Rahman et al., 2011). B) BRD4 interacts with the pTEFb complex for transcriptional elongation. The protein CDK9 from pTEFb complex phosphorylates the RNA polymerase II, guarantying transcriptional elongation. Created with BioRender.

4.3.2. Physiological role of BET proteins

BET proteins have diverse physiological functions as they are distributed in multiple organs throughout the body. These proteins participate in cancer, redox metabolism, inflammatory events, and neuronal activation (N. Wang, Wu, Tang, & Kang, 2021).

BET proteins in inflammation

The role of BET proteins in inflammation has been elucidated by studying the function of BRD4 in NF-Kβ signaling, a pathway responsible for the secretion of a wide array of cytokines and chemokines. In this regard, BRD4 interacts with the NF-Kβ subunit p65/RELA, which has been previously acetylated at its lysine 310 by p300/CBP. The interaction between BRD4 and the acetylated p65/RELA promotes the recruitment of the pTEFb complex, leading to transcriptional elongation of NF-Kβ target genes. Then, the kinase CDK9 from the pTEFb complex phosphorylates the RNA polymerase II, promoting transcriptional elongation (Hajmirza et al., 2018; B. Huang et al., 2009).

In addition, inhibition of BET proteins by I-BET762 in macrophages decreased the expression of several pro-inflammatory cytokines, including IL-1β, IFN1β, IL-6 and Cxcl9 (Nicodeme et al., 2010). Similarly, the use of a BET inhibitor known as JQ1, increased the transcription of the anti-inflammatory cytokines IL-4, IL-10 and IL-13, while decreasing pro-inflammatory mediators both after spinal cord injury and *in vitro* using macrophages (Sanchez-Ventura, Amo-Aparicio, Navarro, & Penas, 2019). Altogether, these findings highlight the role of BET proteins in the modulation of inflammation. However, the mechanism by which BET inhibition promotes anti-inflammatory cytokine transcription remains unknown. Additionally, it is worth noting that although BRD4 has been linked with the NF-Kβ pathway, BRD2 and BRD3 silencing has also been found to reduce pro-inflammatory cytokine expression in macrophages (Belkina, Nikolajczyk, & Denis, 2013).

BET proteins in neuronal activation and neuroprotection

Research assessing the role of BET proteins in the nervous system has been mainly focused on memory and cognitive disorders. However, the effects of BET proteins in axonal regeneration are still unknown.

Current studies have elucidated that BET proteins are implicated in the expression of early neuronal genes. In fact, it has been observed that BET-inhibition using JQ1 reduced the expression of the immediate early genes *Arc*, *Fos* and *Nr4a1* in cortical neuron culture (Korb, Herre, Zucker-Scharff, Darnell, & Allis, 2015). Another study showed that while immediate early genes were decreased after 30 minutes of JQ1 treatment, genes linked with long-term potentiation (LTP), *cFos,* and *JunB*, were enhanced after 24h of BET-inhibition (Benito et al., 2017).

In addition, BET inhibition with JQ1 has improved the outcome to seizures, due to a reduction on the expression of GluA1, an AMPA subunit channel (Korb et al., 2015). Altogether, suggesting an interaction between BET proteins and excitability. This possible causality has been observed in various sequencing studies, where BET-inhibition downregulated the expression of gated ion channels (Benito et al., 2017; Korb et al., 2015). In accordance with the sequencing experiments, a study conducted in rats subjected to inflammatory pain observed increased expression of BRD4 and Nav1.7 in the DRG. Pain was reversed after using siRNA against BRD4, which decreased the expression of Nav1.7 (Hsieh et al., 2017). Therefore,

suggesting that BET proteins act as a link between the inflammatory environment and the expression of sodium channels (Hsieh et al., 2017).

It has also been reported that BET protein inhibition with JQ1 enhances neuroprotection and myelin preservation in animals subjected to spinal cord injury (Sanchez-Ventura et al., 2019). In fact, the BET protein member BRD4 has been found to be a key modulator of apoptosis, pyroptosis and other types of cell death. Although BET inhibitors have been used to prevent cell cycle progression and promote the death of anomalous cancer cells, it has also been observed that under certain conditions BRD4 inhibition avoid apoptosis of non-transformed cells in some pathological conditions (Hu, Pan, Li, Chen, & Hu, 2022). In line with these findings, another study found that BRD4 inhibition with JQ1 ameliorated inflammatory pain, by preventing NF-Kβ inflammasome formation and protecting neuronal cells from pyroptosis (Hua et al., 2022).

In conclusion, BET proteins seem to have a role mediating neuroinflammation, excitability and neuronal survival. Therefore, we hypothesized that they could be suitable targets to improve outcome after nerve injury by preventing pain and promoting neuronal preservation.

4.4 LSD1 as a target to enhance nerve regeneration

Lysine-specific demethylase 1A (LSD1), also known as KDM1A, is an enzyme consisting of 852 amino acids that performs demethylation of lysine residues in histones. It belongs to the superfamily of flavin-dependent monoamine oxidases and the family of lysine-specific demethylases (LSD) (Perillo, Tramontano, Pezone, & Migliaccio, 2020). The LSD and the Jumonji family, are the two most known families of histone demethylases (Hayward & Cole, 2016; Perillo et al., 2020). Additionally, LSD1 shares structural and functional similarities with its homolog LSD2, displaying 30% sequence homology (Perillo et al., 2020).

LSD1 demethylates both mono- and di-methylated forms of Histone 3 lysine 4 (H3K4) and Histone 3 lysine 9 (H3K9) (Maiques-Diaz & Somervaille, 2016; Perillo et al., 2020). The interaction between LSD1 and these methylated histone marks is crucial, as the distinct degrees of methylation in H3K4 and H3K9 play pivotal roles in regulating gene expression. H3K9me2 is a mark associated to gene repression, indicating that LSD1-mediated demethylation can promote gene expression in the previously repressed genes. Contrary,

H3K4 methylation has been classically related to activated gene expression, indicating that demethylation of H3K4me1/2 by LSD1 represses gene transcription (see Figure 9).

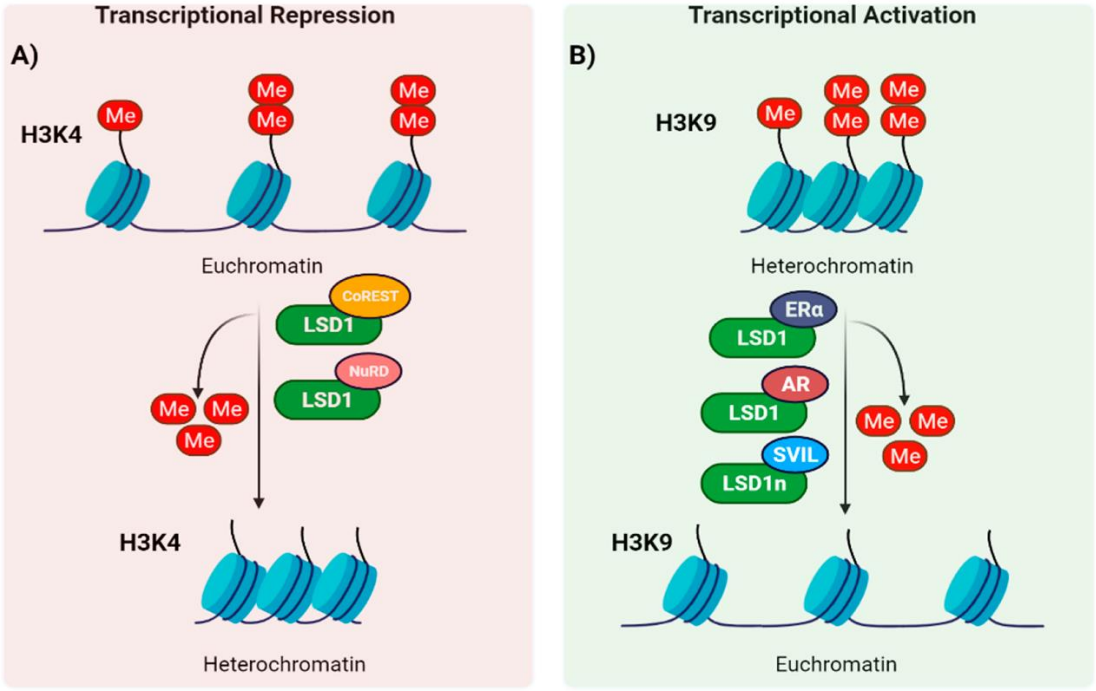

Figure 9: Transcriptional regulation of DNA by the post-translational modifications mediated by LSD1. A) LSD1 can interact with several proteins or complexes, being the most studied CoREST and NuRD, leading to H3K4me2/H3K4me1 demethylation and transcriptional repression. B) H3K9me2/me1 demethylation leads to gene expression. It is regulated by LSD1 along with ERα or AR and by the neural specific isoform LSD1n with SVIL. The LSD1n isoform can target H4K20 methylation but is not displayed in the figure. Extracted from (Martinez-Gamero, Malla, & Aguilo, 2021).

However, H3K4me2 can exhibit diverse effects on transcription and may act as a repressor in certain circumstances. Additionally, H3K4me is also linked to primed enhancers (Christopher, Kyle, et al., 2017; Greer & Shi, 2012; Perillo et al., 2020). Therefore, although it is generally associated with repression, the role of LSD1 in H3K4 should be carefully analyzed to better understand its functional implications in different biological contexts. Moreover, LSD1 is well known to mediate some of its actions by interaction with the repressive complex REST/CoREST (Perillo et al., 2020), the NuRD complex or the MLL coactivator complex (Maiques-Diaz & Somervaille, 2016) (Figure 9).

4.3.1. Physiological roles of LSD1

LSD1 is ubiquitously expressed in the nucleolus of multiple cell types, and it is involved in a diverse range of cellular processes related with the control of cellular differentiation and

homeostasis. These two characteristics imply that alterations on the expression of this enzyme are critical for determining cellular fate and influencing cancer progression.

LSD1 in axonal regeneration

LSD1 is a key regulator of the expression of neuronal genes and the acquisition of neuronal fate, through its interplay with the REST/CoREST complex. In progenitor cells, REST recruits the LSD1-CoREST and HDAC1/2 complex at the promoters of neuronal genes, thereby maintaining a repressed state. Upon differentiation to a neuronal fate the REST complex is degraded, whereas in the commitment to a non-neuronal lineage the integrity of the REST complex is preserved (Ballas, Grunseich, Lu, Speh, & Mandel, 2005; Lunyak et al., 2002; Maiques-Diaz & Somervaille, 2016).

Additionally, LSD1 can be found in four isoforms generated through alterative splicing. These variants depend on the inclusion of the exons E2a and E8a, resulting in the formation of: LSD1, LSD1+2a, LSD1+8a and LSD1+2a+8a. The isoform containing the inclusion of the exon E8a is exclusive of neurons and has also been named LSD1n, whereas LSD1 and LSD1+2a are ubiquitously expressed in several tissues.

LSD1n is implicated in regulating neural differentiation and neurite outgrowth (Zibetti et al., 2010). Functionally, LSD1n lacks H3K4 demethylase activity but acts as a transcriptional activator by promoting H3K9me2 demethylation and H4K20me2/me1 demethylation (Laurent et al., 2015; J. Wang et al., 2015). It is important to note that H3K9me2 is a repressive histone mark, which is downregulated in several RAGs after nerve axotomy. Specifically, the expression of H3K9me2 is inversely correlated with *GAP43, Bdnf, SGC10* and *Galanin* transcription (Puttagunta et al., 2014). Thus, it is possible that demethylation of H3K9me2, mediated by the LSD1n isoform, could promote the expression of certain RAGs. In addition, it has also been proposed that H4K20me2/me1 demethylation may be associated with the expression of early neuronal genes (J. Wang et al., 2015). Nevertheless, the function of LSD1n is dependent on its phosphorylation state at Thr369bAsp. Specifically, phosphorylation of LSD1n is crucial for neuronal arborization and paradoxically represses the LSD1n canonical form (Toffolo et al., 2014).

Additionally, studies that used pharmacological strategies that targeted global LSD1 inhibition described neuroprotection in mouse models of amyotrophic lateral sclerosis (ALS) and spinal

cord injury (Choi et al., 2022; Gu et al., 2021). It has also been reported the upregulation of genes related to plasticity when used as a treatment in a mouse model of Alzheimer's disease (Maes et al., 2020).

LSD1 in inflammation

LSD1 has also been reported to participate in inflammation. In this regard, the NF-Kβ axis depends on the protein p65/RELA for the transcription of pro-inflammatory genes. However, when the p65/RELA is methylated by the methyltransferase SET7/9 it undergoes degradation. Recent findings have shown that LSD1 can maintain the p65/RELA demethylated leading to sustained NF-Kβ expression (D. Kim et al., 2018). Furthermore, administration of GSK-LSD1, an LSD1 inhibitor, resulted in a reduction of the immune response in peripheral blood mononuclear cells from patients with COVID-19 (Hong et al., 2020).

Thus, considering its involvement in the regulation of neuronal differentiation and plasticity, LSD1 could be a promising target for enhancing axonal regeneration. However, since LSD1 also affects the inflammatory environment, it would be also indispensable to determine the effects of targeting LSD1 on the infiltration of macrophages and the proper development of Wallerian degeneration. Provided that these events could also affect axonal growth and functional recovery after a neural injury.

Hypotheses

Hypotheses

Efforts have been made to decipher novel targets to enhance nerve regeneration and reduce neuropathic pain after nerve injury, without much success in the clinical application. Although epigenetics is an emerging field in biomedicine with high therapeutic potential, little research has focused on the use of epigenetic targets after traumatic nerve lesions. In the present Thesis we propose the use of LSD1 and BET proteins as therapeutic targets after nerve injury. In this regard, both proteins are related with neuronal function and neuroinflammation, making them potential candidates to improve functional outcome.

Thus, the general hypotheses are:

Hypothesis 1: BET protein inhibition decreases the expression of pro-inflammatory mediators, while increasing the transcription of anti-inflammatory cytokines. Therefore, we hypothesize that BET protein inhibition may ameliorate pain and improve functional outcome after nerve injury, by accelerating the course of Wallerian degeneration and subsequently enhancing axonal regeneration.

Hypothesis 2: LSD1 inhibition has been previously observed to promote neuroprotection and to influence neuroplasticity. Thus, we hypothesize that LSD1 inhibition will positively affect neurite outgrowth and promote nerve regeneration after nerve injury.

Objectives

Objectives

The main aim of this Thesis is to assess if BET proteins and LSD1 are suitable targets to treat nerve injury. To address this objective, the Thesis has been divided in four chapters with the following specific objectives:

Chapter 1: Nerve excitability and neuropathic pain is reduced by BET protein inhibition after spared nerve injury.

- To determine the consequences of BET inhibition on neural excitability and inflammation *in vivo* after spared nerve injury (SNI).
- To address the therapeutic effect of the BET inhibitor JQ1 on neuropathic pain after SNI.

Chapter 2: BET protein inhibition in macrophages enhances dorsal root ganglion axonal regeneration.

- To ascertain the effects of the BET inhibitor JQ1 on neurite outgrowth *in vitro* and on axonal regeneration *in vivo* after nerve injury.
- To analyze the effects of conditioned media from BET-inhibited macrophages on neurite outgrowth *in vitro*.

Chapter 3: BRD4 prevents anti-inflammatory cytokine transcription in macrophages by binding to their promoters.

- To evaluate the cytokine profile of BET-inhibited primary macrophages.
- To decipher the mechanism by which BET proteins modulate anti-inflammatory cytokine transcription *in vitro*.

Chapter 4: Influence of LSD1 on neurite outgrowth and nerve regeneration.

- To assess the effects of the LSD1 inhibitor RN-1 on neurite outgrowth *in vitro*.
- To determine the consequences of LSD1 inhibition on axonal degeneration after nerve injury.
- To validate the therapeutic effects of RN-1 after peripheral nerve injury *in vivo*.

Experimental design

Methodology and experimental design

The goal of this section is to summarize the methodologies applied in this doctoral thesis to contextualize how the objectives of each chapter will be addressed. Detailed information of each technical procedure can be found in the results section.

Considerations

Although most experimental techniques have been performed by the author of this thesis, Dr. Jordi Badia has collaborated with our research to perform the excitability recordings of Sensory Compound Nerve Action potentials (SNAP) using the QTRAC system (Windows QTRAC v1.0.0; version 23.05.2017, Institute of Neurology, London, UK) providing the electrophysiological data of chapter 1.

Summary of the experimental design

Chapter 1: Nerve excitability and neuropathic pain is reduced by BET protein inhibition after spared nerve injury

In this chapter we aimed to decipher the potential therapeutic effects of BET-inhibition for reducing neuropathic pain after nerve injury. For this purpose, two distinct experiments were set up. In the first experiment, animals were subjected to spared nerve injury (SNI) and treated with the BET inhibitor JQ1 or vehicle. Excitability was assessed by electrophysiological recordings of Sensory Compound Nerve Action potentials (SNAP) and neuropathic pain was determined by mechanical (Randal-Selitto test) and thermal algesimetries (Hargreaves test) at different time-points after injury. At the end of this long-term experiment, spinal cord samples were collected to assess immune cell activity and C-fiber remodeling. In the second experiment, we investigated the molecular pathways that could be involved in the effects produced by the treatment with JQ1. For this purpose, transcriptional alterations of inflammatory markers and ion channels were analyzed at different time points after the injury in L5-L6 DRGs of vehicle or JQ1-treated animals (see Table 4).

Chapter 1: *In vivo* experiments

<table>
<tr><td colspan="3">Long-term in vivo assay: behavioral and histological analysis</td></tr>
<tr><td>Animal model</td><td>Experimental design</td><td>Molecular and functional tests</td></tr>
<tr><td> 
C57BL6/J mouse</td><td> 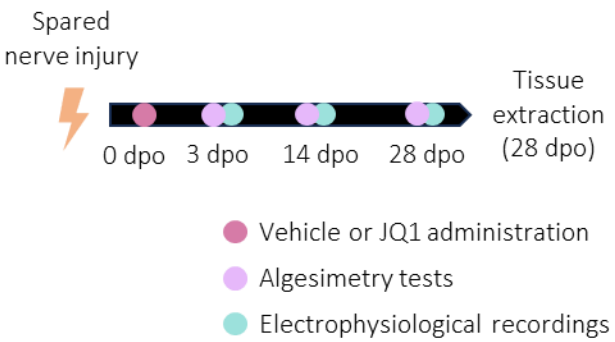 </td><td>Electrophysiological recordings

Algesimetry tests: Randal- Selitto and Hargreaves test

Immunofluorescence (IF) against Iba1, CGRP and IB4 in sections of the spinal cord</td></tr>
<tr><td colspan="3">Long-term in vivo assay: Transcriptional profile of ion channels and inflammation</td></tr>
<tr><td>Animal model</td><td>Experimental design</td><td>Molecular and functional tests</td></tr>
<tr><td> 
C57BL6/J mouse</td><td> 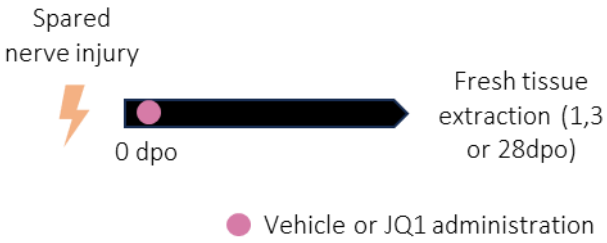 </td><td>Transcriptional analysis of ion channels and inflammatory markers (qPCR)</td></tr>
</table>

Table 4: Experimental design of Chapter 1. In the behavioral and electrophysiological assays, a total of n=5-7 mice per group were used. In this first experiment, tissue extraction was performed after mice perfusion with 4% paraformaldehyde for further histological assessment. Regarding the transcriptional profile of ion channels and markers of inflammation, a total n=3-5 animals per condition were utilized. Fresh tissue was extracted from L5 and L6 dorsal root ganglion (DRG) for further transcriptional characterization. DMSO or JQ1 30 mg/Kg/day were administered intraperitoneally (IP) 2 hours after surgery and daily afterwards in both experimental procedures. Non-injured controls were also included in the immunohistochemical and transcriptional experiments.

Chapter 2: BET protein inhibition in macrophages enhances dorsal root ganglion neurite outgrowth in female mice

In this chapter we wanted to determine the consequences of BET inhibition in neurite growth and nerve regeneration. For this reason, we performed five sets of experiments on *in vitro* and *in vivo* models. First, we realized an *in vivo* short-term study to determine the most appropriate time point of administration of JQ1 after sciatic crush injury in mice. Next, we carried out a long-term experiment to assess motor and sensory reinnervation in animals that underwent sciatic crush injury and treatment with vehicle or JQ1 (see Table 5). Regarding the *in vitro* studies, we determined the effects of JQ1 on neurite outgrowth of DRG explants and assessed neuronal toxicity through an MTT assay. We also analyzed the effects of conditioned media from BET-inhibited macrophages on neurite growth of DRG explants. Finally, we determined the pathway by which BET-inhibited macrophages were promoting neurite outgrowth on DRGs (Table 6).

Chapter 2: *In vivo* assays

<table>
<tr><td colspan="3">Short -term in vivo study: determination of the time point of JQ1 administration</td></tr>
<tr><td>Animal model</td><td>Experimental design</td><td>Molecular and functional tests</td></tr>
<tr><td> 
C57BL6/J mouse</td><td> 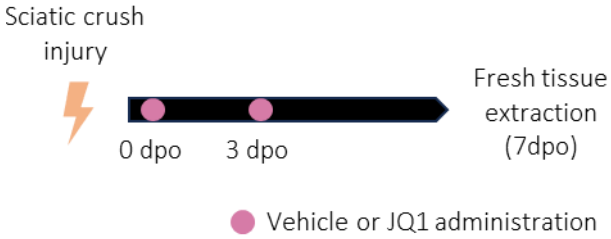 </td><td>Transcriptional analysis (qPCR)</td></tr>
<tr><td colspan="3">Long-term in vivo experiment: assessment of motor and cutaneous reinnervation</td></tr>
<tr><td>Animal model</td><td>Experimental design</td><td>Molecular and functional tests</td></tr>
<tr><td> 
C57BL6/J mouse</td><td> 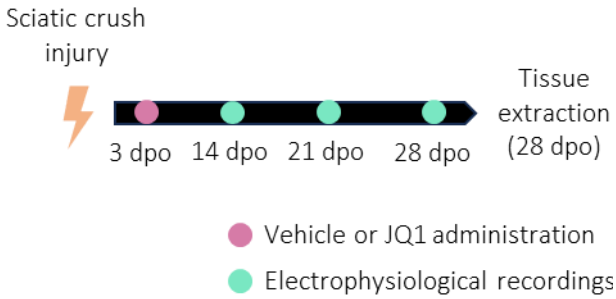 </td><td>CMAP of TA and plantar muscles (Muscle reinnervation)

IF of mouse hind paw pads against PGP 9.5 (Skin reinnervation)</td></tr>
</table>

Table 5: Experimental design of the *in vivo* procedures of chapter 2. In the short-term study n=3-4 mice per condition were used. JQ1 at 30mg/Kg/day or DMSO were administered IP from 2 hours (0 dpo) or 3 days (3 dpo) after injury. At the end of the experiment, the sciatic nerve was extracted for transcriptional analysis. In the long-term study, n=5 animals per condition were tested by nerve conduction studies to record reinnervation, evidenced by the compound muscle action potential (CMAP) of tibialis anterior (TA) and interosseus plantar muscles. Samples were extracted at the endpoint after paraformaldehyde (PFA) perfusion for histological assessment through immunofluorescence (IF) of the skin innervation. In the long-term assessment, treatment begun 3 days after surgery, consisting of DMSO or JQ1 30 mg/Kg/day IP.

Chapter 2: *In vitro* assays

<table>
<tr><td colspan="3">Neurite outgrowth of DRG explants under JQ1 treatment</td></tr>
<tr><td>Animal model</td><td>Experimental design</td><td>Molecular analysis</td></tr>
<tr><td> 
C57BL6/J mouse</td><td>DRG explant culture
 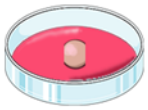
+
48h treatment
DMSO
500 nM JQ1
1000 nM JQ1</td><td>IF against neurofilament heavy chain (NF-H) and neurite length measurements</td></tr>
<tr><td colspan="3">Neuronal viability after JQ1 treatment</td></tr>
<tr><td>Animal model</td><td>Experimental design</td><td>Molecular analysis</td></tr>
<tr><td> 
C57BL6/J mouse</td><td>DRG primary dissociated culture
 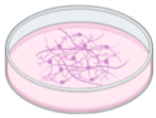
+
48h treatment
DMSO
500 nM JQ1
1000 nM JQ1
5µg cisplatin</td><td>MTT assay</td></tr>
<tr><td colspan="3">Effects of conditioned media from BET-inhibited macrophages on neurite outgrowth and detection of growth associated pathways</td></tr>
<tr><td>Animal model</td><td>Experimental design</td><td>Molecular analysis</td></tr>
<tr><td> 
C57BL6/J mouse</td><td>BMDM conditioned medium
DRG explant culture
 
6h treatment: DMSO or 1 µM JQ1
48h treatment: DMSO or 0,5 µM JQ1</td><td>IF against NF-H and neurite length measurements
WB against STAT3 and STAT6 pathways</td></tr>
</table>

Table 6: Experimental design of the *in vitro* experiments of chapter 2. In the study of the influence of JQ1 in neurite outgrowth, DRG explants were cultured 2 days with different doses of JQ1 or vehicle, prior to fixation and histological analysis. A total n=3 independent cultures were used in this assay. For determining neuronal viability, DRG dissociated cells were left for 2 days in culture before the addition of DMSO, JQ1 or cisplatin (positive control for cell death). MTT viability assay was performed 2 days after treatment. A total of n=5 independent cultures were used in this experiment. For determining the effects of conditioned media from BET-inhibited macrophages on neurite outgrowth, bone marrow-derived macrophages (BMDMs) were differentiated for 10 days and treated 6h with JQ1 or DMSO. Medium from BMDMs was then concentrated and added to DRG explants in culture. DMSO or JQ1 was also added to the DRG explants. The culture was fixed 2 days after treatment or snap frozen for protein analysis. A total of 3 independent cultures were used in this assay.

Chapter 3: BRD4 prevents anti-inflammatory cytokine transcription in macrophages by binding to their promoters

To elucidate the pathway by which BET protein inhibition increases anti-inflammatory cytokine transcription four sets of experiments were carried out. Firstly, we assessed the cytokine profile of BET-inhibited macrophages to corroborate the changes that JQ1 produces in anti-inflammatory cytokine expression, previously observed in our laboratory. Next, we assessed if the BET protein BRD4 and the co-repressor candidates CHD4 and CHD8 could be preventing the transcription of anti-inflammatory cytokines. To address this issue, we performed a knockdown of the three repressor candidates in macrophages and analyzed their effects on anti-inflammatory cytokine expression. Then, we assessed if BRD4 knockdown could have some deleterious effects on macrophage viability. Finally, we performed a ChIP-qPCR to determine if in physiological conditions the repressor complex binds to promoters of anti-inflammatory cytokines (see Table 7).

Chapter 3: *in vitro* experiments

<table>
<tr><td colspan="3">Cytokine profile from bone marrow derived macrophages (BMDM) primary culture</td></tr>
<tr><td>Animal model</td><td>Experimental design</td><td>Molecular analysis</td></tr>
<tr><td> 
C57BL6/J mouse</td><td> 
BMDM culture
+
6h treatment
DMSO
DMSO + LPS (100ng/mL)
1000nM JQ1
1000nM JQ1+LPS (100 ng/mL)</td><td>Transcriptional profile (qPCR)

Protein analysis (Luminex)</td></tr>
<tr><td colspan="3">Assessment of the repressor candidates</td></tr>
<tr><td>Animal model</td><td>Experimental design</td><td>Molecular analysis</td></tr>
<tr><td> 
C57BL6/J mouse</td><td>BMDM culture
 
Accel siRNA delivery
Control siRNA
BRD4 siRNA
Electroporation
Control siRNA
CHD4 siRNA
CHD8 siRNA
  </td><td>Knockdown validation and transcriptional analysis (qPCR)</td></tr>
<tr><td colspan="3">Consequences of BRD4 knockdown on macrophage survival</td></tr>
<tr><td>Animal model</td><td>Experimental design</td><td>Molecular analysis</td></tr>
<tr><td> 
C57BL6/J mouse</td><td>BMDM culture
 
Untreated
Control siRNA
BRD4 siRNA
No M-CSF
Accel siRNA delivery</td><td>MTT assay</td></tr>
<tr><td colspan="3">Repressor-promoter binding assay</td></tr>
<tr><td>Animal model</td><td>Experimental design</td><td>Molecular analysis</td></tr>
<tr><td> 
C57BL6/J mouse</td><td>BMDM culture
 
1h DMSO or 1000nM JQ1
Chromatin immunoprecipitation
 
Antibodies
IgG
CHD4
BRD4</td><td>qPCR from ChIP assay</td></tr>
</table>

Table 7: Experimental design of chapter 3. In all studies macrophages were differentiated 10 days before treatment. A total of n=4 independent cultures were set for the cytokine profile and cell viability studies. For the knockdown experiments of the repressor candidates CHD4 and CHD8, a total of n=3 independent cultures were used. Knockdown of CHD8 and CHD4 was performed by siRNA transfection through electroporation at 10 days *in vitro* (div) and cells were snap-frozen at 13 div. In the case of BRD4, Accel siRNA delivery was used within a total of n=4 independent cultures. BMDMs were transfected at 10 div and cells harvested at 14 div. For the repressor-promoter experiments, a total of n=3 independent cultures were analyzed through qPCR for IL-13, and n=2 independent cultures for IL-4.

Chapter 4: Influence of LSD1 on neurite outgrowth and axonal regeneration

The aim of this chapter was to assess the effects of LSD1 inhibition on neurite outgrowth and axonal regeneration after nerve injury. First, *in vitro* neuronal survival and neurite outgrowth of DRGs were analyzed under the influence of the LSD1 inhibitor RN-1 at variable concentrations (see Table 8). Next, a short-term *in vivo* study was conducted to determine the most adequate time point of administration of the compound after sciatic crush injury. Validation of target engagement of RN-1 was carried out by analyzing histone methylation of H3K4 using samples from the short-term study. Then, a long-term *in vivo* experiment was conducted to determine the influence of RN-1 on cutaneous and muscular reinnervation after sciatic nerve crush injury. Finally, a short-term test was performed to assess the effects of RN-1 on the development of Wallerian degeneration after crush injury (Table 9).

Chapter 4: *In vitro* assays

<table>
<tr><td colspan="3">RN-1 effects on neurite outgrowth of DRG explants</td></tr>
<tr><td>Animal model</td><td>Experimental design</td><td>Molecular analysis</td></tr>
<tr><td> 
C57BL6/J mouse</td><td>DRG explant culture
 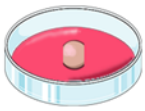
+
48h treatment
DMSO
500 nM RN-1
1000 nM RN-1
2000 nM RN-1</td><td>IF against NF-H and neurite length measurements</td></tr>
<tr><td colspan="3">Impact of RN-1 on neuronal survival</td></tr>
<tr><td>Animal model</td><td>Experimental design</td><td>Molecular analysis</td></tr>
<tr><td> 
C57BL6/J mouse</td><td>DRG primary dissociated culture
 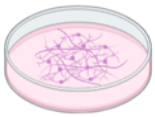
+
48h treatment
DMSO
500 nM RN-1
2000 nM RN-1
5µg cisplatin</td><td>MTT assay</td></tr>
</table>

Table 8: *In vitro* experiments of chapter 4. For assessing neurite outgrowth, DRGs were treated with different concentrations of RN-1 or vehicle, for 2 days and then fixed for immunohistochemical analysis. A total of n=3 independent cultures were performed. For the viability assay, dissociated DRGs were maintained 2 days in vitro before adding DMSO, RN-1 or cisplatin. MTT assay was performed 48 hours after treatment. A total of n=4 independent cultures was performed.

Chapter 4: *In vivo* assays

<table>
<tr><td colspan="3">Short-term regeneration study: determination of the time point of RN-1 treatment</td></tr>
<tr><td>Animal model</td><td>Experimental design</td><td>Molecular and functional tests</td></tr>
<tr><td> 
C57BL6/J mouse</td><td> 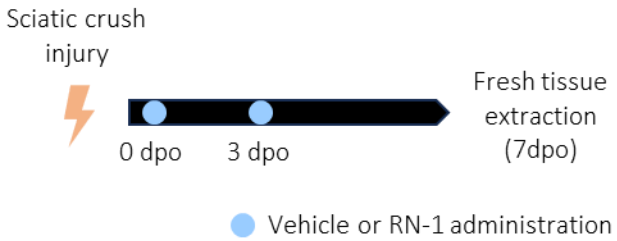 </td><td>Transcriptional analysis (qPCR)

Histone methylation assay</td></tr>
<tr><td colspan="3">Long term regeneration experiment: cutaneous and motor reinnervation assessment</td></tr>
<tr><td>Animal model</td><td>Experimental design</td><td>Molecular and functional tests</td></tr>
<tr><td> 
C57BL6/J mouse</td><td> 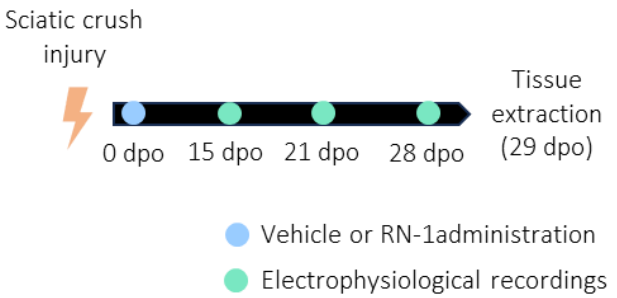 </td><td>CMAP of TA and plantar muscles (Motor reinnervation)

IF of hind paw pads against PGP 9.5 (Skin reinnervation)</td></tr>
<tr><td colspan="3">Short-term degeneration experiment: Effects of RN-1 on Wallerian degeneration</td></tr>
<tr><td>Animal model</td><td>Experimental design</td><td>Molecular and functional tests</td></tr>
<tr><td> 
C57BL6/J mouse</td><td> 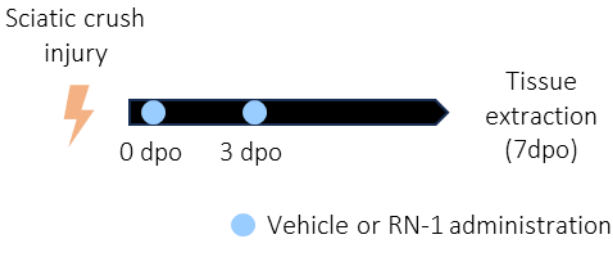 </td><td>Luxol fast blue staining</td></tr>
</table>

Table 9: *In vivo* experimental design of chapter 9. For the short-term regeneration study, animals underwent sciatic crush injury and were administered with DMSO or RN-1 1,52 mg/Kg/day IP, starting at different time points after injury. Fresh tissue from sciatic nerve, L4-L6 DRGs and spinal cord was collected for analyses. N=3-5 animals per group. In the long-term regeneration assay, animals were subjected to sciatic crush injury, treated 2h after operation and daily afterwards. Compound Muscle Action Potential (CMAP) electrophysiological recordings from tibialis anterior (TA) and plantar muscles were performed. At

the endpoint, animals were perfused, and tissue was extracted to study skin reinnervation through immunofluorescence (IF) staining against PGP9.5. N=7 animals per group were used in this study. For the degeneration study, animals underwent sciatic crush injury. RN-1 treatment begun 2 hours after surgery or at 3 dpo, followed by daily administration afterwards. At the endpoint, sciatic nerves were collected for histological assessment with luxol fast blue staining. N=4-5 mice for condition. Non-injured controls were also included in all the *in vivo* assays.

Scientific contributions

Scientific contributions

Chapter 1 and chapter 2 have resulted in the following publications before the presentation of this thesis:

- **Chapter 1:** Palomés-Borrajo G, Badia J, Navarro X, Penas C. Nerve Excitability and Neuropathic Pain is Reduced by BET Protein Inhibition After Spared Nerve Injury. J Pain. 2021 Dec;22(12):1617-1630. doi: 10.1016/j.jpain.2021.05.005. Epub 2021 Jun 19. PMID: 34157407.
- **Chapter 2:** Palomés-Borrajo G, Navarro X, Penas C. BET protein inhibition in macrophages enhances dorsal root ganglion neurite outgrowth in female mice. J Neurosci Res. 2022 Jun;100(6):1331-1346. doi: 10.1002/jnr.25036. Epub 2022 Feb 26. PMID: 35218246; PMCID: PMC9306766.

In addition, we plan to submit the research detailed in Chapter 4 for publication.

Results

Chapter 1

Nerve excitability and neuropathic pain is reduced by BET protein inhibition after spared nerve injury

USASP
US ASSOCIATION FOR THE STUDY OF PAIN

PUBLISHED BY
ELSEVIER

The Journal of Pain, Vol 00, No 00 (), 2021: pp 1–14
Available online at www.jpain.org and www.sciencedirect.com

Original Reports

Nerve Excitability and Neuropathic Pain is Reduced by BET Protein Inhibition After Spared Nerve Injury

Georgina Palomés-Borrajo,[#] Jordi Badia,[#] Xavier Navarro, and Clara Penas

Institute of Neurosciences, Dept. Cell Biology, Physiology and Immunology, Centro de Investigación Biomédica en Red sobre Enfermedades Neurodegenerativas (CIBERNED), Universitat Autònoma de Barcelona, Bellaterra, Spain

Abstract: **Neuropathic pain is a common disability produced by enhanced neuronal excitability after nervous system injury. The pathophysiological changes that underlie the generation and maintenance of neuropathic pain require modifications of transcriptional programs. In particular, there is an induction of pro-inflammatory neuromodulators levels, and changes in the expression of ion channels and other factors intervening in the determination of the membrane potential in neuronal cells. We have previously found that inhibition of the BET proteins epigenetic readers reduced neuroinflammation after spinal cord injury. Within the present study we aimed to determine if BET protein inhibition may also affect neuroinflammation after a peripheral nerve injury, and if this would beneficially alter neuronal excitability and neuropathic pain. For this purpose, C57BL/6 female mice underwent spared nerve injury (SNI), and were treated with the BET inhibitor JQ1, or vehicle. Electrophysiological and algesimetry tests were performed on these mice. We also determined the effects of JQ1 treatment after injury on neuroinflammation, and the expression of neuronal components important for the maintenance of axon membrane potential. We found that treatment with JQ1 affected neuronal excitability and mechanical hyperalgesia after SNI in mice. BET protein inhibition regulated cytokine expression and reduced microglial reactivity after injury. In addition, JQ1 treatment altered the expression of SCN3A, SCN9A, KCNA1, KCNQ2, KCNQ3, HCN1 and HCN2 ion channels, as well as the expression of the Na^+/K^+ ATPase pump subunits. In conclusion, both, alteration of inflammation, and neuronal transcription, could be the responsible epigenetic mechanisms for the reduction of excitability and hyperalgesia observed after BET inhibition. Inhibition of BET proteins is a promising therapy for reducing neuropathic pain after neural injury.**

Key words: *BET proteins, Excitability, Neuropathic pain, Inflammation, Spared nerve injury.*

Introduction

Neuropathic pain is a common maladaptive disorder produced by injuries of the nervous system. It is reflected by presenting pain under non-painful stimulus (allodynia), increased pain after painful stimulus (hyperalgesia) and spontaneous pain without stimuli. Neuropathic pain is considered the result of neural plasticity, produced by an increase in the excitability of primary sensory neurons and nociceptive neurons in the spinal cord and the brain.[26,52] A critical contributor to neuronal excitability, and thus to the induction and maintenance of neuropathic pain, are microglial cells, together with blood borne macrophages.[33] After a neural lesion, these cells release potent neuromodulators, such as pro-inflammatory cytokines and chemokines that regulate synaptic transmission and plasticity[17], and enhance neuronal excitability, by inducing altered expression, trafficking and functioning of ion channels, transporters, receptors and neurotransmitters.[15,18,48] Thus, the pathophysiological changes that underlie the generation and maintenance of neuropathic pain are produced by the induction of pro-inflammatory neuromodulator expression, mainly released by glial cells and

Received March 11, 2021; Revised May 19, 2021; Accepted May 23, 2021.
[#]These authors contributed equally.
Support/grant: This work was supported by grant PID2019-108496RA-I00 from Ministerio de Ciencia e Innovación and Agencia Estatal de Investigación of Spain, CIBERNED (CB06/05/1105) and TERCEL (RD16/0011/0014) funds from the Instituto de Salud Carlos III of Spain, co-funded by European Union (ERDF/ESF, "Investing in your future").
Conflict of interest: The authors declare that they have no conflicts of interest.
Address reprint requests to Clara Penas E-mail: Clara.Penas@uab.cat
1526-5900/$36.00

https://doi.org/10.1016/j.jpain.2021.05.005

macrophages, and by the altered gene expression of neuronal cells.

Regarding neuronal gene expression, transcriptional alterations of components important for the generation of action potentials and maintenance of the membrane potential in axons contribute to the enhancement of neuronal excitability. Voltage gated sodium channels (Nav) are essential for the initiation of action potentials. Several Nav subunits are commonly found altered after nerve injury at early time points, which is related to neuropathic pain generation and excitability.[16,56] Fast voltage gated potassium channels (Kv) are essential for membrane repolarization after an action potential.[31] Then, slow voltage gated potassium channels (Kv) help maintaining the membrane resting potential. In particular, KCNQ2 and KCNQ3 have been reported to be reduced in neuropathic pain conditions, producing hyperexcitability.[44,54] Hyperpolarization-activated cyclic nucleotide-gated (HCN) channels have been also implicated in the development of neuropathic pain. HCN channels produce an excitatory inward current (termed Ih) that depolarizes the membrane potential, which limits electrogenic hyperpolarization[4] and contributes to the resting membrane potential, tending to enhance neuronal excitability. In addition, it has been described that pharmacological blockade of HCN channels decreases mechanical hyperalgesia in different neuropathic pain models (reviewed in[21,50]) and reduces spontaneous activity after nerve damage.[11] Finally, the Na^+/K^+ ATPase pump has also an important role. This pump is required to generate the resting membrane potential in neurons, and thus facilitates excitatory afferent neurotransmission.[51]

Bromodomain and extra-terminal domain (BET) proteins belong to the reader family. BET proteins are characterized by the presence of two tandem bromodomains (BD1 and BD2) and an extra-terminal domain (ET), which are critical for their function.[25,47]These proteins bind to acetylated lysine residues in both histone and non-histone proteins to recruit transcriptional complexes and thus regulate gene expression.[25,36,47] We already described that BET inhibition is a promising strategy to reduce inflammation and promote neuroprotection after spinal cord injury.[43] In the present study, we wanted to ascertain if BET inhibition would also affect neuroinflammation after a peripheral nerve injury and if this would also affect neuronal excitability and appearance of neuropathic pain. For this purpose, we used SNI in mice, since research with this animal model serves as a valuable source of information in many medical areas.[14] We found that treatment with the BET inhibitor JQ1 reduced neuronal excitability and mechanical hyperalgesia after spared nerve injury (SNI). In addition, we found that JQ1 treatment produced an early and long-lasting reduction of neuroinflammation, and alteration of the expression of several contributors of the membrane potential of axons, which could be the responsible mechanisms for the reduced excitability and neuropathic pain observed.

Methods

Spared Nerve Injury (SNI) and JQ1 Treatment

All experimental procedures were approved by the Universitat Autònoma de Barcelona Animal Experimentation Ethical Committee (code 10306) and followed the European Communities Council Directive 2010/63/EU. Female C57BL/6 mice with 7 to 8 weeks of age (22 g) were used for all the procedures and randomly divided into three groups depending on the experimental design. Previous to any animal testing, we confirmed that mice presented a normal behavior, using supervised protocols, approved by the Universitat Autònoma de Barcelona Animal Experimentation Ethical Committee, indicating that mice had a healthy status.

General anesthesia was induced by an intraperitoneal injection (i.p.) of a solution of ketamine (90 mg/kg) and xylazine (10 mg/kg) in saline. To perform the SNI, the sciatic nerve was exposed at the mid-thigh level and freed of adhering tissue. The three terminal branches of the sciatic nerve were gently separated proximal to the poplitea fossa; at this level the tibial and the common peroneal nerves were tightly ligated with 6-0 silk and sectioned distal to the ligation. Care was taken to avoid damage of the sural nerve. After nerve injury, the wound was closed in layers, disinfected, and the animals were kept in a warm environment until recovery from anesthesia. Mice received an i.p. dose of 30mg/kg JQ1, diluted in 5% DMSO and 5% Tween-80 in saline, 2 h post-operation and daily onwards until specified. Vehicle-treated animals received only the vehicle solution. Mice that received different treatments were mixed and housed together in animal cages, to avoid bias on animal welfare. Animal welfare was followed after injury by using protocols held in the animal facility. These included daily weight control, evidence of autotomy and fur appearance among other indicators.

Behavioral Tests

To evaluate neuropathic pain, mechanical and thermal algesimetry tests were performed before surgery and at 3, 14 and 28 days post-operation (dpo). Before the test, animals were acclimated carefully to handling and immobilization for mechanical testing or in a plastic enclosure for thermal algesimetry. Then the tests were performed before surgery and every two weeks after operation. Mechanical nociception threshold was measured by an electronic mouse Randall-Selitto test (Rodent Pincher device, IITC).[42] Briefly, an increasing mechanical force was applied with a probe on the lateral plantar surface of the hind paws until the animal produced retraction of the paw, indicating painful perception. Thermal algesimetry test was performed by the Hargreaves radiant heat method,[19] using a Plantar algesimeter device (Ugo Basile). The lamp focus was applied on the lateral plantar surface of the hind paws and the time that mice can endure heat irradiation was measured. The withdrawal threshold for both tests was calculated as the average of three trials with time interval in between.

Electrophysiological Studies

Electrophysiological evaluation was performed at 3, 14 and 28 days dpo, (n = 5–7 mice per group). During the electrophysiological tests, the animals were placed over a warm flat streamer controlled by a hot water circulating pump to maintain body temperature constant. The right sciatic nerve was percutaneously stimulated with a pair of platinum non-polarizable needle electrodes placed at the sciatic notch. The sensory compound nerve action potential (SNAP) was recorded by custom made microelectrodes placed on the fifth toe in the right paw, near the digital nerve that contains sensory axons. The active electrode was placed at the base of the falanx, the reference at the tip of the toe, and a ground needle subcutaneously placed at the knee. The fifth toe is normally innervated by axons coming in the sural and the tibial/lateral plantar nerves; after the SNI only the intact sural nerve axons remained.

All the animals were submitted to the multiple excitability protocol TRONDNF using the threshold tracking program QTRAC (Windows QTRAC v1.0.0; version 23.05.2017, Institute of Neurology, London, UK).[8,28,29] Electrical stimulus waveforms were generated by the computer and converted to current delivered from a constant current stimulator (Bi-phasic Stimulus Isolator Digitimer DS4, Digitimer Ltd, UK). The evoked potential was amplified and digitized by a computer with an A/D board I/O Tech DaqBoard d2k0 at a sampling rate of 10 kHz. SNAP amplitude was measured from the baseline to-peak, and latency of the fastest conducting axons from stimulus to the peak onset.

The TRONDFN protocol provides five measures of axonal excitability: stimulus–response relationship (SR), strength-duration relationship (QT), threshold electrotonus (TE), current-threshold relationship (I/V) and the recovery cycle (RC). We followed a procedure similar to that previously reported for motor axons in rodents[2,6] but recording the small amplitude digital nerve SNAP as also tested in humans.[22] In short, the first step of the TRONDNF protocol is to determine the stimulus that generates a maximal amplitude SNAP. Then, the software tracks the stimulus needed to elicit a SNAP of 40% of the maximal amplitude, and the result is known as the standard threshold. Each of the tests in the TRONDNF protocol is based on the application of stimuli of different duration and intensity, either by combining with depolarizing or hyperpolarizing conditioning pulses of 20%, 40%, 50%, 70% and 100% of the standard threshold, or by applying pairs of stimuli with different intervals between them and different intensities. The difference between the stimulus needed in the specific test conditioning conditions to reach the threshold value and the initially calculated standard threshold value accounts for changes in excitability membrane properties.[6,28] The following terms correspond to parameters of the TRODNF protocol analyzed in the present study: *Strength duration time constant (SDTC)*, the rate at which the threshold current for a target potential declines as the stimulus duration is increased and is given by the intersection of the line representing the Charge-duration relationship; *Peak response*, is the compound action potential for which a higher delivered stimulus current will not generate an increase on muscle compound potential. *Resting I/V slope*, the slope of the I/V relationship, calculated from the polarizing currents -10% and +10% of threshold; *TEh_{20}(10-20ms), TEh_{20}(10-20ms), TEh(20-40ms) and TEh(90-100ms), and TEd(10-20ms)*, the mean percentage threshold increment or decrement at the specified interval for an hyperpolarizing (h) or depolarizing (d) conditioning pulse of 20%, 40% of the standard threshold (when the hyperpolarizing or depolarizing pulse amplitude is omitted it is understood to refer to 40% of the standard current); TEh(peak, -70%), TEh(peak, -100%), refer to the maximum increase in threshold when a hyperpolarizing conditioning pulse of -70% or -100% of the standard threshold is applied; S3(-70%), S3(-100%), the difference between TEh at the peak and the TEh at the end of the subthreshold hyperpolarizing conditioning pulse of the -70% or -100% of the standard threshold; TEh (slope101-140ms), the slope of the curve from the end of the hyperpolarizing current at 40% of the standard threshold to the start of the overshoot, reflecting the recovering from hyperpolarization; TEd (undershoot), the minimum percentage threshold reduction after 100 ms duration of the depolarizing current.

Immunohistochemistry

Animals used for the functional assessment were sacrificed and perfused with 4% paraformaldehyde in 0.1M phosphate buffer (PB). A 5-mm length of the lumbar spinal cord, containing L5 segment, was dissected, post-fixed in 30% sucrose and cut into 20-μm-thick sagittal sections using a cryostat (Leica CM190, Leica Microsystems). For immunohistochemical staining, a subset of sections was rehydrated in PBS and blocked with 5% normal donkey serum (NDS) in PBS 0.3% Triton-X100 for 1 h at room temperature. The spinal cord sections were then incubated overnight at 4 °C with primary antibodies against calcitonin gene-related peptide (CGRP, for peptidergic fibers; 1:1000; 24112-ImmunoStar), anti-Griffonia Simplicifolia Lectin I (IB4, for non-peptidergic fibers; 1:500; AS-2104 - Vector Laboratories), purified anti-neurofilament H (SMI32, for gray matter neurons, 1:1000; 801701-Biolegend), and ionized calcium-binding adapter molecule 1 (Iba1; for macrophages/ microglia; 1:500, 1919741-Wako). Prior to the addition of IB4 primary antibody, an overnight incubation at 4°C with Lectin 1 (Unconjugated Griffonia Simplicifolia Lectin I; 10 μg/ml; L-1104 – Vector Laboratories) was needed. Nuclei were labeled with DAPI staining (1:1000; D9564-10MG-Sigma). The detection was made with appropriate secondary antibodies conjugated with Alexa Fluor 594 (A21207 for Rabbit and A21203 for Mouse; 1:200; Invitrogen) and Alexa Fluor 488 (A21202 for Mouse and A1105 for Goat; 1:200; Invitrogen). Finally, after several washes in PBS-Tween 0.1%, PBS and PB, a coverslip was applied in Fluoromount-G mounting medium (Southern Biotech). After identifying L5 slices by means of SMI32 staining, microphotographs were taken at 100X (for CGRP and IB4 samples) or 200X (for Iba1

immunohistochemistry) with an Olympus PD37 camera. Immunoreactivity was analyzed by measuring the integrated density of a region of interest (ROI) after defining a threshold for background correction, using ImageJ software. The oval ROI used for IB4 and CGRP analysis measured 125.53 μm width and 50.45 μm height, whereas the oval ROI used for Iba1 had a width of 315.59 μm and a height of 102.95 μm. All ROIs were placed on the centromedial region of the superficial gray matter of the dorsal horn, where the afferent projections of the sciatic nerve are found. Markers were measured from three to five spinal cord sections of each animal (n = 4 mice per group).

RNA Extraction and PCR

Adult mice were perfused with sterile saline at 1, 3, or 28 dpo, (n = 4 mice per group). Then, L5-L6 dorsal root ganglia, or intact sciatic nerve were removed and snap-frozen. Tissue was homogenized with QIAzol lysis reagent (QIAGEN), and RNA was extracted using the RNeasy Mini Kit (QIAGEN) following the manufacturer's guidelines. RNA was quantified with a spectrophotometer (Nano- Drop Technologies) and reverse-transcribed using an Applied Biosystems kit (Thermo Fisher Scientific). Then, the expression of target sequences was quantified by RTqPCR using SYBR Green QPCR Master Mix (Agilent Technologies) and the corresponding primers (Table 1). Glyceraldehyde-3-phosphate dehydrogenase (GAPDH) was used as a housekeeping gene.

Statistical Analysis

Data are expressed as the mean and standard error (SEM) for each group, and analyzed using GraphPad Prism software. For statistical comparisons in behavioral and electrophysiological studies, statistical comparisons between groups were carried out using Two-way ANOVA followed by Sidaks test was performed. For mRNA expression and histological analysis, One-way ANOVA followed by Tukeys post hoc test was used.

Results

BET Inhibition Reduces Neuropathic Pain and Nerve Excitability after SNI

To determine whether BET inhibition reduces neuropathic pain after SNI, mechanical and thermal algesimetry tests were performed in SNI mice treated with the BET inhibitor JQ1 or vehicle (Fig. 1). Despite of the treat-

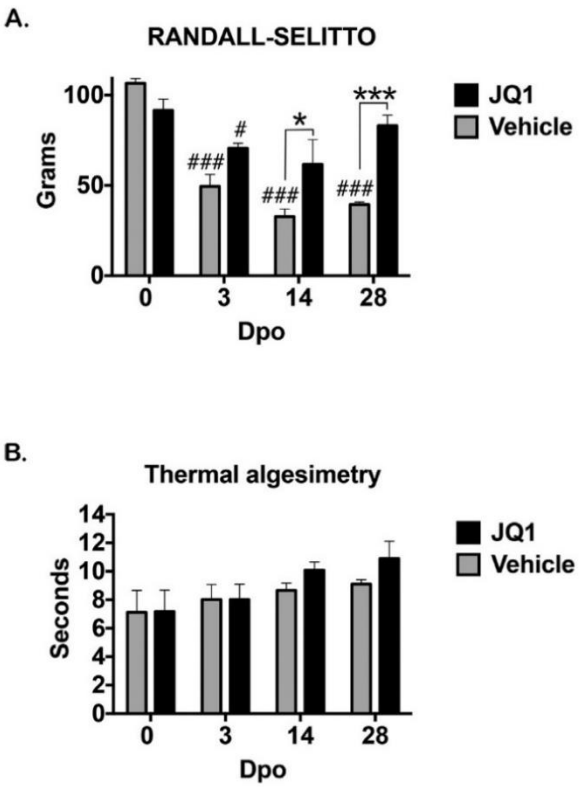

Figure 1. JQ1 treatment reduces mechanical hyperalgesia after SNI. Mechanical algesimetry results (A) and thermal algesimetry results (B) at 3, 14 and 28 dpo. Data are presented as mean ± SEM. N = 6 mice per group. Statistical analysis was performed by Two-way ANOVA followed by Sidak correction for multiple comparisons. Significant differences in parameters measured at 3, 14 and 28 dpo with respect to the control group are indicated as # P <.05, ### P < .001; differences between JQ1 and vehicle groups are denoted by * P <.05, *** P < .001.

Table 1. List of Primers

Primer	Forward	Reverse
TNFα	AGGCACTCCCCCAAAAGATG	TCACCCCGAAGTTCAGTAGAC
TNFR1	GATGAAGAGCGCTGTTTGAA	CAGAGCTCATCCTCCAGCTC
TNFR2	CAGATCCTCGTGTTGGGATT	CAGTCCATGCACTTGTCGAG
IL-6	AACCACGGCCTTCCCTACTTCA	TCATTTCCACGATTTCCCAGAG
IL-4	CATCGGCATTTTGAACGAGGTCA	CTTATCGATGAATCAGGCATCG
IL-10	TGGCCCAGAAATCAAGGAGC	CAGCAGACTCAATACACACT
SCN3A	CCTGGACCCCTACTACGTCA	TGTGTACTCTACATTCTTCGTCCA
SCN9A	GAGGGGCAAACTGACTACA	AGAAACATTCCTACAATGGAG
KCNQ2	CCTCTACAACGTGCTAGAGC	TGCAGCCCAGATCCTCACAA
KCNQ3	CACCGTCAGAAGCACTTTGAG	CCTTTAGTATTGCTACCACGAGG
HCN1	ACTGTGGGCGAATCCCTGG	CCACCAGCAGCTGTGCAGA
HCN2	GGAGAATGCCATCATCCAGG	CAGCAGGCTGTGGCCATGA
α1 NKA	TTTCAGAACGCCTACCTAGAGC	TGGAGATAAGACCCACGAAGC
β1 NKA	GCGACATCAATCACGAACGAG	GTATCCGCCCATCCCAAAGTA
FXYD2	GGGGCGGTAAGAAACATAGGC	CAACTTGGAACAGGGAGTGGG

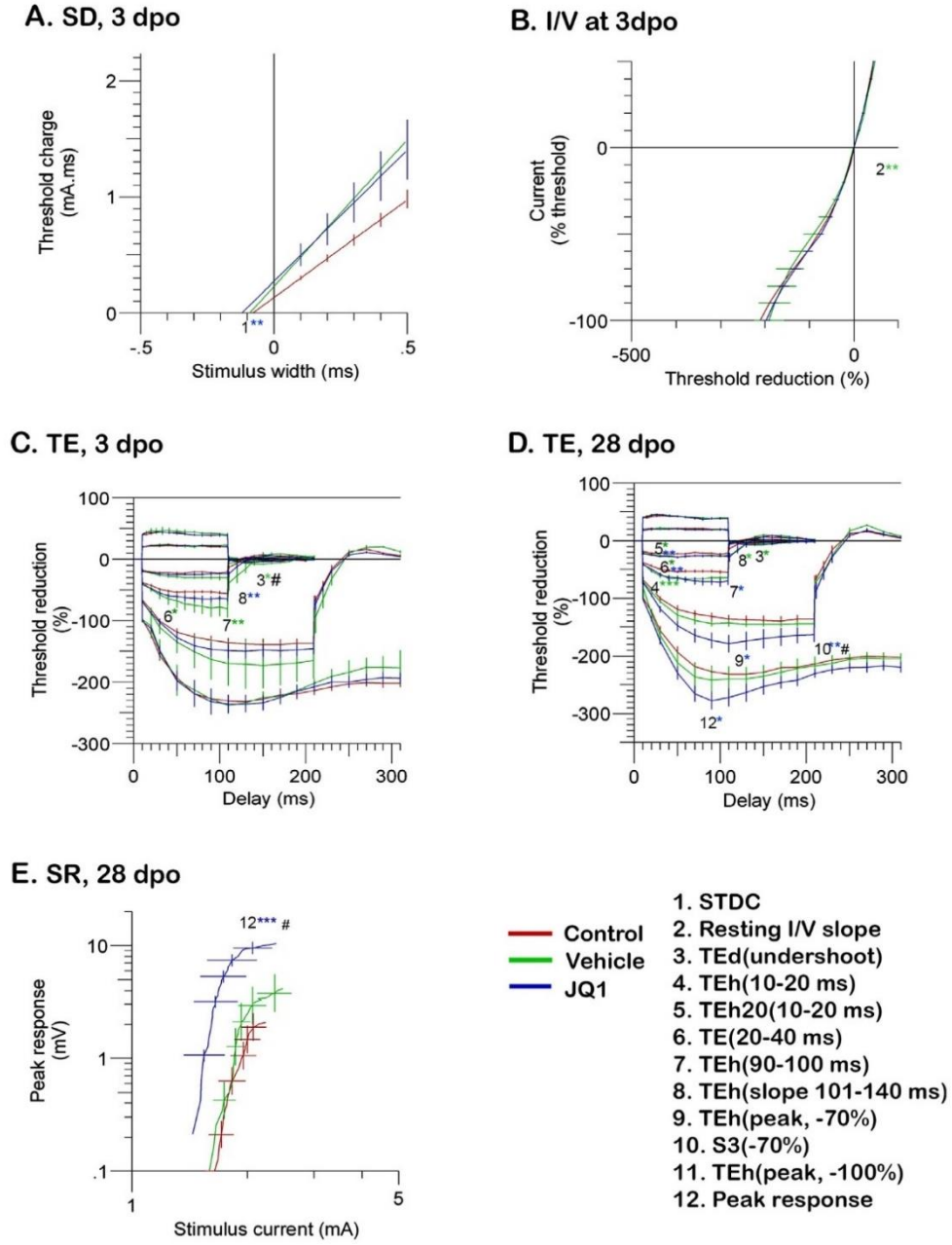

Figure 2. JQ1 modulates axonal excitability after SNI. Plots of sural nerve excitability measurements at 3 dpo (A, B, C) and 28 dpo (D, E), of the control, vehicle and JQ1 groups. (A) The SDTC of the strength-duration (SD) plot has an increased significant value. (B) The resting slope value of the I/V plot shows a significant decreased value. (C), (D) Threshold electrotonus (TE) plot shows the "fanning-out" shape. (E) The peak response of the group JQ1 in the stimulus-response (SR) plot shows a significant increment. These results suggest that the membrane of the axons of the JQ1 and vehicle groups were hyperpolarized except for the parameter SDTC a 3dpo that point to excitability of the axon. The significant differences were found during the application of the SR and TE protocols. N=5-7 per group. * $P < .05$, ** $P < .01$, *** $P < .001$, of the vehicle group compared to the control group (green asterisks) or of the JQ1 group compared to the control group (blue asterisks). #$P < .05$ of the JQ1 group compared to the vehicle group. (Color version of available online)

ment, mice have hyperalgesia at 3 dpo. However, mice treated with JQ1 presented reduced hyperalgesia compared to the vehicle-treated mice, with significant differences at 14 and 28 dpo. The thermal algesimetry test showed a non-significant increase in the withdrawal threshold to hot stimulation in JQ1 with respect to vehicle-treated mice at the three time-points studied (Fig. 1B).

Changes in Axonal Excitability Measures after SNI

To analyze if BET inhibition could induce changes in sensory neuronal excitability, electrophysiological measurements using the TRONDNF protocol were performed. Statistical analyses yielded significant differences between groups in the strength-duration relationship

Table 2. TRONDNF Parameters After SNI

	Control	*Vehicle 3 dpo*	*JQ1 3 dpo*	*Vehicle 14 dpo*	*JQ1 14 dpo*	*Vehicle 28 dpo*	*JQ1 28 dpo*
Strength-duration\t ime	0.08 ± 0.11	0,09± 0,02	0.12± 0.01*	0.10±0.01	0.19±0.01	0.11±0.01	0.10±0.01
Peak response\(mv)	2.11x|/1.32	6.66x|/1,41	1,44x/2.18	3.15x|/1.51	5.14x|/1.15	4.211x|/1.46	10.63x|/1.13*** #
Resting I/V slope	1.07±0.03	0.84±0.04**	1.00±0.04	0.97±0.03	0.99±0.04	0.98±0.04	1.11±0.06
TEd (10-20ms)	42.4 ± 1.3	45.6±4.62	43.59±1.31	47.5 ± 1.7*	46.9 ± 1.1	45.6 ± 0.5	44.5 ± 1.8
TEd (undershoot)	-5.41 ± 0.40	-8.73±1.74*#	-5.52±0.45	-6.60 ± 0.76	-7.92 ± 0.92*	-8.56 ± 0.46*	-7.46 ± 1.19
TEh (10-20ms)	-46.4 ± 1.2	−53.10±5..91	-51.68±1.64	-54.9 ± 1.3**	-56.1 ± 1.6***	-57.3 ± 2.2***	-54.3 ± 2.2**
TEh_{20} (10-20ms)	-21.5 ± 0.7	-23.22±1.71	-23.30±0.52	-25.1 ± 0.9**	-25.3 ± 0.6**	-24.9 ± 0.8*	-25.6 ± 1.3**
TEh (20-40ms)	-51.6 ± 1.9	-63.65±8.49*	-58.72±2.35	-62.5 ± 1.6**	-64.0 ± 2.4**	-62.8 ± 3.0*	-63.4 ± 3.9**
TEh (90-100ms)	-55.2 ± 2.6	-69.98±13.8**	-64.20±3.83	-69.5 ± 2.3*	-71.5 ± 3.0*	-64.6 ± 2.0	-71.1 ± 7.1*
TEh (slope 101-140ms)	0.54 ± 0.08	0.92±0.28**	0.72±0.12	0.94 ± 0.05 *	0.98 ± 0.12*	1.01 ± 0.10*	0.90 ± 0.19
TEh (peak,-70%)	-140.8 ± 7.6	-155.4±32.6	-153.00±10.80	-177.7 ± 5.8*	-192.8 ± 7.0***	-147.8 ± 4.5	-179.5 ±14.4*
S3 (-70%)	4.17 ± 1.14	9.93±5.30	6.00±2.12	13.41 ± 2.88*	16.43 ± 4.63**	3.77 ± 1.20	15.77 ± 2.59** #
TEh (peak,-100%)	-234.7± 9.9	-220.2±19.8	-239.40±14.20	-268.9 ± 9.1	-298.0 ± 13.1**	-243.5 ± 21.5	-278.4 ± 14.4*
S3(-100%)	32.6 ± 6.1	43.03±26NC	45.76±6.65NC	51.1 ± 4.8	66.2 ± 3.8*	38.5 ± 14.2	60.3 ± 7.7

Significant differences in parameters measured at 3, 14 and 28 dpo with respect to the control group are indicated as * $p < 0.05$, ** $p < 0.01$, *** $p < 0.001$; differences between JQ1 and vehicle groups are denoted by # $p < 0.05$.

(SD), the current-threshold relationship (I/V), the threshold electrotonus (TE), and the strength-response relationship (SR), (Fig. 2, Table 2), tests that provide information about the electrical state of the nodal and internodal axonal membrane.[8,27,28]

Results obtained at 3 dpo show a significant increase of de SDTC of the JQ1 treated mice compared to the control group (Fig. 2A). Then, SDTC returned to control values afterwards. This parameter indicate a higher excitability in JQ1-treated animals originated in the nodal membrane region, compared to the vehicle and control group.

We also observed that the resting I/V slope was decreased at 3 dpo in vehicle-treated animals compared to the control group, and returned to control values at 14 and 28 dpo (Fig. 2B). The other significant differences at 3 dpo were obtained within the TE, which tended to have a fanning out shape in vehicle and JQ1-treated animals, compared to the control group (Fig. 2C, D). At 3 dpo, the TEd(undershoot), TEh(20-40ms), TEh(90-100ms) and TEh slope(101-140ms) of the vehicle-treated animals were significantly different to the control group. These results indicate a certain degree of hyperpolarization of the axonal membrane, which was reduced by JQ1 treatment.

At 14 days after SNI, the vehicle and JQ1 groups showed more significant changes in the TEd, TEh, and S3 values respect the control group than at 3 dpo (Table 2). The changes in these values tended to revert at 28 dpo towards control values. However, the parameters TEh(10-20ms),TEh_{20}(10-20ms), TEh(20-40ms), and TEh slope(101-140ms) still remained increased at 28 dpo in the vehicle group. In addition, the value of the TEd (undershoot) increased significantly at 28 dpo, suggesting a persistent membrane hyperpolarization of the sural nerve axons of the vehicle group[28].The parameters that remained significantly increased in the JQ1 group compared with the control group at 28 dpo were TEh (10-20ms), TEh20(10-20ms), TEh(20-40ms), TEh(90-100ms), TEh(peak,-70%), TEh(peak,-100%), and the S3 (-70%), which was also significantly different from the vehicle group. From these, the TEh20(10-20ms), TEh(20-40ms), TEh(90-100ms), indicated persistent membrane hyperpolarization. Then, the TEh(peak,-70%) S3(-70%) and TEh(peak,-100%), indicate a decrease of the inwardly rectifying current (Ih) only in JQ1-treated animals. Finally, from the SR relationship it could be observed that the peak response was increased in the JQ1-treated mice compared with the control group at 28 dpo (Fig. 2E), indicating also membrane hyperpolarization of this group.

BET Inhibition Reduces Inflammation after SNI

JQ1 Reduces Pro-Inflammatory Cytokine Expression after SNI in Lumbar DRG

We assessed if BET inhibition affected neuroinflammation, which has been associated to increased nerve excitability and subsequent neuropathic pain. Thus, we monitored the mRNA expression of pro-inflammatory and anti-inflammatory markers in L5-L6 DRG at 1 and 3 dpo after SNI.

At 1 dpo, JQ1-treated mice showed a significant reduction in TNFα and IL-6 pro-inflammatory cytokines expression in ipsilateral DRGs, compared to vehicle-treated animals (Fig. 3A). However, there were no significant differences on the expression of TNFα receptors, TNFR1 and TNFR2, between treatments. Concerning expression of anti-inflammatory cytokines, BET inhibition produced a significant increase of IL-4 and IL-10 expression in contralateral and ipsilateral DRG when compared to vehicle treatment.

At 3 dpo, JQ1-treated mice had a significant decrease on pro-inflammatory transcription of TNFR2 and IL-6 in ipsilateral DRG (Fig. 3B), and again a significantly increased expression of IL-4 and IL-10 anti-inflammatory cytokines in ipsilateral and contralateral DRG when compared to vehicle-treated animals. Therefore, BET-inhibition with JQ1 reduces pro-inflammatory acute

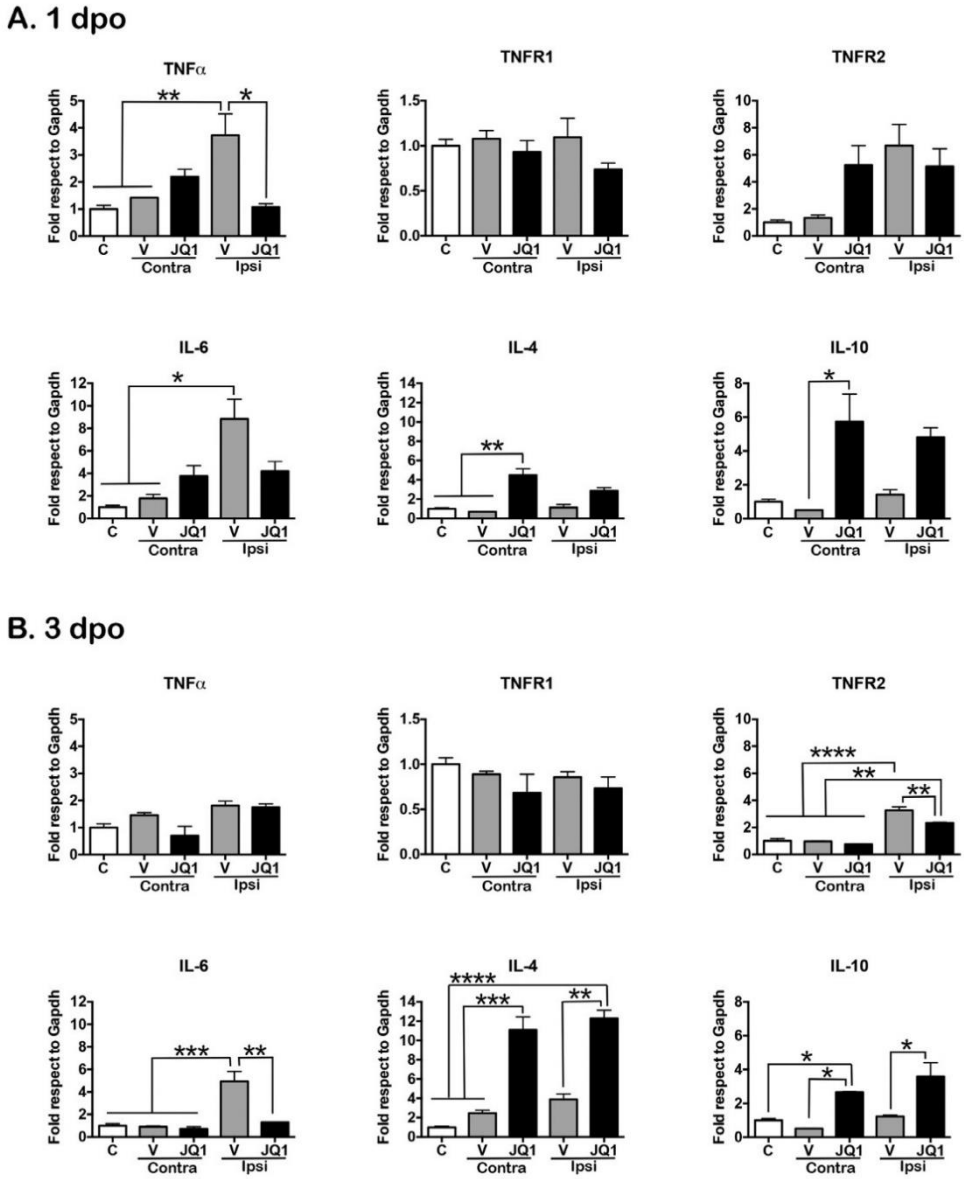

Figure 3. JQ1 reduces inflammation acutely in DRG after SNI. DRG samples were harvested at 1 and 3 dpo. Real-time PCR quantification was normalized to the GAPDH levels. N = 3-5 per group and day. *$P < .05$, **$P < .01$, ***$P < .005$, ****$P < .001$ by One-way ANOVA followed by Tukey post hoc test. Data are presented as mean ± SEM fold changes of gene expression.

response in the DRG after SNI, by decreasing pro-inflammatory and increasing anti-inflammatory cytokine transcription.

JQ1 Reduces Microglial Activation after SNI in the Dorsal Horn of the Spinal Cord

We then assessed if JQ1 treatment produced an effect on microglial reactivity in the dorsal horn, where nociceptive afferents project. At 3 dpo, vehicle-treated animals showed increased immunoreactivity against iba1 in the dorsal horn ipsilateral to the injury, whereas this increase was prevented in JQ1-treated animals (Fig. 4A, B). In contrast, there were no differences between the contralateral and ipsilateral sides of the dorsal horn in JQ1-treated mice, indicating that JQ1 prevents microglial activation at the dorsal horn after the injury. Similar effects were obtaining analyzing a long-lasting effect on inflammatory cell activation at 28 dpo. The increase of Iba1 immunoreactivity at this time point in vehicle-treated animals, lower than in an acute phase after the injury, was also prevented by JQ1 treatment. Therefore, BET inhibition prevents microglial activation, both acutely and chronically after injury.

JQ1 Does not Affect CGRP and IB4 Afferent Projections in the Dorsal Horn of the Spinal Cord

Provided that JQ1 reduced hyperalgesia, we analyzed if BET inhibition lead to changes on the innervation pattern of afferent nociceptive fibers at L5 segment of the spinal cord. To detect peptidergic C fibers and non-peptidergic C fibers, immunohistochemistry against CGRP and IB4 were performed, respectively. Immunoreactivity was measured in lamina I and II of the centro-medial

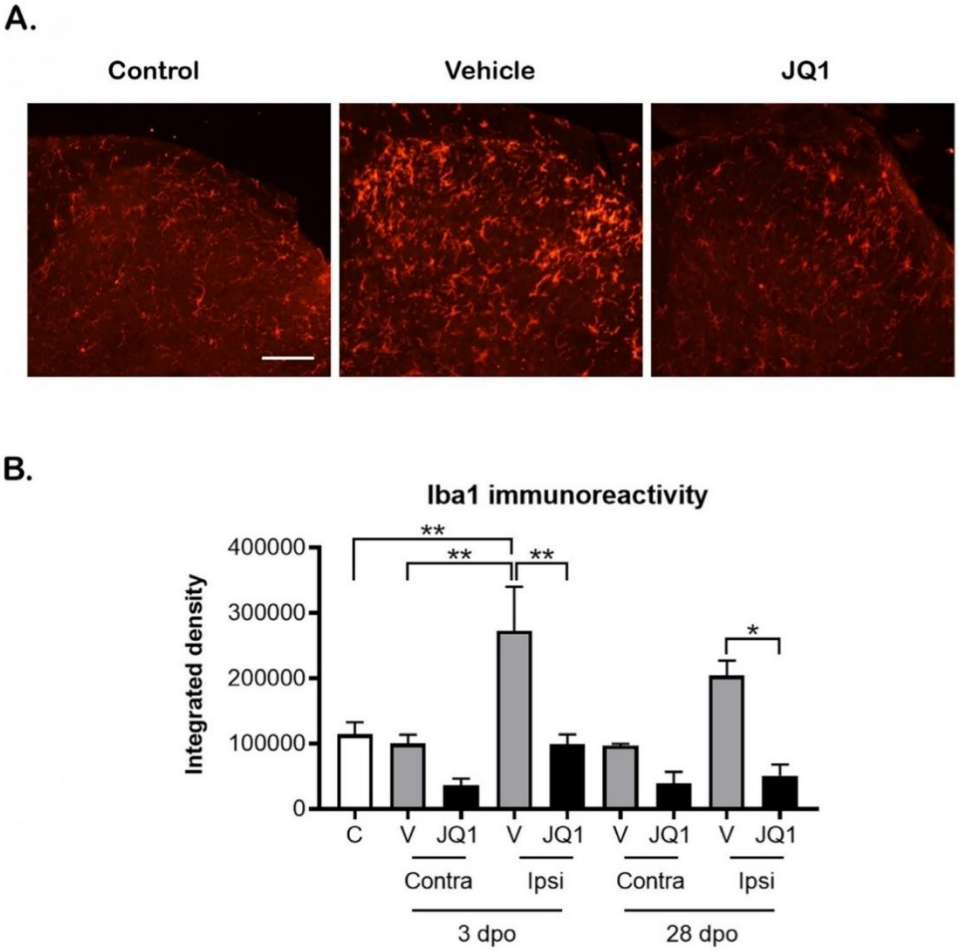

Figure 4. JQ1 reduces long term microglial activation in the dorsal horn of the spinal cord after SNI. (A) Representative microphotographs at 200x from L5 dorsal horn of the ipsilateral hemisections labeled with Iba1 of control and SNI treated mice with vehicle and JQ1 at 3 dpo. Bar = 100 μm. **(B)** Integrated density values of Iba1 immunoreactivity. N= 3-5 per group. *P<.05 and **P<.01, by One-way ANOVA followed by Tukey's multiple comparisons. Data are presented as mean ± SEM.

area of the dorsal horn. No significant differences were found between treatments regarding CGRP immunoreactivity (Fig. 5A left and 5B left). Concerning non-peptidergic C-fibers, both vehicle treated-mice displayed a significant reduction of integrated density values in the ipsilateral compared to the contralateral side and control values (Fig. 5A right and 5B right). In contrast to vehicle, the decrease of non-peptidergic C fibers with JQ1 treatment decreased to a lesser degree, and the difference to the control animals was not significant. However, there were no significant differences between treatments. Therefore, BET-inhibition does not affect the pattern of central projections of nociceptive afferents in the dorsal horn after SNI.

BET Inhibition Affects Ion Channels and $Na^{\pm}/K^{\pm}$ pump mRNA Expression after SNI

SCNA3A and SCNA9A are Nav channel subunits involved in the generation of action potentials. These channels were usually found overexpressed at early time points in neuropathic pain conditions using rat models. However, the same subunits have been found downregulated after SNI in mice[30]. We did not find an enhanced expression in the lumbar DRG after SNI at 3 or 28 dpo (Figs. 6A, 7A). However, JQ1 treatment produced a significant down regulation of both SCN3A and SCN9A, which is in accord to our previous results showing a reduction on nerve excitability and neuropathic pain with JQ1 treatment.

KCNA1 channel is a subunit of the fast Kv channels, present at the juxtaparanodal membrane, which is essential for membrane repolarization[3,40]. We found that its expression was decreased at 3 dpo in both vehicle and JQ1-treated animals, indicating that in both groups there is a decreased ability for repolarization, which could be producing a faster transmission of the action potentials, and thus neuropathic pain generation[31]. Then, KCNA1 levels were normalized by 28 dpo to control values. KCNQ2 and KCNQ3 are subunits of the slow Kv channels involved in the maintenance of membrane potential. At 3 dpo, we found a significant increase of their expression in vehicle-treated animals, which returned to control values at 28 dpo. Further, we found that KCNQ2/3 expression was further decreased by JQ1 treatment (Figs. 6B, 7B).

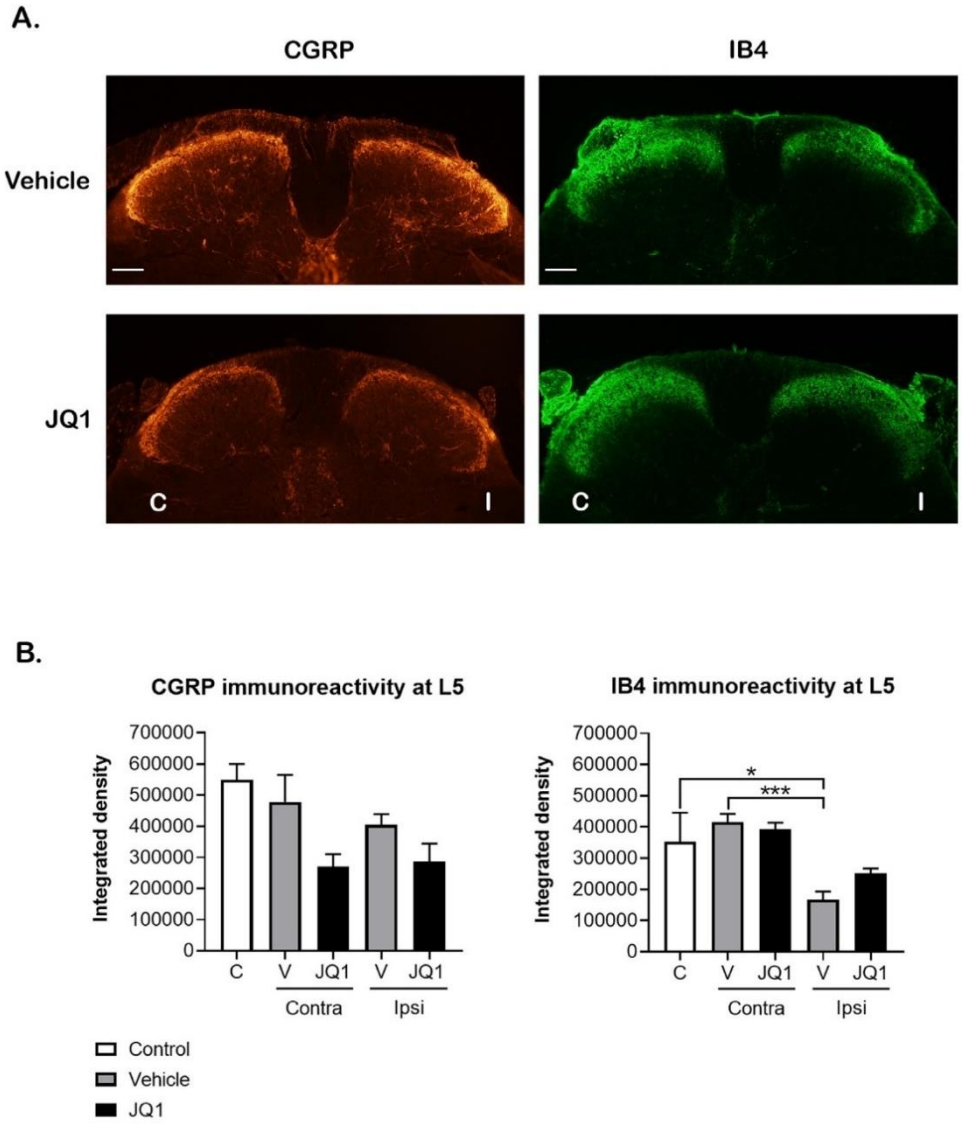

Figure 5. JQ1 does not affect CGRP and IB4 afferent projections in the dorsal horn of the spinal cord. (A) Representative microphotographs at 100x of L5 dorsal horn, labeled against CGRP for peptidergic fibers or IB4 for non-peptidergic fibers in vehicle and JQ1 treatment groups. White bar = 100 μm. C and I letters indicate contralateral and ipsilateral sides to the injury, respectively. **(B)** Integrated density values of CGRP immunoreactivity (left graph) and IB4 (right graph). N=3-4 per group. *P<.05, ***P<.005 and ****P<.001, by One-way ANOVA followed by Tukey's multiple comparisons. Data are presented as mean ± SEM.

The HCN1 and HCN2 are channels thought to limit electrogenic hyperpolarization[4], by enhancing the inwardly rectifying current. From the four isoforms that exist, these ones are the most expressed in sensory neurons[1]. At 3 dpo after SNI, there was an increase of HCN1 expression in vehicle-treated animals. At 28 dpo, both HCN1 and HCN2 levels increased in vehicle-treated animals, which was prevented by JQ1 treatment (Figs. 6C, 7C). These results confirmed the QTRAC TE data, that indicated a decrease of the inwardly rectifying current after JQ1 treatment.

Finally, we determined the levels of the α1NKA, βNKA and FXYD2 (γNKA) subunits of the Na^+/K^+ ATPase pump. At 3 and 28 dpo, the α1NKA and FXYD2 subunits were downregulated by JQ1 treatment, compared to control animals, and at 28 dpo the FXYD2 compared also to vehicle-treated animals (Fig. 6D, 7D). Thus, JQ1 treatment could be producing hyperpolarization by increasing Na^+/K^+ ATPase pump activity, as previously reported[51].

Discussion

In the present study we report that BET inhibition reduces neuronal excitability and neuropathic pain after SNI. Searching for the potential underlying mechanisms of these events, we have found that the BET inhibitor JQ1 reduced the inflammatory response in DRG and spinal cord, and induced changes of the expression of several regulators of the axonal membrane potential. In particular, JQ1 decreased SCN3A, SCN9A, KCNA1, HCN1, HCN2, KCNQ2, KCNQ3 and the α and γ subunits of the Na^+/K^+ ATPase FXYD2, which may be causing membrane hyperpolarization and decreased excitability. Therefore, BET proteins are an efficient epigenetic therapeutic target to reduce neuropathic pain after SNI.

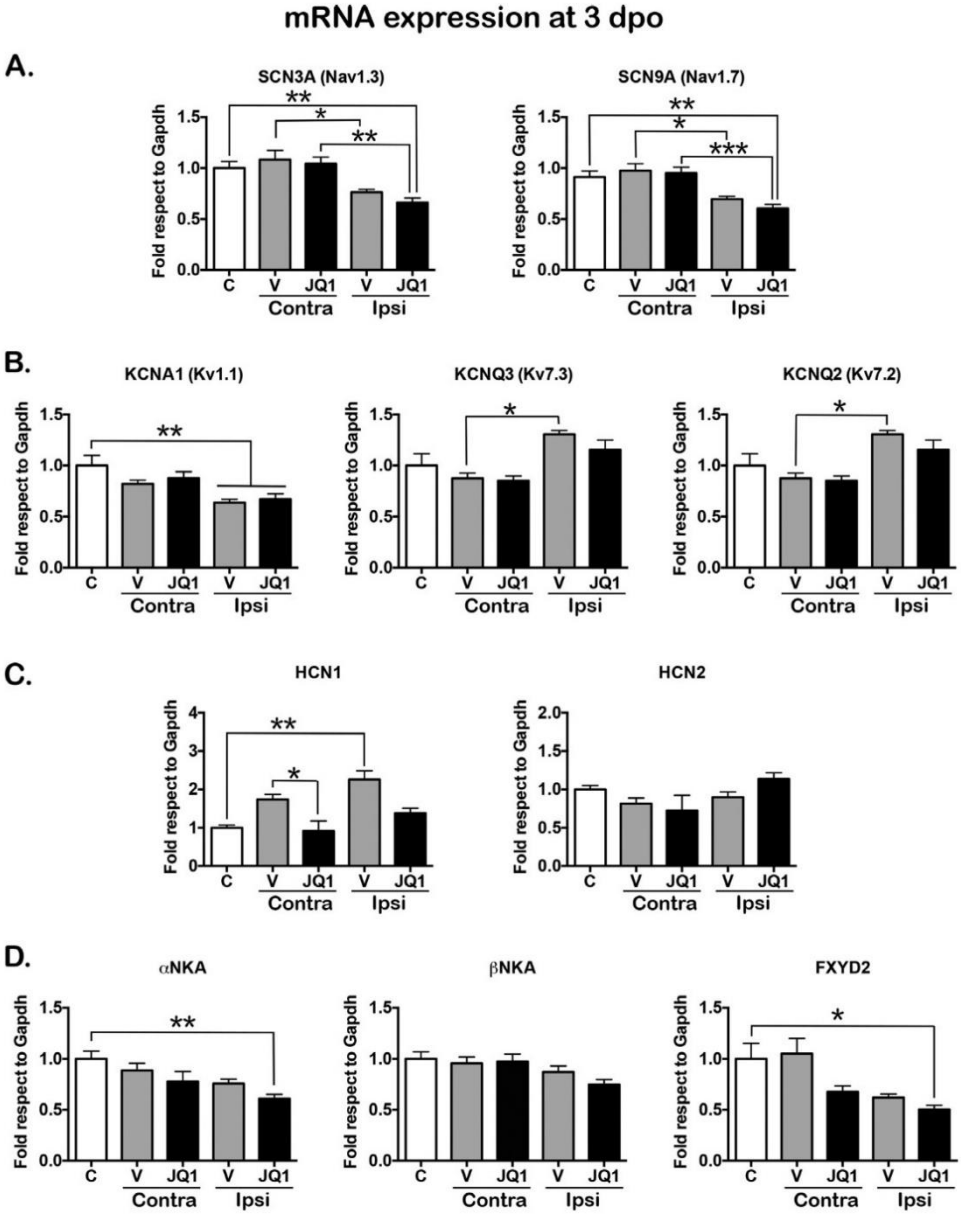

Figure 6. JQ1 affects mRNA expression of ion channels and Na+/K+ pump in DRG at 3 dpo after SNI. DRG samples were harvested at 3 dpo. Real-time PCR quantification was normalized to the GAPDH levels. N = 3-5 per group. *$P < .05$, **$P < .01$, ***$P < .005$, ****$P < .001$ by One-way ANOVA followed by Tukey post hoc test. Data are presented as mean ± SEM fold changes of gene expression.

Effects of BET Inhibition on Neuroinflammation after SNI

We have previously found that BET inhibition reduces inflammation after spinal cord injury. Accordingly, in the present study, BET inhibition also reduced inflammation after SNI. JQ1 acutely decreased the expression of the pro-inflammatory mediators TNFα, TNFR2 and IL-6 in DRG after SNI, and enhanced expression of the anti-inflammatory cytokines IL-4 and IL-10, as we found after SCI.[43] Reduction of cytokine expression is a direct effect of BET inhibition, since BET proteins bind to promoters and enhancers of pro-inflammatory cytokines to promote proinflammatory gene expression,[5,13,36] and due to the interaction of BET proteins with the p65 transactivation domain of NF-Kb.[24,56] However, it still remains to be determined how inhibition of BET proteins promotes anti-inflammatory cytokine expression. Nevertheless, acute inflammatory gene alteration promoted a reduction of microglial activation at longer time points after SNI, since we observed reduced Iba-1 expression in the spinal cord at 28 dpo. Inflammation has profound effects of neuropathic pain generation and maintenance. For instance, cytokine expression alters the expression and activity of several channels, as well as synaptic neurotransmitter release involved in pain transmission.[15,18,48] Therefore, the decrease of mechanical hyperalgesia observed by BET inhibition treatment, could be at least partially explained by the reduction of neural inflammation observed after the treatment.

We analyzed also if BET inhibition and consequent reduction of inflammation affected the spinal

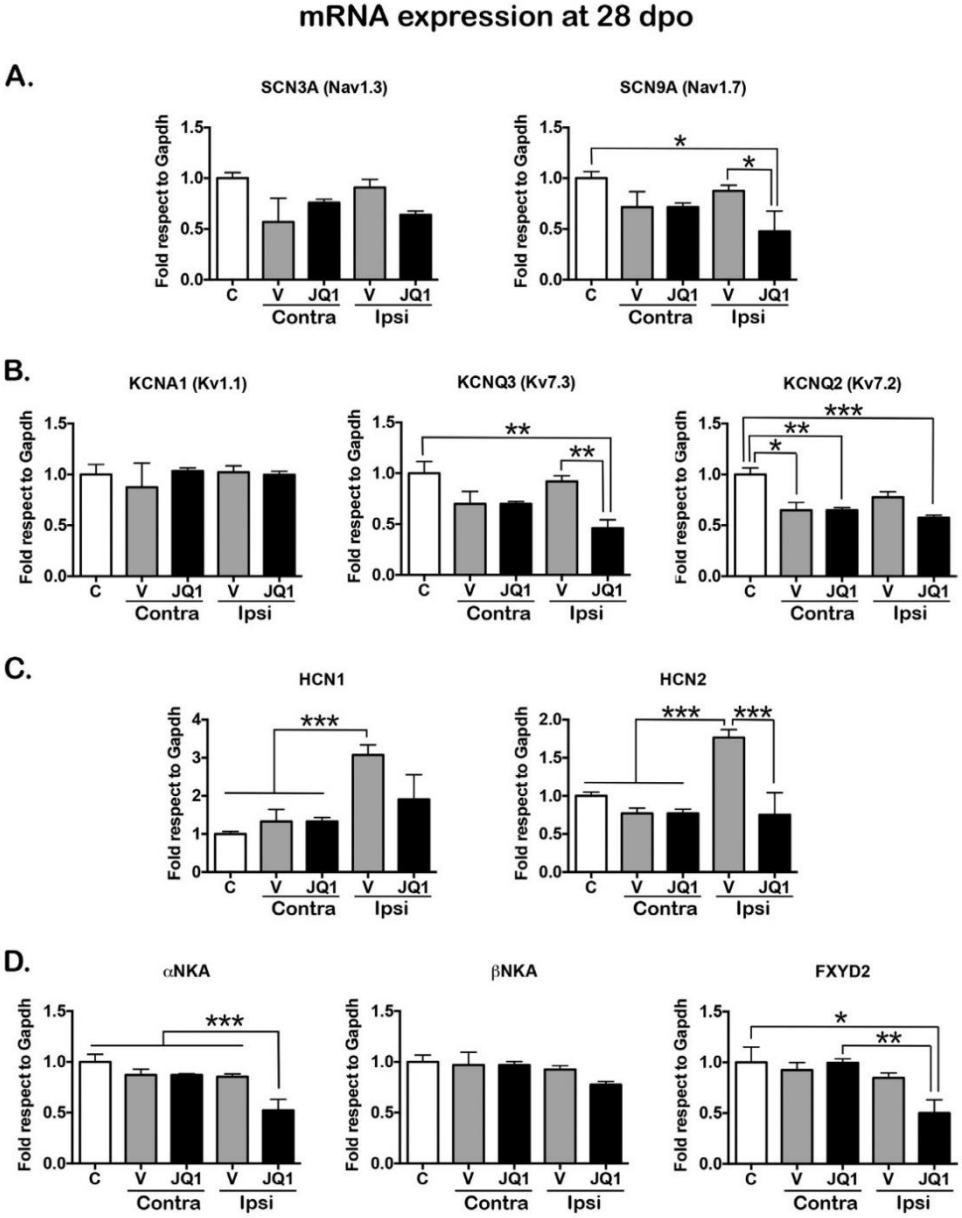

Figure 7. JQ1 affects mRNA expression of ion channels and Na+/K+ pump in DRG at 28 dpo after SNI. DRG samples were harvested at 2 dpo. Real-time PCR quantification was normalized to the GAPDH levels. N = 3-5 per group. *$P < .05$, **$P < .01$, ***$P < .005$, ****$P < .001$ by One-way ANOVA followed by Tukey post hoc test. Data are presented as mean ± SEM fold changes of gene expression.

nociceptive fiber density. We detected a loss of non-peptidergic nociceptive fibers in the dorsal horn after SNI, as previously described in our laboratory,[9] but it was not modified by BET inhibition.

Effects of BET Inhibition on Excitability and Expression of Ion Channels and $Na^{\pm}/K^{\pm}$ Pump

Axonal excitability measurements provide information about the excitability of the axonal membrane, and therefore about the activity of the ion channels and transporters contributing in the determination of the axon membrane potential.[8,28,29] The results obtained from the application of the TRONDNF protocol to the mouse sural nerve are in line to those obtained in previous studies,[32,35,37,38] and indicate reduced excitability caused by JQ1 administration. It has to be pointed out that the sural nerve axons were not injured in the SNI model. Therefore, although alterations in axonal excitability were found by the QTRAC test, they were less prominent compared to other pathologies such as nerve crush, where the tested axons are injured themselves.[34]

BET inhibition modified the expression of several transporters important for the maintenance of the membrane resting polarization and the generation of action potentials. A previous study demonstrated that the BET protein BRD4 binds directly to the SCN9A promoter in DRG cells.[23] However, it is still unknown if the transcriptional regulation of HCN1/2, KCNQ2/3 and the α and γ subunits of the Na^+/K^+ ATPase FXYD2 expression

is produced by direct binding of BET proteins on their promoters. Nonetheless, the altered expression of these genes may contribute to the reduction of neural excitability and the concomitant hyperalgesia observed by JQ1 treatment after SNI.

At 3 dpo, SNI produced neuropathic pain in both the vehicle and the JQ1 treated animals. The electrophysiological results reflected that at 3 dpo, the only significant change observed in JQ1-treated animals was the SDTC, which increased with respect de control group. The SDTC indicates a higher excitability of the axon membrane with the same stimulus applied,[29] and could be produced by an increase of Nav or a decrease of Kv currents.[46] Since increased expression of Nav channels were not observed, the alteration of the SDTC may be produced by the reduction of the KCNA1, a Kv fast channel, which could be responsible for a non-complete repolarization of the action potential generated in the axon node. The KCNA1 was downregulated both vehicle and JQ1 groups. The decrease of KCNA1 channels could partially explain the generation ectopic action potentials at 3 dpo, and thus neuropathic pain in vehicle and JQ1-treated animals.[49] The fact that no SDTC significant change could be observed in the vehicle group, may be due to the higher membrane hyperpolarization of the vehicle group with respect to the JQ1 group (explained below), which may lead to a decrease in the values of the parameters characterizing the membrane depolarization of the node.

As mentioned, the QTRAC results reflected that the vehicle group is hyperpolarized at 3 dpo, which is also known to be involved in neuropathic pain generation.[20,53] Hyperpolarization is demonstrated since the resting I/V slope value was significantly decreased in vehicle-treated animals, and also by the significant changes provided by the TE at this time point. Both, the resting I/V slope, and the altered TE parameter alterations where prevented by JQ1 treatment. This effect is likely caused by the enhanced expression of the KCNQ2/3 channels in the vehicle group, which tend to maintain the membrane potential by inducing membrane hyperpolarization,[7,29] and by the increment of the HCN1 channel.[20] In addition, it could be produced by the enhanced inflammation within the vehicle group, which is also known to produce membrane hyperpolarization.[29,39]

At 28 dpo, vehicle-treated animals maintained neuropathic pain, whereas JQ1-treated animals did not. The electrophysiological results show that both the vehicle and the JQ1 treated animals are hyperpolarized. At this time point, the hyperpolarization of the vehicle group is maintained by the KCNQ2/3 and HCN1 channels, whereas the JQ1 treated may be due to the alterations of the ATPase subunits. The subunit FXYD2 of the Na^+/K^+ATPAase pump interacts with the α1NKA subunit of the pump and negatively regulates the pump activity.[51] Thus, the significant reduction of FXYD2 subunit enhances Na^+/K^+ pump activity after SNI, and may be the cause of the hyperpolarization of the axons.

However, despite both groups are hyperpolarized at 28dpo, JQ1 treated animals have a reduction of the inwardly rectifying channels, which may account for the reduction of pain sensitivity. Several excitability parameters found altered at 28 dpo within the TE test, such as the TEh(peak,-70%), S3(-70%), and TEh(peak,-100%) were specific to the JQ1 group. These parameters indicate the capacity of the axon to return to the basal membrane potential after being submitted to a hyperpolarizing current. Similarly, to the resting I/V slope, the alteration of these parameters on the JQ1 group indicate a less capability to recover the membrane potential, and thus a decrease of the inward rectifying currents produced by the HCN channels. Therefore, in the vehicle group, the resulting inwardly rectifying current from HCN1/2, activated after the hyperpolarization that follows an action potential, leads to a sustained activation of HCN1/2 producing a depolarizing current, resulting in repetitive firing.[53] Thus, the higher expression of HCN1/2 facilitates the transmission of action potentials, and maintains pain sensitivity by the vehicle group at 28 dpo.[20] The fact that the HCN channels in the JQ1 group remain at the level of the control group could be produced by the decreased inflammation produced by the treatment.[12,45] In addition, the expression of SCNA3A and SCNA9A channels is down-regulated at 3 and 28 dpo, only by JQ1 treatment, which also may account by a reduction of the transmission of the neural signal corresponding to neuropathic pain within this group.[10,55]

Conclusion

Treatment with the BET inhibitor JQ1 reduced mechanical pain after SNI. There are 2 main mechanisms which contribute to enhance excitability and thus the generation and maintenance of neuropathic pain.[41] One is the release of neuromodulators such as pro-inflammatory cytokines and chemokines, which enhance neuronal excitability. The other one is the altered expression, trafficking and functioning of receptors and ion channels expressed by primary sensory neurons. In this study, we have found that BET inhibition modulated both mechanisms after SNI. The effect on reducing neuroinflammation may be due to the interaction of BET proteins with the p65 transactivation domain of NF-Kb.[24,56] However, is it still unknown if the effect on ion channels and the Na^+/K^+ pump expression, promoting axonal hyperpolarization and thus decreased excitability, is a direct effect of BET proteins targeting their genes, or an indirect effect promoted by decreasing inflammation. Further studies should be performed to shed light onto these interesting mechanisms. Several drugs targeting BET proteins are currently approved for human use, and therefore this study could be easily translated to the clinic.

Acknowledgments

We acknowledge Dr. James Bradner and Dana-Farber Cancer Institute (DFCI) for kindly providing the compound JQ1. We thank Dr. Mihai Moldovan from the University of Cophenhagen for his technical support.

References

1. Acosta C, McMullan S, Djouhri L, Gao L, Watkins R, Berry C, Dempsey K, Lawson SN: HCN1 and HCN2 in Rat DRG neurons: levels in nociceptors and non-nociceptors, NT3-dependence and influence of CFA-induced skin inflammation on HCN2 and NT3 expression. PLoS One 7:e50442, 2012

2. Arnold R, Moldovan M, Rosberg MR, Krishnan AV, Morris R, Krarup C: Nerve excitability in the rat forelimb: a technique to improve translational utility. J Neurosci Methods 275:19-24, 2017

3. Arroyo EJ, Xu T, Poliak S, Watson M, Peles E, Scherer SS: Internodal specializations of myelinated axons in the central nervous system. Cell Tissue Res 305:53-66, 2001

4. Baker M, Bostock H, Grafe P, Martius P: Function and distribution of three types of rectifying channel in rat spinal root myelinated axons. J Physiol 383:45-67, 1987

5. Belkina AC, Nikolajczyk BS, Denis GV: BET protein function is required for inflammation: Brd2 genetic disruption and BET inhibitor JQ1 impair mouse macrophage inflammatory responses. J Immunol 190:3670-3678, 2013

6. Boerio D, Greensmith L, Bostock H: Excitability properties of motor axons in the maturing mouse. J Peripher Nerv Syst 14(1):45-53, 2009

7. Bostock H, Baker M: Evidence for two types of potassium channel in human motor axons in vivo. Brain Res 462:354-358, 1988

8. Bostock H, Cikurel K, Burke D: Threshold tracking techniques in the study of human peripheral nerve. Muscle Nerve 21:137-158, 1998

9. Casals-Diaz L, Vivo M, Navarro X: Nociceptive responses and spinal plastic changes of afferent C-fibers in three neuropathic pain models induced by sciatic nerve injury in the rat. Exp Neurol 217:84-95, 2009

10. Catterall WA: Voltage-gated sodium channels at 60: structure, function and pathophysiology. J Physiol 590:2577-2589, 2012

11. Chaplan SR, Guo HQ, Lee DH, Luo L, Liu C, Kuei C, Velumian AA, Butler MP, Brown SM, Dubin AE: Neuronal hyperpolarization-activated pacemaker channels drive neuropathic pain. J Neurosci 23:1169-1178, 2003

12. Cho HJ, Staikopoulos V, Furness JB, Jennings EA: Inflammation-induced increase in hyperpolarization-activated, cyclic nucleotide-gated channel protein in trigeminal ganglion neurons and the effect of buprenorphine. Neuroscience 162:453-461, 2009

13. Clifford RL, Patel JK, John AE, Tatler AL, Mazengarb L, Brightling CE, Knox AJ: CXCL8 histone H3 acetylation is dysfunctional in airway smooth muscle in asthma: regulation by BET. Am J Physiol Lung Cell Mol Physiol 308:L962-L972, 2015

14. Colleoni M, Sacerdote P: Murine models of human neuropathic pain. Biochim Biophys Acta 1802:924-933, 2010

15. Dib-Hajj SD, Black JA, Waxman SG: Voltage-gated sodium channels: therapeutic targets for pain. Pain Med 10:1260-1269, 2009

16. Doppler K, Sommer C: [Neuropathic pain associated with Nav1.7 mutations: clinical picture and treatment]. Nervenarzt 84:1428-1435, 2013

17. Gao YJ, Ji RR: Chemokines, neuronal-glial interactions, and central processing of neuropathic pain. Pharmacol Ther 126:56-68, 2010

18. Hains BC, Waxman SG: Sodium channel expression and the molecular pathophysiology of pain after SCI. Prog Brain Res 161:195-203, 2007

19. Hargreaves K, Dubner R, Brown F, Flores C, Joris J: A new and sensitive method for measuring thermal nociception in cutaneous hyperalgesia. Pain 32:77-88, 1988

20. He JT, Li XY, Zhao X, Liu X: Hyperpolarization-activated and cyclic nucleotide-gated channel proteins as emerging new targets in neuropathic pain. Rev Neurosci 30:639-649, 2019

21. Herrmann S, Schnorr S, Ludwig A: HCN channels—modulators of cardiac and neuronal excitability. Int J Mol Sci 16:1429-1447, 2015

22. Howells J, Bostock H, Park SB, Kiernan MC, Burke D: Tracking small sensory nerve action potentials in human axonal excitability studies. J Neurosci Methods 298:45-53, 2018

23. Hsieh MC, Ho YC, Lai CY, Wang HH, Lee AS, Cheng JK, Chau YP, Peng HY: Bromodomain-containing protein 4 activates voltage-gated sodium channel 1.7 transcription in dorsal root Ganglia Neurons to mediate thermal hyperalgesia in rats. Anesthesiology 127:862-877, 2017

24. Hytti M, Tokarz P, Maatta E, Piippo N, Korhonen E, Suuronen T, Honkakoski P, Kaarniranta K, Lahtela-Kakkonen M, Kauppinen A: Inhibition of BET bromodomains alleviates inflammation in human RPE cells. Biochem Pharmacol 110-111:71-79, 2016

25. Jahagirdar R, Attwell S, Marusic S, Bendele A, Shenoy N, McLure KG, Gilham D, Norek K, Hansen HC, Yu R, Tobin J, Wagner GS, Young PR, Wong NCW, Kulikowski E: RVX-297, a BET bromodomain inhibitor, has therapeutic effects in preclinical models of acute inflammation and autoimmune disease. Mol Pharmacol 92:694-706, 2017

26. Julius D, Basbaum AI: Molecular mechanisms of nociception. Nature 413:203-210, 2001

27. Kiernan MC, Bostock H, Park SB, Kaji R, Krarup C, Krishnan AV, Kuwabara S, Lin CS, Misawa S, Moldovan M, Sung J, Vucic S, Wainger BJ, Waxman S, Burke D: Measurement of axonal excitability: Consensus guidelines. Clin Neurophysiol 131:308-323, 2020

28. Kiernan MC, Burke D, Andersen KV, Bostock H: Multiple measures of axonal excitability: a new approach in clinical testing. Muscle Nerve 23:399-409, 2000

29. Krishnan AV, Lin CS, Park SB, Kiernan MC: Axonal ion channels from bench to bedside: A translational neuroscience perspective. Prog Neurobiol 89:288-313, 2009

30. Laedermann CJ, Pertin M, Suter MR, Decosterd I: Voltage-gated sodium channel expression in mouse DRG after SNI leads to re-evaluation of projections of injured fibers. Mol Pain 10:19, 2014

31. Lu Q, Peevey J, Jow F, Monaghan MM, Mendoza G, Zhang H, Wu J, Kim CY, Bicksler J, Greenblatt L, Lin SS, Childers W, Bowlby MR: Disruption of Kv1.1 N-type inactivation by novel small molecule inhibitors (disinactivators). Bioorg Med Chem 16:3067-3075, 2008

32. Makker PGS, Matamala JM, Park SB, Lees JG, Kiernan MC, Burke D, Moalem-Taylor G, Howells J: A unified model of the excitability of mouse sensory and motor axons. J Peripher Nerv Syst 23:159-173, 2018

33. McMahon SB, Cafferty WB, Marchand F: Immune and glial cell factors as pain mediators and modulators. Exp Neurol 192:444-462, 2005

34. Moldovan M, Alvarez S, Rosberg MR, Krarup C: Persistent alterations in active and passive electrical membrane properties of regenerated nerve fibers of man and mice. Eur J Neurosci 43:388-403, 2016

35. Moldovan M, Rosberg MR, Alvarez S, Klein D, Martini R, Krarup C: Aging-associated changes in motor axon voltage-gated Na(+) channel function in mice. Neurobiol Aging 39:128-139, 2016

36. Nicodeme E, Jeffrey KL, Schaefer U, Beinke S, Dewell S, Chung CW, Chandwani R, Marazzi I, Wilson P, Coste H, White J, Kirilovsky J, Rice CM, Lora JM, Prinjha RK, Lee K, Tarakhovsky A: Suppression of inflammation by a synthetic histone mimic. Nature 468:1119-1123, 2010

37. Nodera H, Rutkove SB: Accommodation to hyperpolarizing currents: differences between motor and sensory nerves in mice. Neurosci Lett 518:111-116, 2012

38. Osaki Y, Nodera H, Banzrai C, Endo S, Takayasu H, Mori A, Shimatani Y, Kaji R: Effects of anesthetic agents on in vivo axonal HCN current in normal mice. Clin Neurophysiol 126:2033-2039, 2015

39. Park SB, Kiernan MC, Vucic S: Axonal excitability in amyotrophic lateral sclerosis: Axonal excitability in ALS. Neurotherapeutics 14:78-90, 2017

40. Pathak D, Guan D, Foehring RC: Roles of specific Kv channel types in repolarization of the action potential in genetically identified subclasses of pyramidal neurons in mouse neocortex. J Neurophysiol 115:2317-2329, 2016

41. Penas C, Navarro X: Epigenetic modifications associated to neuroinflammation and neuropathic pain after neural trauma. Front Cell Neurosci 12:158, 2018

42. Randall LO, Selitto JJ: A method for measurement of analgesic activity on inflamed tissue. Arch Int Pharmacodyn Ther 111:409-419, 1957

43. Sanchez-Ventura J, Amo-Aparicio J, Navarro X, Penas C: BET protein inhibition regulates cytokine production and promotes neuroprotection after spinal cord injury. J Neuroinflammation 16:124, 2019

44. Schwarz JR, Glassmeier G, Cooper EC, Kao TC, Nodera H, Tabuena D, Kaji R, Bostock H: KCNQ channels mediate IKs, a slow K+ current regulating excitability in the rat node of Ranvier. J Physiol 573(Pt 1):17-34, 2006

45. Smith T, Al Otaibi M, Sathish J, Djouhri L: Increased expression of HCN2 channel protein in L4 dorsal root ganglion neurons following axotomy of L5- and inflammation of L4-spinal nerves in rats. Neuroscience 295:90-102, 2015

46. Tan ZY, Donnelly DF, LaMotte RH: Effects of a chronic compression of the dorsal root ganglion on voltage-gated Na+ and K+ currents in cutaneous afferent neurons. J Neurophysiol 95:1115-1123, 2006

47. Taniguchi Y: The bromodomain and extra-terminal domain (BET) family: Functional anatomy of BET paralogous proteins. Int J Mol Sci 17, 2016

48. Tibbs GR, Posson DJ, Goldstein PA: Voltage-gated Ion channels in the PNS: Novel therapies for neuropathic pain? Trends Pharmacol Sci 37:522-542, 2016

49. Tsantoulas C, Denk F, Signore M, Nassar MA, Futai K, McMahon SB: Mice lacking Kcns1 in peripheral neurons show increased basal and neuropathic pain sensitivity. Pain 159:1641-1651, 2018

50. Tsantoulas C, Mooney ER, McNaughton PA: HCN2 ion channels: basic science opens up possibilities for therapeutic intervention in neuropathic pain. Biochem J 473:2717-2736, 2016

51. Wang F, Cai B, Li KC, Hu XY, Lu YJ, Wang Q, Bao L, Zhang X: FXYD2, a gamma subunit of Na(+), K(+)-ATPase, maintains persistent mechanical allodynia induced by inflammation. Cell Res 25:318-334, 2015

52. Woolf CJ, Salter MW: Neuronal plasticity: Increasing the gain in pain. Science 288:1765-1769, 2000

53. Yao H, Donnelly DF, Ma C, LaMotte RH: Upregulation of the hyperpolarization-activated cation current after chronic compression of the dorsal root ganglion. J Neurosci 23:2069-2074, 2003

54. Yu T, Li L, Liu H, Li H, Liu Z, Li Z: KCNQ2/3/5 channels in dorsal root ganglion neurons can be therapeutic targets of neuropathic pain in diabetic rats. Mol Pain 14:1744806918793229, 2018

55. Zheng YM, Wang WF, Li YF, Yu Y, Gao ZB: Enhancing inactivation rather than reducing activation of Nav1.7 channels by a clinically effective analgesic CNV1014802. Acta Pharmacol Sin 39:587-596, 2018

56. Zuliani V, Rivara M, Fantini M, Costantino G: Sodium channel blockers for neuropathic pain. Expert Opin Ther Pat 20:755-779, 2010

Chapter 2

BET protein inhibition in macrophages enhances dorsal root ganglion neurite outgrowth in female mice

Received: 16 November 2020 | Revised: 31 January 2022 | Accepted: 13 February 2022

DOI: 10.1002/jnr.25036

RESEARCH ARTICLE

JOURNAL OF Neuroscience Research

BET protein inhibition in macrophages enhances dorsal root ganglion neurite outgrowth in female mice

Georgina Palomés-Borrajo | Xavier Navarro | Clara Penas

Department of Cell Biology, Physiology and Immunology, Centro de Investigación Biomédica en Red sobre Enfermedades Neurodegenerativas (CIBERNED), Institute of Neurosciences, Universitat Autònoma de Barcelona, Bellaterra, Spain

Correspondence
Clara Penas, Department of Cell Biology, Physiology and Immunology, Centro de Investigación Biomédica en Red sobre Enfermedades Neurodegenerativas (CIBERNED), Institute of Neurosciences, Universitat Autònoma de Barcelona, 08193 Bellaterra, Spain.
Email: clara.penas@uab.cat

Funding information
This work was supported by grant PID2019-108496RA-I00 from Ministerio de Ciencia e Innovación and Agencia Estatal de Investigación of Spain, CIBERNED (CB06/05/1105) and TERCEL (RD16/0011/0014) funds from the Instituto de Salud Carlos III of Spain, co-funded by European Union (ERDF/ESF, "Investing in your future")

Abstract

Peripheral nerve regeneration is limited after injury, especially in humans, due to the large distance the axons have to grow in the limbs. This process is highly dependent on the expression of neuroinflammatory factors produced by macrophages and glial cells. Given the importance of the epigenetic BET proteins on inflammation, we aimed to ascertain if BET inhibition may have an effect on axonal outgrowth. For this purpose, we treated female mice with JQ1 or vehicle after sciatic nerve crush injury and analyzed target reinnervation. We also used dorsal root ganglion (DRG) culture explants to analyze the effects of direct BET inhibition or treatment with conditioned medium from BET-inhibited macrophages. We observed that although JQ1 produced an enhancement of IL-4, IL-13, and GAP43 expression, it did not have an effect on sensory or motor reinnervation after crush injury in vivo. In contrast, JQ1 reduced neurite growth when interacting directly with DRG neurons ex vivo, whereas conditioned medium from JQ1-treated macrophages promoted neurite outgrowth. Therefore, BET-inhibited macrophages secrete pro-regenerative factors that induce neurite outgrowth, and that may counteract the direct inhibition of BET proteins in neurons in vivo. Finally, we observed an activation of the STAT6 pathway in DRG explants treated with conditioned medium from JQ1-treated macrophages. In conclusion, this study demonstrates that BET protein inhibition in macrophages provides a mechanism to enhance axonal outgrowth. However, specific targeting of BET proteins to macrophages will be needed to efficiently enhance functional recovery after nerve injury.

KEYWORDS
BET proteins, cytokines, inflammation, neurite outgrowth, regeneration

1 | INTRODUCTION

Peripheral nerve injuries (PNIs) result in the disconnection between the neuronal soma and the distal axon stump, leading to the degeneration of distal fibers and the eventual death of axotomized neurons. As a result, there is a partial or total loss of sensory, motor, and autonomic functions (Allodi et al., 2012; Navarro et al., 2007). PNI affects 1.8% of subjects with traumatic limb injuries in Europe. Patients undergo prolonged rehabilitation and current treatments produce a scarce functional outcome (Huckhagel et al., 2018). Hence, it is important to find novel strategies that promote regeneration and recovery after PNI. In fact, peripheral nerve regeneration is limited after injury, especially in humans, due to the large distances the axons have to grow. One way to overcome this problem is by

Edited by Cristina Antonella Ghiani and Dena R Howland. Reviewed by Lynnette Montgomery, Megan Detloff and John Gensel

promoting an acceleration of axonal regeneration (DeFrancesco-Lisowitz et al., 2015; Ma et al., 2011).

During Wallerian degeneration of the distal stump, a network of different cells, including infiltrating macrophages and Schwann cells, participate in axonal and myelin breakdown, through the release of different products. Between these molecules, cytokines and chemokines are essential to regulate the microenvironment that promotes axonal regeneration (Chen, Lin, et al., 2016; DeFrancesco-Lisowitz et al., 2015). Thus, Wallerian degeneration is a cascade of events that reassemble an immune-like reaction, which can be divided in two main phases. The early phase is characterized by the synthesis of inflammatory cytokines and chemokines such as TNF-α, IL-1α, IL-1ß, IL-6, and CCL2, inducing the recruitment of immune cells. The late phase is defined by the increase in anti-inflammatory cytokines such as IL-13, IL-10, and IL-4, and promotes the clearance of debris (Rotshenker, 2011; Vidal et al., 2013). Both processes are indispensable for successful nerve regeneration. For instance, it has been demonstrated that the enhancement of the anti-inflammatory phase attenuates pro-inflammatory cytokine secretion, concludes degeneration, and increases axonal outgrowth (Fregnan et al., 2012; Siqueira Mietto et al., 2015; Vidal et al., 2013). Thus, to provide a favorable environment for axonal growth, it is crucial to achieve a rapid transition from the pro-inflammatory phase toward the anti-inflammatory phase of Wallerian degeneration. Experimental evidence has shown that cytokines trigger JAK/STAT signaling pathways, which are associated with neural plasticity. Particularly, IL-4 and IL-13 activate STAT6, leading to neuroprotection (Bhattarai et al., 2016; Deboy et al., 2006; Vidal et al., 2013). IL-6 and IL-10 activate the STAT3-mediated pathway, increasing regeneration and neuroprotection of cortical neurons (Chen, Lin, et al., 2016; Dubovy et al., 2019).

BET proteins are epigenetic readers of acetylated lysine residues in histone and nonhistone proteins, and are associated with cellular growth, evasion of apoptosis, and inflammatory response (Filippakopoulos & Knapp, 2014). BET family comprises BRD2, BRD3, BRD4, and the testis-specific protein BRDT. The most studied member of this family is BRD4. BRD4 interacts with an acetylated p65/RELA subunit, triggering the recruitment of p-TEFb complex and stimulating the transcription of NF-kß genes (Hajmirza et al., 2018). Inhibition of BET proteins through the small molecule JQ1 reduces the expression of inflammatory cytokines and prevents TNF-inducible gene expression in macrophages in vitro (Nicodeme et al., 2010). In addition, we have previously found that treatment with the BET inhibitor JQ1 reduces inflammation, increases the presence of anti-inflammatory cytokines, and enhances functional outcome after spinal cord injury (Sanchez-Ventura et al., 2019). Given the importance of BET proteins on inflammatory gene expression, we hypothesized that BET inhibition could favor an early conclusion of Wallerian degeneration through the downregulation of pro-inflammatory cytokines and the upregulation of anti-inflammatory cytokines. Such a process may enhance axonal growth after PNI via JAK/STAT pathways.

We used the BET inhibitor JQ1 and analyzed its effects after PNI in mice. To further analyze the effects of BET proteins on neuronal outgrowth ex vivo, we treated dorsal root ganglion (DRG) neuronal explants with JQ1. In addition, we used conditioned medium from JQ1-treated macrophages, and assessed its effect on DRG neurite growth. In summary, this study aims to determine the role of BET protein inhibition on axonal regeneration and functional recovery after PNI.

Significance

We have found that inhibition of BET proteins in macrophages produce the expression of pro-regenerative factors by these cells. These factors promote neuronal neurite growth. This finding may be important to promote nerve regeneration after peripheral nerve injury.

2 | MATERIALS AND METHODS

2.1 | Animals and surgery

All animal procedures were approved by the Universitat Autònoma de Barcelona Animal Experimentation Ethical Committee (code 10306) and followed the European Commission Directive 2010/63/EU on the protection of animals used for scientific purposes. Female C57BL/6J mice (Charles River Laboratories) were used in all the experiments, which were kept under a 12-hr light cycle and had access to water and food *at libitum*.

To perform nerve injury, 7-week-old female mice were anesthetized by intraperitoneal injection of ketamine (90 mg/kg) and xylazine (10 mg/kg) in saline. Sciatic nerve crush injury was performed on the right hind limb at 45 mm distance from the tip of the fourth digit. The lesion consisted on applying a tight pressure sing forceps (Dumont #5) at the sciatic nerve 3 times during 30 seconds, with different orientations each. Then, the muscle and skin were closed in layers. To prevent reopening and later infection of the wound, the skin was secured with staples and iodine was topically applied. Mice were kept in a warm environment until they recovered from anesthesia. Operated animals were intraperitoneally administered with vehicle (saline with 5% DMSO and 5% Tween-80), or with JQ1 (30 mg/kg, diluted in vehicle) starting at 2 hr (day 0) or at 4 days postoperation (dpo). Each cage of mice contained animals treated with the different conditions, to minimize experimental bias. A total of 27 animals for in vivo studies (15 animals for functional testing and 12 for western blot and qPCR studies) were used.

2.2 | Functional testing

Evaluation of axonal regeneration and target reinnervation was conducted through noninvasive electrophysiological tests at 14, 21, and 28 dpo ($n = 5$ animals per condition). Prior to the functional

test, mice were anesthetized by intraperitoneal injection with 0.04 ml of ketamine/xylazine mixture. For assessment of peripheral nerve conduction, the sciatic nerve was stimulated with single electrical pulses of 0.02-ms duration up to supramaximal intensity, delivered by needles inserted percutaneously at the sciatic notch. Compound muscle action potentials (CMAPs) of the tibialis anterior and plantar muscles were recorded by means of needle electrodes, amplified and displayed on the oscilloscope to measure the amplitude and the latency of the M wave (Navarro, 2016). For sensory nerve conduction, the digital nerve was stimulated similarly, with short-duration electrical pulses of increasing intensity delivered at the sciatic notch. The evoked compound nerve action potentials (CNAPs) were recorded distally at the fourth digit. Functional tests were also performed in the contralateral hind limb as control values for each group.

2.3 | Analysis of skin reinnervation

Animals were intraperitoneally anesthetized with 0.2 ml of 1:1 pentobarbital-saline mixture at 28 dpo and perfused with 4% paraformaldehyde (PFA) ($n = 5$ animals per condition). The distal plantar pads of the hind paw were carefully excised and postfixed with 4% paraformaldehyde for an hour to be later cryopreserved in sucrose 30% solution. Pads 1, referred as the most distal and medial pads that belong to the innervation territory of the sciatic and saphenous nerves, and Pads 2, referred as the most distal and lateral pads that belong only to the innervation territory of the sciatic nerve, were cut longitudinally at 40 μm thickness in a Leica CM190 cryostat (https://drp8p5tqcb2p5.cloudfront.net/fileadmin/downloads_lbs/Leica%20CM1950/User%20Manuals/Leica_CM1950_IFU_2v1N_en.pdf, RRID:SCR_018061). Free-floating samples were washed with PBS and PBS-0.3% Tween, and later incubated overnight at 4°C with PBS-0.3%Triton, 1.5% normal donkey serum, and rabbit anti-PGP9.5 antibody (Table 1). Samples were washed with PBS-0.3% Tween and again incubated overnight at 4°C with PBS 0.3% Triton, normal donkey serum 5% and Alexa fluor 594 donkey anti-rabbit (Table 1) Pad slices were washed with PBS-0.3% Tween, PBS, incubated 1/5,000 in DAPI-PB for 2 min and washed in PB 1x. Samples were then heated at 37°C until dry and mounted with Fluoromount.

Intraepidermal nerve fiber (IENF) density and the number of Meissner corpuscles were estimated using a Olympus BX51 Fluorescence Microscope (https://www.olympus-lifescience.com/en/microscope-resource/primer/techniques/fluorescence/bx51fluorescence/, RRID:SCR_018949). IENFs were counted on the lateral area of the pads, whereas Meissner's corpuscles are found on the apex. To determine the number of IENFs per mm length, the basal layer was localized by the observation of DAPI staining. The ocular 40× grid was oriented following the basal layer to determine the number of nerve fibers that crossed it. A total of two fields per slice were counted. The number of Meissner's corpuscles was also determined at 400× magnification.

2.4 | Analysis of mRNA expression in sciatic nerve

Seven days after the crush injury, mice were perfused with sterile saline ($n = 3$ or 4 mice per group). Then, injured sciatic nerves were removed and snap-frozen. Tissue was homogenized with QIAzol lysis reagent (QIAGEN), and RNA was extracted using the RNeasy Mini Kit (QIAGEN) following the manufacturer's guidelines. RNA was quantified with a Thermo Fisher NanoDrop 1000 Spectrophotometer (http://tools.thermofisher.com/content/sfs/manuals/nd-1000-v3.8-users-manual-8%205x11.pdf, RRID:SCR_016517) and reverse-transcribed using an Applied Biosystems kit (Thermo Fisher Scientific). Then, the expression of target sequences was quantified by RTqPCR using SYBR Green QPCR Master Mix (Agilent Technologies) and the corresponding primers (Table 2). Glyceraldehyde-3-phosphate dehydrogenase (GAPDH) was used as a housekeeping gene.

2.5 | Bone marrow-derived macrophage (BMDM) primary culture

Mice were euthanized with pentobarbital diluted in saline (1:1) and cleaned with ethanol 70%. Femur and tibial bones were dissected, bone epiphyses removed, and bone marrows flushed with chilled PBS using a 10-ml syringe and 25G needle. Cells were centrifuged at 500 RCF for 10 min, to be later cultured in 100 ml Petri plates with DMEM/F12 medium that contained 10% fetal bovine serum, 1% penicillin–streptomycin, and L-glutamine. Macrophage colony-stimulating factor (M-CSF) was added at 10 ng/ml. Medium was replaced every 3 days with the correspondent addition of M-CSF. At 8 days in vitro (div), adherent cells were reseeded in 6-well plate in a density of 1.6×10^6 cells/well with the medium mentioned above, but without the differentiating factor. Cells were treated at 10 div with vehicle containing DMSO or JQ1 1,000 nM for 6 hr ($n = 3$ independent experiments). Then, conditioned medium was harvested and snap-frozen with liquid nitrogen.

Media from treated-BMDM cells were filtered through 10 kDa ultrafiltration filters (Merck Millipore). Samples were centrifuged at 4°C and 10 000× *g* for 1 hr. A concentrated medium volume of 50 μl was obtained from each 1 ml medium sample, thus concentrated 20×. Concentrated media were snap-frozen in liquid nitrogen.

2.6 | DRG explant culture with or without BMDM-conditioned media

Mice were euthanized with pentobarbital diluted in saline (1:1) and washed in 70% ethanol. All DRGs were extracted using sterilized surgery tools and preserved in cold Gey's balanced solution with 0.6% glucose. DRG roots were removed and nervous tissue was exposed. DRGs were placed in a 24-well plate between two droplets of collagen mixture in Neurobasal-A medium with 1% penicillin–streptomycin, 1x B-27, 0.5% glucose, 0.5% glutamax, and murine

TABLE 1 Antibody list

Name of primary antibody	Immunogen	Manufacturer, catalog number, RRID, host	Used concentration, application
RT-97	H-Neurofilament	DSHB Cat# rt97, RRID:AB_528399, mose, monoclonal	1/200, IHC
PGP 9.5 (UCHL1)	PGP 9.5	(CEDARLANE Cat# CL7756AP, RRID:AB_2792979, rabbit, polyclonal	1/500, IHC
Stat3 (79D7)	Stat3	Cell Signaling Technology Cat# 4904, RRID:AB_331269, rabbit, monoclonal	1/1,000, WB
Phospho-Stat3 (Tyr705) (D3A7)	Phospho-Stat3 (Tyr705)	(Cell Signaling Technology Cat# 9145, RRID:AB_2491009), rabbit, monoclonal	1/1,000, WB
Stat6 (D3H4)	Stat6	(Cell Signaling Technology Cat# 5397, RRID:AB_11220421), rabbit, monoclonal	1/1,000, WB
Phospho-STAT6 (Tyr641) (46H1L12)	Phospho-STAT6 (Tyr641)	(Thermo Fisher Scientific Cat# 700247, RRID:AB_2532305), rabbit, monoclonal	1/250, WB
Monoclonal Anti-α-tubulin antibody produced in mouse	α-Tubulin	(Sigma-Aldrich Cat# T9026,RRID:AB_477593) mouse, monoclonal	1/10,000 WB
Name of secondary antibody	**Immunogen**	**Manufacturer, catalog number, RRID, Host**	**Used concentration, application**
Donkey Anti-Rabbit IgG (H + L) Antibody, Alexa Fluor 594 Conjugated	Rabbit IgG (H + L)	(Molecular Probes Cat# A-21207, RRID:AB_141637), donkey	1/200, IHC
Donkey Anti-Mouse IgG (H + L) Antibody, Alexa Fluor 594 Conjugated	Mouse IgG (H+L)	(Molecular Probes Cat# A-21203, RRID:AB_141633), donkey	1/200, IHC
Goat Anti-Rabbit IgG (H L)-HRP Conjugate antibody	Goat Rabbit IgG (H + L)	(Bio-Rad Cat# 170–6515, RRID:AB_11125142), goat	1/3,000, WB
Goat Anti-Mouse IgG (H L)-HRP Conjugate antibody	Goat Mouse IgG (H + L)	(Bio-Rad Cat# 170–6516, RRID:AB_11125547), goat	1/3,000, WB
DAPI		(Sigma-Aldrich Cat#D9564-10MG)	1/5,000 in Pads; 1/1,000 in DRGs

TABLE 2 Primer list

Gene	Forward primer: 5′-3′	Reverse primer: 5′-3′
Mouse BDNF	TGCAGGGGCATAGACAAAAGG	CTTATGAATCGCCAGCCAATTCTC
Mouse CD68	CCAATTCAGGGTGGAAGAAA	ATGGGTACCGTCACAACCTC
Mouse GAPDH	TGGCCTTCCGTGTTCCTAC	GAGTTGCTGTTGAAGTCG
Mouse GAP43	CTGCTGTCACTGATGCTGCT	GGTTTGGCTTCGTCTACAGC
Mouse GDNF	ATTTTATTCAAGCCACCATTA	GATACATCCACACCGTTTAGC
Mouse IL-4	GGCTTTCCTCTTTCCCACTC	AGCCGCCATGAGAGCTAAG
Mouse IL-10	GCTGAGACTTTCGCTCCTCTC	AGCTCCAAGGCACCTGTTC
Mouse IL-13	TCCAATTGCAATGCCATCTA	TGGGCTACTTCGATTTTGGT
Mouse iNOS	GGCCAGCCTGTGAGACCTTT	TTGGAAGTGAAGCGTTTCG
Mouse NGF	CAAGGACGCAGCTTTCTATACTG	CTTCAGGGACAGAGTCTCCTTCT
Mouse SCG-10	TTCTCGTGGAGTGTGTGCTTCACT	TAGCTTTGTGTTTGTGTTCGGCCC

β-NGF (100 ng/ml, Peprotech). The collagen mixture used for the culture consisted in 446.43 µl of rat collagen type 1 (Corning), 50 µl of MEM 10X medium, 2 µl of 7.5% sodium bicarbonate (Gibco), and 1.57 µl of PBS. Either JQ1 (500 or 1,000 nM) or DMSO was added into the collagen and into the medium. The culture was maintained for 2 div before fixation and immunohistochemical analysis.

For DRG explant culture with BMDM-conditioned medium, the procedure was the same except for the preparation of the collagen mixture. In this case, half of the MEM 10x medium was substituted with conditioned medium and the amount of sodium bicarbonate added to the mixture was 8 µl. Provided that JQ1 is a small compound that is filtered during medium concentration, JQ1 or DMSO was also added to collagen

to obtain a 500 nM concentration. This procedure resulted in four experimental culture groups: DMSO-treated DRGs with conditioned medium from DMSO-treated macrophages (D + mD), DMSO-treated DRGs with conditioned medium from JQ1-treated macrophages (D + mJQ1), JQ1-treated DRGs with conditioned medium from DMSO-treated macrophages (JQ1 + mD), and JQ1-treated DRGs with conditioned medium from JQ1-treated macrophages (JQ1 + mJQ1) ($n = 3$ independent experiments). The cultures were also maintained 2 div before fixation.

2.7 | Determination of neurite outgrowth in DRG explants

After 2 div, DRG explants were fixed for 30 min with PFA 4%. Then, samples underwent several washes with TBS-0.1% Tween before being incubated for an hour in citrate buffer (pH = 6.4) heated until boiling temperature, and washed again in TBS-0.1% Tween. DRGs were incubated in increasing concentrations of methanol (50%, 70%, and 100%), washed in TBS-0.1% Tween and incubated for 48 hr at 4°C in TBS-0.3% Triton, 5% normal donkey serum, and anti-H-Neurofilament antibody (Table 1). DRGs were washed with TBS-0.1% Tween and incubated overnight at 4°C with TBS-0.3% Triton, 5% normal donkey serum, and Alexa fluor 594 Donkey anti-mouse (Table 1). Samples were washed, dried, and mounted with Fluoromont.

DRG samples were observed under a fluorescence microscope (Olympus BX51). Images of overlapping territories of each DRG were taken with 20X objective, the microscope camera (Olympus PD37) and CellSens Entry Olympus software (https://www.selectscience.net/products/cellsens-entry---microscopy-imaging-software/?prodID=172461, RRID:SCR_014551). DRG images were reconstructed with Photoshop. Maximum neurite length and the number of neurites of different lengths were measured with the Image J plugin Neurite J (Torres-Espin et al., 2014). The software provided the number of neurite intersections every 25 μm, and the longest neurite value for each DRG. Number of analyzed samples per group was between five and seven DRGs in the BET inhibition study, and between seven and 12 in the conditioned medium study, obtained from three independent cultures in both cases. The analysis of neurite outgrowth was performed by a blinded examiner.

2.8 | Cell viability assay from dissociated DRGs' culture

Mice were euthanized with pentobarbital and saline mixture (1:1). All dorsal root ganglia were extracted with sterilized tools and kept in cold Gey's balanced solution with 2% glucose. DRG roots were cut to disclose nervous tissue. Then, cleaned ganglia underwent an enzymatic digestion with trypsin 1x, collagenase 1x, and DNase (1 mg/ml) diluted in Hank's Balanced Salt Solution (HBSS, Gibco) for 20 min at 37°C. Next, enzymatic digestion was arrested with DMEM/F12 medium containing 10% FBS, 1% penicillin and streptomycin, and L-glutamine, before proceeding with the mechanical digestion. Cells were then filtered within a 70-μm sterile filter to remove myelin fragments. Dissociated ganglia underwent a centrifugation at 900 rpm for 7 min and neurons were counted with a Neubauer chamber. A total of eight wells were seeded per animal in a 96-multiwell plate pretreated with Poly-D-lysine (0.01 mg/ml) and laminin (2 μg/ml). Each well held between 5000 and 6000 neurons that were maintained in Neurobasal-A medium with 2% B-27, 2% glucose at 30%, 1% glutamine, and 1% penicillin and streptomycin. After 2 hr, medium was replaced.

At 2 div, cells were treated in duplicates with vehicle containing DMSO, JQ1 500 nM, JQ1 1000 nM, or cisplatin 5 μg, used as a positive control. At 4 div, an MTT (3-[4,5-dimethylthiazol-2-yl]-2,5-dipheny ltetrazolium bromide) assay was performed to determine cell viability. For this purpose, media was replaced with media containing 0.15 mg/ml MTT. Next, the culture was maintained at 37°C for 2 hr, to finally obtain cells lysed with DMSO. Absorbance was read out through a spectrophotometer (Bio-tek) at 560 nm and 600 nm wavelength using KC Junior software. Readings were normalized against control to obtain the percentage of survival. In total, there were five independent cultures.

2.9 | Western blot

Protein samples for western blot analysis were obtained from DRG explant cultures treated with conditioned medium from DMSO- or JQ1-treated macrophages. At 2 div, collagen layers encapsulating the ganglia were removed using forceps (Dumont #5). DRGs were collected in a cryovial according to the treatment and were immediately snap-frozen in liquid nitrogen. Next, DRGs were homogenized with modified RIPA buffer with protease (100 X) (Sigma) and phosphatase (20X) (Roche) inhibitors. Samples underwent sonication and centrifugation at 14,000 rpm for 20 min at 4°C. Protein concentration of the supernatant was determined with a bicinchoninic acid assay (Pierce). SDS-PAGE was conducted in a 7.5% acrylamide gel, where 20 μg of protein was loaded from each sample. Proteins were transferred to a PVDF membrane, that was blocked in 3% BSA prior to an overnight incubation with the appropriate primary antibodies. Several washings with TBS-Tween 0.1% were performed and the correspondent secondary antibodies incubated during 2 hr at room temperature. Finally, membranes underwent multiple washes with TBS-Tween 0.1% and TBS, before image acquisition with Bio-Rad Chemidoc XRS Gel Imaging System (https://www.bio-rad.com/en-us/product/chemidoc-xrs-system?ID=NINJHRKG4, RRID:SCR_019690). Quantification was then assessed using the ImageLab software (http://www.bio-rad.com/en-us/sku/1709690-image-lab-software, RRID:SCR_014210). Protein levels were analyzed considering the relative intensities of the bands of the phosphorylated protein forms, which were later compared to total non-phosphorylated protein. Then, results were normalized to control. Primary and secondary antibodies used for western blot are in Table 1. There were three blots per protein analysis.

2.10 | Statistical analysis

Data were expressed as mean ± standard deviation (SD) as minimum to maximum in Box and Whisker plots. Data distribution and outliers were determined using the GraphPad Prism software. Results were analyzed with GraphPad Prism 7 software, and significant differences considered when $p < 0.05$. For electrophysiological tests, CMAP values were analyzed by two-way ANOVA followed by Tukey's correction for multiple comparisons, with day and amplitude or latency as factors. The CNAP results were compared with an unpaired *t* test since only a final value was recorded. Histological data of pad reinnervation were analyzed by unpaired *t* test. For statistical analysis of mRNA expression, maximum neurite length of DRG explants treated with increasing doses of JQ1, and cell viability assay, one-way ANOVA followed by a multiple comparison test with Tukey's correction was performed, since only the level of the mRNA, the number of neurites. and % of viable cells were analyzed within the different conditions. The number of neurites at variable distances was analyzed through a two-way ANOVA followed by Sidak's correction for multiple comparisons, using the distance growth and treatments as factors. Maximum neurite length for the conditioned medium experiment was also analyzed using a two-way ANOVA followed by Sidak's correction, in which conditioned media and treatment were factors. For WB analysis, a paired *t* test was conducted, to compare the level of the protein between treatments.

3 | RESULTS

3.1 | Delayed treatment with JQ1 promotes enhanced expression of anti-inflammatory cytokines and the axonal growth marker GAP43 after sciatic nerve crush

Since BET protein inhibition by JQ1 alters macrophage transcriptional state (Nicodeme et al., 2010; Sanchez-Ventura et al., 2019) and macrophage infiltration after PNI occurs early after injury, we compared the effect between an early and a delayed treatment with JQ1 in sciatic nerve (Figure 1a). We observed a reduced expression of the macrophage marker *Cluster of differentiation 68* (CD68) when the treatment started at 0 dpo, indicating a reduction on macrophage infiltration ($F_{2,7} = 4.637$, $p = 0.052$). The expression of *inducible nitric oxide synthase* (iNOS) and CD206, which correspond to M1 and M2 macrophage markers, respectively, was also reduced within this treatment, probably due also to a lessened macrophage infiltration (iNOS, $F_{2,6} = 14.170$, $p = 0.004$) (CD206, $F_{2,6} = 13.660$, $p = 0.006$). However, when the treatment started at 4 dpo, we did not observe changes in CD68, iNOS, or CD206 mRNA expression compared to vehicle-treated animals, indicating that the delayed treatment allowed macrophages to infiltrate, and that JQ1 does not affect M1/M2 macrophage polarization. IL-4 and IL-13 anti-inflammatory cytokine expression was statistically enhanced within animals treated with JQ1 from 4 dpo (IL-4, $F_{2,6} = 20.380$, $p = 0.002$) (IL-13, $F_{2,6} = 10.520$, $p = 0.011$), whereas IL-10 was not altered ($F_{2,7} = 4.023$, $p = 0.069$) (Figure 1b). A mild increase of IL-4 also was observed when the treatment started at 0 dpo. We further studied the effects of JQ1 in neurotrophic factor expression. We did not observe changes of *glial-derived neurotrophic factor* (GDNF) ($F_{2,7} = 0.137$, $p = 0.874$) and *brain-derived neurotrophic factor* (BDNF) ($F_{2,7} = 1.833$, $p = 0.229$) expression, whereas we found a reduction of *nerve growth factor* (NGF) with the treatment starting at 0 dpo ($F_{2,7} = 14.400$, $p = 0.003$), probably due to the reduced infiltration of macrophages.

We then wanted to ascertain if the transcriptional alterations promoted by JQ1 produced an effect on axonal growth markers expression (Figure 1c). We did not observe an alteration in the *superior cervical ganglion-10 protein* (SGC-10) ($F_{2,6} = 1.833$, $p = 0.229$), whereas we found an enhanced expression of the *Growth associated protein 43* (GAP43) when the treatment started at 4 dpo ($F_{2,6} = 6.698$, $p = 0.0270$). Therefore, we planned to further study the effects of axonal regeneration in vivo by a delayed treatment with JQ1.

3.2 | BET protein inhibition does not enhance nerve regeneration after sciatic nerve crush

The analysis of functional and histological outcome was performed in mice with delayed treatment of vehicle and JQ1. Motor nerve conduction tests determine muscle reinnervation, as recorded CMAPs, by regenerated axons after injury. CMAPs were first recorded in the tibialis anterior and plantar muscles at 14 dpo, being of small amplitude and increased latency (Figure 2). At later time points, the latency time decreased indicating axonal enlargement and remyelination after reinnervating the muscle fibers. No differences were found between vehicle and JQ1-treated animals ($F_{2,14} = 1.380$, $p = 0.280$ for tibialis anterior and $F_{2,14} = 0.057$, $p = 0.945$ for plantar muscle). Regarding the amplitude of the CMAP, which determines the amount of innervated muscle fibers, as indicator of nerve regeneration, at 14 dpo the M amplitude was very low in both muscles, around 5% of control values in the tibialis anterior muscle (Figure 2a) and 2.5% in the plantar muscle (Figure 2b). At 21 and 28 dpo, the CMAP amplitude increased in both muscles recorded. However, there were not significant differences between JQ1-treated and vehicle-treated groups ($F_{2,14} = 0.354$, $p = 0.708$ for tibialis anterior and $F_{2,14} = 0.596$, $p = 0.565$ for plantar muscle).

For the sensory nerve conduction test, CNAPs of the digital nerve were recorded only at 28 dpo. The CNAP latency was increased in the two groups of mice ($t_7 = 2.516$, $p = 0.040$). Regarding CNAP amplitude, although JQ1-treated group showed a tendency to be higher (30%) compared to the vehicle-treated group (25%), the difference was not statistically significant (Figure 2c) ($t_7 = 1.126$, $p = 0.297$).

To further study the effects of BET inhibition on axonal regeneration, we analyzed skin reinnervation of the hind paw. Regarding IENF density, JQ1-treated animals showed a tendency of higher number of IENFs/mm (Figure 3b), compared to vehicle-treated animals. However, no statistical differences were found. This was observed in medial Pads 1 (Vehicle: 47.58 ± 5.39; JQ1: 61.17 ± 1.64) ($t_5 = 2.082$, $p = 0.092$), as well as in lateral Pads 2 (Vehicle: 45.05 ± 2.10; JQ1: 48.28 ± 1.81) ($t_7 = 1.166$, $p = 0.280$). Regarding the number of Meissner's corpuscles (Figure 3c), no significant differences were

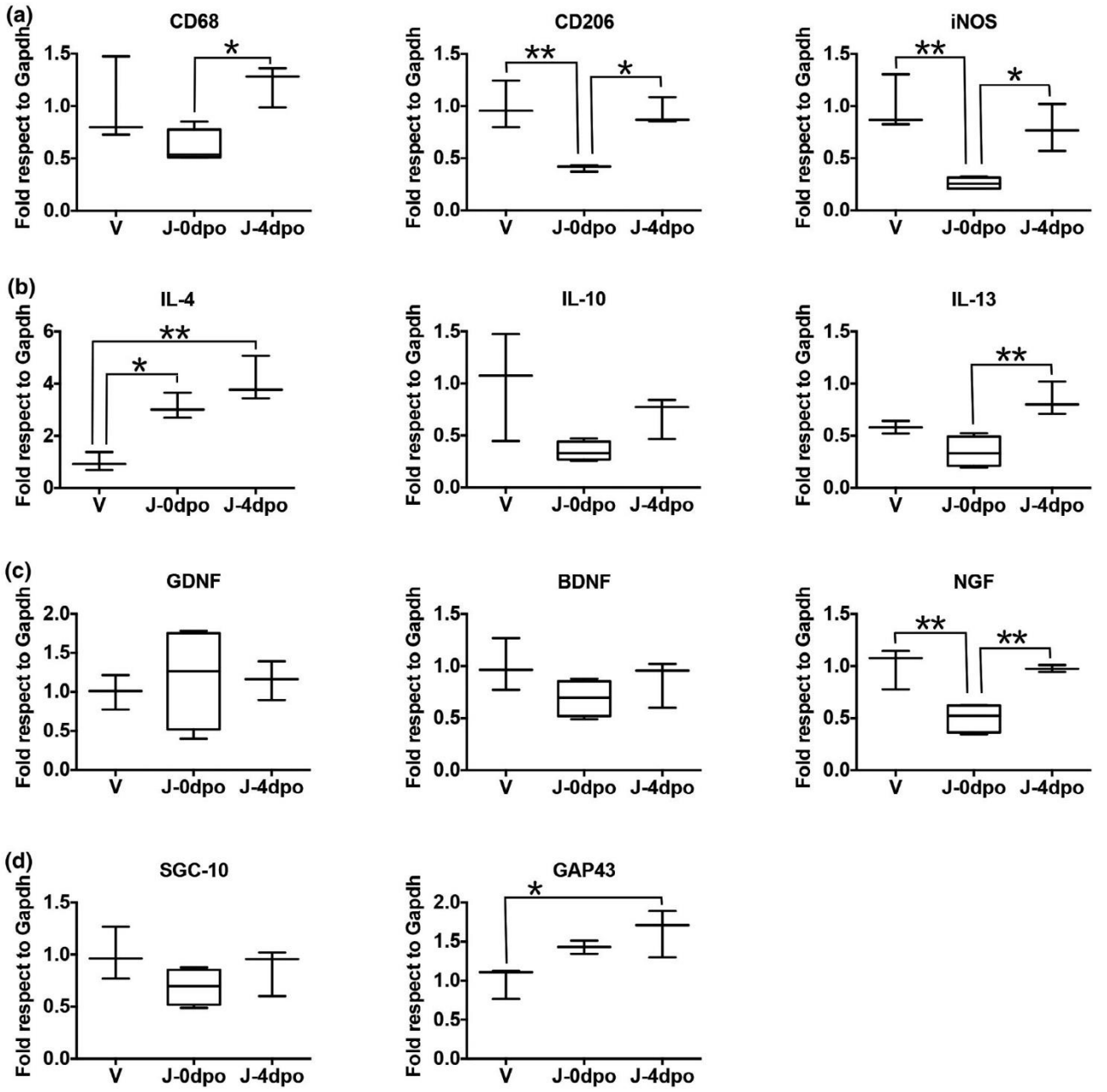

FIGURE 1 Delayed BET inhibition with JQ1 increases anti-inflammatory cytokine and GAP43 transcription in vivo. (a) Early treatment with JQ1 at 0 dpo significantly decreases macrophage infiltration detected with CD68. Neither of the treatments alters M1/M2 polarity as detected with iNOS (M1) and CD206 (M2). (b) Delayed BET inhibition increases the transcription of IL-4 and IL-13 anti-inflammatory cytokines. (c) Immediate administration of JQ1 at 0 dpo decreases NGF mRNA expression. (d) BET inhibition at 4 dpo increases GAP43 transcription, while not altering the mRNA levels of SGC-10. *$p < 0.05$ and **$p < 0.01$ as calculated by one-way ANOVA followed with a multiple comparison with Tukey's correction. Data are shown as minimum to maximum box and whisker graphs

found between treatments in Pads 1 (Vehicle: 3.04 ± 1.14; JQ1: 3.53 ± 0.37) ($t_5 = 0.350$, $p = 0.741$) or Pads 2 (Vehicle: 1.02 ± 0.33; JQ1: 1.14 ± 0.47) ($t_7 = 0.202$, $p = 0.845$).

Therefore, the results of in vivo tests showed that JQ1 administration did not have any significant effect on axonal regeneration in the mice.

3.3 | BET protein inhibition reduces DRG neurite outgrowth

We analyzed the effects of BET protein inhibition on neurite outgrowth in DRG explants ex vivo, by adding to the medium variable doses of JQ1 or DMSO as control. Two parameters were analyzed in

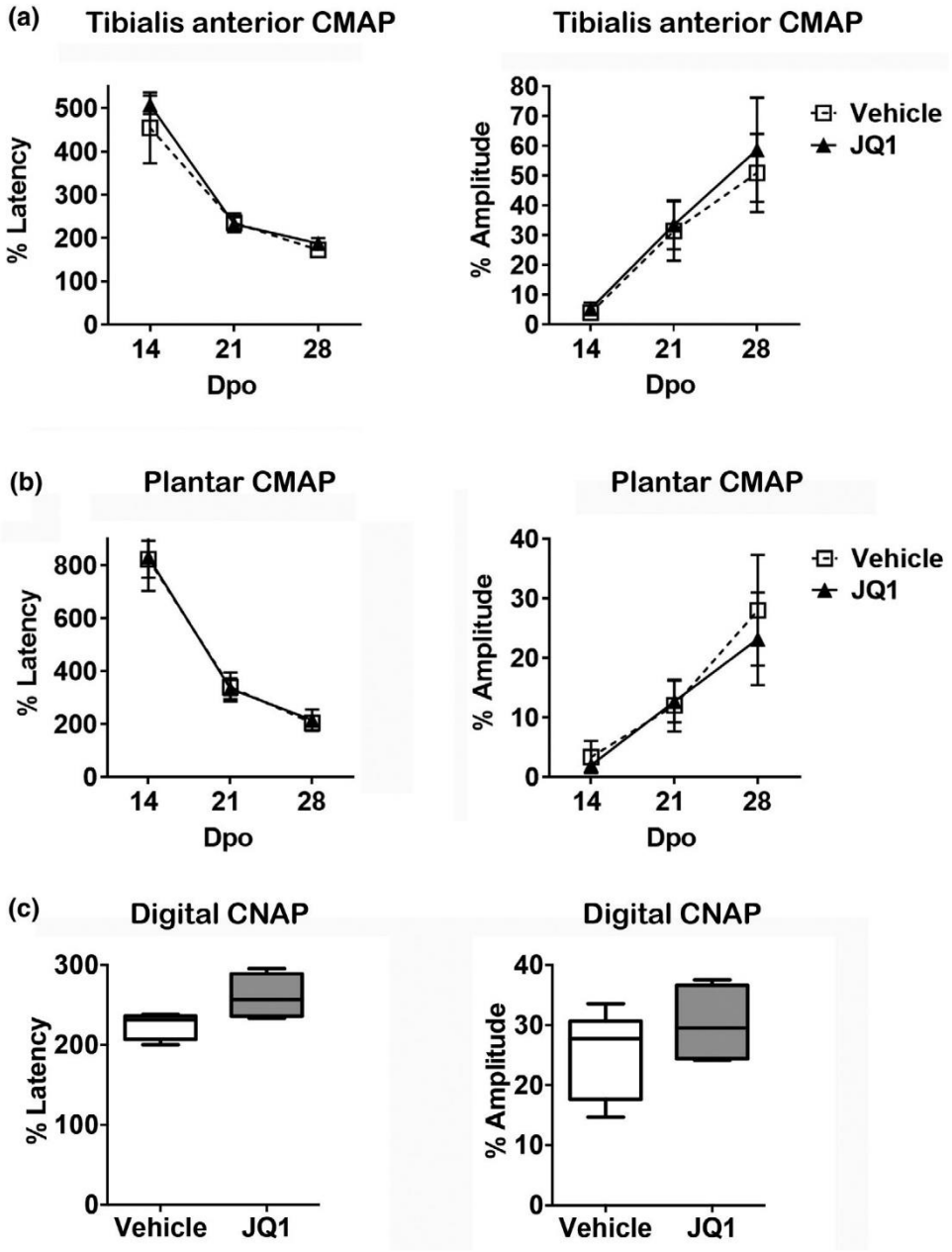

FIGURE 2 BET proteins do not affect nerve regeneration after sciatic nerve crush assessed by electrophysiological tests. No significant differences were found between BET-inhibited animals (JQ1) and control animals (DMSO) in the electrophysiological recordings of the latency and amplitude of the CMAP of tibialis anterior muscle (a), CMAP of plantar muscle (b), and CNAP of the digital nerve (c). Data shown as mean ± SD and minimum to maximum in box and whisker graphs

this study: maximum neurite length and number of neurites of different lengths.

DMSO-treated DRGs had a mean maximal neurite length of 313 μm, whereas JQ1 500 nM and JQ1 1000 nM treatment led to a significant decrease on the maximum neurite length, reaching mean values of 175 μm and 58 μm, respectively (Figure 4a,b) ($F_{2,14}$ = 34.610, $p < 0.001$). The number of neurites grown at different lengths showed that DRGs treated with 500 nM JQ1 had a significant decrease on the number of neurites ranging from 50 μm to 125 μm in length (Upper Figure 4c), compared to DMSO-treated ganglia ($F_{16,340} = 2.280$, $p = 0.004$). The decrement in neurite growth was more pronounced with JQ1 at 1000 nM, showing a significant reduction on the amount of neurites from 0 μm to 150 μm compared with DMSO (Lower Figure 4c) ($F_{16,374} = 16.840$, $p < 0.001$).

Therefore, BET inhibition produced a significant decrease on DRG neurite outgrowth, that was dependent on the JQ1 concentration. To determine if this decrease was due to compound toxicity, we performed an MTT assay (Figure 4d). Results showed that

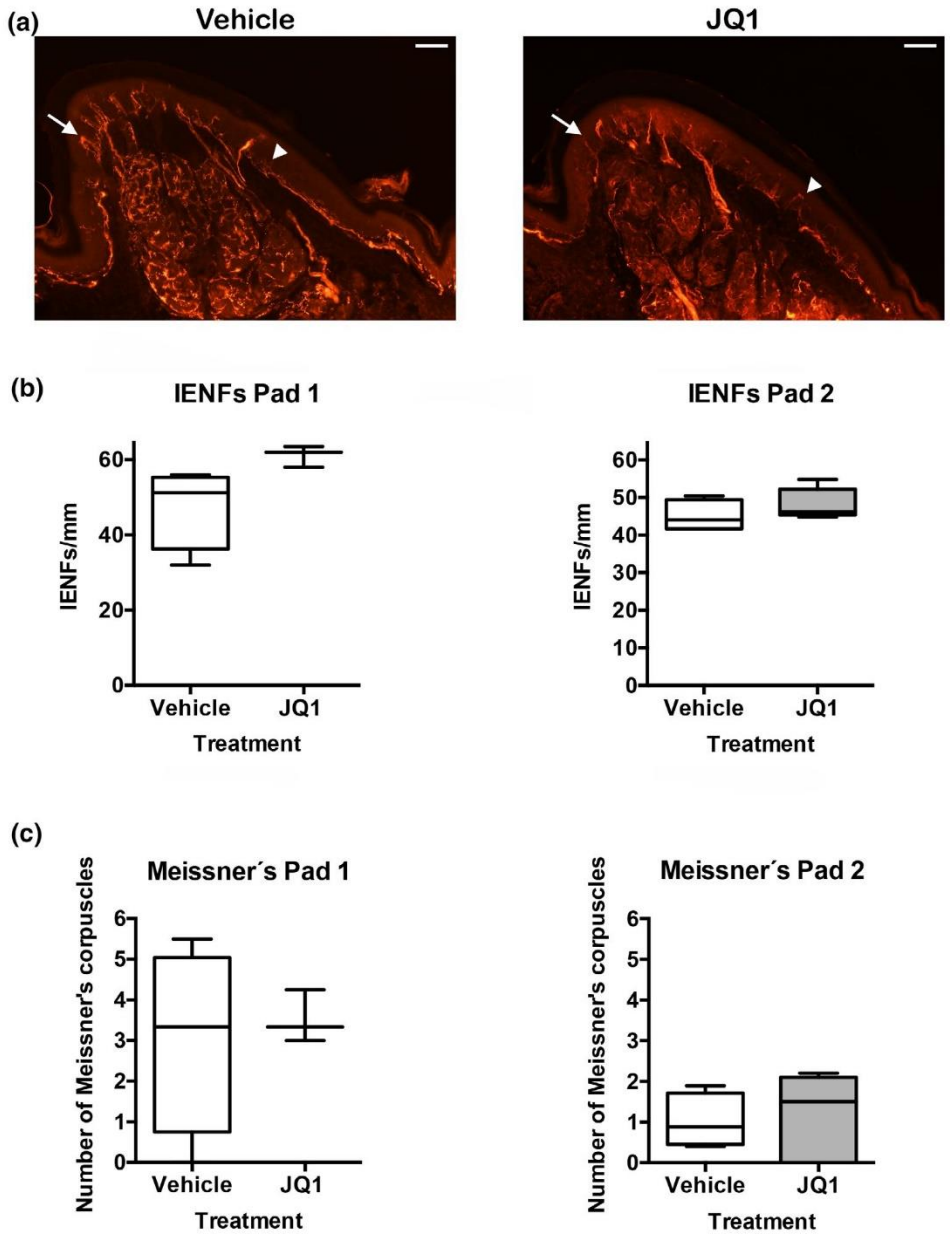

FIGURE 3 BET protein inhibition does not modify sensory reinnervation after sciatic nerve crush. (a) Microphotographs of hind paw pads at ×10 magnification of vehicle and JQ1-treated animals immunolabeled against PGP9.5. Arrow tips point IENFs, whereas arrows exhibit the location of Meissner's corpuscles. Scale bar = 100 μm. (b) No significant differences were found in IENFs density of vehicle and JQ1-treated mice in medial pad 1 and lateral pad 2. (c) No significant differences were found in the number of Meissner's corpuscles of vehicle and JQ1-treated animals in pad 1 and pad 2. Data shown as minimum to maximum in box and whisker graphs

500 or 1,000 nM of JQ1 did not produce cell death, whereas the positive control cisplatin led to 60.07% of cell death ($F_{3,14} = 12.330$, $p < 0.001$).

3.4 | BET protein-inhibited macrophages secrete pro-regenerative factors

Results obtained from in vivo and ex vivo data indicated contradictory effects of BET protein inhibition on axonal growth. Therefore, we hypothesized that these differences might be produced by macrophages, which infiltrate the nerve after lesion in vivo, but were missing in the DRG cultures. To assess the effects that BET-inhibited macrophages have on neurons ex vivo, we cultured DRG explants with conditioned medium from JQ1 or DMSO-treated macrophages added into the collagen matrix.

Control DRGs treated with DMSO-conditioned medium (D + mD) had a maximum neurite length of 258 μm in average. A significant increase in neurite outgrowth was found when DRGs were treated with JQ1 conditioned medium (D + mJQ1), with a mean maximal

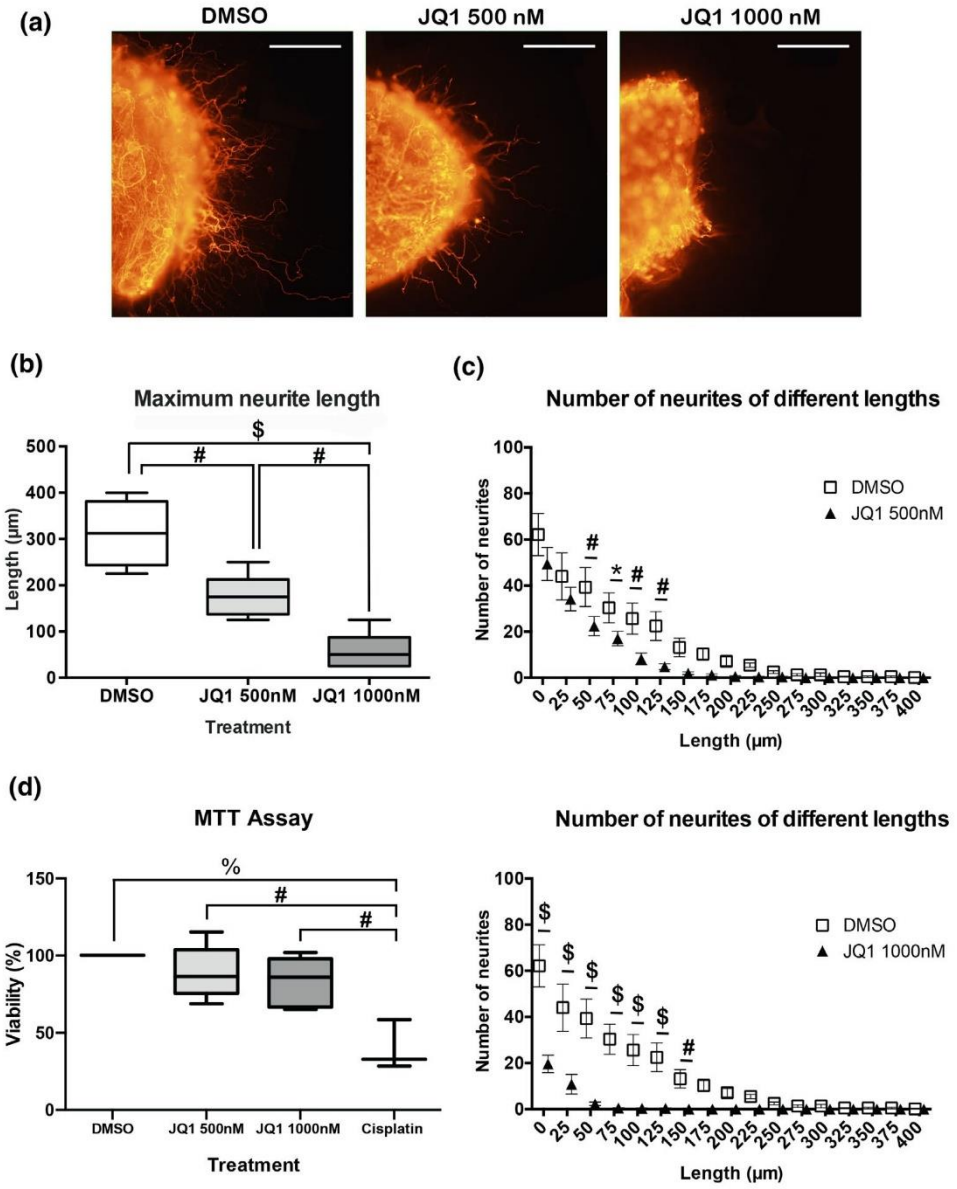

FIGURE 4 BET protein inhibition reduces DRG neurite outgrowth ex vivo. (a) Representative images from DRG explants at ×20 magnification show that BET protein inhibition decreases neurite outgrowth proportionally to JQ1 concentration. Scale bar = 100 µm. (b) BET inhibition with JQ1 reduces maximum neurite length. (c) JQ1 at 500 nM and 1000 nM significantly diminish the number of neurites of different lengths when compared to DMSO-treated ganglia. (d) The different concentrations of JQ1 used in vitro do not produce cell death. $^{*}p < 0.05$, $^{\#}p < 0.01$, $^{\%}p < 0.001$, and $^{\$}p < 0.0001$ as calculated by one-way ANOVA with Tukey's multiple comparison test and two-way ANOVA analysis followed by Sidak's correction of multiple comparisons. Data shown as mean ± SD or minimum to maximum in box and whisker graphs

neurite length of 370 µm (Figure 5a,b). Since conditioned media from macrophages was concentrated by filtration, this media contained 20 times less of JQ1 small compound while increased the concentration of high molecular weight molecules secreted by macrophages. Thus, we can discard any direct effect of JQ1 on the cultured neurons. Therefore, these results indicate that BET-inhibited macrophages secrete pro-regenerative factors that stimulate neurite outgrowth.

Then, we wanted to assess if these pro-regenerative factors were also able to counteract the effects produced by direct BET protein inhibition on DRG neurons. For this purpose, JQ1 was added into the collagen and the medium of DRG explants. When JQ1 was administered in the collagen, it reduced neurite outgrowth, despite the conditioned media added (Figure 5a,b). Significant differences were observed between D + mD (258 µm) and J + mD (107 µm), and between D + mJ (370 µm) and J + mJ (109 µm). In addition, contrarily to what we expected, JQ1 conditioned medium did not overcome the detrimental effects of direct BET inhibition on neurons, since there were no differences between J+ mD (107 µm) and J + mJ (109 µm) (Interaction $F_{1,34} = 2.974$, $p = 0.0937$; Row factor (conditioned media) $F_{1,34} = 3.221$, $p = 0.0816$; and Column factor

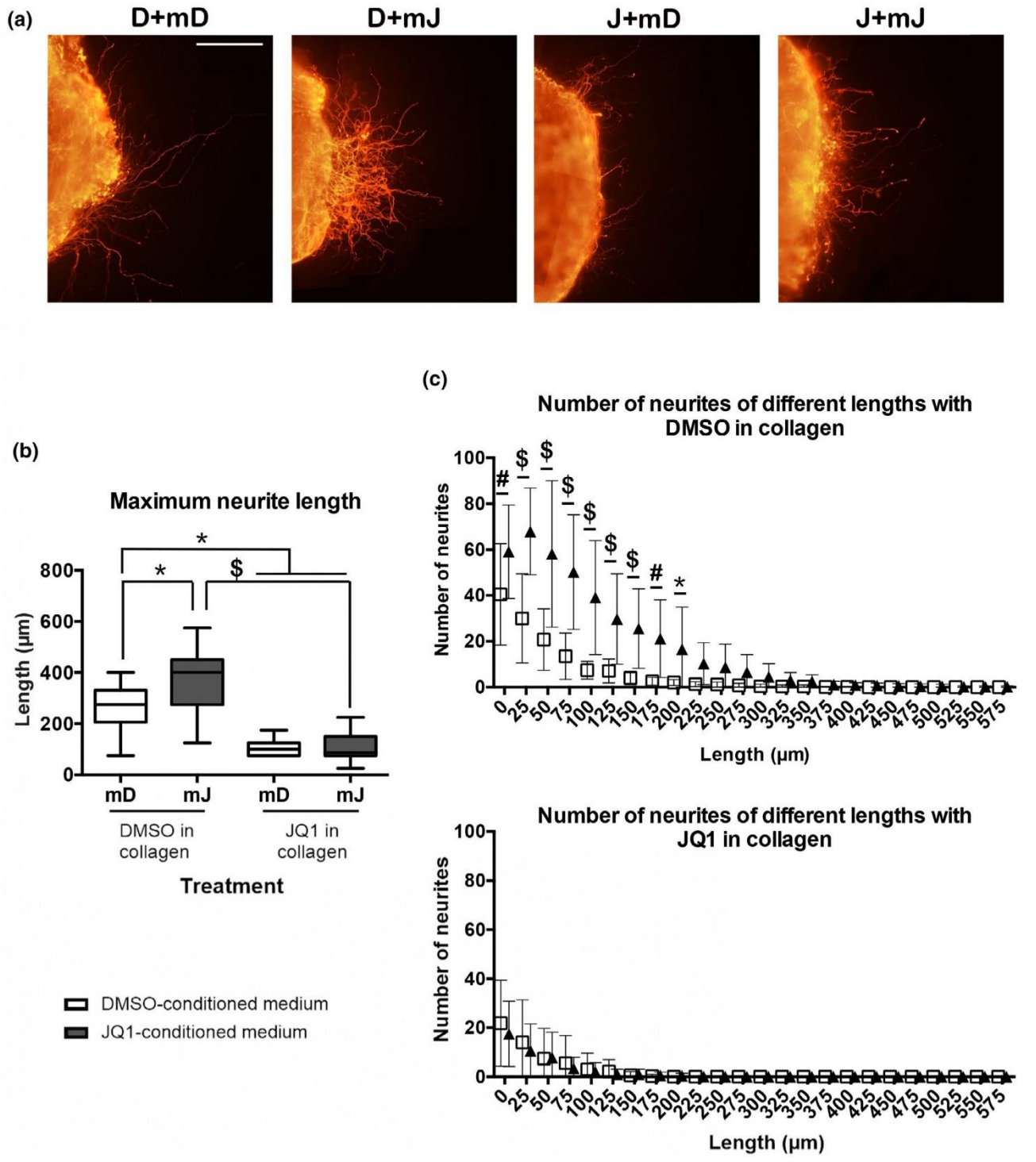

FIGURE 5 Conditioned media from BET-inhibited macrophages enhance DRG neurite outgrowth. (a) Representative images from DRG explants at ×20 magnification show that media from BET-inhibited macrophages enhances neuritogenesis. Scale bar = 100 µm. (b) Conditioned media from BET-inhibited macrophages increases maximum neurite length in vitro. From left to right: DMSO in collagen + DMSO-conditioned medium (D + mD), DMSO in collagen + JQ1-conditioned medium (D + mJ), JQ1 in collagen + DMSO-conditioned medium (J + mD), and JQ1 in collagen + JQ1-conditioned medium (J + mJ). (c) Conditioned media from JQ1-treated macrophages increases the number of neurites of different lengths when DMSO is in collagen (upper graph). No significant differences are found between treatments regarding the number of neurites of different lengths when JQ1 is in collagen (lower graph). $^{*}p < 0.05$, $^{\#}p < 0.01$, and $^{\$}p < 0.0001$ as calculated by two-way ANOVA with Sidak's correction of multiple comparisons. Data shown as mean ± SD or minimum to maximum in box and whisker graphs

(treatment) $F_{1,34} = 41.86, p < 0.0001$) (Figure 5b). Hence, this experiment confirmed our hypothesis that cultured macrophages secreted factors that stimulated neurite growth when treated with JQ1.

To further corroborate our findings, we determined the number of neurites of different lengths. We found that DMSO-treated DRGs with JQ1 conditioned medium (D + mJ) had a significant increase in the number of neurites ranging from 0 μm to 200 μm (Figure 5c, top), when compared to DMSO-treated ganglia with DMSO-conditioned medium (D + mD) (Interaction $F_{23,504} = 8.631, p < 0.0001$; Row factor (length) $F_{23,504} = 48.89, p < 0.0001$; and Column factor (treatment) $F_{1,504} = 152.6, p < 0.0001$). However, no significant differences were found between JQ1-treated DRGs with DMSO-conditioned medium (JQ1 + mD) and JQ1-treated DRGs with JQ1-conditioned medium (JQ1 + mJQ1) (Figure 5c, bottom) (Interaction $F_{23,312} = 0.1894$, $p > 0.9999$; Row factor (length) $F_{23,312} = 11.91$, $p < 0.0001$; and Column factor (treatment) $F_{1,312} = 0.6133$, $p = 0.4342$). These results are consistent with the maximum neurite length analysis, as it demonstrates that JQ1-treated macrophages conditioned medium increased neurite outgrowth. Nonetheless, JQ1-conditioned medium did not overcome the negative effects of direct BET inhibition, probably due to the high concentration of JQ1 used in the ex vivo explants.

3.5 | Conditioned medium from BET-inhibited macrophages induce STAT6 phosphorylation in DRG explants

Our previous experimental study described that BET-inhibited macrophages increase anti-inflammatory cytokine expression of IL-4, IL-10, and IL-13 (Sanchez-Ventura et al., 2019). Moreover, former qPCR analysis demonstrates that JQ1 treatment at 4 dpo after sciatic nerve crush increases IL-4 and IL-13 cytokine transcription. As experimental evidence points that anti-inflammatory cytokines promote neurite outgrowth through acting on JAK/STAT pathways (Vidal et al., 2013), we aimed to determine the activation state of these pathways. For this purpose, DRG explants were treated with conditioned media from JQ1 or DMSO-treated macrophages. We found that ganglia treated with conditioned medium from BET-inhibited macrophages displayed a significant increase in the phosphorylation of STAT6 (Figure 6a,b, Figure S1), being 2.46 times higher than in DRGs treated with conditioned medium from DMSO-treated macrophages ($t_3 = 3.278, p = 0.046$). However, no significant differences between treatments were found regarding the activation of STAT3 pathway (Figure 6c,d, Figure S1) ($t_3 = 1.903, p = 0.153$). Thus, conditioned medium from BET-inhibited macrophages led to an increased phosphorylation of STAT6, probably through an enhanced release of IL-4 and IL-13 anti-inflammatory cytokines.

4 | DISCUSSION

In the present study we have analyzed the effects of BET inhibition on nerve regeneration in vivo and neurite outgrowth ex vivo. Overall, BET inhibition after sciatic nerve crush injury in mice did not produce any effect on axonal regeneration. In contrast, direct inhibition of BET proteins in neurons ex vivo produced a decrease in neuritogenesis. However, BET-inhibited macrophages secrete pro-regenerative factors that promoted neurite outgrowth in DRG cultures, at least by enhancing the STAT6 pathway. Thus, specific targeting of BET proteins in macrophages may be needed to efficiently enhance axonal regeneration and functional recovery after PNI.

The effects of JQ1 treatment on axonal growth were first analyzed after sciatic nerve crush injury in mice. Results of the mRNA expression analysis demonstrated a reduced infiltration of macrophages when JQ1 treatment started at 2 hr postinjury, whereas a delayed treatment did not. In addition, an enhanced expression of IL-4 and IL-13 and GAP43 was found with the delayed treatment of JQ1. It is known that BET protein inhibition reduces chemokine expression in macrophages (Nicodeme et al., 2010; Sanchez-Ventura et al., 2019), which are essential for macrophage infiltration. Thus, we hypothesized that an early treatment with JQ1 would reduce macrophage infiltration, negatively affecting the development of Wallerian degeneration and consequently hindering future outcome. Therefore, we used a delayed treatment with JQ1 since it allows an early macrophage infiltration, which may be useful for further experiments. However, electrophysiological and histological results showed that the delayed treatment with JQ1 did not have any effect on sensory or motor reinnervation after injury. Mice were treated with 30 mg/kg/24 hr, which is the same dose we previously reported to have beneficial effects after spinal cord injury (Sanchez-Ventura et al., 2019). Besides, increasing doses of JQ1 could not be used since long-term administration of higher doses of JQ1 produce a reduction of body weight and eventual death of mice (data not shown). Further, it has been reported by other authors that doses over 50 mg/kg led to detrimental side effects on mice (Korb et al., 2015; Matzuk et al., 2012). Since no changes on nerve regeneration were observed in mice, to better decipher the action of BET proteins on axonal regeneration in neurons, we used DRG ex vivo cultures.

We observed that JQ1 reduced neurite growth when interacting directly with neurons in culture. The mechanisms producing neurite outgrowth inhibition are not known. Cell viability assay demonstrated that JQ1 was not toxic at the used concentrations, confirming the results of other authors in human mesenchymal stem cells and neurons (Bakshi et al., 2018; Li et al., 2020). It has been previously reported that treatment with JQ1 on cortical neurons produce gene repression of immediate early genes such as Arc and Fos Nr4a1 in response to BDNF external stimulation (Korb et al., 2015). Thus, it seems appropriate to hypothesize that JQ1 prevents the expression of genes associated with neurite growth in neurons. However, an exhaustive study remains to be performed to determine which neuronal genes are directly affected by BET inhibition. In addition, several authors have reported that JQ1 treatment leads to a decrease in mTOR phosphorylation (Jang et al., 2017; Li et al., 2019; Li et al., 2020). Therefore,

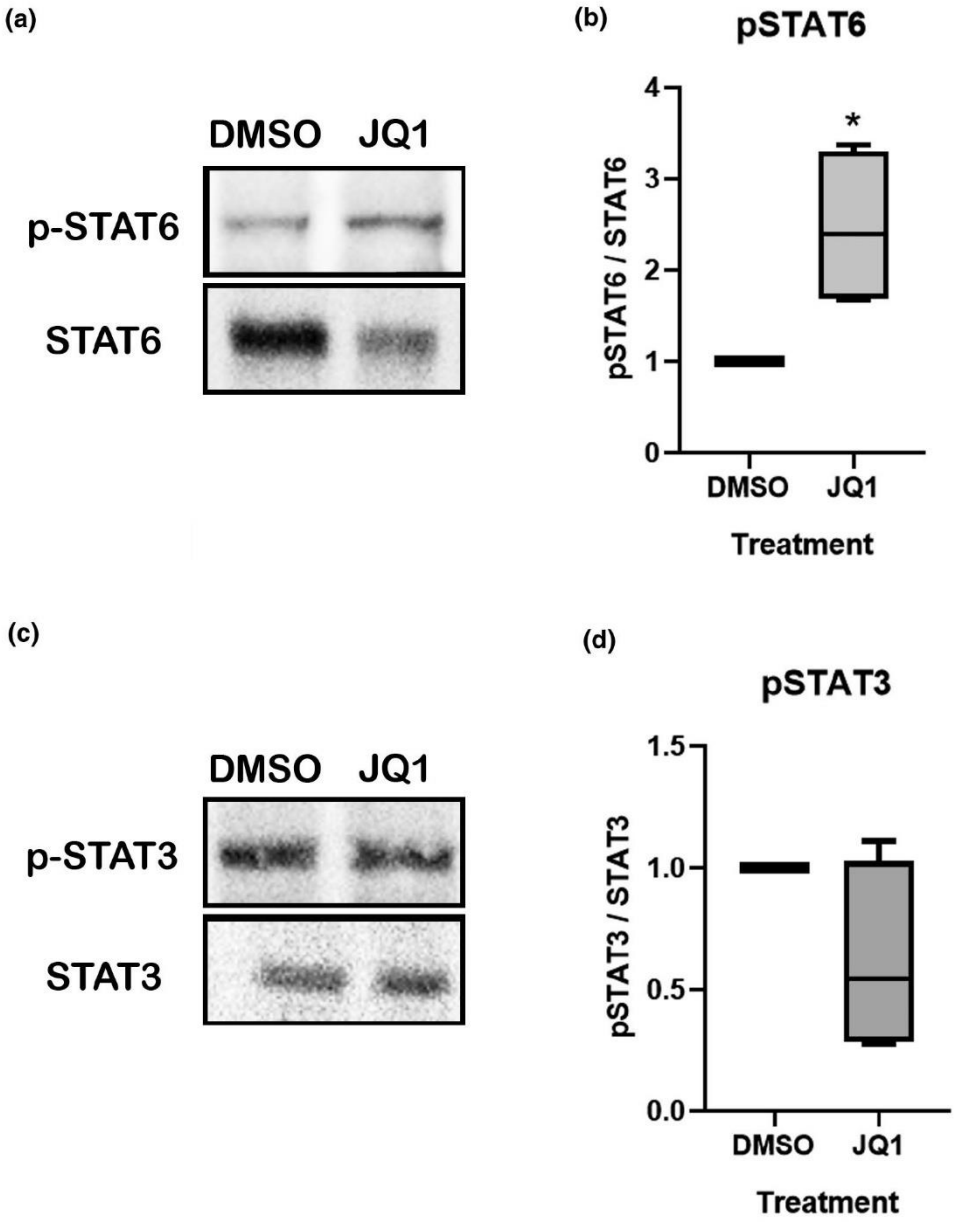

FIGURE 6 STAT6 phosphorylation in DRG explants is produced by conditioned media from BET-inhibited macrophages. (a) Representative images obtained from western blots against p-STAT6 and STAT6 of DRGs treated with conditioned media from macrophages treated with JQ1 or vehicle. (b) Quantification of (a) showing that DRGs treated with conditioned media from BET-inhibited macrophages increase STAT6 phosphorylation relative to STAT6, compared to ganglia treated with conditioned media from DMSO-treated macrophages (DMSO). (c) Representative images from western blots against p-STAT3 and STAT3 of DRGs treated with conditioned media from macrophages treated with JQ1 or vehicle. (d) Quantification of (c) showing that there were no significant differences regarding the protein levels of p-STAT3 relative to STAT3 of DRGs treated with conditioned media from DMSO-treated macrophages and BET-inhibited macrophages. $^{*}p < 0.05$ as calculated by a paired *t* test. Data shown as minimum to maximum in box and whisker graphs

since it has been described that mTOR activation leads to neurite outgrowth and peripheral nerve regeneration (Abe et al., 2010; Chen, Lu, et al., 2016; Liu et al., 2019), it is also possible that BET inhibition in neurons could reduce the intrinsic regenerative capacity of neurons by decreasing the activation of mTOR pathway. Nonetheless, deeper research should be performed to confirm the former hypothesis.

Further studies demonstrated that the discrepancy of the JQ1 effect on axonal growth between the in vivo and ex vivo experimental settings could be accounted to the effect of BET inhibition in macrophages in vivo. Conditioned medium from JQ1-treated macrophages enhanced neurite outgrowth in DRG neurons, thus indicating that BET-inhibited macrophages secrete pro-regenerative factors that induce neuritogenesis. We have previously shown that treatment

with JQ1 to activated macrophages reduced the expression of pro-inflammatory cytokines, such as IL-6, IL-1b, and TNFα, and promoted the expression of anti-inflammatory cytokines IL-4, IL-10, and IL-13 (Sanchez-Ventura et al., 2019). In this study, we further corroborated an enhancement of the expression of IL-4 and IL-13 after crush injury with JQ1. Importantly, anti-inflammatory cytokines, secreted in the denervated distal nerve stump, have a clear role increasing the capacity of proximal axons to cross the lesion zone. It is known that animals lacking IL-10 regenerate worse than WT animals (Siqueira Mietto et al., 2015), and that the administration of IL-4 and IL-10 enhance axonal regeneration (Atkins et al., 2007; Vidal et al., 2013). Therefore, our results suggest that BET inhibition leads to an increase of anti-inflammatory cytokines that compensates the detrimental effects that JQ1 has on neurons in vivo by activating pathways able to increase axonal regeneration. In the ex vivo studies, conditioned medium from JQ1-treated macrophages was not able to overcome the inhibitory signaling of JQ1 present in the collagen matrix embedding the DRG, thus acting directly on neurons. We hypothesize that within these cultures, JQ1 is in higher concentrations than in the in vivo study in mice, producing a stronger effect on neuronal BET proteins in the culture than in vivo.

To determine if cytokines are the potential mediators promoting neurite growth of DRG explants, STAT3 and STAT6 phosphorylation was assessed. We did not observe any changes on STAT3 phosphorylation in DRG samples treated with conditioned media from BET-inhibited macrophages. STAT3 is activated through IL-6 and IL-10. In fact, IL-6 and IL-10 have been reported to produce neuronal regeneration through phosphorylation and concomitant activation of STAT3 (Chen, Lin, et al., 2016; Vidal et al., 2013). However, since our previous studies demonstrated that JQ1 reduces the expression of IL-6, which may compensate for the IL-10-enhanced expression (Sanchez-Ventura et al., 2019), we did not observe an effect on this pathway to explain the enhanced neuritogenesis. In contrast, we found an enhanced phosphorylation of STAT6 in DRG samples treated with conditioned media from BET-inhibited macrophages. The best known activators of STAT6 are IL-13 and IL-4 (Mori et al., 2016) which are, in turn, strongly induced by STAT6 itself (Czimmerer et al., 2018). In fact, we previously found that BET-inhibited macrophages secrete these cytokines (Sanchez-Ventura et al., 2019), and we confirmed these results after a crush injury in sciatic nerve. Since there are previous reports showing that these cytokines promote axonal regeneration (Vidal et al., 2013), the enhanced neuritogenesis in DRG explants observed by the secreted factors from BET-inhibited macrophages could be attributed, at least in part, to this pathway. It should be also considered that macrophages have two variants of IL-4 receptor (IL-4R) that are able to induce STAT6 phosphorylation. Type I IL-4R can also lead to IRS-2 phosphorylation and consequently to the activation of PIP3/Akt and Erk pathways (Czimmerer et al., 2018), which are also related to axonal regeneration (Hausott & Klimaschewski, 2019; Saijilafu et al., 2013). Therefore, further studies should be performed, to also analyze the implication of the PIP3/Akt and ERK pathways on the neural outgrowth induced by BET-inhibited macrophages.

Finally, it should be also pointed out that we have only used females in this study, which may be a limitation for deciphering potential sex differences. Since differential regenerative capacities between males and females is controversial (Kovacic et al., 2004; Wood et al., 2012), a further study with male mice may be performed to obtain a complete vision of the results obtained.

In conclusion, this study demonstrates that BET protein inhibition in macrophages provides a suitable condition to enhance axonal outgrowth, and brings insight on the relevance of the anti-inflammatory cytokines IL-13 and IL-4 and the STAT6 pathway in axonal regeneration. Thus, BET proteins are an effective target to improve axonal regeneration. However, a specific targeting of BET inhibition in macrophages would be needed to efficiently enhance functional recovery after PNI.

DECLARATION OF TRANSPARENCY

The authors, reviewers and editors affirm that in accordance to the policies set by the *Journal of Neuroscience Research*, this manuscript presents an accurate and transparent account of the study being reported and that all critical details describing the methods and results are present.

ACKNOWLEDGMENTS

The authors acknowledge Dr. James Bradner and Dana-Farber Cancer Institute (DFCI) for kindly providing the compound JQ1. They thank the technical help of Monica Espejo and Jessica Jaramillo. The RT-97 antibody was obtained from the Developmental Studies Hybridoma Bank, developed under the auspices of the NICHD and maintained by the University of Iowa, Department of Biology.

CONFLICT OF INTEREST

The authors declare that they have no conflict of interest.

AUTHOR CONTRIBUTIONS

GP and CP performed methodology, investigation and formal analysis. GP, XN and CP performed writing and manuscript preparation. XN and CP did funding acquisition. CP performed study conception and supervision.

PEER REVIEW

The peer review history for this article is available at https://publons.com/publon/10.1002/jnr.25036.

DATA AVAILABILITY STATEMENT

The raw data can be found in the Universitat Autònoma de Barcelona repository, https://ddd.uab.cat/record/243396

ORCID

Xavier Navarro https://orcid.org/0000-0001-9849-902X

REFERENCES

Abe, N., Borson, S. H., Gambello, M. J., Wang, F., & Cavalli, V. (2010). Mammalian target of rapamycin (mTOR) activation increases axonal growth capacity of injured peripheral nerves. *The Journal of Biological Chemistry*, *285*(36), 28034–28043.

Allodi, I., Udina, E., & Navarro, X. (2012). Specificity of peripheral nerve regeneration: Interactions at the axon level. *Progress in Neurobiology*, *98*(1), 16–37.

Atkins, S., Loescher, A. R., Boissonade, F. M., Smith, K. G., Occleston, N., O'Kane, S., Ferguson, M. W. J., & Robinson, P. P. (2007). Interleukin-10 reduces scarring and enhances regeneration at a site of sciatic nerve repair. *Journal of the Peripheral Nervous System*, *12*(4), 269–276.

Bakshi, S., McKee, C., Walker, K., Brown, C., & Chaudhry, G. R. (2018). Toxicity of JQ1 in neuronal derivatives of human umbilical cord mesenchymal stem cells. *Oncotarget*, *9*(73), 33853–33864.

Bhattarai, P., Thomas, A. K., Cosacak, M. I., Papadimitriou, C., Mashkaryan, V., Froc, C., Reinhardt, S., Kurth, T., Dahl, A., Zhang, Y., & Kizil, C. (2016). IL4/STAT6 signaling activates neural stem cell proliferation and neurogenesis upon amyloid-beta42 aggregation in adult zebrafish brain. *Cell Reports*, *17*(4), 941–948.

Chen, H., Lin, W., Zhang, Y., Lin, L., Chen, J., Zeng, Y., Zheng, M., Zhuang, Z., du, H., Chen, R., & Liu, N. (2016). IL-10 promotes neurite outgrowth and synapse formation in cultured cortical neurons after the oxygen-glucose deprivation via JAK1/STAT3 pathway. *Scientific Reports*, *6*, 30459.

Chen, W., Lu, N., Ding, Y., Wang, Y., Chan, L. T., Wang, X., Gao, X., Jiang, S., & Liu, K. (2016). Rapamycin-resistant mTOR activity is required for sensory axon regeneration induced by a conditioning lesion. *eNeuro*, *3*(6), 0358-16.

Czimmerer, Z., Daniel, B., Horvath, A., Rückerl, D., Nagy, G., Kiss, M., Peloquin, M., Budai, M. M., Cuaranta-Monroy, I., Simandi, Z., Steiner, L., Nagy, B., Jr., Poliska, S., Banko, C., Bacso, Z., Schulman, I. G., Sauer, S., Deleuze, J. F., Allen, J. E., … Nagy, L. (2018). The transcription factor STAT6 mediates direct repression of inflammatory enhancers and limits activation of alternatively polarized macrophages. *Immunity*, *48*(1), 75–90.e6.

Deboy, C. A., Xin, J., Byram, S. C., Serpe, C. J., Sanders, V. M., & Jones, K. J. (2006). Immune-mediated neuroprotection of axotomized mouse facial motoneurons is dependent on the IL-4/STAT6 signaling pathway in CD4(+) T cells. *Experimental Neurology*, *201*(1), 212–224.

DeFrancesco-Lisowitz, A., Lindborg, J. A., Niemi, J. P., & Zigmond, R. E. (2015). The neuroimmunology of degeneration and regeneration in the peripheral nervous system. *Neuroscience*, *302*, 174–203.

Dubovy, P., Hradilova-Svizenska, I., Klusakova, I., Brazda, V., & Joukal, M. (2019). Interleukin-6 contributes to initiation of neuronal regeneration program in the remote dorsal root ganglia neurons after sciatic nerve injury. *Histochemistry and Cell Biology*, *152*(2), 109–117.

Filippakopoulos, P., & Knapp, S. (2014). Targeting bromodomains: Epigenetic readers of lysine acetylation. *Nature Reviews. Drug Discovery*, *13*(5), 337–356.

Fregnan, F., Muratori, L., Simoes, A. R., Giacobini-Robecchi, M. G., & Raimondo, S. (2012). Role of inflammatory cytokines in peripheral nerve injury. *Neural Regeneration Research*, *7*(29), 2259–2266.

Hajmirza, A., Emadali, A., Gauthier, A., Casasnovas, O., Gressin, R., & Callanan, M. B. (2018). BET family protein BRD4: An emerging actor in NFkappaB signaling in inflammation and cancer. *Biomedicine*, *6*(1), 1–16.

Hausott, B., & Klimaschewski, L. (2019). Promotion of peripheral nerve regeneration by stimulation of the extracellular signal-regulated kinase (ERK) pathway. *Anatomical Record*, *302*(8), 1261–1267.

Huckhagel, T., Nuchtern, J., Regelsberger, J., Gelderblom, M., Lefering, R., & TraumaRegister DGU. (2018). Nerve trauma of the lower extremity: Evaluation of 60,422 leg injured patients from the TraumaRegister DGU(R) between 2002 and 2015. *Scandinavian Journal of Trauma, Resuscitation and Emergency Medicine*, *26*(1), 40.

Jang, J. E., Eom, J. I., Jeung, H. K., Cheong, J. W., Lee, J. Y., Kim, J. S., & Min, Y. H. (2017). AMPK-ULK1-mediated autophagy confers resistance to BET inhibitor JQ1 in acute myeloid leukemia stem cells. *Clinical Cancer Research*, *23*(11), 2781–2794.

Korb, E., Herre, M., Zucker-Scharff, I., Darnell, R. B., & Allis, C. D. (2015). BET protein Brd4 activates transcription in neurons and BET inhibitor Jq1 blocks memory in mice. *Nature Neuroscience*, *18*(10), 1464–1473.

Kovacic, U., Zele, T., Osredkar, J., Sketelj, J., & Bajrovic, F. F. (2004). Sex-related differences in the regeneration of sensory axons and recovery of nociception after peripheral nerve crush in the rat. *Experimental Neurology*, *189*(1), 94–104.

Li, F., Yang, C., Zhang, H. B., Ma, J., Jia, J., Tang, X., Zeng, J., Chong, T., Wang, X., He, D., & Guo, P. (2019). BET inhibitor JQ1 suppresses cell proliferation via inducing autophagy and activating LKB1/AMPK in bladder cancer cells. *Cancer Medicine*, *8*(10), 4792–4805.

Li, Y., Xiang, J., Zhang, J., Lin, J., Wu, Y., & Wang, X. (2020). Inhibition of Brd4 by JQ1 promotes functional recovery from spinal cord injury by activating autophagy. *Frontiers in Cellular Neuroscience*, *14*, 555591.

Liu, S., Jia, J., Zhou, H., Zhang, C., Liu, L., Liu, J., Lu, L., Li, X., Kang, Y., Lou, Y., Cai, Z., Ren, Y., Kong, X., & Feng, S. (2019). PTEN modulates neurites outgrowth and neuron apoptosis involving the PI3K/Akt/mTOR signaling pathway. *Molecular Medicine Reports*, *20*(5), 4059–4066.

Ma, C. H., Omura, T., Cobos, E. J., Latrémolière, A., Ghasemlou, N., Brenner, G. J., van Veen, E., Barrett, L., Sawada, T., Gao, F., Coppola, G., Gertler, F., Costigan, M., Geschwind, D., & Woolf, C. J. (2011). Accelerating axonal growth promotes motor recovery after peripheral nerve injury in mice. *The Journal of Clinical Investigation*, *121*(11), 4332–4347.

Matzuk, M. M., MR, M. K., Filippakopoulos, P., Li, Q., Ma, L., Agno, J. E., Lemieux, M. E., Picaud, S., Yu, R. N., Qi, J., Knapp, S., & Bradner, J. E. (2012). Small-molecule inhibition of BRDT for male contraception. *Cell*, *150*(4), 673–684.

Mori, S., Maher, P., & Conti, B. (2016). Neuroimmunology of the interleukins 13 and 4. *Brain Sciences*, *6*(2), 1–18.

Navarro, X. (2016). Functional evaluation of peripheral nerve regeneration and target reinnervation in animal models: A critical overview. *The European Journal of Neuroscience*, *43*(3), 271–286.

Navarro, X., Vivo, M., & Valero-Cabre, A. (2007). Neural plasticity after peripheral nerve injury and regeneration. *Progress in Neurobiology*, *82*(4), 163–201.

Nicodeme, E., Jeffrey, K. L., Schaefer, U., Beinke, S., Dewell, S., Chung, C. W., Chandwani, R., Marazzi, I., Wilson, P., Coste, H., White, J., Kirilovsky, J., Rice, C. M., Lora, J. M., Prinjha, R. K., Lee, K., & Tarakhovsky, A. (2010). Suppression of inflammation by a synthetic histone mimic. *Nature*, *468*(7327), 1119–1123.

Rotshenker, S. (2011). Wallerian degeneration: The innate-immune response to traumatic nerve injury. *Journal of Neuroinflammation*, *8*, 109.

Saijilafu, H. E. M., Liu, C. M., Jiao, Z., Xu, W. L., & Zhou, F. Q. (2013). PI3K-GSK3 signalling regulates mammalian axon regeneration by inducing the expression of Smad1. *Nature Communications*, *4*, 2690.

Sanchez-Ventura, J., Amo-Aparicio, J., Navarro, X., & Penas, C. (2019). BET protein inhibition regulates cytokine production and promotes neuroprotection after spinal cord injury. *Journal of Neuroinflammation*, *16*(1), 124.

Siqueira Mietto, B., Kroner, A., Girolami, E. I., Santos-Nogueira, E., Zhang, J., & David, S. (2015). Role of IL-10 in resolution of inflammation and functional recovery after peripheral nerve injury. *The Journal of Neuroscience*, *35*(50), 16431–16442.

Torres-Espin, A., Santos, D., Gonzalez-Perez, F., del Valle, J., & Navarro, X. (2014). Neurite-J: An image-J plug-in for axonal growth analysis in organotypic cultures. *Journal of Neuroscience Methods*, *236*, 26–39.

Vidal, P. M., Lemmens, E., Dooley, D., & Hendrix, S. (2013). The role of "anti-inflammatory" cytokines in axon regeneration. *Cytokine & Growth Factor Reviews*, *24*(1), 1–12.

Wood, K., Wilhelm, J. C., Sabatier, M. J., Liu, K., Gu, J., & English, A. W. (2012). Sex differences in the effectiveness of treadmill training in enhancing axon regeneration in injured peripheral nerves. *Developmental Neurobiology*, *72*(5), 688–698.

SUPPORTING INFORMATION

Additional supporting information may be found in the online version of the article at the publisher's website.

FIGURE S1 Uncropped images of WB from DRGs treated with media from DMSO- (marked as V) and JQ1-treated macrophages (referred as J). (a) Pictures of samples from the first and second culture. (b) Membranes belonging to the third culture

Transparent Science Questionnaire for Authors

How to cite this article: Palomés-Borrajo, G., Navarro, X. & Penas, C. (2022). BET protein inhibition in macrophages enhances dorsal root ganglion neurite outgrowth in female mice. *Journal of Neuroscience Research*, 100, 1331–1346. https://doi.org/10.1002/jnr.25036

Chapter 3

BRD4 prevents anti-inflammatory cytokine transcription in macrophages by binding to their promoters

BRD4 prevents anti-inflammatory cytokine transcription in macrophages by binding to their promoters

Georgina Palomés-Borrajo, Xavier Navarro, Clara Penas

Institute of Neurosciences, Dept. Cell Biology, Physiology and Immunology, Centro de Investigación Biomédica en Red sobre Enfermedades Neurodegenerativas (CIBERNED), Universitat Autònoma de Barcelona, Bellaterra, Spain.

Abstract

Inflammation is a physiological mechanism that protects the organism against damage and provides favorable conditions for tissue repair. However, dysregulation of the inflammatory response can lead to delayed recovery, chronic pain, and to development of inflammatory diseases. Thus, research has focused on elucidating the molecular pathways that control the expression of pro- and anti-inflammatory mediators. Epigenetic post-translational modifications have been found to exert a pivotal role in the regulation of the inflammatory response. Particularly, acetylation facilitates the expression of inflammatory genes by inducing chromatin relaxation and favoring the recruitment of transcription-promoting factors. Nevertheless, the molecular mechanisms behind the production of anti-inflammatory mediators remains partly unknown.

In this regard, the Bromodomain and Extraterminal domain (BET) protein family constitutes a group of epigenetic readers that detect acetylated residues in both histone and non-histone proteins. Although the impact of BET proteins on pro-inflammatory mediator secretion has been described, little is known about the role of these reader proteins on the production of anti-inflammatory mediators. In this study, we analyzed the outcome of BET-inhibition on inflammation by using the small-molecule JQ1, a pan-BET inhibitor with high affinity towards the BET family member BRD4. We confirmed that JQ1 raised the transcription of anti-inflammatory cytokines, while decreased the expression of pro-inflammatory mediators in primary macrophages. Moreover, knockdown of BRD4 and CHD4 *in vitro* increased the transcription of the anti-inflammatory cytokines IL-4 and IL-13, suggesting that both proteins were potentially repressing the expression of these anti-inflammatory mediators. Finally, we determined that under physiological conditions BRD4 and CHD4 are recruited in the IL-13

promoter and upon JQ1 treatment both proteins are released from this genetic region. Thus, we suggest that BRD4 and CHD4 proteins prevent the transcription of IL-13, and probably of IL-4, by creating a repressive complex in their promoters. In conclusion, this study sheds light on the regulatory mechanisms behind the production of anti-inflammatory mediators and provides two novel targets for modulating the immune response.

Introduction

Inflammation is a physiological mechanism that defends the organism against pathogens and creates a favorable environment to resolve tissue damage and facilitate repair. However, chronic inflammation can have detrimental consequences, including increased chronic pain, delayed recovery, and the development of inflammatory diseases. In the case of chronic neuroinflammation, it also contributes to the etiopathogenesis of neurodegenerative disorders such as multiple sclerosis, Alzheimer's and Parkinson's disease (Scotece & Conde-Aranda, 2022). Thus, considering that inflammation intervenes in health and sickness of various body systems, there is considerable interest on unraveling the regulatory mechanisms of the inflammatory response.

In this context, it is well-known that NF-Kβ signaling plays a pivotal role in conducting the immune response by controlling the expression of inflammatory genes (D. Li & Wu, 2021). However, it has been reported that epigenetic modifications also participate in inflammation. Particularly, acetylation is a key mechanism that orchestrates early and late inflammatory gene transcription (Saccani, Pantano, & Natoli, 2001). In this regard, it is worth noting that histone acetylation can be subjected to environmental alterations. For instance, lipopolysaccharide (LPS) stimulation promotes the acetylation of H3 and H4 histones, facilitating DNA accessibility on promoters or enhancers of pro-inflammatory genes like TNF-α and IL-12b (Lauterbach et al., 2019; K. E. Sullivan et al., 2007). Additionally, several studies have shown that alterations on the expression of histone deacetylases negatively affect LPS-induced gene expression (W. F. Fang et al., 2018; Wu, Li, Hu, & Kang, 2019). Thus, considering the relevance of acetylation in immunoregulatory events, epigenetic readers of acetylated histones could be relevant tools for modulating inflammation.

Bromodomain and Extra terminal domain (BET) proteins are a family of epigenetic readers that bind to acetylated residues of histone and non-histone proteins. This family is comprised

of four members, BRD2, BRD3, BRD4 and BRDT (Hajmirza et al., 2018; Liu et al., 2021). The most studied enzyme of the BET family is BRD4, which has been closely associated with inflammatory events. Mechanistically, the histone acetyltransferase p300/CBP, acetylates at its lysine 310 the NF-Kβ subunit p65/RelA (Bhatt & Ghosh, 2014; B. Huang et al., 2009). Then, the epigenetic reader BRD4 binds to the acetylated subunit of the p65/RelA, promoting the recruitment of the positive transcription elongator factor (pTEFb) complex, and thus facilitating the expression of NF-Kβ genes (Hajmirza et al., 2018; B. Huang et al., 2009). To note, BET inhibitors decrease LPS-induced pro-inflammatory cytokine transcription, and we previously observed that they also raise anti-inflammatory cytokine expression when given after spinal cord and nerve injuries (Nicodeme et al., 2010; Palomes-Borrajo, Navarro, & Penas, 2022; Sanchez-Ventura et al., 2019). Further, previous results from our laboratory showed that primary macrophages treated for 2 hours with the BET inhibitor JQ1 *in vitro* display increased expression of IL-4, IL-10, and IL-13 cytokines (Sanchez-Ventura et al., 2019). Additionally, conditioned media from JQ1-treated macrophages enhances neurite outgrowth in DRG explants through the STAT6 pathway, whose activation depends on IL-4 and IL-13 anti-inflammatory mediators (Junttila, 2018; Palomes-Borrajo et al., 2022). Despite evidence suggest that BET proteins may modulate anti-inflammatory cytokine expression, the regulation behind these events remains unknown.

Thus, in the present study we aimed to elucidate the mechanism by which BET proteins, and particularly BRD4, affect anti-inflammatory cytokine transcription. We hypothesized that under physiological conditions BRD4 may form a repressor complex on promoters of anti-inflammatory genes preventing their transcription. Then, upon BET inhibition, which promotes BRD4 release from the chromatin, there would be a disassembly of the repressive complex, facilitating the transcription of anti-inflammatory cytokines.

Regarding potential partners that can constitute the mentioned repressor complex, it has been described that the extra terminal region of BRD4 has high binding affinity to the Chromodomain-helicase-DNA-binding protein 4 (CHD4) and Nuclear Receptor Binding SET Domain Protein 3 (NSD3) (Rahman et al., 2011). However, NSD3 has a short isoform that lacks the methyltransferase activity and serves as a scaffold between the chromatin remodeler CHD8 and BRD4 (Shen et al., 2015). Specifically, CHD8 has been described to have both activator and transcriptionally repressor properties (Hurley et al., 2021). In addition, it has

been reported that the chromatin remodeler CHD4 belongs to the repressor complex Nucleosome-Remodeling Deacetylase (NuRD) (Micucci et al., 2015). Apart from their repressor function, both proteins have been linked to regulatory roles in hematopoietic cells. For instance, CHD4 controls hematopoietic cell lineage renewal and differentiation, and intervenes in Th2 lymphocyte differentiation (Hosokawa et al., 2013; Micucci et al., 2015; Yoshida et al., 2008). Whereas CHD8 is responsible for the maintenance of the hematopoietic stem cell lineage pool (Nita et al., 2021). Considering their repressor role and their influence on hematopoietic cells, we aimed to assess if CHD4 or CHD8 might be co-repressors along BRD4 of anti-inflammatory cytokine transcription.

In this study, we investigated the effects of BET-inhibition in the transcription of anti-inflammatory and pro-inflammatory cytokines, by using JQ1 as a treatment on primary macrophages. We also assessed the potential contribution of BRD4 and CHD4 on the regulation of anti-inflammatory cytokine expression.

Materials and methods

Bone Marrow Derived Macrophage (BMDM) culture

C57BL6/J female mice were euthanized with intraperitoneal administration of pentobarbital and disinfected with 70% ethanol. Femurs and tibias were extracted from the animals, and bone epiphyses were removed to flush the bone marrow with chilled PBS using a 10 mL syringe and 26G needle. Cells were centrifuged at 500 RCF for 10 minutes and cultured in 100 mm petri dishes with DMEM/F12 medium containing 10% fetal bovine serum (FBS), 1% penicillin-streptomycin (P/S) and L-glutamine. Macrophage colony stimulating factor (M-CSF) was added at a concentration of 10 ng/ml. Medium was replaced every three days. At 8 days in vitro (div) cells were seeded at different densities depending on the experiment and M-CSF was added at 10 ng/ml.

For assessing the cytokine profile, macrophages were seeded in a 12-well plate with a density of $3.5x10^5$ cells/well, using the medium indicated above. At 10 div cells were treated with vehicle DMSO or JQ1 at 1000 nM during 6h, with or without a pre-treatment with LPS (100 ng/mL) during 1h. This resulted in four experimental conditions: DMSO, DMSO+LPS, JQ1 and JQ1+LPS. For protein cytokine analysis, the medium from macrophage cultures was snap frozen in liquid nitrogen. Whereas to assess RNA cytokine analysis, cells were lysed with lysis

buffer from RNeasy Micro kit (Qiagen) containing 1/100 β-mercaptoethanol. A total of 4 independent cultures was set for determining the transcriptional and secreted cytokine profile.

Detection of secreted cytokines

Medium from macrophages was processed using the Miliplex MAP Mouse Cytokine/Chemokine magnetic bead panel (Milipore) following the manufacturer's protocol. Samples were then analyzed on a Luminex (Milipore) reader, following manufacturer´s instructions.

Silencing of CHD4, CHD8 and BRD4 proteins

For BRD4 knockdown, macrophages were seeded at 8 div with a density of $4x10^5$ cells/well in 12-well plate containing DMEM/F12 medium enriched with 10 % FBS, 1 % P/S and L-glutamine. M-CSF was added to the medium at a concentration of 10 ng/ml. At 10 div culture medium was replaced by Accel siRNA delivery media (Horizon) containing 3 % fetal bovine serum. Cells were treated with Accel non-targeting control siRNA #1 (Horizon, Catalog ID: D-001910-01-05) or with Accel Mouse BRD4 siRNA-SMARTPool (Horizon, Catalog ID: E-041493-00-0005) at 1 µM concentration and M-CSF added at 10 ng/ml. At 13 div DMEM/F12 containing 10 % FBS, 1 % P/S and L-glutamine was added at 1/4 proportion considering the final volume per well. M-CSF was also added at the same concentration. Cells were collected at 14 div for RNA extraction. A total of 4 independent cultures was set for BRD4 silencing.

For CHD4 and CHD8 knockdown, BMDMs were separated in falcons at 10 div with a density of $3x10^6$ cells/condition and cells were electroporated using an Amaxa Nucleofector device (Lonza). The knockdown was performed following the manufacturer's guidelines of the Mouse Amaxa Nucleofector Kit (Lonza) and using ON-TAGETplus Mouse Chd4 siRNA-SMARTPool (Horizon, Catalog ID: L-052142-00-0005), ON-TARGETplus Mouse Chd8 siRNA-SMARTPool (Horizon, Catalog ID: L-063710-00-0005) and ON-TARGETplus Mouse Control-SMARTPool (Horizon, Catalog ID: D-001910-01-05). Cells were seeded in a 60 mm petri dish with DMEM/F12 containing 10 % FBS, 1 % P/S and L-glutamine. At 13 div cells were recovered for further RNA extraction. A total of 3 independent cultures were stablished.

Cell viability assay from BMDM culture

Differentiated macrophages were seeded at 8 div at a density of 30,000 cells/well in a 96-well plate. At 10 div cells were treated in duplicates with Accel non-targeting control siRNA or with Accel Mouse BRD4 siRNA-SMARTPool (Horizon) at 1 µM concentration. M-CSF at 10 ng/ml was added in the Accel treated wells. The remaining seeded wells had their media replaced with factor, except for two duplicates that were left without M-CSF. Wells deprived from factor were used as cell death positive controls. At 13 div DMEM/F12 containing 10 % FBS, 1 % P/S and L-glutamine was added at 1/4 proportion considering the final volume per well. M-CSF was added again to all conditions, except to the duplicates left without M-CSF.

At 14 div an MTT (3-(4,5-dimethylthiazol-2-yl)-2,5-diphenyltetrazolium bromide) assay was performed to determine cell viability. Media was replaced with media containing 0.15 mg/mL MTT. The culture was maintained at 37ºC for 3 hours to finally lyse the cells with DMSO. Absorbance was read out through a spectrophotometer (Bio-tek) at 560 nm and 600 nm wavelength using KC Junior software. Readings were normalized against untreated cells with M-CSF to obtain the percentage of survival. A total of 4 independent cultures were performed.

Chromatin immunoprecipitation (ChIP)-qPCR

At 8 div primary BMDMs were seeded at a density of ~$5x10^6$ cells per condition in 100 mm petri dishes. At 10 div cells were treated with DMSO or JQ1 1000 nM for an hour. Then, samples were crosslinked with 1% formaldehyde (Sigma) for 10 minutes and quenched with 0,125 M of glycine for 5 minutes. Cells were washed with PBS, collected in 15mL tubes (Falcon) and frozen at -80 ºC. Pellets were resuspended in 0,25 mL of Lysis buffer (1%SDS, 10mM EDTA and 50nM Tris-Hcl pH=8) containing protease (Sigma) and phosphatase (Roche) inhibitors at 1x. Samples were then transferred to Bioruptor tubes and finally sonicated using a Bioruptor Pico (Diagenode) at 4ºC during 8 cycles (30 seconds ON and 30 seconds OFF). DNA size of sonicated samples was validated to be from 300 bp to 1000 bp in a 1% agarose gel. After size determination samples were centrifuged at 4ºC and 15000g for 10 minutes. The supernatant was kept and used for chromatin immunoprecipitations with antibodies pre-bound to A/G-protein beads (Sigma and Invitrogen). The antibodies used for immunoprecipitation are listed in Table 1.

Name	Immunogen	Manufacturer, catalog number, RRID, host	Concentration and application
BRD4 Polyclonal Antibody	BRD4	Bethyl Laboratories – Thermo fisher, Cat#A301-985A50, RRID: AB_2631449, Rabbit, polyclonal	3 µg, ChIP
Recombinant Anti-CHD4 Antibody	CHD4	Abcam, Cat#ab240640, RRID: RRID:AB_2941814, Rabbit, monoclonal	3 µg, ChIP
Normal Rabbit IgG	IgG	Cell signaling technology, Cat#2729, RRID: AB_1031062, Rabbit	3 µg, ChIP

Table 1: Antibody list

Immunoprecipitated DNA was de-crosslinked and digested with RNAse A (Invitrogen) and Proteinase K (Thermo Fisher Scientific). DNA was purified using the Clean-Easy PCR Purification Kit (Canvax Biotech) and used for quantitative PCR. A total of three independent cultures were set to assess chromatin immunoprecipitation at IL-13 promoter and two independent cultures were established to assess provisional tendencies at IL-4 promoter. Primers used for ChIP-qPCR are displayed in table 2. The IL-4 ChIP primer is located 345 bp before the transcription start site (TSS), whereas the IL-13 ChIP primer is directly located in the TSS.

RNA isolation, Reverse transcription PCR and quantitative PCR

RNA was extracted using the RNeasy Micro Kit (QIAGEN) following the manufacturer's guidelines. RNA quantification was performed with a NanoDrop 1000 Spectrophotometer (Thermo Fisher Scientific) and reverse-transcribed using the High-capacity cDNA Reverse Transcription kit (Applied Biosystems – Thermo Fisher Scientific). The expression of target genes was determined through qPCR using iTaq Universal SYBR Green Supermix (BioRad) and the corresponding primers (Table 2, see next page). Glyceraldehyde-3-phosphate dehydrogenase (GAPDH) was used as a housekeeping gene.

Gene	Forward primer: 5'– 3'	Reverse primer: 3'– 5'
Mouse Arg1	GTGAAGAACCCACGGTCTGT	CCAGAGATGCTTCCAACTGC
Mouse BRD2	CCCACCCATCAGTCATCTCT	GGGGTGGTAGTATCCGCTTT
Mouse BRD3	AAGAAGGCCAACAGCACAAC	CCCTCCTCCTCTTCCTCTGA
Mouse BRD4	TGCTCAGAGTGGTGCTCAAG	TCCCATATCCATGGGTGTTT
Mouse ChIP IL-13	GCATGCCTTCTGCTTGTCTTGA	GAACTGGAAATCTGCCTCCGTC
Mouse ChIP IL-4	ACTTTCTTGATATTACTCTGTCTTTCC	GTTGCCACTGGCTCTCCTC
Mouse CHD4	CAAGGCCAAGACCAAGGAG	CCCAGCTTGATCTTCAGAGG
Mouse CHD8	CAGCCAGTAAAGGGTTCAGC	AGGACCAAAGTGATGCGTTT
Mouse CD206	ATTGTGGAGCAGATGGAAGG	ATTTGCATTGCCCAGTAAGG
Mouse GAPDH	TGGCCTTCCGTGTTCCTAC	GAGTTGCTGTTGAAGTCG
Mouse IL-1β	CTTCAAATCTCACAGCAGCACATC	CCACGGGAAAGACACAGGTAG
Mouse IL-4	GGCTTTCCTCTTTCCCACTC	AGCCGCCATGAGAGCTAAG
Mouse IL-6	AACCACGGCCTTCCCTACTTCA	TCATTTCCACGATTTCCCAGAG
Mouse IL-10	GCTGAGACTTTCGCTCCTCTC	AGCTCCAAGGCACCTGTTC
Mouse IL-13	TCCAATTGCAATGCCATCTA	TGGGCTACTTCGATTTTGGT
Mouse TNF-α	AGGCACTCCCCCAAAAGATG	TCACCCCGAAGTTCAGTAGAC

Table 2: Primer list.

Statistical analysis

Results were analyzed using GraphPad Prism 7 software and differences were considered significant when $p<0,05$. For statistical analysis of mRNA expression and secreted proteins, a One-way ANOVA for multiple comparisons with Tukey's correction was performed. The qPCR values for BRD4 knockdown were statistically analyzed through a T-test. For the ChIP experiment at the IL-13 promoter, a Sidak's Two-way ANOVA was assessed using treatment and the antibody selected for immunoprecipitation as factors. For all experiments data is shown in bar graphs as mean ± SEM.

Results

BET-inhibition by JQ1 reduces pro-inflammatory cytokine secretion, and increases anti-inflammatory cytokine transcription in macrophages

In the previous chapter we observed that the conditioned medium from JQ1-treated macrophages increased neurite outgrowth through the STAT6 pathway, which is activated under the influence of IL-4 and IL-13 (Junttila, 2018; Palomes-Borrajo et al., 2022). However, we did not test the presence of these anti-inflammatory mediators in the macrophage-derived

media. To address this issue, we aimed to determine if the conditioned media used in the former experiment contained IL-4 and IL-13.

Firstly, we assessed the transcriptional profile of macrophages treated with the BET inhibitor JQ1 and its effects after LPS-mediated macrophage activation. We observed that the transcription profile of IL-4 and IL-13 was not affected by LPS stimulation. However, treatment with JQ1 for 6 hours significantly raised the expression of both anti-inflammatory cytokines with an average of 5,42-fold for IL-4 and 3,91-fold for IL-13 (Figure 1A). These effects on anti-inflammatory cytokine transcription were counteracted when BET-inhibition occurred after LPS pre-activation, which returned their expression close to basal levels.

This pattern differed when considering the anti-inflammatory cytokine IL-10, which transcription is influenced by LPS (Barsig et al., 1995). We detected a raise on IL-10 expression after LPS activation, although it was not significant. Although, BET inhibition alone did not alter the transcription levels of this cytokine, JQ1 treatment displayed a tendency of downregulating IL-10 expression on macrophages that underwent previous LPS stimulation (Figure 1A).

Regarding the pro-inflammatory cytokines TNF-α, IL-1β and IL-6, BET-inhibition significantly reduced the effects of LPS transcriptional activation (Figure 1B). Thus, JQ1 and LPS carry out opposing roles. While LPS counteracts the increase of IL-4 and IL-13 transcription carried out after BET-inhibition, JQ1 prevents the transcription of inflammatory mediators conducted by LPS.

Next, we assessed the protein levels of secreted cytokines present in the macrophage's media. In the assay we were only able to detect the secreted form of TNF-α, IL-6 and IL-10. These three inflammatory mediators followed a similar pattern than their respective mRNA analysis, where their secretion was upregulated after LPS stimulation. JQ1 treatment after LPS activation significantly reduced the transcription of IL-6. Although TNF-α and IL-10 followed a similar dynamic, the decrease on their expression was not significant (Figure 1C).

To summarize, JQ1 treatment for 6 h raises the transcription of the anti-inflammatory cytokines IL-4 and IL-13. However, we were unable to detect their secreted form in the macrophage-derived conditioned medium. In addition, BET protein inhibition in activated macrophages downregulates the transcription and secretion of pro-inflammatory mediators.

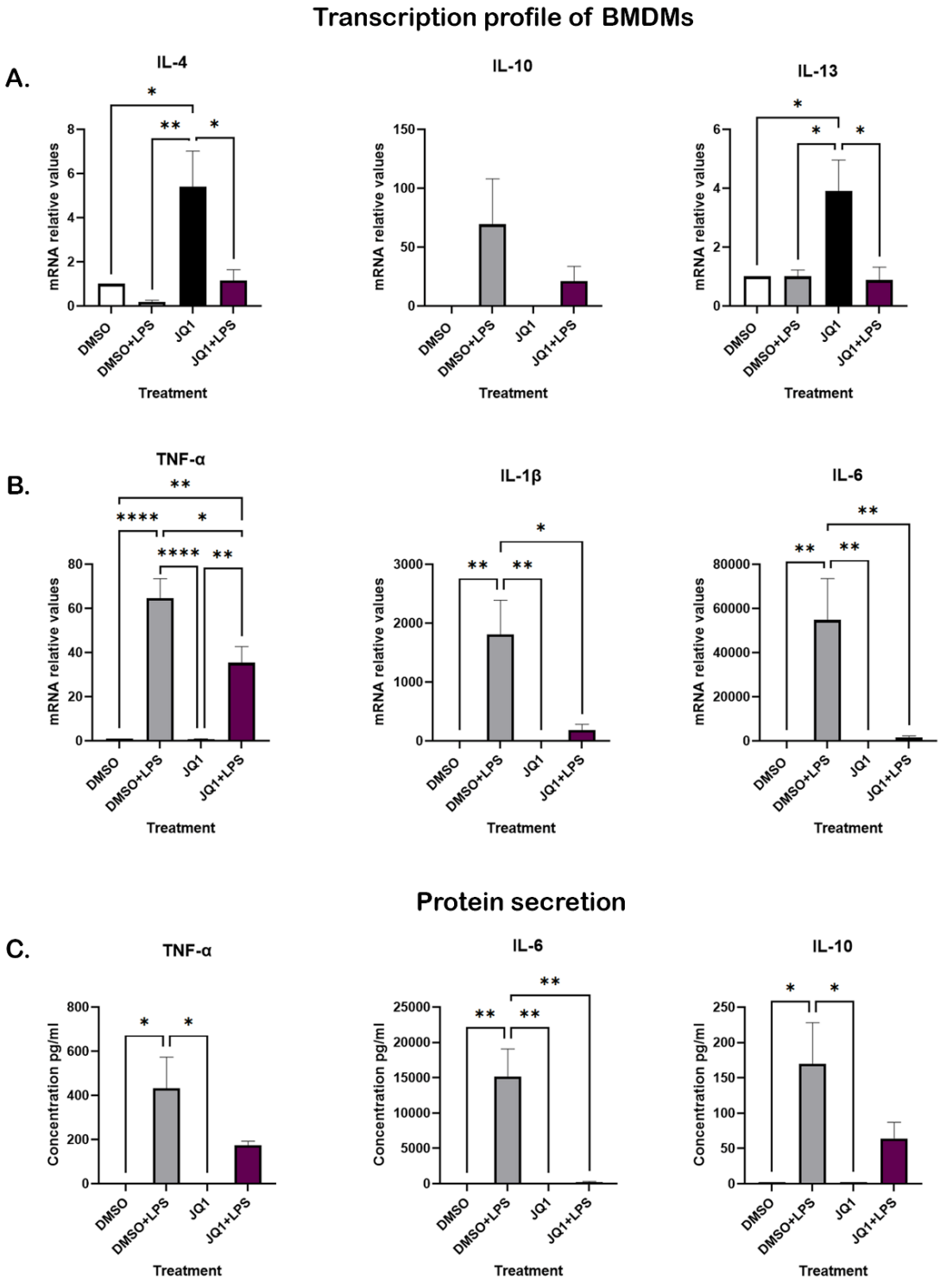

Figure 1: BET-inhibition with JQ1 increases anti-inflammatory cytokine transcription while decreasing the pro-inflammatory profile of macrophages. A) JQ1 increases IL-4 and IL-13 anti-inflammatory cytokine gene expression. B) JQ1 treatment decreases the LPS-induced transcription of IL-1β, IL-6 and TNF-α. C) BET-inhibition impairs the LPS dependent protein secretion. *p<0.05, **p<0.01 and ****p<0.0001 as calculated by a One-way ANOVA for multiple comparisons followed by Tukey's correction. Results are shown in bar graphs as mean ± SEM. N= 4 independent cultures.

Thus, BET proteins seem to play a role in regulating the inflammatory response in macrophages.

BRD4 knockdown increases the transcription of the anti-inflammatory cytokines IL-4 and IL-13 without affecting macrophage viability

Since JQ1 treatment enhances the transcription of the anti-inflammatory cytokines IL-4 and IL-13, it can be hypothesized that in basal conditions BET proteins may be preventing anti-inflammatory cytokine expression. Provided that JQ1 is a pan-BET inhibitor, we aimed to underscore which BET protein may be implicated in the repression of these anti-inflammatory mediators. As BRD4 is associated with inflammation and its preferentially targeted by JQ1, we performed a knockdown to assess its potential role as a regulator of IL-4 and IL-13 transcription (Filippakopoulos et al., 2010; Hajmirza et al., 2018).

Knockdown of BRD4 using short interference RNA (siRNA) resulted in significant downregulation of its transcription, up to 27.6%, without altering the expression of the other BET proteins. This ensures that any alteration observed in cytokine transcription can be directly attributed to BRD4 instead of other members of the BET protein family (Figure 2A). BRD4 knockdown led to a significant increase on the transcription of IL-4 and IL-13, which were upregulated 1.54-fold and 2.06-fold respectively. The expression of the cytokine IL-10 displayed a tendency to increase after BRD4 silencing, but these changes were not significant (Figure 2B). Finally, there were no differences in the transcription of the M2 polarity markers Arginine 1 (Arg1) and Cluster of differentiation 206 (CD206) under BRD4 knockdown (Figure 2C).

In addition, BRD4 has been reported to compromise development and proliferation of resident peritoneal macrophages on a $BRD4^{fl/fl}$ LysM-Cre transgenic mouse strain (Dey et al., 2019). However, in our conditions, silencing of BRD4 did not significantly affect macrophage viability, that had a survival rate of 77% (Figure 2D). Thus, our results suggest that BRD4 could be repressing the expression of IL-4 and IL-13 anti-inflammatory cytokines in basal conditions without compromising macrophage viability.

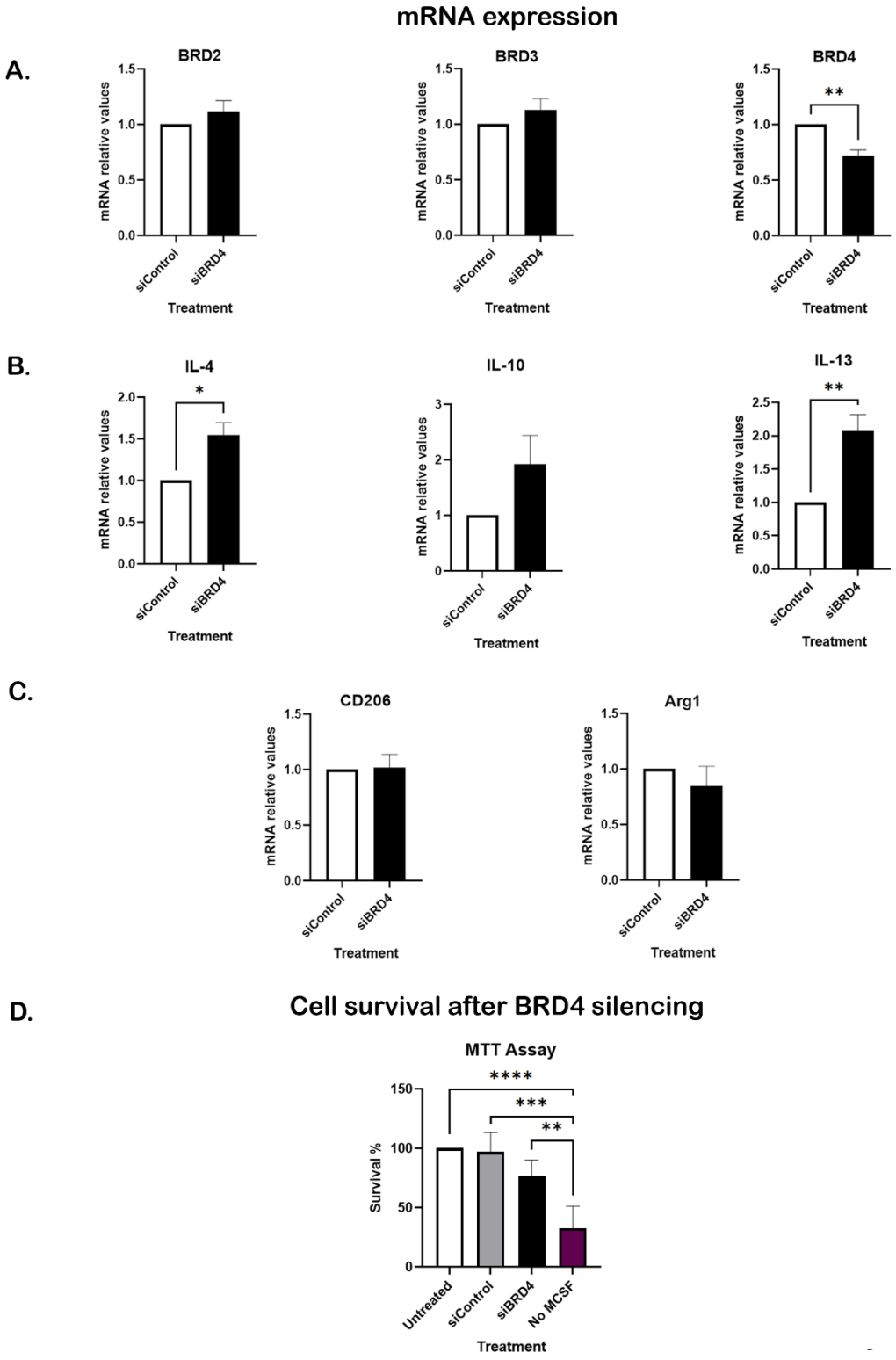

Figure 2: BRD4 prevents anti-inflammatory gene expression and does not affect macrophage viability. A) Knockdown of BRD4 did not affect other BET family members. B) siBRD4 increases IL-4 and IL-13 transcription. C) BRD4 knockdown does not alter the transcription of the M2 polarity markers CD206 and Arg1. D) BRD4 silencing does not affect macrophage survival. *p<0.05, **p<0.01, ***p<0.001 and ****p<0.0001 as calculated by a T-test. Results are displayed as mean ± SEM. A total of n=4 independent cultures were used for the transcriptional profile after BRD4 knockdown and for the cell survival assay.

CHD4 silencing raises anti-inflammatory cytokine transcription

Since BRD4 is an epigenetic reader and we observed that it hinders anti-inflammatory cytokine production, we intended to assess if it binds to other proteins forming a repressor complex that prevents IL-4 and IL-13 transcription. As BRD4 has high binding affinity with the repressive proteins CHD4 and CHD8, we studied them as possible partners.

We performed knockdown using siRNA against CHD4 and CHD8, which were significantly downregulated, leaving an expression of 32% for CHD4 and 24% for CHD8. Moreover, knockdown of both repressors did not affect the transcription of each other, allowing the attribution of any altered parameter to the silenced target (Figure 3A). To assess that alterations on the cytokine transcriptional profiles were due to the knockdown of the repressor candidates, we also assessed possible alterations on the profile of BET proteins. In this regard, we did not observe any variation on the expression of the members of the BET protein family (Figure 3B).

Concerning anti-inflammatory cytokines, silencing of CHD4 significantly raised the transcription of IL-4 and IL-13 anti-inflammatory mediators about 2-fold. In contrast, knockdown of CHD8 did not induce any changes in the expression of both cytokines. Coinciding with the observations made after JQ1 treatment and BRD4 silencing, the anti-inflammatory cytokine IL-10 was unaffected under siCHD4 and siCHD8 administration (Figure 3C). We also assessed if CHD4 and CHD8 knockdowns affected M2 macrophage polarity and found that siCHD4 significantly upregulated the transcription of the M2 markers Arg1 and CD206 a total of 4-fold and 2,9-fold each (Figure 3D). These results prove that CHD4 is preventing the expression of the anti-inflammatory cytokines IL-4 and IL-13, suggesting that it may be a repressive partner of BRD4.

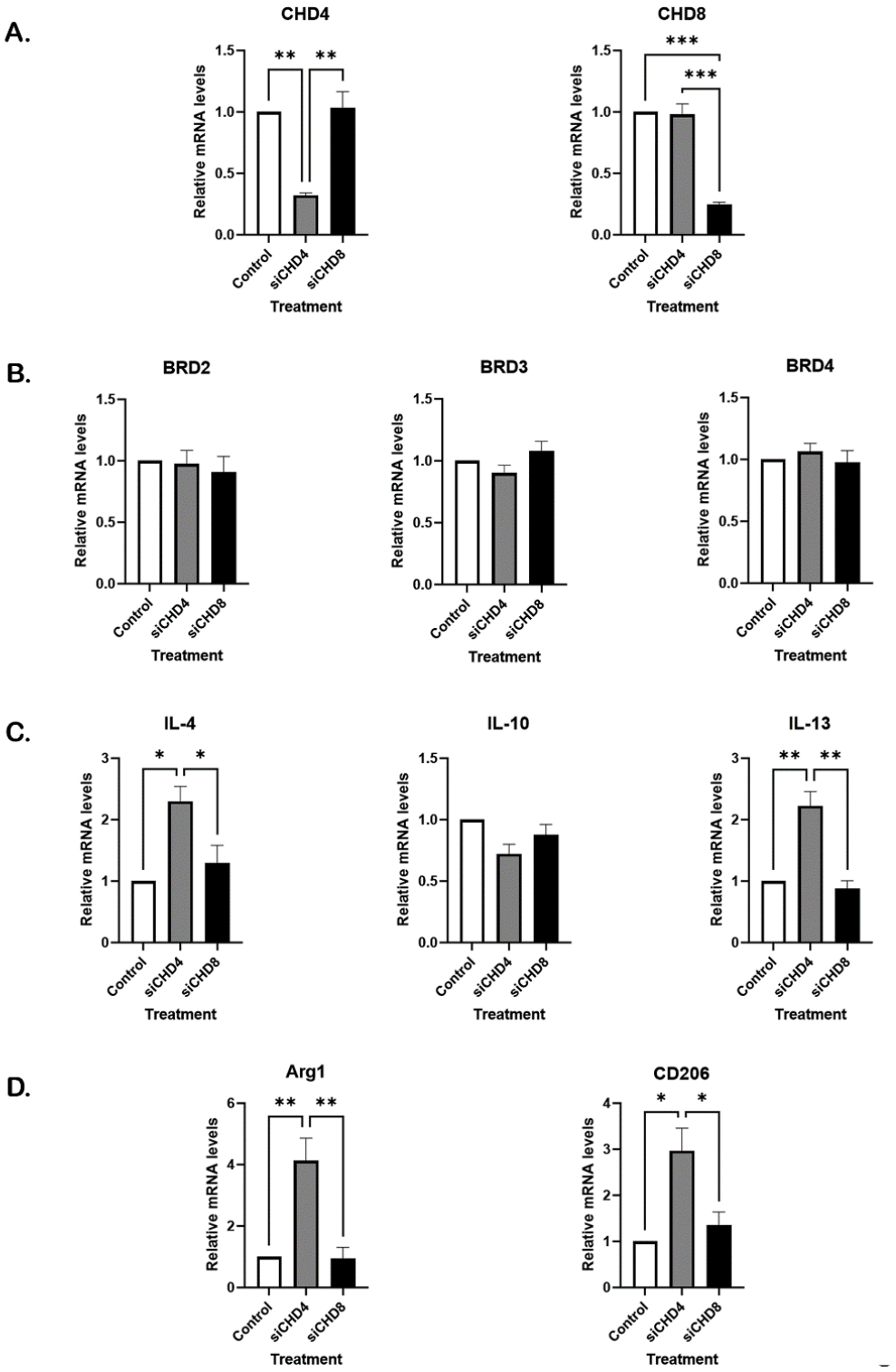

Figure 3: CHD4 represses IL-4 and IL-13 transcription. A) Knockdown successfully reduced the expression of each target gene without affecting the other repressor candidate. B) BET protein expression was unaffected after CHD4 and CHD8 silencing. C) CHD4 knockdown increased IL-4 and IL-13 transcription. D) siCHD4 raised the expression of the M2 polarity markers Arg1 and CD206. *p<0.05, **p<0.01 and ***p<0.001 as calculated by a One-way ANOVA for multiple comparisons followed by Tukey's correction. Results are shown in bar graphs as mean ± SEM. N=3 independent cultures.

BRD4 and CHD4 prevent IL-13 transcription by binding to its promoter

We hypothesized that under physiological conditions BRD4 may form a repressor complex on promoters of anti-inflammatory genes preventing their transcription. Then, upon BET inhibition there would be a release of the repressive complex from the DNA, facilitating IL-4 and IL-13 expression. To prove our hypothesis, we aimed to demonstrate that both BRD4 and CHD4 proteins bind to the promoters of IL-4 and IL-13 genes and that JQ1 treatment disrupts this binding.

For this purpose, we performed ChIP-qPCR of BRD4 and CHD4 proteins. The results show that basal binding at the IL-13 promoter was of 2.5-fold for BRD4 and 3.2-fold for CHD4 with respect to IgG. This union was interrupted in macrophages treated with the BET inhibitor JQ1, where there was a significant release of BRD4 and CHD4 from the IL-13 promoter. Specifically, when JQ1 was used as a treatment, binding at the promoter region of IL-13 was 0.6-fold for BRD4 and 1.2-fold for CHD4 with respect to IgG (Figure 4A). Thus, in basal conditions BRD4 and CHD4 bind to the IL-13 promoter and upon BET-inhibition they disassemble from chromatin.

We observed a similar tendency on IL-4, where BET-inhibition seems to reduce the union of BRD4 and CHD4 at the IL-4 promoter (Figure 4B). Nevertheless, we need to replicate the IL-4 experiment for these observations to be conclusive.

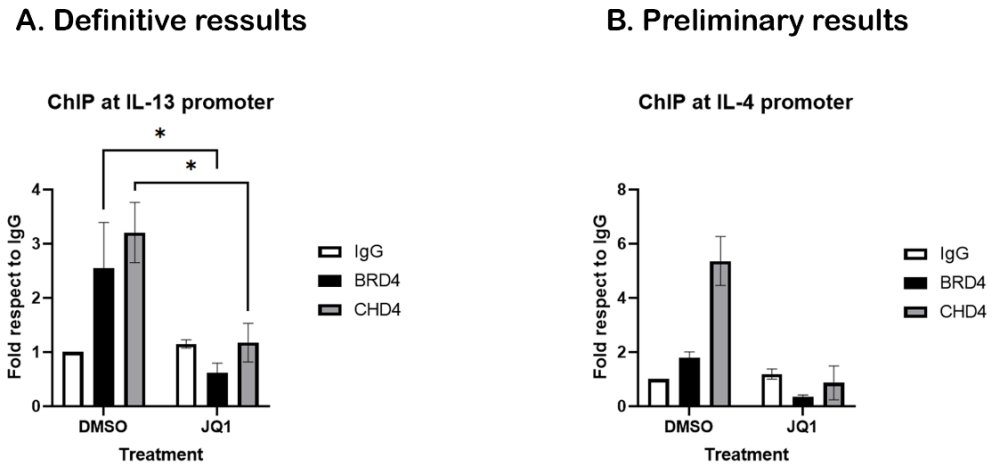

Figure 4: BRD4 and CHD4 bind to IL-13 promoter under physiological conditions and are released upon JQ1 treatment. A) JQ1 disrupts the union of BRD4 and CHD4 at the IL-13 promoter. B) Preliminary results of BRD4 and CHD4 union at IL-4 promoter. *p<0.05, as calculated by a Two-way ANOVA for multiple comparisons followed by Sidak's correction. Results are shown in bar graphs as mean ± SEM. N=3 independent cultures for IL-13 promoter and n=2 independent cultures for the preliminary study in the IL-4 promoter.

Thus, these results demonstrate that BRD4 and CHD4 bind to the IL-13 promoter, and probably to the IL-4 promoter. Then, upon JQ1 stimulation these proteins release from the chromatin, presumably facilitating anti-inflammatory cytokine transcription.

Discussion

Inflammation is a complex mechanism subjected under epigenetic control. However, few studies had focused on unraveling the role of epigenetic readers in inflammatory events. In this study, we provide information about the role of BET proteins on anti-inflammatory cytokine production. Specifically, we assessed the consequences of pan-BET inhibition and BRD4 knockdown, on the inflammatory transcriptional profile of macrophages. We also determined that BET-inhibition by JQ1 promotes the release of the repressor proteins BRD4 and CHD4 from the IL-13 promoter, probably facilitating its transcription in primary macrophages. Thus, this study provides new insights and possible targets to regulate the expression of anti-inflammatory mediators.

BET inhibition using JQ1 in cultured macrophages increased the transcription of IL-4 and IL-13 anti-inflammatory cytokines, while it negatively regulated the LPS-induced pro-inflammatory mediators TNF-α, IL-1β and IL-6. Next, using medium from the same samples, we determined the concentration of secreted cytokines employing Luminex technology. We observed that JQ1 treatment significantly decreased the secretion of the LPS-induced protein IL-6. Additionally, the LPS-regulated cytokines TNF-α and IL-10 followed a similar dynamic although the reduction was not significant. Overall, these results are concordant with other scientific reports. In fact, our laboratory had previously observed that cultured macrophages treated with 1 µM of JQ1 for 2 hours had an increase on the transcription of IL-4 and IL-13 (Sanchez-Ventura et al., 2019). However, in that experiment an increase on IL-10 transcription was also reported, a change that was not observed in the present study. Probably the discrepancy regarding IL-10 gene expression is due to the different time exposure to treatment, which was longer in our present investigation. Moreover, our results are also coincident with those of Nicodeme et al. who reported that BET-inhibition using I-BET762 downregulates LPS-induced gene expression (Nicodeme et al., 2010). On the other hand, there are conflicting results on the effects of BET-inhibition on TNF-α transcription. For instance, it has been described in transcriptomic studies that the pro-inflammatory cytokine TNF-α was not affected by I-BET762

and JQ1 in macrophages (Das et al., 2015; Nicodeme et al., 2010). Contrarily, the use of JQ1 in the macrophage cell line RAW 264.7 and after spinal cord injury promoted the downregulation of TNF-α transcription (S. Meng et al., 2014; Sanchez-Ventura et al., 2019). These differences between studies could be attributed to the compound, cell type or the duration of treatment. Thus, further studies should clarify this issue.

Paradoxically, in our research we did not identify the presence of the secreted anti-inflammatory cytokines IL-4 and IL-13 in the macrophages' medium, although we observed an increase on their transcription upon JQ1 treatment. We attribute this discrepancy to the selected assay for protein detection, which may have not enough sensibility. To support this idea, we observed that upon LPS stimulation the transcription of pro-inflammatory genes is upregulated more than 70-fold, and the decrease with JQ1 treatment is around the same magnitude. In the case of anti-inflammatory cytokines, the increase of anti-inflammatory gene expression with JQ1 is less than 6-fold. Thus, although there is an increase in anti-inflammatory cytokine transcription, the rate of transcription is very different between IL-4 and IL-13 compared to the rest of cytokines. Thus, to solve this issue we could further perform a proteomic analysis or use a qPCR-based ELISA kit which have higher sensibility and could possibly allow to identify these proteins. Nevertheless, with an appropriate assay we would expect to detect IL-4 and IL-13, as we previously observed that conditioned media from BET-inhibited macrophages that followed the same treatment was able to activate STAT6 pathway in dorsal root ganglia explants (Palomes-Borrajo et al., 2022).

Provided that BET inhibition increased the transcription of anti-inflammatory mediators in macrophages, we hypothesized that BET proteins may form a repressor complex on the promoters of anti-inflammatory cytokines preventing their expression in basal conditions. Then, with JQ1 treatment, the BET-repressor complex would release from the promoters of anti-inflammatory cytokines allowing IL-4 and IL-13 transcription. Provided that BRD4 is the BET family member that has been more closely related to inflammation (Hajmirza et al., 2018; B. Huang et al., 2009), we performed a knockdown of this protein in primary macrophages. As a result, BRD4 silencing raised the transcription of the anti-inflammatory mediators IL-4 and IL-13, without affecting other BET family members. However, after BRD4 knockdown we did not observe an increase on the expression of the M2 polarity markers *Arg1* and *CD206*. These results differed from what we expected, as anti-inflammatory cytokines trigger M2 polarity in

macrophages (Morris, Kershaw, & Babon, 2018). Nevertheless, science reports also indicate that BET inhibition does not lead to M2 polarization. In fact, mice that received JQ1 treatment after spinal cord injury did not display alterations on these polarity markers (Sanchez-Ventura et al., 2019). Additionally, animals that underwent a BRD4 knockout in macrophages have been reported to display a fall of M2 markers and diminished M1 responses under IFN-γ stimulation (Dey et al., 2019; Sanchez-Ventura et al., 2019). Thus, it seems that although BRD4 enhances the expression of anti-inflammatory mediators it also may trigger a pathway that compromises macrophage polarity. In this regard, a study made in ovarian cancer cell lines indicated that JQ1 treatment for 72 hours downregulated the expression of the Janus Kinases JAK1, JAK2 and JAK3 (Bagratuni et al., 2020). These proteins phosphorylate STAT proteins, a step necessary for their translocation to the cell nucleus. Thus, it could be that BRD4 knockdown in macrophages is inhibiting JAK1 or JAK2 pathways and subsequently not activating STAT6, preventing the acquisition of the M2 phenotype in macrophages (Morris et al., 2018). Nevertheless, more research should be done to address this issue.

We also observed that BRD4 knockdown in *vitro* did not compromise cell viability. This result coincides with a study made in microglia *in vitro,* but differs from an *in vivo* experiment that pointed that macrophage specific BRD4 KO compromises development and proliferation of resident peritoneal macrophages (Dey et al., 2019; Matuszewska, Cieslik, Wilkaniec, Strawski, & Czapski, 2022). Concerning these discrepancies, it is possible that the differences reside in the maturation stage of cells. Whereas cultured cells are already differentiated, *in vivo* cells are in variable maturity stages. Nevertheless, considering cell viability and macrophage polarization, we must acknowledge that it could also be possible that BRD4 knockdown is not efficient enough to detect alterations in those parameters. Thus, it would be suitable to stablish a stronger knockdown method and observe the effects on cell viability and macrophage polarity. It would be also convenient to assess the effects of the knockdown of other members of the BET protein family, as it has been described that BRD2 can also be involved in inflammatory events (Belkina et al., 2013).

Next, we aimed to assess if BRD4 could conform a repressor complex with other proteins preventing IL-4 and IL-13 expression. We considered the proteins CHD4 and CHD8 as possible candidates, as they form part of repressor complexes, are involved with the hematopoietic lineage and have been found to bind the extra terminal domain of BRD4 (Hurley et al., 2021;

Rahman et al., 2011; Shen et al., 2015). We observed that upon CHD4 silencing there was an increase in the transcription of IL-4 and IL-13 anti-inflammatory mediators, without affecting the expression profile of BET proteins. These effects were not observed by knocking down CHD8. Thus, evidence suggest that CHD4 could be repressing the secretion of anti-inflammatory cytokines on physiological conditions.

To note, CHD4 and CHD8 are epigenetic readers that belong to the Chromodomain superfamily. Chromodomains (CHDs) are ATP-dependent chromatin remodeling enzymes that utilize ATP hydrolysis to promote nucleosome sliding and alter chromatin conformation (Boulasiki, Tan, Spinelli, & Riccio, 2023). Specifically, CHD4 is included in the NuRD repressive complex, and can bind to epigenetic modifications on histone 3 (Boulasiki et al., 2023; Mansfield et al., 2011). The former complex is comprised by many proteins, between them special interest resides in the histone deacetylases (HDAC1 and 2) which removes acetylation marks from the histone tails closing the chromatin conformation (Boulasiki et al., 2023). Nevertheless, recent evidence proved that CHD4 can also promote alterations in DNA disposition without depending on other NuRD complex proteins (Zhong et al., 2020). Thus, the repressive mechanism of CHD4 in physiological conditions could reside in the deacetylase activity of the NuRD complex or in the intrinsic capacity of CHD4 of promoting nucleosome displacement. Future research should elucidate by which concrete mechanism CHD4 is preventing anti-inflammatory cytokine transcription by analyzing HDAC activity. In addition, CHD4 knockdown raised the expression of M2 polarity markers in macrophages. In this regard, it has already been assessed that CHD4 contributed to the induction of Th2 cell identity on undifferentiated CD4 lymphocytes (Hosokawa et al., 2013). Thus, it is possible that CHD4 triggers a similar effect on macrophages being an important catalyzer of M2 polarization.

Finally, we observed that JQ1 treatment released BRD4 and CHD4 from the promoter of IL-13, which confirmed our hypothesis. However, the experiment should be replicated for the IL-4 promoter to achieve definitive results suitable for statistical analysis. In addition, further experiments should validate by co-immunoprecipitation the formation of a BRD4-CHD4 complex in the promoter of these anti-inflammatory cytokines in primary macrophages.

Conclusions

In conclusion, this study provides insights on the relation between BRD4 and IL-4/IL-13 anti-inflammatory cytokine transcription and suggests two new valuable targets to regulate inflammation in multiple diseases.

References

Bagratuni, T., Mavrianou, N., Gavalas, N. G., Tzannis, K., Arapinis, C., Liontos, M., . . . Bamias, A. (2020). JQ1 inhibits tumour growth in combination with cisplatin and suppresses JAK/STAT signalling pathway in ovarian cancer. *Eur J Cancer, 126*, 125-135. doi:10.1016/j.ejca.2019.11.017

Barsig, J., Kusters, S., Vogt, K., Volk, H. D., Tiegs, G., & Wendel, A. (1995). Lipopolysaccharide-induced interleukin-10 in mice: role of endogenous tumor necrosis factor-alpha. *Eur J Immunol, 25*(10), 2888-2893. doi:10.1002/eji.1830251027

Belkina, A. C., Nikolajczyk, B. S., & Denis, G. V. (2013). BET protein function is required for inflammation: Brd2 genetic disruption and BET inhibitor JQ1 impair mouse macrophage inflammatory responses. *J Immunol, 190*(7), 3670-3678. doi:10.4049/jimmunol.1202838

Bhatt, D., & Ghosh, S. (2014). Regulation of the NF-kappaB-Mediated Transcription of Inflammatory Genes. *Front Immunol, 5*, 71. doi:10.3389/fimmu.2014.00071

Boulasiki, P., Tan, X. W., Spinelli, M., & Riccio, A. (2023). The NuRD Complex in Neurodevelopment and Disease: A Case of Sliding Doors. *Cells, 12*(8). doi:10.3390/cells12081179

Das, A., Chai, J. C., Yang, C. S., Lee, Y. S., Das, N. D., Jung, K. H., & Chai, Y. G. (2015). Dual transcriptome sequencing reveals resistance of TLR4 ligand-activated bone marrow-derived macrophages to inflammation mediated by the BET inhibitor JQ1. *Sci Rep, 5*, 16932. doi:10.1038/srep16932

Dey, A., Yang, W., Gegonne, A., Nishiyama, A., Pan, R., Yagi, R., . . . Ozato, K. (2019). BRD4 directs hematopoietic stem cell development and modulates macrophage inflammatory responses. *EMBO J, 38*(7). doi:10.15252/embj.2018100293

Fang, W. F., Chen, Y. M., Lin, C. Y., Huang, H. L., Yeh, H., Chang, Y. T., . . . Lin, M. C. (2018). Histone deacetylase 2 (HDAC2) attenuates lipopolysaccharide (LPS)-induced inflammation by regulating PAI-1 expression. *J Inflamm (Lond), 15*, 3. doi:10.1186/s12950-018-0179-6

Filippakopoulos, P., Qi, J., Picaud, S., Shen, Y., Smith, W. B., Fedorov, O., . . . Bradner, J. E. (2010). Selective inhibition of BET bromodomains. *Nature, 468*(7327), 1067-1073. doi:10.1038/nature09504

Hajmirza, A., Emadali, A., Gauthier, A., Casasnovas, O., Gressin, R., & Callanan, M. B. (2018). BET Family Protein BRD4: An Emerging Actor in NFkappaB Signaling in Inflammation and Cancer. *Biomedicines, 6*(1). doi:10.3390/biomedicines6010016

Hosokawa, H., Tanaka, T., Suzuki, Y., Iwamura, C., Ohkubo, S., Endoh, K., . . . Nakayama, T. (2013). Functionally distinct Gata3/Chd4 complexes coordinately establish T helper 2 (Th2) cell identity. *Proc Natl Acad Sci U S A, 110*(12), 4691-4696. doi:10.1073/pnas.1220865110

Huang, B., Yang, X. D., Zhou, M. M., Ozato, K., & Chen, L. F. (2009). Brd4 coactivates transcriptional activation of NF-kappaB via specific binding to acetylated RelA. *Mol Cell Biol, 29*(5), 1375-1387. doi:10.1128/MCB.01365-08

Hurley, S., Mohan, C., Suetterlin, P., Ellingford, R., Riegman, K. L. H., Ellegood, J., . . . Basson, M. A. (2021). Distinct, dosage-sensitive requirements for the autism-associated factor CHD8 during cortical development. *Mol Autism, 12*(1), 16. doi:10.1186/s13229-020-00409-3

Junttila, I. S. (2018). Tuning the Cytokine Responses: An Update on Interleukin (IL)-4 and IL-13 Receptor Complexes. *Front Immunol, 9*, 888. doi:10.3389/fimmu.2018.00888

Lauterbach, M. A., Hanke, J. E., Serefidou, M., Mangan, M. S. J., Kolbe, C. C., Hess, T., . . . Latz, E. (2019). Toll-like Receptor Signaling Rewires Macrophage Metabolism and Promotes Histone Acetylation via ATP-Citrate Lyase. *Immunity, 51*(6), 997-1011 e1017. doi:10.1016/j.immuni.2019.11.009

Li, D., & Wu, M. (2021). Pattern recognition receptors in health and diseases. *Signal Transduct Target Ther, 6*(1), 291. doi:10.1038/s41392-021-00687-0

Liu, L., Yang, C., & Candelario-Jalil, E. (2021). Role of BET Proteins in Inflammation and CNS Diseases. *Front Mol Biosci, 8*, 748449. doi:10.3389/fmolb.2021.748449

Mansfield, R. E., Musselman, C. A., Kwan, A. H., Oliver, S. S., Garske, A. L., Davrazou, F., . . . Mackay, J. P. (2011). Plant homeodomain (PHD) fingers of CHD4 are histone H3-binding modules with preference for unmodified H3K4 and methylated H3K9. *J Biol Chem, 286*(13), 11779-11791. doi:10.1074/jbc.M110.208207

Matuszewska, M., Cieslik, M., Wilkaniec, A., Strawski, M., & Czapski, G. A. (2022). The Role of Bromodomain and Extraterminal (BET) Proteins in Controlling the Phagocytic Activity of Microglia In Vitro: Relevance to Alzheimer's Disease. *Int J Mol Sci, 24*(1). doi:10.3390/ijms24010013

Meng, S., Zhang, L., Tang, Y., Tu, Q., Zheng, L., Yu, L., . . . Chen, J. (2014). BET Inhibitor JQ1 Blocks Inflammation and Bone Destruction. *J Dent Res, 93*(7), 657-662. doi:10.1177/0022034514534261

Micucci, J. A., Sperry, E. D., & Martin, D. M. (2015). Chromodomain helicase DNA-binding proteins in stem cells and human developmental diseases. *Stem Cells Dev, 24*(8), 917-926. doi:10.1089/scd.2014.0544

Morris, R., Kershaw, N. J., & Babon, J. J. (2018). The molecular details of cytokine signaling via the JAK/STAT pathway. *Protein Sci, 27*(12), 1984-2009. doi:10.1002/pro.3519

Nicodeme, E., Jeffrey, K. L., Schaefer, U., Beinke, S., Dewell, S., Chung, C. W., . . . Tarakhovsky, A. (2010). Suppression of inflammation by a synthetic histone mimic. *Nature, 468*(7327), 1119-1123. doi:10.1038/nature09589

Nita, A., Muto, Y., Katayama, Y., Matsumoto, A., Nishiyama, M., & Nakayama, K. I. (2021). The autism-related protein CHD8 contributes to the stemness and differentiation of mouse hematopoietic stem cells. *Cell Rep, 34*(5), 108688. doi:10.1016/j.celrep.2021.108688

Palomes-Borrajo, G., Navarro, X., & Penas, C. (2022). BET protein inhibition in macrophages enhances dorsal root ganglion neurite outgrowth in female mice. *J Neurosci Res, 100*(6), 1331-1346. doi:10.1002/jnr.25036

Rahman, S., Sowa, M. E., Ottinger, M., Smith, J. A., Shi, Y., Harper, J. W., & Howley, P. M. (2011). The Brd4 extraterminal domain confers transcription activation independent of pTEFb by recruiting multiple proteins, including NSD3. *Mol Cell Biol, 31*(13), 2641-2652. doi:10.1128/MCB.01341-10

Saccani, S., Pantano, S., & Natoli, G. (2001). Two waves of nuclear factor kappaB recruitment to target promoters. *J Exp Med, 193*(12), 1351-1359. doi:10.1084/jem.193.12.1351

Sanchez-Ventura, J., Amo-Aparicio, J., Navarro, X., & Penas, C. (2019). BET protein inhibition regulates cytokine production and promotes neuroprotection after spinal cord injury. *J Neuroinflammation, 16*(1), 124. doi:10.1186/s12974-019-1511-7

Scotece, M., & Conde-Aranda, J. (2022). Inflammation in Health and Disease: New Insights and Therapeutic Avenues. *Int J Mol Sci, 23*(15). doi:10.3390/ijms23158392

Shen, C., Ipsaro, J. J., Shi, J., Milazzo, J. P., Wang, E., Roe, J. S., . . . Vakoc, C. R. (2015). NSD3-Short Is an Adaptor Protein that Couples BRD4 to the CHD8 Chromatin Remodeler. *Mol Cell, 60*(6), 847-859. doi:10.1016/j.molcel.2015.10.033

Sullivan, K. E., Reddy, A. B., Dietzmann, K., Suriano, A. R., Kocieda, V. P., Stewart, M., & Bhatia, M. (2007). Epigenetic regulation of tumor necrosis factor alpha. *Mol Cell Biol, 27*(14), 5147-5160. doi:10.1128/MCB.02429-06

Wu, C., Li, A., Hu, J., & Kang, J. (2019). Histone deacetylase 2 is essential for LPS-induced inflammatory responses in macrophages. *Immunol Cell Biol, 97*(1), 72-84. doi:10.1111/imcb.12203

Yoshida, T., Hazan, I., Zhang, J., Ng, S. Y., Naito, T., Snippert, H. J., . . . Georgopoulos, K. (2008). The role of the chromatin remodeler Mi-2beta in hematopoietic stem cell self-renewal and multilineage differentiation. *Genes Dev, 22*(9), 1174-1189. doi:10.1101/gad.1642808

Zhong, Y., Paudel, B. P., Ryan, D. P., Low, J. K. K., Franck, C., Patel, K., . . . Mackay, J. P. (2020). CHD4 slides nucleosomes by decoupling entry- and exit-side DNA translocation. *Nat Commun, 11*(1), 1519. doi:10.1038/s41467-020-15183-2

Chapter 4

Influence of LSD1 on neurite outgrowth and nerve regeneration

Influence of LSD1 on neurite outgrowth and nerve regeneration

Georgina Palomés-Borrajo, Xavier Navarro, Clara Penas

Institute of Neurosciences, Dept. Cell Biology, Physiology and Immunology, Centro de Investigación Biomédica en Red sobre Enfermedades Neurodegenerativas (CIBERNED), Universitat Autònoma de Barcelona, Bellaterra, Spain.

Abstract

Recovery after nerve injury relies in mechanisms that enhance axonal regeneration and facilitate successful reinnervation of target organs. Nowadays, there are not available treatments to improve the functional outcome after severe nerve injuries, and patients usually remain with deficits during a lifetime. Thus, research of novel strategies to improve nerve regeneration after injury is essential.

LSD1 is a lysine demethylase that targets H3K4me2/me1 and H3K9me2/me1, leading to gene repression and expression respectively. In this study, we investigated the possible role of LSD1 in nerve regeneration. We first found that LSD1 inhibition using RN-1 increases neurite outgrowth in DRG explants. We also identified that LSD1 inhibition enhances the expression of RAGs in the sciatic nerve, spinal cord, and dorsal root ganglion of mice after sciatic nerve injury. Specifically, RN-1 treatment raises the expression of Sox11, a transcription factor of utmost importance in the axonal regeneration program. Although RN-1 leads to a positive regulation of RAGs, it does not improve motor and sensory axon regeneration, nor affects the development of Wallerian degeneration. In conclusion, this study provides evidence of the positive influence of LSD1 inhibition in neuroplasticity, although more refined strategies must be developed to use this epigenetic enzyme as a target to enhance regeneration after nerve injury.

Introduction

Peripheral nerve injuries (PNI) lead to the interruption of the continuity of axons within the nerve, disconnecting the nervous system from the target organs. PNI causes paralysis, loss of sensibility and of autonomic control of the denervated territory and leads to serious

complications such as neuropathic pain. Altogether, negatively impacting the patient's functional status and quality of life. Although injured axons can regrow to some extent, the regenerative process is usually incomplete and functional deficits can last a lifetime (Navarro et al., 2018). Nowadays, there are no available treatments that allow complete functional restoration, and therapy is limited to surgical repair when indicated, and to rehabilitation measures. Thus, research on novel therapeutic targets that improve functional outcome after injury is necessary.

LSD1 is a histone demethylase important for brain function and neuronal development, whose alterations have been linked to several neurodegenerative diseases (D. Kim, Kim, & Baek, 2021). LSD1 removes methyl groups from histone 3 at its lysine 4 (H3K4) and 9 (H3K9), promoting repression and activation of gene expression, respectively (Maiques-Diaz & Somervaille, 2016). The impact of LSD1 on neuronal function is controversial, pointing to an incomplete understanding of its biological actions within the nervous system. Alternative splicing of LSD1 generates a neuronal isoform (LSD1n), which specific genetic deletion impairs neuronal maturation and neurite outgrowth (Rusconi, Grillo, Toffolo, Mattevi, & Battaglioli, 2017; Zibetti et al., 2010). Although, LSD1n expression has been classically associated with neurite growth, recent research has suggested that the responsible for increasing neurite outgrowth is the overexpression of the phosphorylated form of LSD1n (Thr369bAsp) (Toffolo et al., 2014; Zibetti et al., 2010). Specifically, phosphorylated LSD1n losses the capacity to recruit the corepressors CoREST and HDAC1/2. Thus, it may be that LSD1n phosphorylation acts as a negative regulator of LSD1n, impairing its activity and promoting neurite extension (Toffolo et al., 2014).

Considering ubiquitous LSD1, its neuronal deletion promotes neurodegeneration in hippocampus and brain cortex (Christopher, Myrick, et al., 2017). However, inhibition of LSD1 has been found to reduce neurological deficits in several neuropathological conditions, suggesting a role in enhancing neuroplasticity. ORY-2001, a brain penetrant inhibitor of LSD1 corrected memory deficits in the Senescence Accelerated Mouse Prone 8 (SAMP8) model for accelerated aging and Alzheimer's disease, as well as reduced aggression and improved social behavior (Maes et al., 2020). In this context, this treatment upregulated the expression of genes related to synaptic plasticity, neurogenesis and memory, and downregulated genes

overexpressed in SAMP8 mice and in AD patients within the hippocampus. In addition, combined administration of the class I histone deacetylase inhibitor Romidepsin and the LSD1 inhibitor GSK-LSD1 ameliorated clinical deficits of Autism spectrum disorder (ASD) in a model of adult Shank3-deficient mice by restoring NMDAR synaptic function in pyramidal neurons (Zhang et al., 2021). Other studies reported beneficial effects of LSD1 inhibition by promoting neuroprotection in an Experimental Autoimmune Encephalomyelitis (EAE) induced model (Cavalcanti et al., 2022), in a mouse model of Amyotrophic Lateral Sclerosis (ALS) (Choi et al., 2022), and after spinal cord injury (Gu et al., 2021). In general, these studies pointed out that neuroprotective effects were produced by reducing the alterations of gene expression produced by the pathology and by enhancing autophagic flux.

Therefore, since inhibition of LSD1 and LSD1n have been previously related to neuroprotection and neuroplasticity, we aimed to ascertain the effects of global LSD1 inhibition to promote axonal regeneration after injury. Thus, we hypothesized that global LSD1 inhibition using RN-1 could promote neurite growth in DRG neurons and may lead to axonal regeneration after nerve injury.

Materials and methods

DRG explant culture

Ten-week-old female C57BL6/J mice (Charles River Laboratories) were euthanized with pentobarbital (200 mg/kg i.p.). Lumbar DRGs were extracted using sterilized surgery tools and were preserved in chilled Gey's balanced salt solution containing 0.6% glucose. Connective tissue and roots were removed and DRGs were placed between two droplets of a collagen mixture in 24 well plates. The collagen mixture consisted of 446.43 µl of rat collagen type 1 (Corning), 50 µl MEM 10X medium, 2 µl 7.5% sodium bicarbonate (Gibco), and 1.57 µl PBS. Then, the wells were filled with culture medium: Neurobasal, 1x B-27, 1% penicillin-streptomycin, 0.5% glucose, 0.5% glutamax and 100 ng/mL murine β-NGF (Peprotech). RN-1 dissolved in DMSO at 500nM, 1000nM or 2000nM, or the vehicle DMSO, were added as a treatment on the same day. Culture was maintained for two days prior to fixation with 4% paraformaldehyde (PFA) for 30 minutes. A total of 3 independent cultures were made per condition.

Neurite growth analysis

After fixation, DRG explants underwent several washes with TBS-Tween 0.1% and were then incubated for 1 hour in citrate buffer heated until boiling temperature. Then, samples were washed again and incubated with increasing concentrations of methanol (50%, 70% and 100%). After further washes, the samples were incubated in TBS-triton 0.3% with 5% normal donkey serum and anti-H-Neurofilament antibody for 48h at 4ºC (see Table 1) Samples were then washed with TBS-Tween 0.1% and incubated overnight at 4ºC with TBS-triton 0.3% containing 5% normal donkey serum and Alexa fluor 594 donkey anti-mouse. Samples underwent several washes before being incubated with DAPI diluted in TBS. Finally, samples were washed, dried, and mounted with Fluoromount-G (Southern Biotech).

Name	Immunogen	Manufacturer, catalog number, RRID, host	Concentration and application
PGP 9.5 (UCHL1)	PGP9.5	CEDARLANE Cat# CL7756AP, RRID: AB_2792979, rabbit, polyclonal	1/500, IHQ
RT-97	Neurofilament-H	DSHB Cat# rt97, RRID: AB_528399, mouse, monoclonal	1/200, IHQ
Donkey anti-Mouse Secondary Antibody, Alexa Fluor™ 594	IgG (H+L)	Thermo Fisher Scientific Cat# A-21203, RRID: AB_141633, donkey, polyclonal	1/200, IHQ
Donkey anti-Rabbit Secondary Antibody, Alexa Fluor™ 594	IgG (H+L)	Thermo Fisher Scientific Cat# A-21207, RRID: AB_141637, donkey, polyclonal	1/200, IHQ
DAPI		Sigma-Aldrich Cat#D9564-10MG	1/5000 in pads 1/1000 in DRG

Table 1: List of antibodies used in the study.

The immunolabeled DRGs were observed at X20 in an Olympus BX51 microscope and images were captured through a DP73 camera. Microphotographs at 200x of overlapping territories of the DRGs were acquired and merged with Adobe Photoshop 2020 software. Neurite length and number were determined using an Image J plugin known as Neurite J (Torres-Espin, Santos, Gonzalez-Perez, del Valle, & Navarro, 2014). The software facilitated values of the longest neurite and the number of neurite intersections at every 25µm steps. The analysis was performed blindly regarding to culture treatment.

DRG dissociated neuron cultures and cell viability assay

Animals were euthanized with pentobarbital and DRGs were extracted, as above. Samples were cleaned from debris and washed before undergoing an enzymatic digestion for 20 minutes at 37 ºC with a solution consisting of trypsin 1x, collagenase 1x, and DNase (1 mg/ml) diluted in Hank's Balanced Salt Solution (HBSS, Gibco). The enzymatic digestion was arrested with the addition of DMEM/F12 containing 10% FBS and L-glutamine. Next, samples underwent mechanical digestion and were filtered through a 70µm cell strainer to be later centrifuged at 900 rpm for 7 minutes. The pellet was resuspended in Neurobasal A medium with 2% B-27, 2% glucose at 30%, 1% glutamine, and 1% penicillin and streptomycin. Cell density was determined using a Neubauer chamber. A total of eight wells were seeded per animal in a 96-well plate pre-treated with Poly-D-Lysine (0.01 mg/mL) and laminin (2 µg/mL). Each well contained 5,000-6,000 cells and the medium was replaced after 2h.

Two days after the stabilization of the culture, cells were treated in duplicates with the vehicle DMSO, 500nM RN-1, 2000nM RN-1, or 5 µg cisplatin for 48 hours. This last compound was used as a positive control of cell death. To determine cell viability, the medium was replaced with medium containing 0.15 mg/mL MTT (3-[4,5-dimethylthiazol-2-yl]-2,5-diphenyltetrazolium bromide) and kept at 37ºC for 2 hours. Cells were then lysed with DMSO and absorbance was read out in a spectrophotometer (Bio-tek) at 560 nm and 600 nm wavelength using the KC Junior software. Blank was subtracted and readings were normalized against control to obtain the percentage of survival. A total of four independent cultures were performed.

Animals and nerve injury

Animal procedures were approved by the Animal Experimentation Ethical Committee of the Universitat Autònoma de Barcelona (code 10306) and followed the European Commission Directive 2010/63/EU on the protection of animals for scientific purposes. Ten-week-old female C57BL6/J mice (Charles River Laboratories) were used in all the *in vivo* experiments. Animals had access to food and water *ad libitum* and were kept under a 12-hour light cycle.

For the surgical procedure, mice were anesthetized by intraperitoneal injection of ketamine (90 mg/Kg) and xylazine (10 mg/Kg) diluted in saline. The sciatic nerve of the right hindlimb was exposed and subjected to a crush injury, at 45 mm from the tip of the third

digit. The injury was conducted by applying pressure with Dumont #5 forceps 3 times during 30 seconds in different orientations. Then, muscle and skin were closed by suture, and the wound disinfected with iodine solution. Operated animals were kept in a warm environment until recovered from anesthesia, and closely supervised during the post-operation follow-up.

Operated animals were administered daily by intraperitoneal injection of vehicle (5% DMSO and 5% Tween-80 in saline) or RN-1 (1,52 mg/kg) diluted in vehicle. In the short-term regeneration assay, treatment started at two different time points: at 2 hours post-operation (0 dpo) or at 3 dpo. Then, at 7 dpo the animals were terminated for molecular analyses. In the degeneration and the long-term regeneration studies, animals begun the treatment 2 hours after surgery and were euthanized at 7 and 29 dpo. To avoid any possible bias, animals from both treatments were mixed in the same cages.

mRNA expression

Mice from the short-term regeneration study were euthanized with pentobarbital at 7dpo and then perfused in saline. Fresh tissue from the sciatic nerve, spinal cord and L4-L6 DRGs were extracted and snap frozen in liquid nitrogen. Spinal cord samples were later sectioned to keep a 4mm ventral lumbar section for RNA extraction. Samples were lysed using a TissueRuptor (QIAGEN) and QIAzol lysis reagent (QIAGEN) following manufacturer's guidelines. The aqueous phase obtained from the protocol was then processed with RNeasy MiniKit (QIAGEN) following the producer's instructions.

Gene	Forward primer: 5'– 3'	Reverse primer: 3'– 5'
Mouse β-III tubulin	CGGCAACTATGTAGGGGACT	CATGGTTCCAGGTTCCAAGT
Mouse BDNF	TGCAGGGGCATAGACAAAAGG	CTTATGAATCGCCAGCCAATTCTC
Mouse GAP43	CTGCTGTCACTGATGCTGCT	GGTTTGGCTTCGTCTACAGC
Mouse GAPDH	TGGCCTTCCGTGTTCCTAC	GAGTTGCTGTTGAAGTCG
Mouse IL-4	GGCTTTCCTCTTTCCCACTC	AGCCGCCATGAGAGCTAAG
Mouse IL-6	AACCACGGCCTTCCCTACTTCA	TCATTTCCACGATTTCCCAGAG
Mouse IL-10	GCTGAGACTTTCGCTCCTCTC	AGCTCCAAGGCACCTGTTC
Mouse IL-13	TCCAATTGCAATGCCATCTA	TGGGCTACTTCGATTTTGGT
Mouse Sox11	TTGGTGTCTCAGCATCCAACCAG	AGCCTGCCCTAAGCATCACTTC
Mouse TNF-α	AGGCACTCCCCCAAAAGATG	TCACCCCGAAGTTCAGTAGAC

Table 2: List of primers used in the study

RNA concentration was measured with a Nanodrop 2000 spectrophotometer (Thermo Scientific) and reverse transcription PCR was conducted using a High-capacity cDNA reverse transcription Kit (Applied Biosystems). Expression of target genes was determined through RT-qPCR using iTaq Universal SYBR Green Supermix (BioRad) and the corresponding primers (see Table 2). Glyceraldehyde-3-phosphate dehydrogenase (GAPDH) was used as a housekeeping gene. A total of 3-5 animals per condition were analyzed.

Histone methylation analysis

To assess the histone methylation profile, fresh tissue samples from the short-term study were sectioned to obtain a 4mm fragment of the cervical spinal cord. Protein was extracted using a potter homogenizer and following the manufacturer instructions for histone extraction of the EpiQuick^{TM} Global Pan-Methyl Histone H3-K4 Quantification Kit Colorimetric (Epigentek). Protein concentration was determined with a bicinchoninic acid assay (Pierce). Finally, samples were processed following the indications of the EpiQuick^{TM} Global Pan-Methyl Histone H3-K4 Quantification Kit Colorimetric (Epigentek) and read out at 450 nm wavelength using a microplate reader (BioTek) and the KC Junior Software. Blank was subtracted from the readings and values were normalized against the average for control animals to obtain the degree of H3K4 mono- di- and tri- methylation. A total of 4 animals per condition were analyzed.

Assessment of Wallerian degeneration

Animals from the degeneration study were also euthanized at 7dpo and perfused with 4% PFA. Sciatic nerves from the ipsilateral and the contralateral hindlimbs were extracted and kept in PFA for 1 hour before cryopreservation in phosphate buffer (PB) with 30% glucose and 1% azide. Sciatic nerves were cut into 10 µm-thick longitudinal sections, using a cryostat Leica CM 1950. Samples were submitted to dehydration in increasing concentrations of ethanol (50%, 70%, 80% and 95%) and then placed overnight at 37 ºC with luxol fast blue solution. Next, excess of colorant was removed with ethanol 95% and distilled water before applying lithium carbonate 0.05%. Afterwards, samples were put in distilled water and dehydrated with various washes of increasing concentration of ethanol (70%, 80%, 95% and 100%). Finally, samples were dipped in xylol and mounted using DPX.

Microphotographs were captured from distal segments of the sciatic nerves using the 20x objective of an Olympus BX40 microscope and a DP50 camera. The stained area was calculated using Image J software in a constant rectangular area of 281.13 µm width x 292.29 µm height. A total of 3 nerves per animal were analyzed. In this study, 4-5 animals were processed per condition.

Motor reinnervation

Mice of the long-term regeneration experiment were submitted to electrophysiological tests at days 15, 21 and 28 after injury. Under anesthesia with ketamine/xylazine, stimulating needle electrodes were placed at the sciatic notch and single electrical pulses of 0.02 ms duration were delivered up to supramaximal intensity using a Grass S88 stimulator. The compound muscle action potentials (CMAPs) were recorded by means of microneedle electrodes placed in the plantar interosseus and the tibialis anterior muscles. The signals were amplified and displayed on the oscilloscope to obtain the amplitude and the latency of the M wave (Navarro, 2016). Electrophysiological recordings were also obtained for the contralateral hind paw as control value for each animal. A total of 7 animals per group underwent functional testing.

Skin reinnervation

Animals from the long-term regeneration study were euthanized at 29 dpo and perfused with 4% PFA. Paw pads from the ipsilateral and contralateral hindlimbs were extracted and maintained in PFA for 1 hour, to be finally kept in PB containing 30% glucose and 1% azide. To assess skin reinnervation, we analyzed the pad located proximal to the second toe, as it is fully innervated by the sciatic nerve. Pads were cut longitudinally at 60 µm-thick sections using a Leica CM 1950 cryostat. Then, free-floating sections were washed with PBS and PBS plus Triton 0.3%, before being blocked with PBS-0.3% triton X-100 containing 1.5% normal donkey serum. Pads were finally incubated overnight at 4ºC with PBS-0.3% triton X-100 enriched with 1.5% normal donkey serum and rabbit anti-PGP 9.5 antibody (Table 1). Next, samples underwent several washes with PBS-triton 0.3% to be incubated overnight at 4ºC with PBS-triton 0.3% containing 1.5% normal donkey serum and Alexa fluor 594 anti-rabbit (see Table1). Thereafter, pads were washed with PBS-triton 0.3% and incubated with PB containing 1/5000

DAPI (Sigma) during 2 minutes at room temperature. Finally, samples were washed with PB and dried to be mounted with Fluoromount-G (Southern Biotech).

The number of Meissner's corpuscles and intraepidermal nerve fibers (IENFs) were determined using an Olympus BX51 microscope. To estimate the number of IENFs, the basal layer of the skin was localized by observation of DAPI staining. Then, a grid was overlayed on the lateral side of the pad following the basal layer to assess the number of nerve fibers that crossed it. Two fields per slice were counted. Meissner's corpuscles were found at the apex of the pads and counted at 40x. A total of 3-7 animals per treatment were used.

Statistical analysis

Data from experimental procedures was analyzed using GraphPad Prism 7 software. Data were expressed as mean±SEM. For the statistical analysis of the number of neurites at different distances of DRG explants, a two-way ANOVA with Sidak's correction for multiple comparisons was applied, using distance from the surface and treatment as factors. For comparisons of the maximum neurite length of cultured DRGs, cell viability *in vitro*, mRNA expression of the short-term study and myelin clearance, a one-way ANOVA followed by Tukey's correction for multiple comparisons was used. To assess histone methylation, results were analyzed through an unpaired t-test. For comparisons of data of motor reinnervation, a two-way ANOVA followed by Sidak's correction for multiple comparisons was applied. In this experiment, time and percentage of the amplitude with respect to the contralateral values were used as variables. For the determination of cutaneous reinnervation, the number of IENFs and Meissner's corpuscles were submitted to a one-way ANOVA followed by Tukey's correction for multiple comparisons.

Results

LSD1 inhibition using RN-1 increases neurite outgrowth in DRG explants *in vitro*

To assess the consequences of global LSD1 inhibition in neuronal outgrowth, DRG explant cultures were treated with DMSO or increasing concentrations of RN-1.

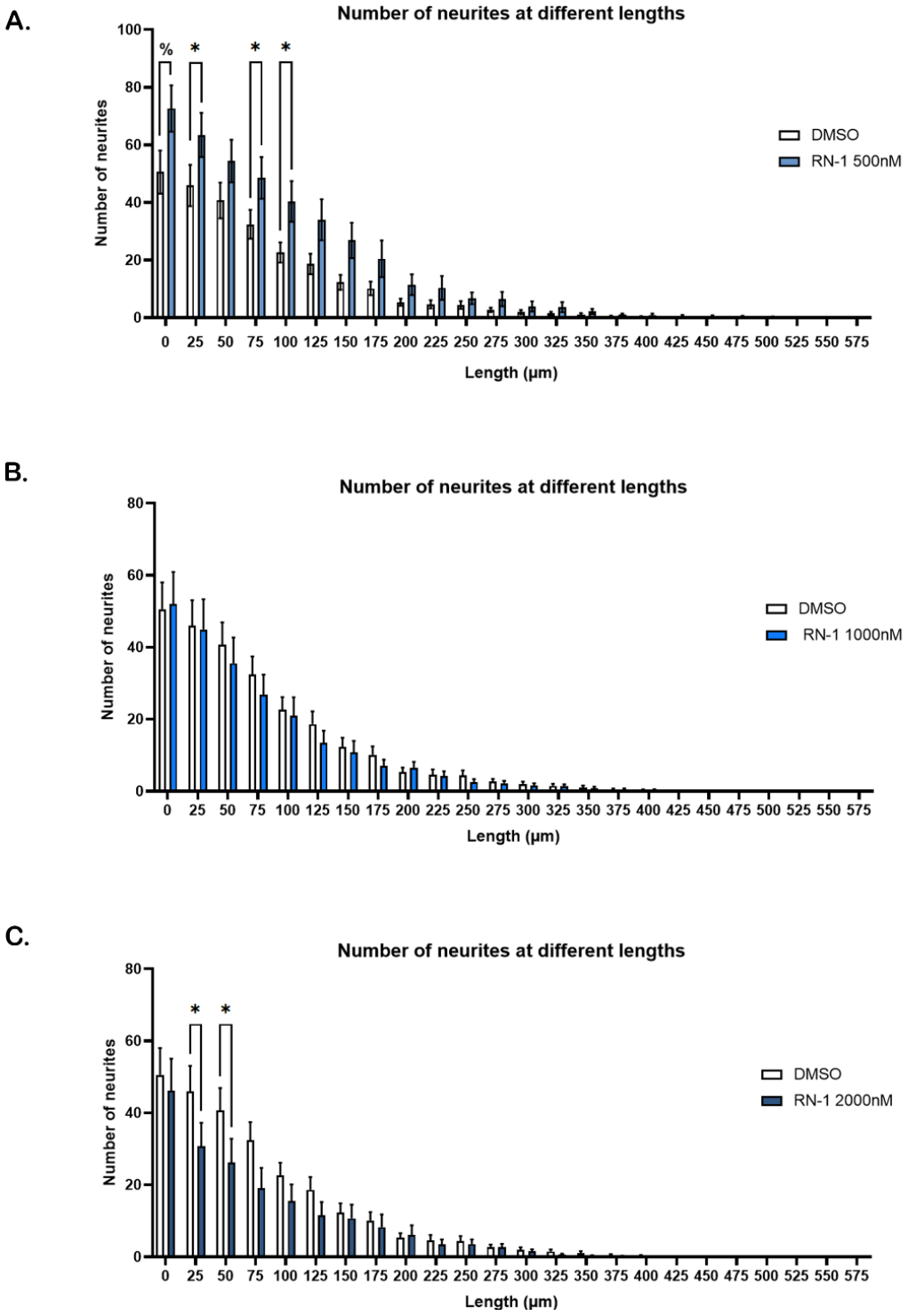

Figure 1: LSD1 inhibition using RN-1 at low concentration increases neurite number of DRG explants. Number of neurites every 25µm for DMSO and (A) RN-1 at 500nM, (B) RN-1 at 1000nM, and (C) RN-1 at 2000nM. *p<0.05 and % p<0.001 calculated by two-way ANOVA for multiple comparisons followed by Sidak's correction. Results are displayed in bar graphs as mean ± SEM. N= 3 independent cultures.

Considering the number of neurites, RN-1 treatment at a low concentration (500nM) promotes a significant increase in the number of neurites ranging 0 - 25µm and 75 - 100µm (Figure 1A, 2A). Contrarily, a high concentration of the compound (2000nM) produced the opposite effect, leading to a significant decrease in neurite number of 25-50µm when compared to the control (Figure 1C, 2A). Intermediate concentrations of RN-1 of 1000nM showed no significant differences compared to control ganglia (Figure 1B, 2A).

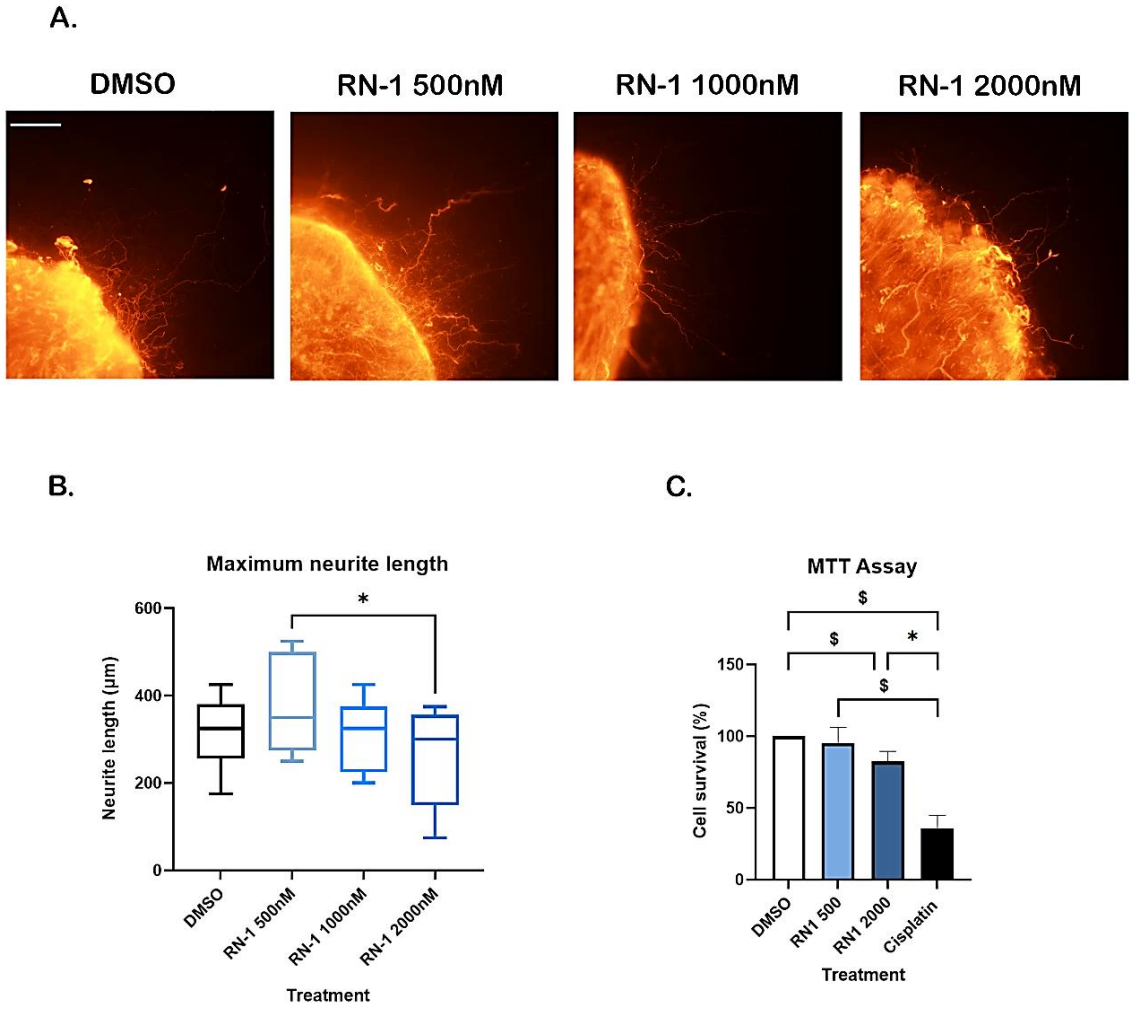

Figure 2: High concentrations of RN-1 decreased maximum neurite length and cell survival. A) Representative microphotographs at 200x of DRGs treated with DMSO and RN-1 at 500nM, 1000nM and 2000nM. White bar represents 100µm. B) Maximum neurite length of the DRG explants for each treatment. C) Results of the MTT assay. *p<0.05 and $p<0.0001 by a One-way ANOVA followed by Tukey's correction. Results are displayed in box and whisker graphs as minimum to maximum and in bar graphs as mean ± SEM. N=3 independent cultures for neurite length assessment and n=4 for the MTT assay.

Next, the longest neurite per DRG was calculated. For DRGs treated with DMSO the maximum neurite length was 316µm, whereas for DRGs cultured with RN-1 at 500nM was 377µm. Hereof, there were no significant differences between both conditions. RN-1 at 2000nM

reduced the maximal neurite length to 263µm, which was significantly shorter than RN-1 at 500nM (Figure 2B). Thus, high concentrations of the compound have negative effects on sensory neurite growth.

Provided that RN-1 at 2000nM was affecting neurite outgrowth and density, we wondered if the observed detrimental effects were consequence of poor cellular survival. To address this issue, an MTT assay was performed on dissociated DRG cultures, and the neurotoxic drug cisplatin was used as a positive control. We observed that high doses of RN-1 were inducing a significant decrease of neuronal survival when compared to control, reducing neural viability up to 80% (Figure 2C). Thus, it is feasible that the decreased neurite growth observed with the high concentration treatment was due to adverse toxic effects of RN-1 on the explants.

RN-1 increases the expression of regeneration associated genes, affects the inflammatory environment after nerve injury and enhances H3K4me1 expression *in vivo*

Since the low concentrations of RN-1 increased neurite density and tended to raise neurite length *ex vivo*, we performed a short-term experiment to discern the most appropriate time point of administration of this compound *in vivo* to enhance axonal regeneration. For this purpose, changes on the transcription of Regeneration Associated Genes (RAGs) and cytokines were assessed in the sciatic nerves of non-injured control mice, in vehicle and in RN-1 treated mice that underwent nerve crush. These changes were analyzed in 2 settings, starting treatment at early (0 dpo) and delayed (3 dpo) time points.

We first validated if RN-1 treatment affected LSD1 *in vivo,* by analyzing the methylation levels of injured animals that underwent vehicle or early RN-1 treatment in one of the LSD1 downstream targets, the histone 3 lysine 4 (H3K4). Mono-methylation was significantly increased up to 36% in cervical spinal cord segments of injured animals treated with RN-1. RN-1 also displayed a tendency to increase H3K4me2, although in this case the changes were not significant (Figure 3A). The increase on the monomethylated levels of H3K4 demonstrate that RN-1 is properly reaching its target, as LSD1 acts on mono- and di-methylated H3K4. Additionally, RN-1 also led to a significant increment of H3K4 tri-methylation, which is not a direct target of LSD1. In this case, the methylation levels raised by 32%. Thus, it is possible that under the influence of RN-1 other enzymes act upon H3K4me. However, further research should be performed to validate this hypothesis.

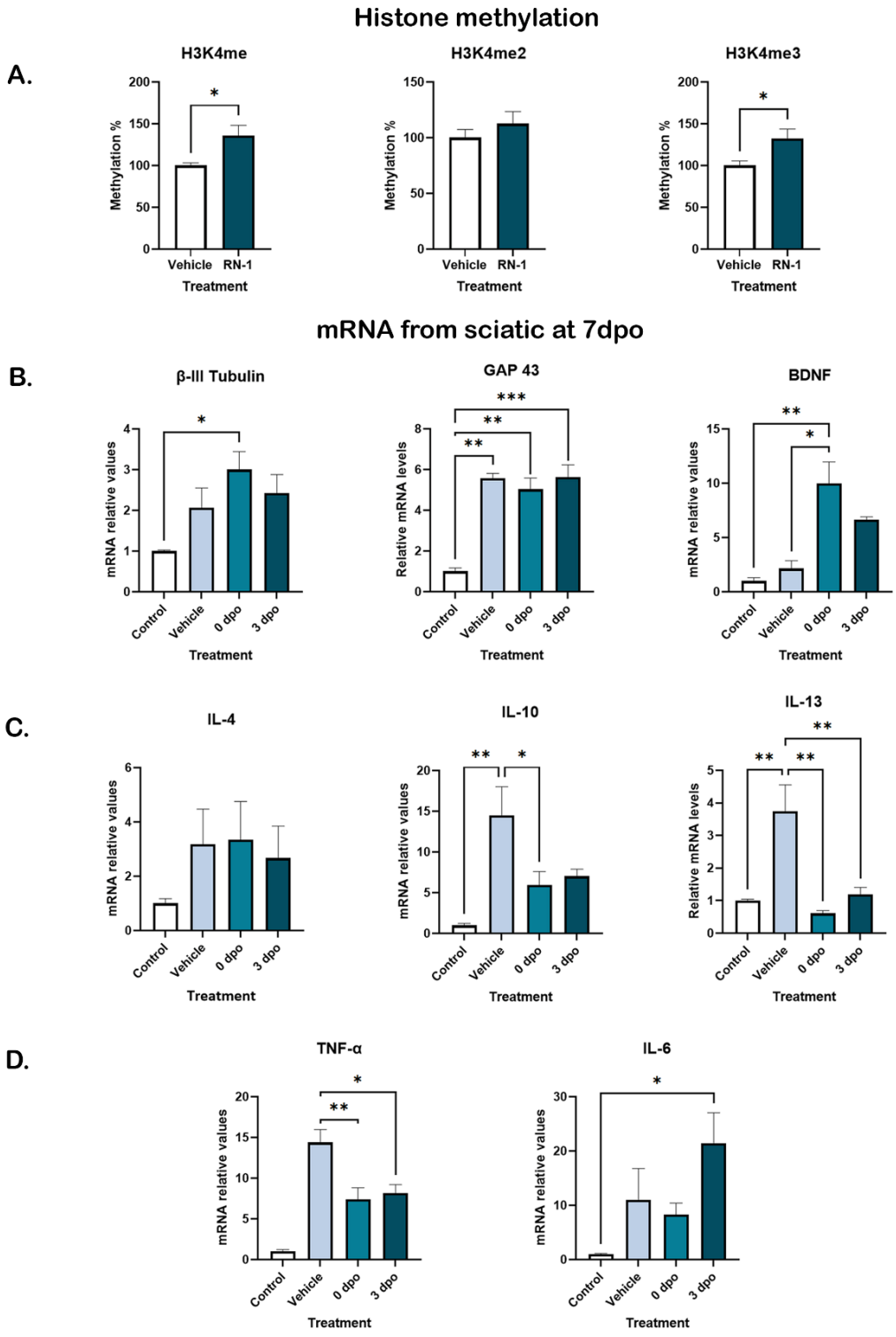

Figure 3: RN-1 administration increases the transcription of RAGs in the sciatic nerve and diminishes the inflammatory response. A) Methylation levels of mono-, di- and trimethylated H3K4. B) mRNA expression of RAGs in sciatic nerve. C) Transcriptional profile of anti-inflammatory cytokines in the sciatic nerve. D) mRNA expression of pro-inflammatory mediators. *p<0.05, **p<0.01 and ***p<0.001 by One-way ANOVA followed by Tukey's correction. Results are displayed in bar graphs as mean ± SEM. N= 3 – 5 animals per group in the transcriptional assessment and n=4 samples for each condition in the histone methylation analysis.

Regarding the expression of RAGs, early administration of RN-1 significantly raises up to 3-fold the transcription of β-III tubulin in the injured sciatic nerve when compared to non-injured animals. Moreover, LSD1 inhibition at 0 dpo also increases the expression of the neurotrophic factor BDNF with respect to non-injured controls and vehicle animals. This increase is 9.9-fold and 4.58-fold respectively. Concerning GAP43, all treatments significantly enhanced its expression against control animals. However, no differences are found between the treatments regarding the expression of this gene (Figure 3B).

Considering the inflammatory environment, RN-1 decreases the whole inflammatory response affecting both pro- and anti-inflammatory cytokines. In fact, early administration of RN-1 significantly decreases the transcription of IL-10 compared to vehicle. This decline on IL-10 expression is around 2.43-fold. The anti-inflammatory cytokine IL-13 follows a similar change. In this case, LSD1 inhibition significantly reduces IL-13 expression when both time-points are contrasted to vehicle. The magnitude of variation is 6.11-fold for the early treatment and 3.15-fold for the delayed treatment with respect to vehicle values. IL-4 is the only anti-inflammatory cytokine that remains unaffected under RN-1 treatment (Figure 3C).

Considering pro-inflammatory mediators, LSD1 inhibition significantly reduces TNF-α transcription at both time points compared to vehicle. These changes are around 1.94-fold for the early treatment and 1.75-fold for the delayed treatment against vehicle. However, IL-6 is significantly increased in the delayed administration group when compared to control around 21.45-fold (Figure 3D).

Altogether these results show that LSD1 inhibition can act as an immunosuppressor affecting the whole inflammatory environment. In addition, we found that early administration of RN-1 facilitates the transcription of certain RAGs, like β-III tubulin and BDNF, in the sciatic nerve.

LSD1 inhibition by RN-1 increases the expression of RAGs in the DRG and the spinal cord

β-III tubulin is a RAG, regulated by various members of the Sox family. For instance, Sox4 and Sox11 have been associated to promoter elements of this gene. Moreover, REST/NRSF complex has been reported to restrict the expression of the transcription factor Sox11, which has been linked to axonal regeneration (Bergsland et al., 2006; Jankowski et al., 2009). Since, LSD1 can participate in the formation of the REST/NRSF complex and we found an increase in the expression of β-III tubulin in the sciatic nerve after treatment, we hypothesized that LSD1

inhibition could also upregulate the expression of Sox11. To address this idea, we analyzed the transcription of multiple RAGs and Sox11 in the spinal cord and lumbar DRGs from non-injured controls and crush-injured mice treated with vehicle or RN-1.

The analysis demonstrated that an early treatment with RN-1 led to a significant increase of 2.83-fold in Sox11 transcription when compared to non-injured controls in the spinal cord (Figure 4A). A significant increase was also detected in the DRGs, where Sox11 is significantly raised under LSD1 inhibition at both time points when compared to non-injured controls (Figure 4B). Thus, these results indicated that LSD1 may be repressing the expression of Sox11.

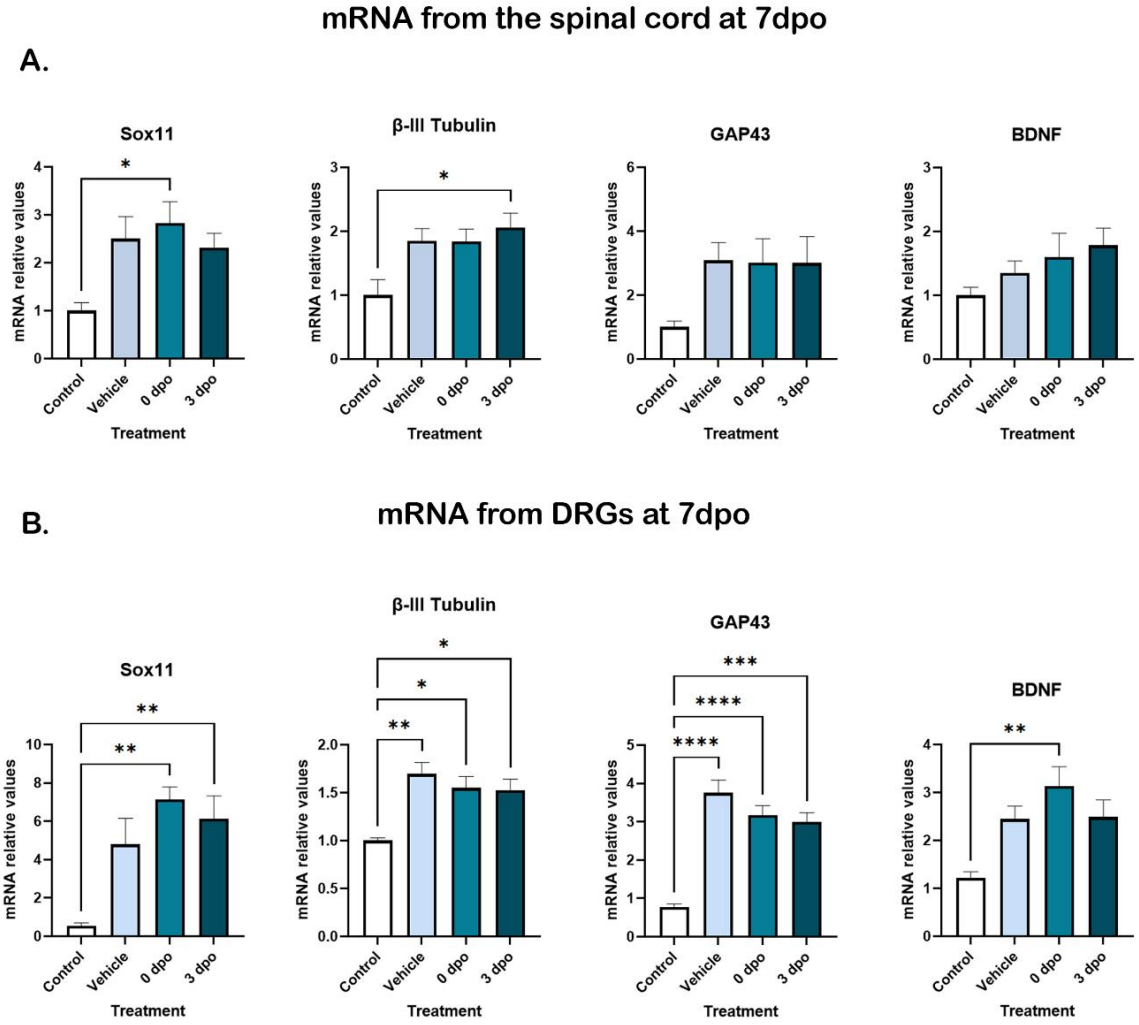

Figure 4: LSD1 inhibition by RN-1 increases the transcription of RAGs in the ventral spinal cord (A) and in DRGs (B) after nerve injury. *p<0.05, **p<0.01 by One-way ANOVA followed by Tukey's correction. Results are displayed in bar graphs as mean ± SEM. N= 3 – 5 animals per group in the transcriptional analysis.

Regarding the expression of RAGs, β-III tubulin is significantly increased a total of 2.06-fold in the spinal cord when comparing the delayed treatment of RN-1 to control (Figure 4A). In DRG samples, all treatments show a significant enhancement on the expression of this gene when compared to control (Figure 4B). These alterations are 1.69-fold for vehicle, 1.55-fold for early RN-1 administration and 1.52 for the delayed treatment. These results differ from the observations made in the sciatic nerve, where β-III tubulin was only significantly raised against control in the early RN-1 treatment.

There are no significant differences between treatments and the control in the expression of GAP43 in the spinal cord, which is probably justified by the high variability of measures for this marker (Figure 4A). Regarding DRG samples, GAP43 is significantly increased around 3-fold for all treatments compared to control (Figure 4B).

The neurotrophic factor BDNF is significantly raised by the early RN-1 treatment compared to vehicle in DRGs, following a similar pattern than the one observed in the sciatic nerve (Figure 4B). However, LSD1 inhibition using RN-1 does not lead to significant transcriptional changes of BDNF in the spinal cord (Figure 4A).

Provided that early administration of RN-1 facilitates the transcription of certain RAGs in the sciatic nerve, spinal cord and DRGs, we resorted to this experimental setting for further regeneration studies.

Inhibition of LSD1 does not affect Wallerian Degeneration

Since we previously reported that LSD1 inhibition decreases the secretion of inflammatory mediators, we wondered if this leads to a lack of infiltrating macrophages within the nerve and to possible myelin clearance defects.

To test this idea, the area of myelin within the nerve from non-injured mice and crush-injured animals was analyzed at 7dpo through Luxol Fast Blue (LFB) staining. Hence, lesioned mice were administered with vehicle or RN-1, delivered at 0 dpo or at 3 dpo.

For non-injured controls the myelin-stained area was 19845 arbitrary units in average, for vehicle animals 2552 units, for early RN-1 treatment 2929 units and for delayed RN-1 administration 3405 arbitrary units (Figure 5A and 5B). Thus, we observed that injured sciatic nerves displayed a significant decrease of myelin within the nerve, demonstrating that crush-

injured mice underwent Wallerian degeneration. In addition, the lack of differences between treatments suggest that RN-1 is not affecting the degenerative process.

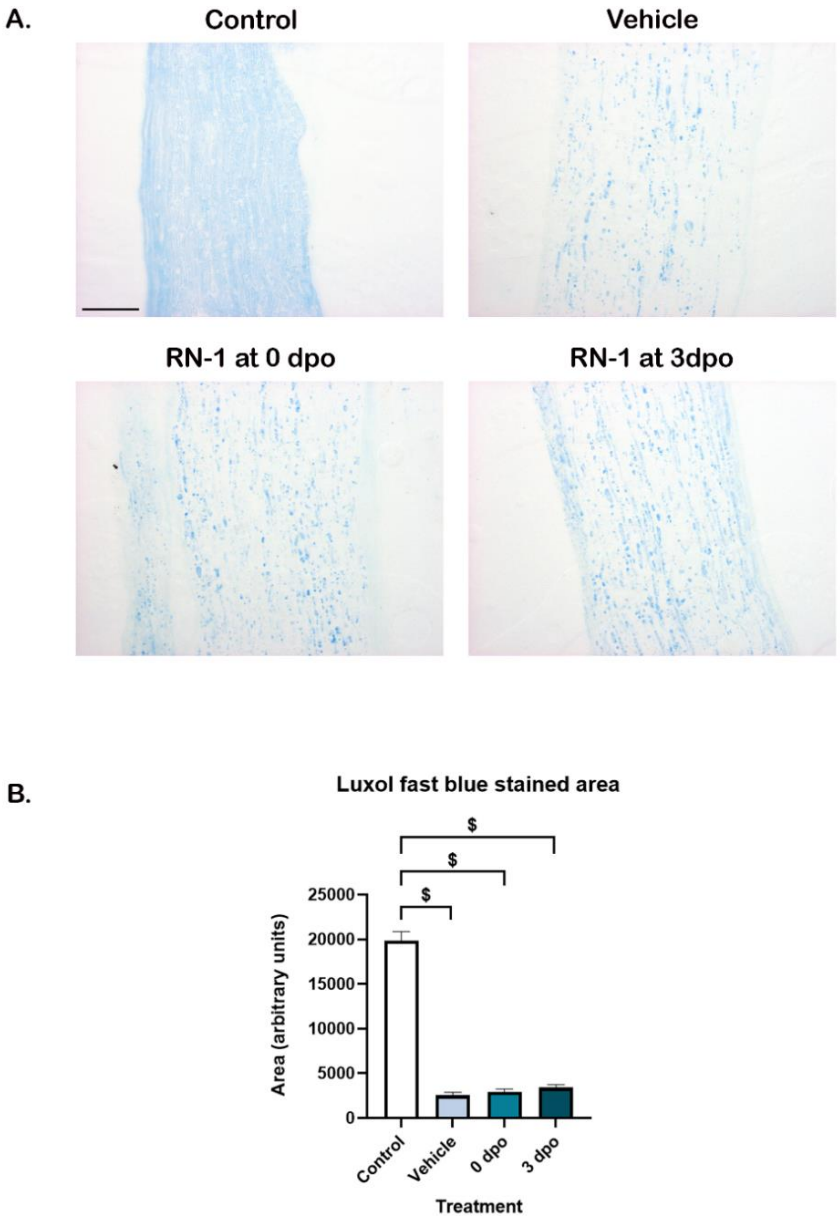

Figure 5: LSD1 inhibition with RN-1 does not affect Wallerian degeneration. A) Representative microphotographs of nerves stained with LFB at 100x. Black bar represents 100µm. B) Luxol fast blue stained area within the nerve for each condition. $p<0.0001 as calculated by One-way ANOVA followed by Tukey's correction. Data is expressed in bar graphs as mean+SEM. N= 4 – 5 mice per group.

LSD1 inhibition does not improve motor and sensory axonal regeneration after nerve injury

Given that we observed that early administration of RN-1 raises the transcription of multiple RAGs and Sox11 after nerve injury, we hypothesized that this treatment could positively favor

nerve regeneration. To test this premise, we performed a sciatic nerve crush and analyzed the effects of LSD1 inhibition on motor and nerve reinnervation.

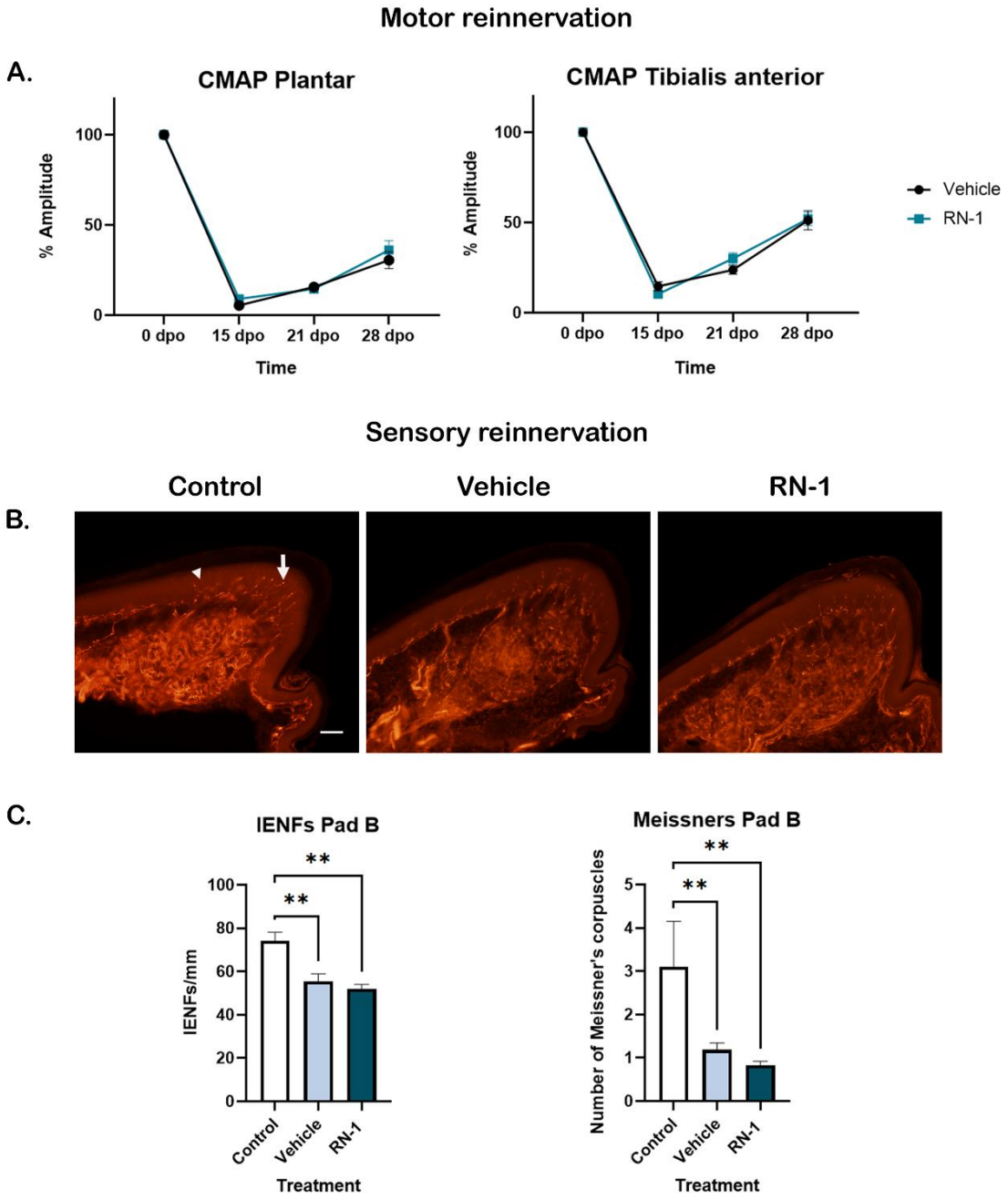

Figure 6: LSD1 inhibition using RN-1 does not improve motor and sensory axonal regeneration. A) Mean values of the CMAP of tibialis anterior and plantar muscles during the follow-up. B) Representative microphotographs of mouse hind paw pads at 100x. White bar represents 100µm; arrow points at Meissner's corpuscles and arrow tip at intraepidermal nerve fibers (IENFs). C) Analysis of the number of IENFs (left graph) and Meissner's corpuscles (right graph) per treatment. **p<0.01 by One-way ANOVA followed by Tukey's correction. Results are shown as mean ± SEM and connected superimposed symbols at mean ± SEM. N=7 animals for treatment.

After sciatic nerve crush injury, we observed that M wave amplitude was decreased in both of the sciatic nerve target muscles at 15 dpo. In the plantar muscle the M wave amplitude was 5-9% of control values, whereas in the tibialis anterior muscle the values were around 10-14% from control values. At 21 and 28 dpo CMAP amplitude increased progressively in both muscles, but there were no significant differences between vehicle and RN-1 treated animals (Figure 6A).

In the immunohistochemical analysis of hind paw pads, both the number of Meissner's corpuscles and the density of IENFs were significantly decreased after nerve injury. The density of IENFs per millimeter in the controls was 74.2 on average, whereas for vehicle and RN-1 treated animals was 55.4 and 51.9 respectively. Regarding the number of reinnervated Meissner's corpuscles, control animals had an average of 3.1, vehicle mice had 1.19 and LSD1-inhibited mice had an average of 0.83. There were not significant differences between vehicle and RN-1-treated mice (Figure 6B,6C).

Discussion

LSD1 inhibition has been associated with neuroprotection and neuroplasticity in several conditions (Gu et al., 2021; Maes et al., 2020), and therefore, we wondered if it could also facilitate axonal outgrowth after nerve injury. Our results demonstrate that LSD1 inhibition enhanced neurite outgrowth within DRG *ex vivo* explants and potentiated the expression of RAGs after nerve injury. However, administration of RN-1, an LSD1 inhibitor, did not improve nerve regeneration after sciatic crush injury.

In cultured DRG explants RN-1 treatment at 500 nM significantly enhanced neurite sprouting and displayed a tendency to increase neurite length. However, raising concentrations of RN-1 decreased its positive effects on neurite density and extension, leading to a significant reduction of both factors at the 2000 nM concentration. Since 2000 nM of RN-1 led also to a significant reduction of cell survival, we concluded that elevated concentrations of RN-1 have toxic effects on neurons or glial cells. Thus, LSD1 inhibition may favor neurite outgrowth but within a critical range of concentrations.

Consistent with our findings, knockdown of LSD1 in the leukemia-like cell line MOLT-4 has been found to increase apoptosis (Zou, Huang, Zou, Zheng, & Ma, 2017). Contrarily, it has also been described that LSD1 inhibition prevents cell death by promoting autophagy (Gu et al.,

2021) and that LSD1 knockdown averts apoptosis under oxidative stress (Tsutsumi et al., 2016). These discrepancies in the effects of LSD1, could be due to the differences in the studies regarding cell type, environment, and dosage. In addition, autophagy is a double edged sword capable of promoting and preventing cell death (Yonekawa & Thorburn, 2013). Thus, further studies should unravel the influence of high concentrations of RN-1 in the regulation of autophagy and apoptosis balance. Another explanation for the observed toxic effects, may be that high concentration of RN-1 could be hitting off-targets. RN-1 exhibits high affinity to LSD1 (IC50=70nM) but it can also bind to MAO-A (IC50=0.51µM) and to MAO-B in a lesser degree (IC50= 2.8 µM) (Rivers et al., 2015). Hence, the high concentration of our compound at 2000nM could be also targeting MAO-A. Since administration of low doses of the MAO-A specific inhibitor Clorgyline promotes neuronal death (Naoi, Maruyama, Akao, Yi, & Yamaoka, 2006; Ou, Chen, & Shih, 2006), the affinity of RN-1 to MAO-A could be also deleterious to cell survival. Nevertheless, further research should be done to fully unravel the mechanism behind cell death in this experiment.

As we observed that global LSD1 inhibition raised neurite outgrowth at low concentrations *in vitro*, we assessed if RN-1 could also improve outcome after nerve injury *in vivo*. We first validated that RN-1 was effectively inhibiting LSD1, as mono-methylation levels of H3K4 were significantly increased. Next, we assessed the impact of RN-1 on the neuroinflammatory response after nerve injury by means of a short-term study. We determined that TNF-α, IL-10 and IL-13 transcription were decreased in the sciatic nerve, suggesting that LSD1 inhibition was promoting the suppression of the inflammatory response. These results are consistent with previous findings that reported that LSD1 contributes to the development of NF-Kβ signaling (D. Kim et al., 2018). Lastly, we analyzed the influence of LSD1 inhibition on the expression of RAGs. We found that early administration of RN-1 enhanced the expression of BDNF, βIII-tubulin and Sox11, and subsequently we chose this timeframe of administration for the long-term study.

In this regard, BDNF is regulated by LSD1 (Kyzar, Bohnsack, Zhang, & Pandey, 2019; Sagarkar et al., 2021) and it has been reported that decreased levels of the LSD1-dependent histone modification H3K4me2 diminish BDNF expression (Sagarkar et al., 2021). Thus, in our study, BDNF transcription may be partly justified by the slight increment on H3K4me2 expression under LSD1 inhibition. In addition, other epigenetic alterations triggered after injury are also

involved in BDNF expression. For instance, H3K9ac raises after nerve injury and is known to promote BDNF transcription (Puttagunta et al., 2014). Thus, it is also possible that the injury-triggered H3K9ac together the little increase of H3K4me2 after LSD1-inhibition contributed to the raise of BDNF transcription. Although, further experiments should assess the certainty of this idea.

The increment of β-III tubulin under RN-1 treatment is consistent with previous reports, where knockdown of LSD1 in embryonic stem cells raised β-III tubulin expression (X. Han et al., 2014). To note, the β-III tubulin gene contains RE-1 binding sites that are suitable for the union of the repressor complex REST. Hereof, knockdown of REST has been found to increase β-III tubulin expression (Aoki, Hara, Era, Kunisada, & Yamada, 2012). Since LSD1 can belong to the REST/CoREST complex (Maiques-Diaz & Somervaille, 2016), LSD1 inhibition with RN-1 may disrupt the integrity of REST complex increasing β-III tubulin transcription.

In addition, β-III tubulin is regulated by several members of the transcription factor family Sox (Duly, Kao, Teo, & Kavallaris, 2022). Between them, Sox11 raised our interest as it is linked with nerve regeneration after injury (Jankowski et al., 2009). As Sox11 expression is negatively regulated by the REST complex (Ballas et al., 2005), we hypothesized that LSD1 inhibition could lead to REST complex disruption and further promote the transcription of Sox11. In our experimental settings, we observed that LSD1 inhibition was increasing the expression of Sox11 at distinct time points at the DRG and spinal cord, partially validating our idea.

Within the long-term study, we observed that animals that underwent crush-injury and RN-1 treatment did not show enhancement in motor and skin reinnervation. In this regard, nerve regeneration depends on the expression of RAGs and on the correct development of Wallerian degeneration (Menorca et al., 2013). Since LSD1 inhibition leads to immunosuppression, this could affect the infiltration of hematogenous macrophages within the nerve leading to Wallerian degeneration deficits. These complications would further affect the regenerative capacity of the nerve and could justify the null effects of our compound in reinnervation after injury. However, no significant differences were observed in the development of Wallerian degeneration between vehicle and LSD1-inhibited animals. Therefore, RN-1 did not inhibit myelin degradation, which could potentially interfere with the regenerative process. Even though, it would be suitable to assess macrophage accumulation and axonal degeneration at

7 dpo and earlier time points to fully validate that Wallerian degeneration remains unaffected after LSD1 inhibition.

Another possible explanation for the lack of regenerative success is the severity of the injury. Provided that the nerve regeneration rate after crush injury is quicker than after a transection injury, it is probable that the high velocity of the regeneration events may mask the positive effects of our treatment in this study (B. B. Wang et al., 2023).

Conclusions

In conclusion, this study shows that global LSD1 inhibition can increase neurite outgrowth *ex vivo* and promote the expression of Regeneration Associated Genes (RAGs) after nerve injury. However, LSD1 inhibition was not potent enough to produce long lasting effects and, it did not improve nerve regeneration in vivo. Thus, LSD1 function within the nervous system should be carefully dissected to clarify its potential as a therapeutic target.

References

Aoki, H., Hara, A., Era, T., Kunisada, T., & Yamada, Y. (2012). Genetic ablation of Rest leads to in vitro-specific derepression of neuronal genes during neurogenesis. *Development, 139*(4), 667-677. doi:10.1242/dev.072272

Ballas, N., Grunseich, C., Lu, D. D., Speh, J. C., & Mandel, G. (2005). REST and its corepressors mediate plasticity of neuronal gene chromatin throughout neurogenesis. *Cell, 121*(4), 645-657. doi:10.1016/j.cell.2005.03.013

Bergsland, M., Werme, M., Malewicz, M., Perlmann, T., & Muhr, J. (2006). The establishment of neuronal properties is controlled by Sox4 and Sox11. *Genes Dev, 20*(24), 3475-3486. doi:10.1101/gad.403406

Cavalcanti, F., Gonzalez-Rey, E., Delgado, M., Falo, C. P., Mestre, L., Guaza, C., . . . Maes, T. (2022). Efficacy of Vafidemstat in Experimental Autoimmune Encephalomyelitis Highlights the KDM1A/RCOR1/HDAC Epigenetic Axis in Multiple Sclerosis. *Pharmaceutics, 14*(7). doi:10.3390/pharmaceutics14071420

Choi, S. H., Yousefian-Jazi, A., Hyeon, S. J., Nguyen, P. T. T., Chu, J., Kim, S., . . . Lee, J. (2022). Modulation of histone H3K4 dimethylation by spermidine ameliorates motor neuron survival and neuropathology in a mouse model of ALS. *J Biomed Sci, 29*(1), 106. doi:10.1186/s12929-022-00890-3

Christopher, M. A., Myrick, D. A., Barwick, B. G., Engstrom, A. K., Porter-Stransky, K. A., Boss, J. M., . . . Katz, D. J. (2017). LSD1 protects against hippocampal and cortical neurodegeneration. *Nat Commun, 8*(1), 805. doi:10.1038/s41467-017-00922-9

Duly, A. M. P., Kao, F. C. L., Teo, W. S., & Kavallaris, M. (2022). betaIII-Tubulin Gene Regulation in Health and Disease. *Front Cell Dev Biol, 10*, 851542. doi:10.3389/fcell.2022.851542

Gu, Y., Chen, D., Zhou, L., Zhao, X., Lin, J., Lin, B., . . . Liu, W. (2021). Lysine-specific demethylase 1 inhibition enhances autophagy and attenuates early-stage post-spinal cord injury apoptosis. *Cell Death Discov, 7*(1), 69. doi:10.1038/s41420-021-00455-7

Han, X., Gui, B., Xiong, C., Zhao, L., Liang, J., Sun, L., . . . Shang, Y. (2014). Destabilizing LSD1 by Jade-2 promotes neurogenesis: an antibraking system in neural development. *Mol Cell, 55*(3), 482-494. doi:10.1016/j.molcel.2014.06.006

Jankowski, M. P., McIlwrath, S. L., Jing, X., Cornuet, P. K., Salerno, K. M., Koerber, H. R., & Albers, K. M. (2009). Sox11 transcription factor modulates peripheral nerve regeneration in adult mice. *Brain Res, 1256*, 43-54. doi:10.1016/j.brainres.2008.12.032

Kim, D., Kim, K. I., & Baek, S. H. (2021). Roles of lysine-specific demethylase 1 (LSD1) in homeostasis and diseases. *J Biomed Sci, 28*(1), 41. doi:10.1186/s12929-021-00737-3

Kim, D., Nam, H. J., Lee, W., Yim, H. Y., Ahn, J. Y., Park, S. W., . . . Baek, S. H. (2018). PKCalpha-LSD1-NF-kappaB-Signaling Cascade Is Crucial for Epigenetic Control of the Inflammatory Response. *Mol Cell, 69*(3), 398-411 e396. doi:10.1016/j.molcel.2018.01.002

Kyzar, E. J., Bohnsack, J. P., Zhang, H., & Pandey, S. C. (2019). MicroRNA-137 Drives Epigenetic Reprogramming in the Adult Amygdala and Behavioral Changes after Adolescent Alcohol Exposure. *eNeuro, 6*(6). doi:10.1523/ENEURO.0401-19.2019

Maes, T., Mascaro, C., Rotllant, D., Lufino, M. M. P., Estiarte, A., Guibourt, N., . . . Buesa Arjol, C. (2020). Modulation of KDM1A with vafidemstat rescues memory deficit and behavioral alterations. *PLoS One, 15*(5), e0233468. doi:10.1371/journal.pone.0233468

Maiques-Diaz, A., & Somervaille, T. C. (2016). LSD1: biologic roles and therapeutic targeting. *Epigenomics, 8*(8), 1103-1116. doi:10.2217/epi-2016-0009

Menorca, R. M., Fussell, T. S., & Elfar, J. C. (2013). Nerve physiology: mechanisms of injury and recovery. *Hand Clin, 29*(3), 317-330. doi:10.1016/j.hcl.2013.04.002

Naoi, M., Maruyama, W., Akao, Y., Yi, H., & Yamaoka, Y. (2006). Involvement of type A monoamine oxidase in neurodegeneration: regulation of mitochondrial signaling leading to cell death or neuroprotection. *J Neural Transm Suppl*(71), 67-77. doi:10.1007/978-3-211-33328-0_8

Navarro, X. (2016). Functional evaluation of peripheral nerve regeneration and target reinnervation in animal models: a critical overview. *Eur J Neurosci, 43*(3), 271-286. doi:10.1111/ejn.13033

Navarro, X., Geuna, S., Grothe, C., & Haastert-Talini, K. (2018). Introduction: Thematic Papers Issue on Peripheral Nerve Regeneration and Repair. *Anat Rec (Hoboken), 301*(10), 1614-1617. doi:10.1002/ar.23941

Ou, X. M., Chen, K., & Shih, J. C. (2006). Monoamine oxidase A and repressor R1 are involved in apoptotic signaling pathway. *Proc Natl Acad Sci U S A, 103*(29), 10923-10928. doi:10.1073/pnas.0601515103

Puttagunta, R., Tedeschi, A., Soria, M. G., Hervera, A., Lindner, R., Rathore, K. I., . . . Di Giovanni, S. (2014). PCAF-dependent epigenetic changes promote axonal regeneration in the central nervous system. *Nat Commun, 5*, 3527. doi:10.1038/ncomms4527

Rivers, A., Vaitkus, K., Ruiz, M. A., Ibanez, V., Jagadeeswaran, R., Kouznetsova, T., . . . Lavelle, D. (2015). RN-1, a potent and selective lysine-specific demethylase 1 inhibitor, increases gamma-globin expression, F reticulocytes, and F cells in a sickle cell disease mouse model. *Exp Hematol, 43*(7), 546-553 e541-543. doi:10.1016/j.exphem.2015.04.005

Rusconi, F., Grillo, B., Toffolo, E., Mattevi, A., & Battaglioli, E. (2017). NeuroLSD1: Splicing-Generated Epigenetic Enhancer of Neuroplasticity. *Trends Neurosci, 40*(1), 28-38. doi:10.1016/j.tins.2016.11.002

Sagarkar, S., Choudhary, A. G., Balasubramanian, N., Awathale, S. N., Somalwar, A. R., Pawar, N., . . . Sakharkar, A. J. (2021). LSD1-BDNF activity in lateral hypothalamus-medial forebrain bundle area is essential for reward seeking behavior. *Prog Neurobiol, 202*, 102048. doi:10.1016/j.pneurobio.2021.102048

Toffolo, E., Rusconi, F., Paganini, L., Tortorici, M., Pilotto, S., Heise, C., . . . Battaglioli, E. (2014). Phosphorylation of neuronal Lysine-Specific Demethylase 1LSD1/KDM1A impairs transcriptional repression by regulating interaction with CoREST and histone deacetylases HDAC1/2. *J Neurochem, 128*(5), 603-616. doi:10.1111/jnc.12457

Torres-Espin, A., Santos, D., Gonzalez-Perez, F., del Valle, J., & Navarro, X. (2014). Neurite-J: an image-J plug-in for axonal growth analysis in organotypic cultures. *J Neurosci Methods, 236*, 26-39. doi:10.1016/j.jneumeth.2014.08.005

Tsutsumi, T., Iwao, K., Hayashi, H., Kirihara, T., Kawaji, T., Inoue, T., . . . Tanihara, H. (2016). Potential Neuroprotective Effects of an LSD1 Inhibitor in Retinal Ganglion Cells via p38 MAPK Activity. *Invest Ophthalmol Vis Sci, 57*(14), 6461-6473. doi:10.1167/iovs.16-19494

Wang, B. B., Guo, C., Sun, S. Q., Zhang, X. N., Li, Z., Li, W. J., . . . Liu, S. (2023). Comparison of the Nerve Regeneration Capacity and Characteristics between Sciatic Nerve Crush and Transection Injury Models in Rats. *Biomed Environ Sci, 36*(2), 160-173. doi:10.3967/bes2023.001

Yonekawa, T., & Thorburn, A. (2013). Autophagy and cell death. *Essays Biochem, 55*, 105-117. doi:10.1042/bse0550105

Zhang, F., Rein, B., Zhong, P., Shwani, T., Conrow-Graham, M., Wang, Z. J., & Yan, Z. (2021). Synergistic inhibition of histone modifiers produces therapeutic effects in adult Shank3-deficient mice. *Transl Psychiatry, 11*(1), 99. doi:10.1038/s41398-021-01233-w

Zibetti, C., Adamo, A., Binda, C., Forneris, F., Toffolo, E., Verpelli, C., . . . Battaglioli, E. (2010). Alternative splicing of the histone demethylase LSD1/KDM1 contributes to the modulation of neurite morphogenesis in the mammalian nervous system. *J Neurosci, 30*(7), 2521-2532. doi:10.1523/JNEUROSCI.5500-09.2010

Zou, Z. K., Huang, Y. Q., Zou, Y., Zheng, X. K., & Ma, X. D. (2017). Silencing of LSD1 gene modulates histone methylation and acetylation and induces the apoptosis of JeKo-1 and MOLT-4 cells. *Int J Mol Med, 40*(2), 319-328. doi:10.3892/ijmm.2017.3032

Discussion

Discussion

Peripheral nerve injuries disrupt the connection between the nervous system and the target organs, leading to functional loss and to the appearance of secondary problems like neuropathic pain. Currently, there is a lack of therapies that can ameliorate pain and promote functional recovery after nerve injury. For this reason, it is necessary to identify novel treatments that can address both conditions to effectively improve patient's outcome. In this regard, epigenetic research is a growing field that has triggered the development of new strategies for the treatment of diverse neuropathological diseases. However, investigations involving epigenetic modulation following nerve trauma are still limited. Thus, the identification of epigenetic targets capable of effectively enhancing axonal growth and reducing neuropathic pain could provide new treatments for traumatic nerve injuries. To address this issue, the main objective of this thesis was to underscore if the epigenetic targets LSD1 and BET proteins could be suitable candidates to promote a better outcome after nerve injury.

The former objective was elaborated under two main hypotheses. Firstly, we proposed that BET protein inhibition might improve functional outcome after sciatic nerve injury by accelerating the course of Wallerian degeneration. This idea was sustained on the evidence that BET proteins are involved in inflammation. In fact, inhibition of BET proteins has been found to decrease pro-inflammatory gene expression, while it increased the transcription of anti-inflammatory mediators (Nicodeme et al., 2010; Sanchez-Ventura et al., 2019). Subsequently, the change on the inflammatory environment could potentially reduce pain and accelerate the conclusion of Wallerian degeneration, favoring axonal regeneration. Secondly, provided that LSD1 inhibition has been associated with neuroplasticity and neuroprotection (Choi et al., 2022; Christopher, Myrick, et al., 2017; Gu et al., 2021; Maes et al., 2020), we hypothesized that LSD1 inhibition could positively influence axonal outgrowth after nerve injury.

BET proteins as a target to treat nerve injury

Targeting BET proteins for reducing neuropathic pain

Spared nerve injury (SNI) is a neuropathic pain model first described by Decosterd and Woolf (Decosterd & Woolf, 2000). Use of this injury model consistently induces thermal hyperalgesia, as well as mechanical allodynia and hyperalgesia in mice (Bourquin et al., 2006; Bravo-Caparros et al., 2019; Casals-Diaz, 2011). Hereof, in chapter 1 we observed that BET inhibition using JQ1, significantly reduced mechanical hyperalgesia in mice that underwent SNI. This result is coherent with other scientific reports, showing that JQ1 reduces mechanical hyperalgesia and allodynia in mice subjected to SCI and to trigeminal neuralgia (Sanchez-Ventura et al., 2019; Vasavda et al., 2022). In addition, other BET inhibitors displayed similar effects in the amelioration of mechanical-based pain. For instance, the use of I-BET762 after SNI and after HIV-induced neuropathy (Borgonetti & Galeotti, 2021; Takahashi et al., 2018), or treatment with DDO-8926 after SNI, ameliorated mechanical allodynia (X. Chen et al., 2023). Thus, evidence proves that BET inhibition reduces the perception of mechanical-based pain in distinct neuropathic pain models.

Nevertheless, contradicting results are found when analyzing the effects of BET inhibition on thermal hyperalgesia. We did not observe any improvement in heat-dependent hyperalgesia after JQ1 treatment, coinciding with previous results from our laboratory in a study conducted in mice that underwent SCI (Sanchez-Ventura et al., 2019). In contrast, reports that used other BET inhibitors, as I-BET762, stated that heat-based pain was reduced after treatment (Borgonetti & Galeotti, 2021; Borgonetti et al., 2022). These discrepancies between studies may be dependent on the selected compound, and differences in sex and mice strain. Firstly, JQ1 and I-BET762 have been defined as pan-BET inhibitors, but their binding affinity towards the distinct BET family members differs (Filippakopoulos et al., 2010; Nicodeme et al., 2010; Shorstova, Foulkes, & Witcher, 2021). Subsequently, distinct attachment preferences between BET inhibitors could lead to different outcomes in pain. In second place, we used C57BL6/J female mice, while studies that show effects on thermal pain assessment used CD1 male animals (Borgonetti & Galeotti, 2021; Borgonetti, Meacci, Pierucci, Romanelli, & Galeotti, 2022). In this regard, several reports pointed that the genetic background of mice strain and sex influences the responsiveness of the animals to pain (Marmiroli et al., 2017; Presto, Mazzitelli, Junell, Griffin, & Neugebauer, 2022; J. C. Smith, 2019; Vacca et al., 2014;

Wilson et al., 2003). Thus, provided that multiple variables differ between experiments it is difficult to assess the role of BET-proteins on thermal-induced pain.

BET proteins and their effects on mechanisms of neuropathic pain

To assess the impact of BET protein inhibition on pain, we analyzed the effects of JQ1 on two physiopathological mechanisms that contribute to its appearance: inflammation and excitability. To our knowledge, our study is the first to report that inhibition of BET proteins dually modulates both mechanisms, by altering the expression of ion channels and by facilitating an anti-inflammatory response. Specifically, in chapter 1 we observed that BET inhibition reduced the expression of pro-inflammatory mediators, while increased the transcription of anti-inflammatory cytokines early after injury. In addition, JQ1 also prevented microglial reactivity without affecting nociceptive fiber density in the dorsal horn of the spinal cord. Consistent with our findings, similar effects on inflammation have been observed in reports that used other BET inhibitors after SNI (Borgonetti & Galeotti, 2021; X. Chen et al., 2023).

Neural excitability is also altered after nerve injuries and in other neuropathic pain conditions. It is originated by changes in ion channel expression, inflammation, and collateral axon growth (Costigan et al., 2009). Considering the mechanisms that contribute to excitability, BET proteins have been associated with the expression of sodium channels (Hsieh et al., 2017). Subsequently, we proceeded to assess the effects of BET inhibition over ion channels in animals that underwent SNI. In chapter 1 we determined that JQ1 led to alterations in ion channel expression, resulting in increased axonal hyperpolarization and reduced neural excitability. Specifically, Nav1.3, Nav1.7, Kv7.2, Kv7.3, HCN1, HCN2 ion channels and distinct subunits of the sodium-potassium pump were affected after treatment. Importantly, these findings are consistent with other scientific publications. Hereof, treatment with the BET-inhibitor DDO-8926 after SNI led to alterations on Nav1.3, Kv7.2, Kv7.3 and the sodium potassium pump (X. Chen et al., 2023). In addition, an RNA sequencing of cortical neurons that underwent JQ1 treatment detected a downregulation of genes involved in voltage-gated channel activity and potassium channel activity (Korb et al., 2015). Another RNA sequencing conducted in a mouse model of Alzheimer's disease, described that JQ1 decreased Nav1.3, Nav1.7 and HCN2 transcriptional levels when compared to vehicle-treated animals (Benito et al., 2017).

Besides, JQ1-dependent alteration of neural excitability improved the symptomatology of epilepsy and Rett Syndrome affecting other parameters that were not included in our study (Korb et al., 2015; Xiang et al., 2020). BET inhibition in Rett Syndrome recovered the expression of the glutamate receptor $mGlu_7$ and the chloride transporter KCC2 in GABAergic neurons (Xiang et al., 2020). In epilepsy, JQ1 may reduce the expression of *gria1*, a gene that conforms a subunit of the $AMPA_R$ (Korb et al., 2015; Singh, Babigian, & Sartor, 2022). Considering the findings reported in Rett syndrome and epilepsy, further experiments should assess if JQ1 may also modulate glutamate channels and facilitate the action of inhibitory pathways in models of neuropathic pain. Lastly, reactive oxygen species have been reported to contribute to neuropathic pain (Kallenborn-Gerhardt et al., 2012; D. Kim et al., 2010). In this regard, JQ1 decreased oxidative stress in a mouse model of trigeminal neuralgia (Vasavda et al., 2022).

In conclusion, we determined that BET inhibition modulates inflammation and excitability after SNI. However, BET proteins could also potentially modulate other physiological mechanisms that contribute to the appearance of neuropathic pain.

JQ1 as a potential treatment for neuropathic pain

Neuropathic pain management requires of more effective and safer treatments. Current first line and second line treatments for neuropathic pain, summarized in Table 10, coincide with BET inhibitors in their effects on ion channels and inflammation. For instance, tricyclic antidepressants like amitriptyline can block sodium channels and modulate potassium currents (Dick et al., 2007; Wolff et al., 2016). Similarly, the second-line treatment lidocaine blocks voltage gated sodium channels (Cavalli, Mammana, Nicoletti, Bramanti, & Mazzon, 2019). JQ1 also shares mechanism of action with other first-line drugs, such as duloxetine, which, besides regulating serotonin-noradrenaline reuptake, participates in inflammation and oxidative stress (Demirdas, Naziroglu, & Ovey, 2017; J. Meng et al., 2019; Yamashita et al., 2016). Importantly, BET inhibitors have also demonstrated similar efficacy than first-line drugs. Specifically, the BET-inhibitor DDO-8926 also displayed similar effects in the amelioration of mechanical-based pain when compared to gabapentin (X. Chen et al., 2023).

Although our results suggest that BET inhibitors could be a promising therapy for nerve injury, further studies should clarify the consequences of BET inhibition in substance abuse and in mood alterations to offer a secure pharmacological alternative to patients. In this regard, one

of the current problems with prevailing contemporary treatments involve safety concerns. For instance, opioid derivates, which are proposed as second- or third-line recommendations, can lead to addiction (Miotto et al., 2017) and gabapentinoids have been associated with suicidal thoughts in patients (Molero, Larsson, D'Onofrio, Sharp, & Fazel, 2019).

Summary of pharmacotherapies for neuropathic pain

Priority	*Drug name*	*Mechanism of action*	*Use*
First line	Gabapentin	Probable binding to calcium voltage-dependent channels, reducing Ca^{2}+ influx to the cells. Previously used against epilepsy.	All
	Pregabalin		All
	Duloxetine or venlafaxine	Inhibits serotonin-noradrenaline reuptake from presynaptic terminals.	All
	Amitriptyline (Tricyclic antidepressants)	Inhibits serotonin-noradrenaline reuptake. It also acts as an inhibitor of cholinergic, adrenergic, and histaminergic receptors, and ion channels.	All
Second line	Capsaicin 8% patches	TRPV1 agonist. Its prolonged activation leads to desensitization.	Peripheral pain
	Lidocaine patches	Promote blockage of voltage-gated sodium channels, leading to a reduction of ectopic firing.	Peripheral pain
	Tramadol	Weak opioid agonist and inhibitor of serotonin noradrenaline reuptake.	All
Third line	Oxycodone and morphine (Strong opioids)	Agonists of μ-opioid receptors.	All
	Botulinum toxin A	Inhibitor of synaptic exocytosis.	Peripheral pain

Table 10: Recommendations on pharmacotherapies for neuropathic pain proposed by the IASP. Treatments are classified as first-, second- and third-line options based on their efficacy and safety (Cavalli et al., 2019; Finnerup et al., 2015)

In conclusion, BET protein inhibition targets some of the underlying mechanisms of neuropathic pain, coinciding with the effects of other first- and second-line accepted drugs. In addition, inhibition of BET proteins displayed similar performance in the amelioration of pain than the first-line drug gabapentin. Thus, JQ1 and other BET inhibitors seem potentially good candidates for the treatment of neuropathic pain.

Targeting BET proteins to enhance nerve regeneration

DRG explant cultures preserve the structure and cellular interactions between neurons and the peripheral glia present *in vivo*, being a good *ex vivo* alternative to study axonal regeneration (Fornaro, Sharthiya, & Tiwari, 2018). By using this methodology in chapter 2, we observed that BET inhibition with JQ1 led to a decrease in neurite outgrowth without affecting cell viability. These results are consistent with other reports in which BET inhibition in cortical cultures altered the expression of immediate early genes (IEGs) and downregulated the expression of genes associated with synapse formation and axon-dendrite development (Benito et al., 2017; Korb et al., 2015; J. M. Sullivan et al., 2015).

As a drawback, DRG explant cultures miss the inclusion of other cell types involved in nerve repair, such as fibroblasts and infiltrating immune cells. To address this issue, we used conditioned medium from BET-inhibited macrophages in explant cultures and observed a significant increase in neurite outgrowth through STAT6 pathway. In line with the idea that cultures must include various cell types to mimic physiological events, another report stated that BET protein inhibition only enhanced synapse formation when human IPs-derived neurons where co-cultured with IPS-derived astrocytes (Berryer et al., 2023). Therefore, BET-inhibition directly in neurons may not facilitate plasticity, but it may favor neuronal function when targeting other cell types. In addition, and in concordance with our observations, it has been stated that phosphorylation of STAT6 increased the growth on retinal axons of rats (Goulart et al., 2018). Importantly, STAT6 is activated by IL-4 and IL-13 cytokines which both have also been linked to nerve regeneration (Ali et al., 2020; Kelly-Welch et al., 2005; Van Broeckhoven et al., 2022).

Apart from assessing the effects of BET-inhibition *ex vivo*, we assessed the effects of JQ1 in nerve regeneration *in vivo*. Firstly, we performed a short-term study to determine the most adequate treatment regimen when using JQ1 after sciatic crush injury. As a result, delayed administration of the compound promoted the transcription of GAP43 and IL-4. Despite delayed JQ1 treatment enhanced the expression of pro-regenerative markers, its long-term administration after nerve injury did not lead to motor and sensory reinnervation. Contrary to our findings, BET-inhibition ameliorated outcome after SCI and increased the expression of anti-inflammatory cytokines IL-4, IL-13 and IL-10 (Sanchez-Ventura et al., 2019). Additionally, exogenous administration of IL-4 improved early axonal regeneration after various models of

nerve injury (Ali et al., 2020; Pan et al., 2022). Nevertheless, this permissive environment did not lead to a significant increase on axonal regeneration in our long-term experiment.

Although not studied in detail in chapter 2, other proteins that conform the regenerative environment have been reported to be affected by BET inhibition. For instance, JQ1 treatment and BRD4 knockdown *in vitro* were found to reduce BDNF transcription (Sartor et al., 2019). In addition, BET inhibition with I-BET858 decreased the transcription of semaphorin-3a, TrkC and calcium/calmodulin dependent protein kinase II delta in cortical neurons (J. M. Sullivan et al., 2015). However, we did not see negative effects in the transcription of neurotrophic factors after sciatic nerve injury when JQ1 was used as a delayed treatment. It is possible that in our assay other cell types, such as Schwann cells, may compensate the negative effects on neurotrophic factor transcription that have been described in neurons using *in vitro* models.

Despite the regenerative environment can be slightly permissive due to BET-inhibition in macrophages, it may only compensate the negative effects that BET-inhibition has on peripheral neurons, only guaranteeing a regeneration comparable to vehicle animals.

Future considerations

In this thesis we have hypothesized that switching the inflammatory state towards an anti-inflammatory environment could promote regeneration. In this regard, a similar approach that used thrombomodulin to transition towards an anti-inflammatory milleu has obtained good prognosis after sciatic nerve transection (T. C. Huang, Wu, Chen, Wang, & Wu, 2020). Thus, it would be advisable to refine the experimental design to potentiate the effects of BET proteins as regulators of the environment to treat nerve injuries.

To further assess the regenerative potential of BET-inhibition after nerve injury and avoid its negative effects in neurons, it would be interesting to use transgenic animals with an inducible knockout (KO) of BRD4 in macrophages. Between the distinct BET family members, BRD4 KO seems more convenient since we demonstrated its involvement in the transcription of anti-inflammatory cytokines in chapter 3. In addition, an inducible KO would permit to switch towards an anti-inflammatory environment without suppressing the pro-inflammatory phase of Wallerian degeneration, which is necessary to promote macrophage recruitment and debris clearance after injury (P. Chen et al., 2015). Possible positive results of this proposal

could grant a novel possibility to develop treatments for humans by using specific drug delivery of BET inhibitors towards macrophages or by employing gene therapy.

Considering the current results, inhibition of BET proteins seems not suitable to dually modulate axonal regeneration and ameliorate pain, since it is probable that different cell targets would be needed in each case. In future works it would be recommendable to assess the efficacy of the proposed study with transgenic animals for enhancing nerve regeneration, and if the approach turns out to be successful, it would be essential to determine if this novel strategy also affects neuropathic pain. By doing so, we could elucidate if BET proteins can be used as a dual therapy or should be applied in combination with other therapies to ameliorate the outcome after nerve injury.

BET proteins in inflammation

Inflammation is a complex physiological mechanism subjected under epigenetic control. In this regard, the epigenetic reader family of BET proteins have been described to be involved in inflammatory events (Hajmirza et al., 2018).

Despite the modulation of pro-inflammatory gene expression has been widely studied in distinct BET family members, we wanted to determine the mechanisms by which BET inhibition promotes anti-inflammatory cytokine transcription in macrophages. To our knowledge, our results are the first to report that the BET family member BRD4 acts as a repressor on the promoter of the anti-inflammatory cytokine IL-13, and possibly of IL-4, in macrophages. In chapter 3 we analyzed the transcriptional and translational alterations on cytokine expression using JQ1 on macrophages. We corroborated that BET-inhibition reduces the expression of LPS-induced inflammatory mediators and increases the transcription of IL-4 and IL-13, coinciding with the evidence stated by other reports (Nicodeme et al., 2010; Sanchez-Ventura et al., 2019). Considering LPS-dependent cytokines, their expression under the regulation of BET proteins has largely been studied in macrophages. For instance, it has been demonstrated that LPS treatment triggers the association of BET proteins to the IL-6 promoter and TNF-α promoter. This binding is disrupted upon JQ1 treatment, probably leading to the disassembly of p-65/RelA complex on pro-inflammatory genes (Belkina et al., 2013). In line with these results, a study showed that LPS stimulated IL-10 transcription in B lymphocytes, and JQ1 treatment counteracted these effects. They elucidated that LPS

treatment significantly enhanced BRD4 and p65 binding onto IL-10 proximal promoters and that these effects were neutralized after JQ1 treatment (Lee et al., 2017). Altogether these findings corroborate the effects that we saw in chapter 3, where BET-inhibition decreased the transcription and protein expression of LPS-mediated cytokines.

In the following experiments, we observed that independent knockdown of the BET protein family member BRD4 and the repressor CHD4, were able to increase the transcription of IL-4 and IL-13 anti-inflammatory mediators. These results suggested that BRD4 and CHD4 probably formed a repressive complex in the promoters of these anti-inflammatory cytokines, preventing their expression. Then, upon JQ1 treatment these effects could be counteracted leading to transcription. This idea was corroborated by chromatin immunoprecipitation in the promoter of IL-13.

Although we are the first to assess that BRD4 and CHD4 repress the IL-13 promoter in macrophages, we are not the first authors to establish that BRD4 can bind to anti-inflammatory cytokine promoters (Zhao et al., 2023). Contrary to our findings, Zhao et al. stated that BRD4 promoted Gata3 transcriptional activation of IL-4, IL-5 and IL-13 by mediating the repression of the Th2 negative regulators Foxp3 and Fbxw7 (Zhao et al., 2023). Thus, while previous findings attribute to BRD4 a pro-transcriptional role of anti-inflammatory mediators, we unraveled that BRD4 also harbors a direct repressive function over these genes. In fact, we observed that BET inhibition promotes anti-inflammatory cytokine transcription, while in the experiments of Zhao et al. it promotes a transcriptional downregulation of these cytokines. These discrepancies between studies may be due to cell type or cell polarization, as Zhao et al. used differentiated Th2 lymphocytes. To further support this idea, it has been described that IL-4 activated macrophages display another inflammatory transcriptional program than non-polarized macrophages (Czimmerer et al., 2022). Therefore, immune cell status could potentially affect the role of BRD4 in inflammation.

In conclusion, BET inhibition in macrophages can act as an inflammatory switch, reducing the production of pro-inflammatory mediators and enhancing the transcription of anti-inflammatory cytokines. This mechanism harbors a great therapeutic potential to a wide variety of diseases that depend upon inflammatory dysregulation.

LSD1 as a target to improve regeneration

LSD1 in axonal growth and inflammation

Previous research has suggested that LSD1 inhibition promotes plasticity and neuroprotection when used as a treatment in various neurological diseases (Choi et al., 2022; Christopher, Myrick, et al., 2017; Gu et al., 2021; Maes et al., 2020). However, limited research has focused on elucidating the role of LSD1 in axonal growth. In chapter 4 we observed that LSD1 inhibition with RN-1 at 500 nM raised the number of neurites in DRG explants *ex vivo*. In line with our research, Toffolo et al. also studied the effects of LSD1 and its isoforms on neurite morphogenesis. Although they observed a small increase on neurite length when comparing LSD1 knockdown to control, the differences were not significant (Toffolo et al., 2014). We attribute our discrepancies to the fact that pharmacotherapy and gene silencing may lead to distinct degrees of expression of the target protein or gene. In this regard, RN-1 permitted neurite growth in a very limited therapeutic window which can be hardly mimicked using a knockdown. In addition, our study is performed using a DRG explant culture instead of a cortical culture, which preserves the structure, and the diversity of cellular populations present within the ganglia (Fornaro et al., 2018). Consistent with the *ex vivo* results, early RN-1 treatment to mice that underwent nerve injury increased the expression of Regeneration Associated Genes (RAGs) in the sciatic nerve, in the DRG and in the spinal cord. In agreement with our findings, other authors already reported that LSD1 could regulate the expression of *bdnf* and *tubulin* genes (X. Han et al., 2014; Sagarkar et al., 2021).

We also assessed that RN-1 treatment affected the inflammatory environment *in vivo*. In this regard, it has already been reported that LSD1 affects pro-inflammatory and anti-inflammatory cytokine expression (Hong et al., 2020; D. Kim et al., 2018; Sobczak et al., 2021). Provided that RN-1 leads to immunosuppression *in vivo*, we analyzed the consequences of LSD1 inhibition on Wallerian degeneration. Contrarily to what we expected and to other studies, LSD1 inhibition did not affect the course of Wallerian degeneration (Boivin et al., 2007). Taking into account that macrophages and Schwann cells participate in debris clearance, it would be necessary to assess the effects of RN-1 treatment on macrophage recruitment and in Schwann cell phagocytosis to fully elucidate the consequences of LSD1 inhibition on Wallerian degeneration (Stoll, Griffin, Li, & Trapp, 1989).

Despite the positive effects of LSD1 on the expression of RAGs, we did not observe significant differences between treatments regarding cutaneous and muscular reinnervation after injury. One of the obstacles that may limit the observation of results is the selection of the injury. While crush injury has been proposed as an adequate model to study the cellular and molecular changes after nerve damage, more severe injuries like complete transection and suture repair may be more adequate to assess the differences on reinnervation and axonal regeneration (B. B. Wang et al., 2023).

Future work

Chapter 4 suggests that RN-1 has potential as a treatment to increase axonal regeneration, as seen in the *ex vivo* assay and with the expression of RAGs in the short-term study. However, it remains to fully clarify the influence of RN-1 inhibition on Wallerian degeneration. As mentioned in the previous paragraphs, it would be needed to assess the effects of RN-1 inhibition in Schwann cell and macrophage phagocytic activity *in vitro* as well as on macrophage recruitment after injury. Once the effects of LSD1 inhibition on Wallerian degeneration had been fully elucidated, RN-1 might be applied in a more severe nerve injury to assess potential effects on the rate of axonal regeneration. Finally, the effects of RN-1 as an immunosuppressor could negatively affect the regenerative environment (Boivin et al., 2007; Vidal et al., 2013). Thus, it would also be advisable to assess specific LSD1 knockdown in neurons after nerve injury. Approaches to address this idea, could be the use of viral vectors containing siRNA against LSD1 to specifically target the neuronal population *in vivo* (Tiscornia, Singer, Ikawa, & Verma, 2003; Yang, Bailey, Baltimore, & Wang, 2006), or by using transgenic animals to promote specific knockdown of LSD1 in neurons.

Limitations of the study

Epigenetics as a whole-body therapy

One problem when facing the use of epigenetic drugs is that epigenetic alterations can have distinct effects in each cell type or organoid. This is clearly demonstrated in the present Thesis with the epigenetic inhibitors JQ1 and RN-1. We observed that the pan-BET inhibitor JQ1 prevents growth on DRG explants, however the use of this epigenetic target on macrophages creates a favorable environment that facilitates axon growth. Another example found in our work with RN-1, is that we observed that LSD1 inhibition could increase the expression of

RAGs but led to immunosuppression. As epigenetic alterations affect the whole body, a favorable balance on the outcome targeting the distinct cellular types involved is challenging. In fact, it has been described that HDACs in clinical trials led to several side effects such fatigue, diarrhea, and nausea (Nepali & Liou, 2021). Side effects have also been reported in clinical trials that used BET and LSD1 inhibitors (Amorim et al., 2016; Y. Fang, Liao, & Yu, 2019). Thus, a possible way to overcome these issues and potentiate the favorable results of epigenetic drugs is to promote cell-type specific delivery such as using modified nanoparticles or viral vectors under de regulation of specific cell-type promoters. This delivery system could be used to specifically deliver the compounds, shRNAs, or crisp-dCAS9 systems to facilitate epigenetic modifications only on the cell types of interest.

Sex as a variable in the enhancement of functional outcome after injury

Sexual dimorphism has become important in the last decades, demonstrating that physiological functions are differently regulated between both sexes. In fact, research has shown that pain perception, regeneration and inflammation may be distinct between males and females. For instance, some studies indicate that females are more susceptible to pain after nerve injury and report differences in the physiological mechanisms that regulate its appearance between sexes (Presto et al., 2022; Sorge et al., 2015; Vacca et al., 2014). Regarding axonal regeneration, it has been revealed that sexual dimorphism does not lead to significant differences in axonal growth *in vitro* and after crush injury in mice (Jang et al., 2021). Specifically, while axon guidance and regeneration-related gene expression was similar between both sexes (between 65 and 81 % coincidence), differences were detected in genes associated with inflammation (15 to 29% coincidence). In line with these results, different genetic expression has been detected between male and female mice involving the expression of structural proteins, ion channels, neurotrophic and immune genes after nerve axotomy (Chernov & Shubayev, 2022). Thus, while some common regenerative pathways are maintained, males and females employ distinct mechanisms to confront neuronal damage.

Special account should be taken when using inflammation-derived approaches between female and male mice. The impact of sexual dimorphism on inflammation considering different animals has been reviewed in various articles (Klein & Flanagan, 2016; Martinez de Toda et al., 2023). In fact, age and strain are also critical when considering the consequences

of inflammation in mice and should also be considered (Sans-Fons et al., 2013; Wong, Magnusson, & Ho, 2013).

To note, our targets participate in sex-specific programs which may exacerbate possible differences between sexes. Specifically, LSD1 couples with the androgen receptor and the BET member BRDT is selectively expressed in the reproductive organs (Martinez-Gamero et al., 2021; N. Wang et al., 2021). In conclusion, parallel studies regarding the role of BET and LSD1 must also be assessed in male subjects in future studies.

Conclusions

Conclusions

The main conclusions of the present thesis are:

BET proteins as an epigenetic target to treat nerve injuries

- Administration of the BET-inhibitor JQ1 immediately after injury reduced mechanical pain in mice that underwent SNI, by regulating excitability through the alteration of ion channel expression and the modulation of the inflammatory environment.
- *In vitro,* JQ1 treatment in primary macrophages generated a pro-regenerative conditioned media that promoted neurite outgrowth in DRG explants through the STAT6 pathway. However, direct action of JQ1 in neuronal and glial populations of DRG explant cultures decreased neurite number and length, without affecting cellular viability. This effect demonstrates that BET-inhibition improves neurite outgrowth through an indirect action in macrophages.
- Administration of JQ1 since day 4 after injury did not affect macrophage infiltration and increased the transcription of anti-inflammatory cytokines and RAGs in the sciatic nerve of crush-injured mice.
- JQ1 treatment since day 4 after injury did not improve motor and sensory reinnervation after sciatic crush injury, suggesting that more refined delivery strategies must be developed to apply BET protein inhibition as a therapy to promote nerve regeneration.
- Six-hour treatment of JQ1 in primary macrophages *in vitro* increases the transcription of the anti-inflammatory cytokines IL-4 and IL-13, while decreases the expression of the pro-inflammatory mediators TNF-α, IL-1β and IL-6.
- Knockdown of BRD4 and CHD4 raises the transcription of the anti-inflammatory mediators IL-4 and IL-13.
- JQ1 administration in primary macrophages releases BRD4 and CHD4 from the promoter of the IL-13 gene, indicating that these enzymes may work as co-repressive partners preventing anti-inflammatory cytokine transcription.

LSD1 as a potential epigenetic target to treat nerve injury

- Administration of the LSD1 inhibitor RN-1 at 500nM in DRG explants *in vitro* enhances neurite number and displays a positive tendency to increase neurite length.
- LSD1 inhibition increases the expression of the regeneration associated genes β-III tubulin and BDNF in crush-injured animals and leads to immunosuppression.
- RN-1 mediated LSD1 inhibition *in vivo* raises the transcription of the pro-regenerative factor Sox11 after sciatic crush injury.
- LSD1 inhibition does not affect the development of Wallerian degeneration and does not promote motor and sensory reinnervation after nerve injury. These results suggest that the role of LSD1 after nerve injury must be carefully dissected to apply it as a potential treatment after nerve injury.

References

References

Abe, N., Borson, S. H., Gambello, M. J., Wang, F., & Cavalli, V. (2010). Mammalian target of rapamycin (mTOR) activation increases axonal growth capacity of injured peripheral nerves. *J Biol Chem, 285*(36), 28034-28043. doi:10.1074/jbc.M110.125336

Ali, S. A., Hanks, J. E., Stebbins, A. W., Alkhalili, O., Cohen, S. T., Chen, J. Y., . . . Brenner, M. J. (2020). Delivery of Interleukin-4-Encoding Lentivirus Using Multiple-Channel Bridges Enhances Nerve Regeneration. *Laryngoscope, 130*(12), 2802-2810. doi:10.1002/lary.28629

Alles, S. R. A., & Smith, P. A. (2021). Peripheral Voltage-Gated Cation Channels in Neuropathic Pain and Their Potential as Therapeutic Targets. *Front Pain Res (Lausanne), 2*, 750583. doi:10.3389/fpain.2021.750583

Allodi, I., Udina, E., & Navarro, X. (2012). Specificity of peripheral nerve regeneration: interactions at the axon level. *Prog Neurobiol, 98*(1), 16-37. doi:10.1016/j.pneurobio.2012.05.005

Alpsoy, A., & Dykhuizen, E. C. (2018). Glioma tumor suppressor candidate region gene 1 (GLTSCR1) and its paralog GLTSCR1-like form SWI/SNF chromatin remodeling subcomplexes. *J Biol Chem, 293*(11), 3892-3903. doi:10.1074/jbc.RA117.001065

Amorim, S., Stathis, A., Gleeson, M., Iyengar, S., Magarotto, V., Leleu, X., . . . Thieblemont, C. (2016). Bromodomain inhibitor OTX015 in patients with lymphoma or multiple myeloma: a dose-escalation, open-label, pharmacokinetic, phase 1 study. *Lancet Haematol, 3*(4), e196-204. doi:10.1016/S2352-3026(16)00021-1

Angius, D., Wang, H., Spinner, R. J., Gutierrez-Cotto, Y., Yaszemski, M. J., & Windebank, A. J. (2012). A systematic review of animal models used to study nerve regeneration in tissue-engineered scaffolds. *Biomaterials, 33*(32), 8034-8039. doi:10.1016/j.biomaterials.2012.07.056

Aoki, H., Hara, A., Era, T., Kunisada, T., & Yamada, Y. (2012). Genetic ablation of Rest leads to in vitro-specific derepression of neuronal genes during neurogenesis. *Development, 139*(4), 667-677. doi:10.1242/dev.072272

Atanasoski, S., Scherer, S. S., Sirkowski, E., Leone, D., Garratt, A. N., Birchmeier, C., & Suter, U. (2006). ErbB2 signaling in Schwann cells is mostly dispensable for maintenance of

myelinated peripheral nerves and proliferation of adult Schwann cells after injury. *J Neurosci, 26*(7), 2124-2131. doi:10.1523/JNEUROSCI.4594-05.2006

Atkins, S., R Loescher, A., M Boissonade, F., G Smith, K., Occleston, N., O'Kane, S., . . . P Robinson, P. (2007). Interleukin-10 reduces scarring and enhances regeneration at a site of sciatic nerve repair. *Journal of the Peripheral Nervous System, 12*(4), 269–276. doi:doi:10.1111/j.1529-8027.2007.00148.x

Austin, P. J., & Moalem-Taylor, G. (2010). The neuro-immune balance in neuropathic pain: involvement of inflammatory immune cells, immune-like glial cells and cytokines. *J Neuroimmunol, 229*(1-2), 26-50. doi:10.1016/j.jneuroim.2010.08.013

Austin, P. J., & Moalem-Taylor, G. (2013). Pathophysiology of neuropathic pain: inflammatory mediators. In *Neuropathic Pain* (pp. 77-89).

Bagratuni, T., Mavrianou, N., Gavalas, N. G., Tzannis, K., Arapinis, C., Liontos, M., . . . Bamias, A. (2020). JQ1 inhibits tumour growth in combination with cisplatin and suppresses JAK/STAT signalling pathway in ovarian cancer. *Eur J Cancer, 126*, 125-135. doi:10.1016/j.ejca.2019.11.017

Ballas, N., Grunseich, C., Lu, D. D., Speh, J. C., & Mandel, G. (2005). REST and its corepressors mediate plasticity of neuronal gene chromatin throughout neurogenesis. *Cell, 121*(4), 645-657. doi:10.1016/j.cell.2005.03.013

Barral, A., & Dejardin, J. (2023). The chromatin signatures of enhancers and their dynamic regulation. *Nucleus, 14*(1), 2160551. doi:10.1080/19491034.2022.2160551

Barsig, J., Kusters, S., Vogt, K., Volk, H. D., Tiegs, G., & Wendel, A. (1995). Lipopolysaccharide-induced interleukin-10 in mice: role of endogenous tumor necrosis factor-alpha. *Eur J Immunol, 25*(10), 2888-2893. doi:10.1002/eji.1830251027

Belkina, A. C., Nikolajczyk, B. S., & Denis, G. V. (2013). BET protein function is required for inflammation: Brd2 genetic disruption and BET inhibitor JQ1 impair mouse macrophage inflammatory responses. *J Immunol, 190*(7), 3670-3678. doi:10.4049/jimmunol.1202838

Beltran, B., Mathur, A., Duchen, M. R., Erusalimsky, J. D., & Moncada, S. (2000). The effect of nitric oxide on cell respiration: A key to understanding its role in cell survival or death. *Proceedings of the National Academy of Sciences, 97*(26), 14602–14607. doi:doi:10.1073/pnas.97.26.14602

Benito, E., Ramachandran, B., Schroeder, H., Schmidt, G., Urbanke, H., Burkhardt, S., . . . Fischer, A. (2017). The BET/BRD inhibitor JQ1 improves brain plasticity in WT and APP mice. *Transl Psychiatry, 7*(9), e1239. doi:10.1038/tp.2017.202

Bennett, D. L., Clark, A. J., Huang, J., Waxman, S. G., & Dib-Hajj, S. D. (2019). The Role of Voltage-Gated Sodium Channels in Pain Signaling. *Physiol Rev, 99*(2), 1079-1151. doi:10.1152/physrev.00052.2017

Bergmeister, K. D., Grosse-Hartlage, L., Daeschler, S. C., Rhodius, P., Bocker, A., Beyersdorff, M., . . . Harhaus, L. (2020). Acute and long-term costs of 268 peripheral nerve injuries in the upper extremity. *PLoS One, 15*(4), e0229530. doi:10.1371/journal.pone.0229530

Bergsland, M., Werme, M., Malewicz, M., Perlmann, T., & Muhr, J. (2006). The establishment of neuronal properties is controlled by Sox4 and Sox11. *Genes Dev, 20*(24), 3475-3486. doi:10.1101/gad.403406

Berryer, M. H., Rizki, G., Nathanson, A., Klein, J. A., Trendafilova, D., Susco, S. G., . . . Barrett, L. E. (2023). High-content synaptic phenotyping in human cellular models reveals a role for BET proteins in synapse assembly. *Elife, 12*. doi:10.7554/eLife.80168

Bhatt, D., & Ghosh, S. (2014). Regulation of the NF-kappaB-Mediated Transcription of Inflammatory Genes. *Front Immunol, 5*, 71. doi:10.3389/fimmu.2014.00071

Black, J. A., Cummins, T. R., Plumpton, C., Chen, Y. H., Hormuzdiar, W., Clare, J. J., & Waxman, S. G. (1999). Upregulation of a silent sodium channel after peripheral, but not central, nerve injury in DRG neurons. *J Neurophysiol, 82*(5), 2776-2785. doi:10.1152/jn.1999.82.5.2776

Boadas-Vaello, P., Castany, S., Homs, J., Álvarez-Pérez, B., Deulofeu, M., & Verdú, E. (2016). Neuroplasticity of ascending and descending pathways after somatosensory system injury: reviewing knowledge to identify neuropathic pain therapeutic targets. *Spinal Cord, 54*(5), 330-340. doi:10.1038/sc.2015.225

Boissonnas, A., Louboutin, F., Laviron, M., Loyher, P. L., Reboussin, E., Barthelemy, S., . . . Combadiere, C. (2020). Imaging resident and recruited macrophage contribution to Wallerian degeneration. *J Exp Med, 217*(11). doi:10.1084/jem.20200471

Boivin, A., Pineau, I., Barrette, B., Filali, M., Vallieres, N., Rivest, S., & Lacroix, S. (2007). Toll-like receptor signaling is critical for Wallerian degeneration and functional recovery

after peripheral nerve injury. *J Neurosci, 27*(46), 12565-12576. doi:10.1523/JNEUROSCI.3027-07.2007

Borgonetti, V., & Galeotti, N. (2021). Combined inhibition of histone deacetylases and BET family proteins as epigenetic therapy for nerve injury-induced neuropathic pain. *Pharmacol Res, 165*, 105431. doi:10.1016/j.phrs.2021.105431

Borgonetti, V., Meacci, E., Pierucci, F., Romanelli, M. N., & Galeotti, N. (2022). Dual HDAC/BRD4 Inhibitors Relieves Neuropathic Pain by Attenuating Inflammatory Response in Microglia After Spared Nerve Injury. *Neurotherapeutics, 19*(5), 1634-1648. doi:10.1007/s13311-022-01243-6

Bouhassira, D., Attal, N., Fermanian, J., Alchaar, H., Gautron, M., Masquelier, E., . . . Boureau, F. (2004). Development and validation of the Neuropathic Pain Symptom Inventory. *Pain, 108*(3), 248-257. doi:10.1016/j.pain.2003.12.024

Bouhassira, D., Lanteri-Minet, M., Attal, N., Laurent, B., & Touboul, C. (2008). Prevalence of chronic pain with neuropathic characteristics in the general population. *Pain, 136*(3), 380-387. doi:10.1016/j.pain.2007.08.013

Boulasiki, P., Tan, X. W., Spinelli, M., & Riccio, A. (2023). The NuRD Complex in Neurodevelopment and Disease: A Case of Sliding Doors. *Cells, 12*(8). doi:10.3390/cells12081179

Bourquin, A. F., Suveges, M., Pertin, M., Gilliard, N., Sardy, S., Davison, A. C., . . . Decosterd, I. (2006). Assessment and analysis of mechanical allodynia-like behavior induced by spared nerve injury (SNI) in the mouse. *Pain, 122*(1-2), 14 e11-14. doi:10.1016/j.pain.2005.10.036

Bravo-Caparros, I., Perazzoli, G., Yeste, S., Cikes, D., Baeyens, J. M., Cobos, E. J., & Nieto, F. R. (2019). Sigma-1 Receptor Inhibition Reduces Neuropathic Pain Induced by Partial Sciatic Nerve Transection in Mice by Opioid-Dependent and -Independent Mechanisms. *Front Pharmacol, 10*, 613. doi:10.3389/fphar.2019.00613

Brugger, V., Duman, M., Bochud, M., Munger, E., Heller, M., Ruff, S., & Jacob, C. (2017). Delaying histone deacetylase response to injury accelerates conversion into repair Schwann cells and nerve regeneration. *Nat Commun, 8*, 14272. doi:10.1038/ncomms14272

Brushart, T., Gerber, J., Kessens, P., Chen, Y., & Royall, R. (1998). Contributions of pathway and neuron to preferential motor reinnervation. *The Journal of Neuroscience, 18*(21), 8674–8681. doi:10.1523/JNEUROSCI.18-21-08674.1998

Brushart, T. M. (1988). Preferential Reinnervation of Motor Nerves by Regenerating Motor Axons *The Journal of Neuroscience, 8*(3), 1026-1031. doi:10.1523/JNEUROSCI.08-03-01026.1988

Buttner, R., Schulz, A., Reuter, M., Akula, A. K., Mindos, T., Carlstedt, A., . . . Morrison, H. (2018). Inflammaging impairs peripheral nerve maintenance and regeneration. *Aging Cell, 17*(6), e12833. doi:10.1111/acel.12833

Casals-Diaz, L. (2011). *Neuroimmune interactions in neuropathic pain. Involvement of TNF-α and voltage-gated sodium channels in sensory neurons after peripheral nerve injury.* (PhD), Universitat Autònoma de Barcelona,

Casals-Diaz, L., Vivo, M., & Navarro, X. (2009). Nociceptive responses and spinal plastic changes of afferent C-fibers in three neuropathic pain models induced by sciatic nerve injury in the rat. *Exp Neurol, 217*(1), 84-95. doi:10.1016/j.expneurol.2009.01.014

Caterina, M. J., Leffler, A., Malmberg, A. B., Martin, W. J., Trafton, J., Petersen-Zeitz, K. R., . . . Julius, D. (2000). Impaired Nociception and Pain Sensation in Mice Lacking the Capsaicin Receptor. *Science, 288*(5464), 306-313. doi:10.1126/science.288.5464.30

Cavalcanti, F., Gonzalez-Rey, E., Delgado, M., Falo, C. P., Mestre, L., Guaza, C., . . . Maes, T. (2022). Efficacy of Vafidemstat in Experimental Autoimmune Encephalomyelitis Highlights the KDM1A/RCOR1/HDAC Epigenetic Axis in Multiple Sclerosis. *Pharmaceutics, 14*(7). doi:10.3390/pharmaceutics14071420

Cavalli, E., Mammana, S., Nicoletti, F., Bramanti, P., & Mazzon, E. (2019). The neuropathic pain: An overview of the current treatment and future therapeutic approaches. *Int J Immunopathol Pharmacol, 33*, 2058738419838383. doi:10.1177/2058738419838383

Cervero, F. (2009). Pain: friend or foe? A Neurobiologic perspective: the 2008 Bonica Award Lecture. *Reg Anesth Pain Med, 34*(6), 569-574. doi:10.1097/aap.0b013e3181b4c517

Chaplan, S. R., Guo, H. Q., Lee, D. H., Luo, L., Liu, C., Kuei, C., . . . Dubin, A. E. (2003). Neuronal hyperpolarization-activated pacemaker channels drive neuropathic pain. *J Neurosci, 23*(4), 1169-1178. doi:10.1523/JNEUROSCI.23-04-01169.2003

Chen, H., Lin, W., Zhang, Y., Lin, L., Chen, J., Zeng, Y., . . . Liu, N. (2016). IL-10 Promotes Neurite Outgrowth and Synapse Formation in Cultured Cortical Neurons after the Oxygen-

Glucose Deprivation via JAK1/STAT3 Pathway. *Sci Rep, 6*, 30459. doi:10.1038/srep30459

Chen, P., Piao, X., & Bonaldo, P. (2015). Role of macrophages in Wallerian degeneration and axonal regeneration after peripheral nerve injury. *Acta Neuropathol, 130*(5), 605-618. doi:10.1007/s00401-015-1482-4

Chen, X., Cao, D., Liu, C., Meng, F., Zhang, Z., Xu, R., . . . Jiang, Z. (2023). Discovery of 1H-Imidazo[4,5-b]pyridine Derivatives as Potent and Selective BET Inhibitors for the Management of Neuropathic Pain. *J Med Chem, 66*(13), 8725-8744. doi:10.1021/acs.jmedchem.3c00372

Cheng, Y., Song, H., Ming, G. L., & Weng, Y. L. (2023). Epigenetic and epitranscriptomic regulation of axon regeneration. *Mol Psychiatry*. doi:10.1038/s41380-023-02028-9

Chernov, A. V., & Shubayev, V. I. (2022). Sexually dimorphic transcriptional programs of early-phase response in regenerating peripheral nerves. *Frontiers in Molecular Neuroscience, 15*. doi:10.3389/fnmol.2022.958568

Chhabra, A., Ahlawat, S., Belzberg, A., & Andreseik, G. (2014). Peripheral nerve injury grading simplified on MR neurography: As referenced to Seddon and Sunderland classifications. *Indian J Radiol Imaging, 24*(3), 217-224. doi:10.4103/0971-3026.137025

Choi, S. H., Yousefian-Jazi, A., Hyeon, S. J., Nguyen, P. T. T., Chu, J., Kim, S., . . . Lee, J. (2022). Modulation of histone H3K4 dimethylation by spermidine ameliorates motor neuron survival and neuropathology in a mouse model of ALS. *J Biomed Sci, 29*(1), 106. doi:10.1186/s12929-022-00890-3

Christopher, M. A., Kyle, S. M., & Katz, D. J. (2017). Neuroepigenetic mechanisms in disease. *Epigenetics Chromatin, 10*(1), 47. doi:10.1186/s13072-017-0150-4

Christopher, M. A., Myrick, D. A., Barwick, B. G., Engstrom, A. K., Porter-Stransky, K. A., Boss, J. M., . . . Katz, D. J. (2017). LSD1 protects against hippocampal and cortical neurodegeneration. *Nat Commun, 8*(1), 805. doi:10.1038/s41467-017-00922-9

Chung, D., Shum, A., & Caraveo, G. (2020). GAP-43 and BASP1 in Axon Regeneration: Implications for the Treatment of Neurodegenerative Diseases. *Front Cell Dev Biol, 8*, 567537. doi:10.3389/fcell.2020.567537

Cisneros, E., Roza, C., Jackson, N., & López-García, J. A. (2015). A New Regulatory Mechanism for Kv7.2 Protein During Neuropathy: Enhanced Transport from the Soma to Axonal

Terminals of Injured Sensory Neurons. *Frontiers in Cellular Neuroscience, 9*. doi:10.3389/fncel.2015.00470

Clark, A. K., Old, E. A., & Malcangio, M. (2013). Neuropathic pain and cytokines: current perspectives. *J Pain Res, 6*, 803-814. doi:10.2147/JPR.S53660

Costigan, M., Scholz, J., & Woolf, C. J. (2009). Neuropathic pain: a maladaptive response of the nervous system to damage. *Annu Rev Neurosci, 32*, 1-32. doi:10.1146/annurev.neuro.051508.135531

Coutaux, A., Adam, F., Willer, J. C., & Le Bars, D. (2005). Hyperalgesia and allodynia: peripheral mechanisms. *Joint Bone Spine, 72*(5), 359-371. doi:10.1016/j.jbspin.2004.01.010

Czimmerer, Z., Halasz, L., Daniel, B., Varga, Z., Bene, K., Domokos, A., . . . Nagy, L. (2022). The epigenetic state of IL-4-polarized macrophages enables inflammatory cistromic expansion and extended synergistic response to TLR ligands. *Immunity, 55*(11), 2006-2026 e2006. doi:10.1016/j.immuni.2022.10.004

Daines, J. M., Schellhardt, L., & Wood, M. D. (2021). The Role of the IL-4 Signaling Pathway in Traumatic Nerve Injuries. *Neurorehabil Neural Repair, 35*(5), 431-443. doi:10.1177/15459683211001026

Daou, I., Beaudry, H., Ase, A. R., Wieskopf, J. S., Ribeiro-da-Silva, A., Mogil, J. S., & Seguela, P. (2016). Optogenetic Silencing of Nav1.8-Positive Afferents Alleviates Inflammatory and Neuropathic Pain. *eNeuro, 3*(1). doi:10.1523/ENEURO.0140-15.2016

Das, A., Chai, J. C., Yang, C. S., Lee, Y. S., Das, N. D., Jung, K. H., & Chai, Y. G. (2015). Dual transcriptome sequencing reveals resistance of TLR4 ligand-activated bone marrow-derived macrophages to inflammation mediated by the BET inhibitor JQ1. *Sci Rep, 5*, 16932. doi:10.1038/srep16932

Deboy, C. A., Xin, J., Byram, S. C., Serpe, C. J., Sanders, V. M., & Jones, K. J. (2006). Immune-mediated neuroprotection of axotomized mouse facial motoneurons is dependent on the IL-4/STAT6 signaling pathway in CD4(+) T cells. *Exp Neurol, 201*(1), 212-224. doi:10.1016/j.expneurol.2006.04.028

Decosterd, I., & Woolf, C. J. (2000). Spared nerve injury: an animal model of persistent peripheral neuropathic pain. *Pain, 87*(2), 149-158. doi:10.1016/S0304-3959(00)00276-1

DeFrancesco-Lisowitz, A., Lindborg, J. A., Niemi, J. P., & Zigmond, R. E. (2015). The neuroimmunology of degeneration and regeneration in the peripheral nervous system. *Neuroscience, 302*, 174-203. doi:10.1016/j.neuroscience.2014.09.027

Demirdas, A., Naziroglu, M., & Ovey, I. S. (2017). Duloxetine Reduces Oxidative Stress, Apoptosis, and Ca(2+) Entry Through Modulation of TRPM2 and TRPV1 Channels in the Hippocampus and Dorsal Root Ganglion of Rats. *Mol Neurobiol, 54*(6), 4683-4695. doi:10.1007/s12035-016-9992-1

Denny, J. B. (2006). Molecular Mechanisms, Biological Actions, and Neuropharmacology of the Growth-Associated Protein GAP-43. *Current Neuropharmacology, 4*, 293-304 doi:10.2174/157015906778520782

Deprez, M., Lubke, U., Verlaet, M., Debrus, S., Delvenne, P., & Martin, J. J. (2001). Detection of cytokines in human sural nerve biopsies: an immunohistochemical and molecular study. *Acta Neuropathol, 101*(4), 393-404. doi:10.1007/s004010000300

Dey, A., Yang, W., Gegonne, A., Nishiyama, A., Pan, R., Yagi, R., . . . Ozato, K. (2019). BRD4 directs hematopoietic stem cell development and modulates macrophage inflammatory responses. *EMBO J, 38*(7). doi:10.15252/embj.2018100293

Dick, I. E., Brochu, R. M., Purohit, Y., Kaczorowski, G. J., Martin, W. J., & Priest, B. T. (2007). Sodium channel blockade may contribute to the analgesic efficacy of antidepressants. *J Pain, 8*(4), 315-324. doi:10.1016/j.jpain.2006.10.001

Duly, A. M. P., Kao, F. C. L., Teo, W. S., & Kavallaris, M. (2022). betaIII-Tubulin Gene Regulation in Health and Disease. *Front Cell Dev Biol, 10*, 851542. doi:10.3389/fcell.2022.851542

Ellis, A., & Bennett, D. L. (2013). Neuroinflammation and the generation of neuropathic pain. *Br J Anaesth, 111*(1), 26-37. doi:10.1093/bja/aet128

Emery, E. C., Young, G. T., Berrocoso, E. M., Chen, L., & McNaughton, P. A. (2011). HCN2 ion channels play a central role in inflammatory and neuropathic pain. *Science, 333*(6048), 1462-1466. doi:10.1126/science.1206243

Esiri, M. M., & Reading, M. C. (1989). Macrophages, lymphocytes and major histocompatibility complex (HLA) class II antigens in adult human sensory and sympathetic ganglia *Journal of Neuroimmunology, 23*, 187-193. doi:10.1016/0165-5728(89)90050-7

Facer, P., Casula, M. A., Smith, G. D., Benham, C. D., Chessell, I. P., Bountra, C., . . . Anand, P. (2007). Differential expression of the capsaicin receptor TRPV1 and related novel

receptors TRPV3, TRPV4 and TRPM8 in normal human tissues and changes in traumatic and diabetic neuropathy. *BMC Neurol, 7*, 11. doi:10.1186/1471-2377-7-11

Fang, W. F., Chen, Y. M., Lin, C. Y., Huang, H. L., Yeh, H., Chang, Y. T., . . . Lin, M. C. (2018). Histone deacetylase 2 (HDAC2) attenuates lipopolysaccharide (LPS)-induced inflammation by regulating PAI-1 expression. *J Inflamm (Lond), 15*, 3. doi:10.1186/s12950-018-0179-6

Fang, Y., Liao, G., & Yu, B. (2019). LSD1/KDM1A inhibitors in clinical trials: advances and prospects. *J Hematol Oncol, 12*(1), 129. doi:10.1186/s13045-019-0811-9

Filippakopoulos, P., & Knapp, S. (2014). Targeting bromodomains: epigenetic readers of lysine acetylation. *Nat Rev Drug Discov, 13*(5), 337-356. doi:10.1038/nrd4286

Filippakopoulos, P., Qi, J., Picaud, S., Shen, Y., Smith, W. B., Fedorov, O., . . . Bradner, J. E. (2010). Selective inhibition of BET bromodomains. *Nature, 468*(7327), 1067-1073. doi:10.1038/nature09504

Finelli, M. J., Wong, J. K., & Zou, H. (2013). Epigenetic regulation of sensory axon regeneration after spinal cord injury. *J Neurosci, 33*(50), 19664-19676. doi:10.1523/JNEUROSCI.0589-13.2013

Finnerup, N. B., Attal, N., Haroutounian, S., McNicol, E., Baron, R., Dworkin, R. H., . . . Wallace, M. (2015). Pharmacotherapy for neuropathic pain in adults: a systematic review and meta-analysis. *Lancet Neurol, 14*(2), 162-173. doi:10.1016/S1474-4422(14)70251-0

Finnerup, N. B., Kuner, R., & Jensen, T. S. (2021). Neuropathic Pain: From Mechanisms to Treatment. *Physiol Rev, 101*(1), 259-301. doi:10.1152/physrev.00045.2019

Fonseca, M. M., Davoli-Ferreira, M., Santa-Cecilia, F., Guimaraes, R. M., Oliveira, F. F. B., Kusuda, R., . . . Cunha, T. M. (2019). IL-27 Counteracts Neuropathic Pain Development Through Induction of IL-10. *Front Immunol, 10*, 3059. doi:10.3389/fimmu.2019.03059

Fornaro, M., Marcus, D., Rattin, J., & Goral, J. (2021). Dynamic Environmental Physical Cues Activate Mechanosensitive Responses in the Repair Schwann Cell Phenotype. *Cells, 10*(2). doi:10.3390/cells10020425

Fornaro, M., Sharthiya, H., & Tiwari, V. (2018). Adult Mouse DRG Explant and Dissociated Cell Models to Investigate Neuroplasticity and Responses to Environmental Insults Including Viral Infection. *J Vis Exp*(133). doi:10.3791/56757

Gibson, G. (2007). Peripheral Nerve Injuries. In *Physical Rehabilitation* (pp. 473-513).

Giovannini, S., Weller, M. C., Hanzlikova, H., Shiota, T., Takeda, S., & Jiricny, J. (2020). ATAD5 deficiency alters DNA damage metabolism and sensitizes cells to PARP inhibition. *Nucleic Acids Res, 48*(9), 4928-4939. doi:10.1093/nar/gkaa255

Golz, G., Uhlmann, L., Ludecke, D., Markgraf, N., Nitsch, R., & Hendrix, S. (2006). The cytokine/neurotrophin axis in peripheral axon outgrowth. *Eur J Neurosci, 24*(10), 2721-2730. doi:10.1111/j.1460-9568.2006.05155.x

Goulart, V. G., Menezes, G. D., Espirito-Santo, S., Faria-Melibeu, A. D. C., Serfaty, C. A., & Campello-Costa, P. (2018). Interleukin 4 Leads to Sustained Phosphorylation of the STAT6 and ERK Pathways in the Retina and Disrupts Subcortical Visual Circuitry in Rodents. *Neuroimmunomodulation, 25*(2), 96-102. doi:10.1159/000490895

Greer, E. L., & Shi, Y. (2012). Histone methylation: a dynamic mark in health, disease and inheritance. *Nat Rev Genet, 13*(5), 343-357. doi:10.1038/nrg3173

Gu, Y., Chen, D., Zhou, L., Zhao, X., Lin, J., Lin, B., . . . Liu, W. (2021). Lysine-specific demethylase 1 inhibition enhances autophagy and attenuates early-stage post-spinal cord injury apoptosis. *Cell Death Discov, 7*(1), 69. doi:10.1038/s41420-021-00455-7

Hains, B. C., Saab, C. Y., Klein, J. P., Craner, M. J., & Waxman, S. G. (2004). Altered sodium channel expression in second-order spinal sensory neurons contributes to pain after peripheral nerve injury. *J Neurosci, 24*(20), 4832-4839. doi:10.1523/JNEUROSCI.0300-04.2004

Hajmirza, A., Emadali, A., Gauthier, A., Casasnovas, O., Gressin, R., & Callanan, M. B. (2018). BET Family Protein BRD4: An Emerging Actor in NFkappaB Signaling in Inflammation and Cancer. *Biomedicines, 6*(1). doi:10.3390/biomedicines6010016

Han, F., Zhang, L., Chen, C., Wang, Y., Zhang, Y., Qian, L., . . . Lai, M. (2019). GLTSCR1 Negatively Regulates BRD4-Dependent Transcription Elongation and Inhibits CRC Metastasis. *Adv Sci (Weinh), 6*(23), 1901114. doi:10.1002/advs.201901114

Han, S. B., Kim, H., Lee, H., Grove, M., Smith, G. M., & Son, Y. J. (2017). Postinjury Induction of Activated ErbB2 Selectively Hyperactivates Denervated Schwann Cells and Promotes Robust Dorsal Root Axon Regeneration. *J Neurosci, 37*(45), 10955-10970. doi:10.1523/JNEUROSCI.0903-17.2017

Han, X., Gui, B., Xiong, C., Zhao, L., Liang, J., Sun, L., . . . Shang, Y. (2014). Destabilizing LSD1 by Jade-2 promotes neurogenesis: an antibraking system in neural development. *Mol Cell, 55*(3), 482-494. doi:10.1016/j.molcel.2014.06.006

Hanz, S., & Fainzilber, M. (2006). Retrograde signaling in injured nerve--the axon reaction revisited. *J Neurochem, 99*(1), 13-19. doi:10.1111/j.1471-4159.2006.04089.x

Hao, J., Padilla, F., Dandonneau, M., Lavebratt, C., Lesage, F., Noel, J., & Delmas, P. (2013). Kv1.1 channels act as mechanical brake in the senses of touch and pain. *Neuron, 77*(5), 899-914. doi:10.1016/j.neuron.2012.12.035

Hayward, D., & Cole, P. A. (2016). LSD1 Histone Demethylase Assays and Inhibition. *Methods Enzymol, 573*, 261-278. doi:10.1016/bs.mie.2016.01.020

Hong, K. S., Ahn, J. H., Jang, J. G., Lee, J. H., Kim, H. N., Kim, D., & Lee, W. (2020). GSK-LSD1, an LSD1 inhibitor, quashes SARS-CoV-2-triggered cytokine release syndrome in-vitro. *Signal Transduct Target Ther, 5*(1), 267. doi:10.1038/s41392-020-00391-5

Hosokawa, H., Tanaka, T., Suzuki, Y., Iwamura, C., Ohkubo, S., Endoh, K., . . . Nakayama, T. (2013). Functionally distinct Gata3/Chd4 complexes coordinately establish T helper 2 (Th2) cell identity. *Proc Natl Acad Sci U S A, 110*(12), 4691-4696. doi:10.1073/pnas.1220865110

Hsieh, M. C., Ho, Y. C., Lai, C. Y., Wang, H. H., Lee, A. S., Cheng, J. K., . . . Peng, H. Y. (2017). Bromodomain-containing Protein 4 Activates Voltage-gated Sodium Channel 1.7 Transcription in Dorsal Root Ganglia Neurons to Mediate Thermal Hyperalgesia in Rats. *Anesthesiology, 127*(5), 862-877. doi:10.1097/ALN.0000000000001809

Hu, J., Pan, D., Li, G., Chen, K., & Hu, X. (2022). Regulation of programmed cell death by Brd4. *Cell Death Dis, 13*(12), 1059. doi:10.1038/s41419-022-05505-1

Hua, T., Wang, H., Fan, X., An, N., Li, J., Song, H., . . . Yuan, H. (2022). BRD4 Inhibition Attenuates Inflammatory Pain by Ameliorating NLRP3 Inflammasome-Induced Pyroptosis. *Front Immunol, 13*, 837977. doi:10.3389/fimmu.2022.837977

Huang, B., Yang, X. D., Zhou, M. M., Ozato, K., & Chen, L. F. (2009). Brd4 coactivates transcriptional activation of NF-kappaB via specific binding to acetylated RelA. *Mol Cell Biol, 29*(5), 1375-1387. doi:10.1128/MCB.01365-08

Huang, T. C., Wu, H. L., Chen, S. H., Wang, Y. T., & Wu, C. C. (2020). Thrombomodulin facilitates peripheral nerve regeneration through regulating M1/M2 switching. *J Neuroinflammation, 17*(1), 240. doi:10.1186/s12974-020-01897-z

Huckhagel, T., Nuchtern, J., Regelsberger, J., Gelderblom, M., Lefering, R., & TraumaRegister, D. G. U. (2018). Nerve trauma of the lower extremity: evaluation of 60,422 leg injured

patients from the TraumaRegister DGU(R) between 2002 and 2015. *Scand J Trauma Resusc Emerg Med, 26*(1), 40. doi:10.1186/s13049-018-0502-5

Hurley, S., Mohan, C., Suetterlin, P., Ellingford, R., Riegman, K. L. H., Ellegood, J., . . . Basson, M. A. (2021). Distinct, dosage-sensitive requirements for the autism-associated factor CHD8 during cortical development. *Mol Autism, 12*(1), 16. doi:10.1186/s13229-020-00409-3

Hutson, T. H., Kathe, C., Palmisano, I., Bartholdi, K., Hervera, A., De Virgiliis, F., . . . Di Giovanni, S. (2019). Cbp-dependent histone acetylation mediates axon regeneration induced by environmental enrichment in rodent spinal cord injury models. *Sci Transl Med, 11*(487). doi:10.1126/scitranslmed.aaw2064

Hwang, J. Y., Aromolaran, K. A., & Zukin, R. S. (2017). The emerging field of epigenetics in neurodegeneration and neuroprotection. *Nat Rev Neurosci, 18*(6), 347-361. doi:10.1038/nrn.2017.46

Ikeda, H., Heinke, B., Ruscheweyh, R., & Sandkuhler, J. (2003). Synaptic plasticity in spinal lamina I projection neurons that mediate hyperalgesia. *Science, 299*(5610), 1237-1240. doi:10.1126/science.1080659

Italiani, P., & Boraschi, D. (2014). From Monocytes to M1/M2 Macrophages: Phenotypical vs. Functional Differentiation. *Front Immunol, 5*, 514. doi:10.3389/fimmu.2014.00514

Jang, E. H., Bae, Y. H., Yang, E. M., Gim, Y., Suh, H. J., Kim, S., . . . Hur, E. M. (2021). Comparing axon regeneration in male and female mice after peripheral nerve injury. *J Neurosci Res, 99*(11), 2874-2887. doi:10.1002/jnr.24955

Jankowski, M. P., McIlwrath, S. L., Jing, X., Cornuet, P. K., Salerno, K. M., Koerber, H. R., & Albers, K. M. (2009). Sox11 transcription factor modulates peripheral nerve regeneration in adult mice. *Brain Res, 1256*, 43-54. doi:10.1016/j.brainres.2008.12.032

Jensen, T. S., Baron, R., Haanpaa, M., Kalso, E., Loeser, J. D., Rice, A. S. C., & Treede, R. D. (2011). A new definition of neuropathic pain. *Pain, 152*(10), 2204-2205. doi:10.1016/j.pain.2011.06.017

Jessen, K. R., & Mirsky, R. (2008). Negative regulation of myelination: relevance for development, injury, and demyelinating disease. *Glia, 56*(14), 1552-1565. doi:10.1002/glia.20761

Jessen, K. R., & Mirsky, R. (2016). The repair Schwann cell and its function in regenerating nerves. *J Physiol, 594*(13), 3521-3531. doi:10.1113/JP270874

Jessen, K. R., Mirsky, R., & Lloyd, A. C. (2015). Schwann Cells: Development and Role in Nerve Repair. *Cold Spring Harb Perspect Biol, 7*(7), a020487. doi:10.1101/cshperspect.a020487

Jiang, Y. Q., Xing, G. G., Wang, S. L., Tu, H. Y., Chi, Y. N., Li, J., . . . Wan, Y. (2008). Axonal accumulation of hyperpolarization-activated cyclic nucleotide-gated cation channels contributes to mechanical allodynia after peripheral nerve injury in rat. *Pain, 137*(3), 495-506. doi:10.1016/j.pain.2007.10.011

Joshi, S., Singh, A. R., Zulcic, M., Bao, L., Messer, K., Ideker, T., . . . Durden, D. L. (2014). Rac2 controls tumor growth, metastasis and M1-M2 macrophage differentiation in vivo. *PLoS One, 9*(4), e95893. doi:10.1371/journal.pone.0095893

Junttila, I. S. (2018). Tuning the Cytokine Responses: An Update on Interleukin (IL)-4 and IL-13 Receptor Complexes. *Front Immunol, 9*, 888. doi:10.3389/fimmu.2018.00888

Kallenborn-Gerhardt, W., Schroder, K., Del Turco, D., Lu, R., Kynast, K., Kosowski, J., . . . Schmidtko, A. (2012). NADPH oxidase-4 maintains neuropathic pain after peripheral nerve injury. *J Neurosci, 32*(30), 10136-10145. doi:10.1523/JNEUROSCI.6227-11.2012

Kawasaki, A., Okada, M., Tamada, A., Okuda, S., Nozumi, M., Ito, Y., . . . Igarashi, M. (2018). Growth Cone Phosphoproteomics Reveals that GAP-43 Phosphorylated by JNK Is a Marker of Axon Growth and Regeneration. *iScience, 4*, 190-203. doi:10.1016/j.isci.2018.05.019

Kawasaki, Y., Zhang, L., Cheng, J. K., & Ji, R. R. (2008). Cytokine mechanisms of central sensitization: distinct and overlapping role of interleukin-1beta, interleukin-6, and tumor necrosis factor-alpha in regulating synaptic and neuronal activity in the superficial spinal cord. *J Neurosci, 28*(20), 5189-5194. doi:10.1523/JNEUROSCI.3338-07.2008

Kaya, Y., & Sarikcioglu, L. (2015). Sir Herbert Seddon (1903-1977) and his classification scheme for peripheral nerve injury. *Childs Nerv Syst, 31*(2), 177-180. doi:10.1007/s00381-014-2560-y

Kelly-Welch, A., M. Hanson, E., & D. Keegan, A. (2005). Interleukin-13 (IL-13) Pathway. *Science's STKE, 2005*(293). doi:https://doi.org/10.1126/stke.2932005cm8open_in_new

Kim, D., Kim, K. I., & Baek, S. H. (2021). Roles of lysine-specific demethylase 1 (LSD1) in homeostasis and diseases. *J Biomed Sci, 28*(1), 41. doi:10.1186/s12929-021-00737-3

Kim, D., Nam, H. J., Lee, W., Yim, H. Y., Ahn, J. Y., Park, S. W., . . . Baek, S. H. (2018). PKCalpha-LSD1-NF-kappaB-Signaling Cascade Is Crucial for Epigenetic Control of the Inflammatory Response. *Mol Cell, 69*(3), 398-411 e396. doi:10.1016/j.molcel.2018.01.002

Kim, D., You, B., Jo, E. K., Han, S. K., Simon, M. I., & Lee, S. J. (2010). NADPH oxidase 2-derived reactive oxygen species in spinal cord microglia contribute to peripheral nerve injury-induced neuropathic pain. *Proc Natl Acad Sci U S A, 107*(33), 14851-14856. doi:10.1073/pnas.1009926107

Kim, H. Y., Park, C. K., Cho, I. H., Jung, S. J., Kim, J. S., & Oh, S. B. (2008). Differential Changes in TRPV1 expression after trigeminal sensory nerve injury. *J Pain, 9*(3), 280-288. doi:10.1016/j.jpain.2007.11.013

King, C. H., Lancaster, E., Salomon, D., Peles, E., & Scherer, S. S. (2014). Kv7.2 regulates the function of peripheral sensory neurons. *J Comp Neurol, 522*(14), 3262-3280. doi:10.1002/cne.23595

Klein, S. L., & Flanagan, K. L. (2016). Sex differences in immune responses. *Nat Rev Immunol, 16*(10), 626-638. doi:10.1038/nri.2016.90

Klimovich, P., Rubina, K., Sysoeva, V., & Semina, E. (2021). New Frontiers in Peripheral Nerve Regeneration: Concerns and Remedies. *Int J Mol Sci, 22*(24). doi:10.3390/ijms222413380

Korah, H. E., Cheng, K., Washington, S. M., Flowers, M. E., Stratton, H. J., Patwardhan, A., . . . Martin, L. F. (2022). Partial Sciatic Nerve Ligation: A Mouse Model of Chronic Neuropathic Pain to Study the Antinociceptive Effect of Novel Therapies. *J Vis Exp*(188). doi:10.3791/64555

Korb, E., Herre, M., Zucker-Scharff, I., Darnell, R. B., & Allis, C. D. (2015). BET protein Brd4 activates transcription in neurons and BET inhibitor Jq1 blocks memory in mice. *Nat Neurosci, 18*(10), 1464-1473. doi:10.1038/nn.4095

Korn, T., Magnus, T., & Jung, S. (2005). Autoantigen specific T cells inhibit glutamate uptake in astrocytes by decreasing expression of astrocytic glutamate transporter GLAST: a mechanism mediated by tumor necrosis factor-alpha. *FASEB J, 19*(13), 1878-1880. doi:10.1096/fj.05-3748fje

Kumar, V., Rayan, N. A., Muratani, M., Lim, S., Elanggovan, B., Xin, L., . . . Prabhakar, S. (2016). Comprehensive benchmarking reveals H2BK20 acetylation as a distinctive signature of

cell-state-specific enhancers and promoters. *Genome Res, 26*(5), 612-623. doi:10.1101/gr.201038.115

Kyzar, E. J., Bohnsack, J. P., Zhang, H., & Pandey, S. C. (2019). MicroRNA-137 Drives Epigenetic Reprogramming in the Adult Amygdala and Behavioral Changes after Adolescent Alcohol Exposure. *eNeuro, 6*(6). doi:10.1523/ENEURO.0401-19.2019

Lackington, W. A., Ryan, A. J., & O'Brien, F. J. (2017). Advances in Nerve Guidance Conduit-Based Therapeutics for Peripheral Nerve Repair. *ACS Biomater Sci Eng, 3*(7), 1221-1235. doi:10.1021/acsbiomaterials.6b00500

Latremoliere, A., & Woolf, C. J. (2009). Central Sensitization: A Generator of Pain Hypersensitivity by Central Neural Plasticity. *The Journal of Pain, 10*(9), 895-926. doi:10.1016/j.jpain.2009.06.012

Laumet, G., Garriga, J., Chen, S. R., Zhang, Y., Li, D. P., Smith, T. M., . . . Pan, H. L. (2015). G9a is essential for epigenetic silencing of K(+) channel genes in acute-to-chronic pain transition. *Nat Neurosci, 18*(12), 1746-1755. doi:10.1038/nn.4165

Laurent, B., Ruitu, L., Murn, J., Hempel, K., Ferrao, R., Xiang, Y., . . . Shi, Y. (2015). A specific LSD1/KDM1A isoform regulates neuronal differentiation through H3K9 demethylation. *Mol Cell, 57*(6), 957-970. doi:10.1016/j.molcel.2015.01.010

Lauterbach, M. A., Hanke, J. E., Serefidou, M., Mangan, M. S. J., Kolbe, C. C., Hess, T., . . . Latz, E. (2019). Toll-like Receptor Signaling Rewires Macrophage Metabolism and Promotes Histone Acetylation via ATP-Citrate Lyase. *Immunity, 51*(6), 997-1011 e1017. doi:10.1016/j.immuni.2019.11.009

Lee, M. B., Lee, J. H., Hong, S. H., You, J. S., Nam, S. T., Kim, H. W., . . . Choi, W. S. (2017). JQ1, a BET inhibitor, controls TLR4-induced IL-10 production in regulatory B cells by BRD4-NF-kappaB axis. *BMB Rep, 50*(12), 640-646. doi:10.5483/bmbrep.2017.50.12.194

Li, A., Pereira, C., Hill, E. E., Vukcevich, O., & Wang, A. (2022). In Vitro, In Vivo and Ex Vivo Models for Peripheral Nerve Injury and Regeneration. *Curr Neuropharmacol, 20*(2), 344-361. doi:10.2174/1570159X19666210407155543

Li, D., & Wu, M. (2021). Pattern recognition receptors in health and diseases. *Signal Transduct Target Ther, 6*(1), 291. doi:10.1038/s41392-021-00687-0

Li, R., Li, D. H., Zhang, H. Y., Wang, J., Li, X. K., & Xiao, J. (2020). Growth factors-based therapeutic strategies and their underlying signaling mechanisms for peripheral nerve

regeneration. *Acta Pharmacol Sin, 41*(10), 1289-1300. doi:10.1038/s41401-019-0338-1

Lien, B. V., Brown, N. J., Ransom, S. C., Lehrich, B. M., Shahrestani, S., Tafreshi, A. R., . . . Sahyouni, R. (2020). Enhancing peripheral nerve regeneration with neurotrophic factors and bioengineered scaffolds: A basic science and clinical perspective. *J Peripher Nerv Syst, 25*(4), 320-334. doi:10.1111/jns.12414

Lindia, J. A., Kohler, M. G., Martin, W. J., & Abbadie, C. (2005). Relationship between sodium channel NaV1.3 expression and neuropathic pain behavior in rats. *Pain, 117*(1-2), 145-153. doi:10.1016/j.pain.2005.05.027

Lis-Lopez, L., Bauset, C., Seco-Cervera, M., & Cosin-Roger, J. (2021). Is the Macrophage Phenotype Determinant for Fibrosis Development? *Biomedicines, 9*(12). doi:10.3390/biomedicines9121747

Liu, L., Yang, C., & Candelario-Jalil, E. (2021). Role of BET Proteins in Inflammation and CNS Diseases. *Front Mol Biosci, 8*, 748449. doi:10.3389/fmolb.2021.748449

Lopes, B., Coelho, A., Alvites, R., Sousa, A. C., Sousa, P., Moreira, A., . . . Mauricio, A. C. (2023). Animal models in peripheral nerve transection studies: a systematic review on study design and outcomes assessment. *Regen Med*. doi:10.2217/rme-2023-0102

López-Álvarez, V. M. (2017). *Activity-dependent treatments for neuropathic pain.* Autonomous Univerity of Barcelona,

Lowery, L. A., & Van Vactor, D. (2009). The trip of the tip: understanding the growth cone machinery. *Nat Rev Mol Cell Biol, 10*(5), 332-343. doi:10.1038/nrm2679

Lunyak, V. V., Burgess, R., Prefontaine, G. G., Nelson, C., Sze, S. H., Chenoweth, J., . . . Rosenfeld, M. G. (2002). Corepressor-dependent silencing of chromosomal regions encoding neuronal genes. *Science, 298*(5599), 1747-1752. doi:10.1126/science.1076469

M. R. Wells, S. P. Racis, & Vaidya, U. (1992). Changes in plasma cytokines associated with peripheral

nerve injury. *Journal of Neuroimmunology,, 39*, 261-268.

Ma, W., & Quirion, R. (2008). Does COX2-dependent PGE2 play a role in neuropathic pain? *Neurosci Lett, 437*(3), 165-169. doi:10.1016/j.neulet.2008.02.072

Maes, T., Mascaro, C., Rotllant, D., Lufino, M. M. P., Estiarte, A., Guibourt, N., . . . Buesa Arjol, C. (2020). Modulation of KDM1A with vafidemstat rescues memory deficit and behavioral alterations. *PLoS One, 15*(5), e0233468. doi:10.1371/journal.pone.0233468

Maiques-Diaz, A., & Somervaille, T. C. (2016). LSD1: biologic roles and therapeutic targeting. *Epigenomics, 8*(8), 1103-1116. doi:10.2217/epi-2016-0009

Mansfield, R. E., Musselman, C. A., Kwan, A. H., Oliver, S. S., Garske, A. L., Davrazou, F., . . . Mackay, J. P. (2011). Plant homeodomain (PHD) fingers of CHD4 are histone H3-binding modules with preference for unmodified H3K4 and methylated H3K9. *J Biol Chem, 286*(13), 11779-11791. doi:10.1074/jbc.M110.208207

Marmiroli, P., Riva, B., Pozzi, E., Ballarini, E., Lim, D., Chiorazzi, A., . . . Carozzi, V. A. (2017). Susceptibility of different mouse strains to oxaliplatin peripheral neurotoxicity: Phenotypic and genotypic insights. *PLoS One, 12*(10), e0186250. doi:10.1371/journal.pone.0186250

Martinez-Gamero, C., Malla, S., & Aguilo, F. (2021). LSD1: Expanding Functions in Stem Cells and Differentiation. *Cells, 10*(11). doi:10.3390/cells10113252

Martinez de Toda, I., Gonzalez-Sanchez, M., Diaz-Del Cerro, E., Valera, G., Carracedo, J., & Guerra-Perez, N. (2023). Sex differences in markers of oxidation and inflammation. Implications for ageing. *Mech Ageing Dev, 211*, 111797. doi:10.1016/j.mad.2023.111797

Martini, R., Fischer, S., Lopez-Vales, R., & David, S. (2008). Interactions between Schwann cells and macrophages in injury and inherited demyelinating disease. *Glia, 56*(14), 1566-1577. doi:10.1002/glia.20766

Matuszewska, M., Cieslik, M., Wilkaniec, A., Strawski, M., & Czapski, G. A. (2022). The Role of Bromodomain and Extraterminal (BET) Proteins in Controlling the Phagocytic Activity of Microglia In Vitro: Relevance to Alzheimer's Disease. *Int J Mol Sci, 24*(1). doi:10.3390/ijms24010013

Meng, J., Zhang, Q., Yang, C., Xiao, L., Xue, Z., & Zhu, J. (2019). Duloxetine, a Balanced Serotonin-Norepinephrine Reuptake Inhibitor, Improves Painful Chemotherapy-Induced Peripheral Neuropathy by Inhibiting Activation of p38 MAPK and NF-kappaB. *Front Pharmacol, 10*, 365. doi:10.3389/fphar.2019.00365

Meng, S., Zhang, L., Tang, Y., Tu, Q., Zheng, L., Yu, L., . . . Chen, J. (2014). BET Inhibitor JQ1 Blocks Inflammation and Bone Destruction. *J Dent Res, 93*(7), 657-662. doi:10.1177/0022034514534261

Menorca, R. M., Fussell, T. S., & Elfar, J. C. (2013). Nerve physiology: mechanisms of injury and recovery. *Hand Clin, 29*(3), 317-330. doi:10.1016/j.hcl.2013.04.002

Metwally, E., Zhao, G., & Zhang, Y. Q. (2021). The calcium-dependent protease calpain in neuronal remodeling and neurodegeneration. *Trends Neurosci, 44*(9), 741-752. doi:10.1016/j.tins.2021.07.003

Michaelevski, I., Segal-Ruder, Y., Rozenbaum, M., Medzihradszky, K. F., Shalem, O., Coppola, G., . . . Fainzilber, M. (2010). Signaling to transcription networks in the neuronal retrograde injury response. *Sci Signal, 3*(130), ra53. doi:10.1126/scisignal.2000952

Micucci, J. A., Sperry, E. D., & Martin, D. M. (2015). Chromodomain helicase DNA-binding proteins in stem cells and human developmental diseases. *Stem Cells Dev, 24*(8), 917-926. doi:10.1089/scd.2014.0544

Milligan, E. D., Penzkover, K. R., Soderquist, R. G., & Mahoney, M. J. (2012). Spinal interleukin-10 therapy to treat peripheral neuropathic pain. *Neuromodulation, 15*(6), 520-526; discussion 526. doi:10.1111/j.1525-1403.2012.00462.x

Mills, C. D., Kincaid, K., Alt, J. M., Heilman, M. J., & Hill, A. M. (2000). M-1/M-2 macrophages and the Th1/Th2 paradigm. *J Immunol, 164*(12), 6166-6173. doi:10.4049/jimmunol.164.12.6166

Minett, M. S., Falk, S., Santana-Varela, S., Bogdanov, Y. D., Nassar, M. A., Heegaard, A. M., & Wood, J. N. (2014). Pain without nociceptors? Nav1.7-independent pain mechanisms. *Cell Rep, 6*(2), 301-312. doi:10.1016/j.celrep.2013.12.033

Miotto, K., Cho, A. K., Khalil, M. A., Blanco, K., Sasaki, J. D., & Rawson, R. (2017). Trends in Tramadol: Pharmacology, Metabolism, and Misuse. *Anesth Analg, 124*(1), 44-51. doi:10.1213/ANE.0000000000001683

Molero, Y., Larsson, H., D'Onofrio, B. M., Sharp, D. J., & Fazel, S. (2019). Associations between gabapentinoids and suicidal behaviour, unintentional overdoses, injuries, road traffic incidents, and violent crime: population based cohort study in Sweden. *BMJ, 365*, l2147. doi:10.1136/bmj.l2147

Morgado-Pascual, J. L., Rayego-Mateos, S., Tejedor, L., Suarez-Alvarez, B., & Ruiz-Ortega, M. (2019). Bromodomain and Extraterminal Proteins as Novel Epigenetic Targets for Renal Diseases. *Front Pharmacol, 10*, 1315. doi:10.3389/fphar.2019.01315

Morii, H., Shiraishi-Yamaguchi, Y., & Mori, N. (2006). SCG10, a microtubule destabilizing factor, stimulates the neurite outgrowth by modulating microtubule dynamics in rat hippocampal primary cultured neurons. *J Neurobiol, 66*(10), 1101-1114. doi:10.1002/neu.20295

Morris, R., Kershaw, N. J., & Babon, J. J. (2018). The molecular details of cytokine signaling via the JAK/STAT pathway. *Protein Sci, 27*(12), 1984-2009. doi:10.1002/pro.3519

Msheik, Z., El Massry, M., Rovini, A., Billet, F., & Desmouliere, A. (2022). The macrophage: a key player in the pathophysiology of peripheral neuropathies. *J Neuroinflammation, 19*(1), 97. doi:10.1186/s12974-022-02454-6

Mueller, M., Leonhard, C., Wacker, K., Ringelstein, E. B., Okabe, M., Hickey, W. F., & Kiefer, R. (2003). Macrophage response to peripheral nerve injury: the quantitative contribution of resident and hematogenous macrophages. *Lab Invest, 83*(2), 175-185. doi:10.1097/01.lab.0000056993.28149.bf

Muheremu, A., & Ao, Q. (2015). Past, Present, and Future of Nerve Conduits in the Treatment of Peripheral Nerve Injury. *Biomed Res Int, 2015*, 237507. doi:10.1155/2015/237507

Murphy, M. P. (1999). Nitric oxide and cell death. *Biochimica et Biophysica Acta (BBA) - Bioenergetics*, 401–414. doi:doi:10.1016/s0005-2728(99)00029-8

Murray, P. J., Allen, J. E., Biswas, S. K., Fisher, E. A., Gilroy, D. W., Goerdt, S., . . . Wynn, T. A. (2014). Macrophage activation and polarization: nomenclature and experimental guidelines. *Immunity, 41*(1), 14-20. doi:10.1016/j.immuni.2014.06.008

Naoi, M., Maruyama, W., Akao, Y., Yi, H., & Yamaoka, Y. (2006). Involvement of type A monoamine oxidase in neurodegeneration: regulation of mitochondrial signaling leading to cell death or neuroprotection. *J Neural Transm Suppl*(71), 67-77. doi:10.1007/978-3-211-33328-0_8

Nassar, M. A., Baker, M. D., Levato, A., Ingram, R., Mallucci, G., McMahon, S. B., & Wood, J. N. (2006). Nerve injury induces robust allodynia and ectopic discharges in Nav1.3 null mutant mice. *Mol Pain, 2*, 33. doi:10.1186/1744-8069-2-33

Nassar, M. A., Levato, A., Stirling, L. C., & Wood, J. N. (2005). Neuropathic pain develops normally in mice lacking both Na(v)1.7 and Na(v)1.8. *Mol Pain, 1*, 24. doi:10.1186/1744-8069-1-24

Navarro, X. (2016). Functional evaluation of peripheral nerve regeneration and target reinnervation in animal models: a critical overview. *Eur J Neurosci, 43*(3), 271-286. doi:10.1111/ejn.13033

Navarro, X., Geuna, S., Grothe, C., & Haastert-Talini, K. (2018). Introduction: Thematic Papers Issue on Peripheral Nerve Regeneration and Repair. *Anat Rec (Hoboken), 301*(10), 1614-1617. doi:10.1002/ar.23941

Navarro, X., Verdu, E., & Buti, M. (1994). Comparison of regenerative and reinnervating capabilities of different functional types of nerve fibers. *Exp Neurol, 129*(2), 217-224. doi:10.1006/exnr.1994.1163

Navarro, X., Vivo, M., & Valero-Cabre, A. (2007). Neural plasticity after peripheral nerve injury and regeneration. *Prog Neurobiol, 82*(4), 163-201. doi:10.1016/j.pneurobio.2007.06.005

Nepali, K., & Liou, J. P. (2021). Recent developments in epigenetic cancer therapeutics: clinical advancement and emerging trends. *J Biomed Sci, 28*(1), 27. doi:10.1186/s12929-021-00721-x

Nicodeme, E., Jeffrey, K. L., Schaefer, U., Beinke, S., Dewell, S., Chung, C. W., . . . Tarakhovsky, A. (2010). Suppression of inflammation by a synthetic histone mimic. *Nature, 468*(7327), 1119-1123. doi:10.1038/nature09589

Ninova, M., Fejes Toth, K., & Aravin, A. A. (2019). The control of gene expression and cell identity by H3K9 trimethylation. *Development, 146*(19). doi:10.1242/dev.181180

Nita, A., Muto, Y., Katayama, Y., Matsumoto, A., Nishiyama, M., & Nakayama, K. I. (2021). The autism-related protein CHD8 contributes to the stemness and differentiation of mouse hematopoietic stem cells. *Cell Rep, 34*(5), 108688. doi:10.1016/j.celrep.2021.108688

Nitarska, J., Smith, J. G., Sherlock, W. T., Hillege, M. M., Nott, A., Barshop, W. D., . . . Riccio, A. (2016). A Functional Switch of NuRD Chromatin Remodeling Complex Subunits Regulates Mouse Cortical Development. *Cell Rep, 17*(6), 1683-1698. doi:10.1016/j.celrep.2016.10.022

Noguchi, K. (2006). Chapter 20 Central sensitization following nerve injury: molecular mechanisms. *Handb Clin Neurol, 81*, 277-291. doi:10.1016/S0072-9752(06)80024-2

Okada, M., Kawagoe, Y., Sato, Y., Nozumi, M., Ishikawa, Y., Tamada, A., . . . Igarashi, M. (2021). Phosphorylation of GAP-43 T172 is a molecular marker of growing axons in a wide range of mammals including primates. *Mol Brain, 14*(1), 66. doi:10.1186/s13041-021-00755-0

Okutani, H., Yamanaka, H., Kobayashi, K., Okubo, M., & Noguchi, K. (2018). Recombinant interleukin-4 alleviates mechanical allodynia via injury-induced interleukin-4 receptor alpha in spinal microglia in a rat model of neuropathic pain. *Glia, 66*(8), 1775-1787. doi:10.1002/glia.23340

Ou, X. M., Chen, K., & Shih, J. C. (2006). Monoamine oxidase A and repressor R1 are involved in apoptotic signaling pathway. *Proc Natl Acad Sci U S A, 103*(29), 10923-10928. doi:10.1073/pnas.0601515103

Padeken, J., Methot, S. P., & Gasser, S. M. (2022). Establishment of H3K9-methylated heterochromatin and its functions in tissue differentiation and maintenance. *Nat Rev Mol Cell Biol, 23*(9), 623-640. doi:10.1038/s41580-022-00483-w

Palomes-Borrajo, G., Navarro, X., & Penas, C. (2022). BET protein inhibition in macrophages enhances dorsal root ganglion neurite outgrowth in female mice. *J Neurosci Res, 100*(6), 1331-1346. doi:10.1002/jnr.25036

Pan, D., Schellhardt, L., Acevedo-Cintron, J. A., Hunter, D., Snyder-Warwick, A. K., Mackinnon, S. E., & Wood, M. D. (2022). IL-4 expressing cells are recruited to nerve after injury and promote regeneration. *Exp Neurol, 347*, 113909. doi:10.1016/j.expneurol.2021.113909

Papalampropoulou-Tsiridou, M., Labrecque, S., Godin, A. G., De Koninck, Y., & Wang, F. (2020). Differential Expression of Acid - Sensing Ion Channels in Mouse Primary Afferents in Naive and Injured Conditions. *Front Cell Neurosci, 14*, 103. doi:10.3389/fncel.2020.00103

Patodia, S., & Raivich, G. (2012). Role of transcription factors in peripheral nerve regeneration. *Front Mol Neurosci, 5*, 8. doi:10.3389/fnmol.2012.00008

Penas, C., & Navarro, X. (2018). Epigenetic Modifications Associated to Neuroinflammation and Neuropathic Pain After Neural Trauma. *Front Cell Neurosci, 12*, 158. doi:10.3389/fncel.2018.00158

Perillo, B., Tramontano, A., Pezone, A., & Migliaccio, A. (2020). LSD1: more than demethylation of histone lysine residues. *Exp Mol Med, 52*(12), 1936-1947. doi:10.1038/s12276-020-00542-2

Perrin, F. E., Lacroix, S., Aviles-Trigueros, M., & David, S. (2005). Involvement of monocyte chemoattractant protein-1, macrophage inflammatory protein-1alpha and interleukin-1beta in Wallerian degeneration. *Brain, 128*(Pt 4), 854-866. doi:10.1093/brain/awh407

Poirot, O., Berta, T., Decosterd, I., & Kellenberger, S. (2006). Distinct ASIC currents are expressed in rat putative nociceptors and are modulated by nerve injury. *J Physiol, 576*(Pt 1), 215-234. doi:10.1113/jphysiol.2006.113035

Presto, P., Mazzitelli, M., Junell, R., Griffin, Z., & Neugebauer, V. (2022). Sex differences in pain along the neuraxis. *Neuropharmacology, 210*, 109030. doi:10.1016/j.neuropharm.2022.109030

Puttagunta, R., Tedeschi, A., Soria, M. G., Hervera, A., Lindner, R., Rathore, K. I., . . . Di Giovanni, S. (2014). PCAF-dependent epigenetic changes promote axonal regeneration in the central nervous system. *Nat Commun, 5*, 3527. doi:10.1038/ncomms4527

Rahman, S., Sowa, M. E., Ottinger, M., Smith, J. A., Shi, Y., Harper, J. W., & Howley, P. M. (2011). The Brd4 extraterminal domain confers transcription activation independent of pTEFb by recruiting multiple proteins, including NSD3. *Mol Cell Biol, 31*(13), 2641-2652. doi:10.1128/MCB.01341-10

Raivich, G., & Makwana, M. (2007). The making of successful axonal regeneration: genes, molecules and signal transduction pathways. *Brain Res Rev, 53*(2), 287-311. doi:10.1016/j.brainresrev.2006.09.005

Ramirez, D., Zuniga, R., Concha, G., & Zuniga, L. (2018). HCN Channels: New Therapeutic Targets for Pain Treatment. *Molecules, 23*(9). doi:10.3390/molecules23092094

Rivers, A., Vaitkus, K., Ruiz, M. A., Ibanez, V., Jagadeeswaran, R., Kouznetsova, T., . . . Lavelle, D. (2015). RN-1, a potent and selective lysine-specific demethylase 1 inhibitor, increases gamma-globin expression, F reticulocytes, and F cells in a sickle cell disease mouse model. *Exp Hematol, 43*(7), 546-553 e541-543. doi:10.1016/j.exphem.2015.04.005

Ronchi, G., Morano, M., Fregnan, F., Pugliese, P., Crosio, A., Tos, P., . . . Gambarotta, G. (2019). The Median Nerve Injury Model in Pre-clinical Research - A Critical Review on Benefits and Limitations. *Front Cell Neurosci, 13*, 288. doi:10.3389/fncel.2019.00288

Rotshenker, S. (2011). Wallerian degeneration: the innate-immune response to traumatic nerve injury. *J Neuroinflammation, 8*, 109. doi:10.1186/1742-2094-8-109

Ruiz, L., Liedgens, H., & Obradovic, M. (2013). Cost of Illness of Neuropathic Pain in Spain in 2012 from a Societal Perspective. *Value in Health, 16*(7). doi:10.1016/j.jval.2013.08.336

Rusconi, F., Grillo, B., Toffolo, E., Mattevi, A., & Battaglioli, E. (2017). NeuroLSD1: Splicing-Generated Epigenetic Enhancer of Neuroplasticity. *Trends Neurosci, 40*(1), 28-38. doi:10.1016/j.tins.2016.11.002

Saccani, S., Pantano, S., & Natoli, G. (2001). Two waves of nuclear factor kappaB recruitment to target promoters. *J Exp Med, 193*(12), 1351-1359. doi:10.1084/jem.193.12.1351

Sagarkar, S., Choudhary, A. G., Balasubramanian, N., Awathale, S. N., Somalwar, A. R., Pawar, N., . . . Sakharkar, A. J. (2021). LSD1-BDNF activity in lateral hypothalamus-medial forebrain bundle area is essential for reward seeking behavior. *Prog Neurobiol, 202*, 102048. doi:10.1016/j.pneurobio.2021.102048

Salonen, V., Aho, H., Roytta, M., & Peltonen, J. (1988). Quantitation of Schwann cells and endoneurial fibroblast-like cells after experimental nerve trauma. *Acta Neuropathologica, 75*, 331-338. doi: 10.1007/BF00687785

Sanchez-Huertas, C., & Herrera, E. (2021). With the Permission of Microtubules: An Updated Overview on Microtubule Function During Axon Pathfinding. *Front Mol Neurosci, 14*, 759404. doi:10.3389/fnmol.2021.759404

Sanchez-Ventura, J., Amo-Aparicio, J., Navarro, X., & Penas, C. (2019). BET protein inhibition regulates cytokine production and promotes neuroprotection after spinal cord injury. *J Neuroinflammation, 16*(1), 124. doi:10.1186/s12974-019-1511-7

Sans-Fons, M. G., Yeramian, A., Pereira-Lopes, S., Santamaria-Babi, L. F., Modolell, M., Lloberas, J., & Celada, A. (2013). Arginine transport is impaired in C57Bl/6 mouse macrophages as a result of a deletion in the promoter of Slc7a2 (CAT2), and susceptibility to Leishmania infection is reduced. *J Infect Dis, 207*(11), 1684-1693. doi:10.1093/infdis/jit084

Sartor, G. C., Malvezzi, A. M., Kumar, A., Andrade, N. S., Wiedner, H. J., Vilca, S. J., . . . Wahlestedt, C. (2019). Enhancement of BDNF Expression and Memory by HDAC Inhibition Requires BET Bromodomain Reader Proteins. *J Neurosci, 39*(4), 612-626. doi:10.1523/JNEUROSCI.1604-18.2018

Schafers, M., & Sorkin, L. (2008). Effect of cytokines on neuronal excitability. *Neurosci Lett, 437*(3), 188-193. doi:10.1016/j.neulet.2008.03.052

Scotece, M., & Conde-Aranda, J. (2022). Inflammation in Health and Disease: New Insights and Therapeutic Avenues. *Int J Mol Sci, 23*(15). doi:10.3390/ijms23158392

Seddon. (1942). A Classification of Nerve Injuries. *British Medical Journal (BMJ), 2*, 237–239. doi:10.1136/bmj.2.4260.237

Shen, C., Ipsaro, J. J., Shi, J., Milazzo, J. P., Wang, E., Roe, J. S., . . . Vakoc, C. R. (2015). NSD3-Short Is an Adaptor Protein that Couples BRD4 to the CHD8 Chromatin Remodeler. *Mol Cell, 60*(6), 847-859. doi:10.1016/j.molcel.2015.10.033

Shields, S. D., Deng, L., Reese, R. M., Dourado, M., Tao, J., Foreman, O., . . . Hackos, D. H. (2018). Insensitivity to Pain upon Adult-Onset Deletion of Nav1.7 or Its Blockade with Selective Inhibitors. *J Neurosci, 38*(47), 10180-10201. doi:10.1523/JNEUROSCI.1049-18.2018

Shin, J. E., Geisler, S., & DiAntonio, A. (2014). Dynamic regulation of SCG10 in regenerating axons after injury. *Exp Neurol, 252*, 1-11. doi:10.1016/j.expneurol.2013.11.007

Shorstova, T., Foulkes, W. D., & Witcher, M. (2021). Achieving clinical success with BET inhibitors as anti-cancer agents. *Br J Cancer, 124*(9), 1478-1490. doi:10.1038/s41416-021-01321-0

Singh, M. B., Babigian, C. J., & Sartor, G. C. (2022). Domain-selective BET inhibition attenuates transcriptional and behavioral responses to cocaine. *Neuropharmacology, 210*, 109040. doi:10.1016/j.neuropharm.2022.109040

Siqueira Mietto, B., Kroner, A., Girolami, E. I., Santos-Nogueira, E., Zhang, J., & David, S. (2015). Role of IL-10 in Resolution of Inflammation and Functional Recovery after Peripheral Nerve Injury. *J Neurosci, 35*(50), 16431-16442. doi:10.1523/JNEUROSCI.2119-15.2015

Sitcheran, R., Gupta, P., Fisher, P. B., & Baldwin, A. S. (2005). Positive and negative regulation of EAAT2 by NF-kappaB: a role for N-myc in TNFalpha-controlled repression. *EMBO J, 24*(3), 510-520. doi:10.1038/sj.emboj.7600555

Smith, J. C. (2019). A Review of Strain and Sex Differences in Response to Pain and Analgesia in Mice. *Comp Med, 69*(6), 490-500. doi:10.30802/AALAS-CM-19-000066

Smith, P. A. (2020). K(+) Channels in Primary Afferents and Their Role in Nerve Injury-Induced Pain. *Front Cell Neurosci, 14*, 566418. doi:10.3389/fncel.2020.566418

Sobczak, M., Strachowska, M., Gronkowska, K., Karwaciak, I., Pulaski, L., & Robaszkiewicz, A. (2021). LSD1 Facilitates Pro-Inflammatory Polarization of Macrophages by Repressing Catalase. *Cells, 10*(9). doi:10.3390/cells10092465

Sorge, R. E., Mapplebeck, J. C., Rosen, S., Beggs, S., Taves, S., Alexander, J. K., . . . Mogil, J. S. (2015). Different immune cells mediate mechanical pain hypersensitivity in male and female mice. *Nat Neurosci, 18*(8), 1081-1083. doi:10.1038/nn.4053

Sousa, A. M., Lages, G. V., Pereira, C. L., & Slullitel, A. (2016). Experimental models for the study of neuropathic pain. *Revista Dor, 17*. doi:10.5935/1806-0013.20160043

Stein. M, Keshav. S, Harris. N, & Gordon. S. (1992). Interleukin 4 potently enhances murine macrophage mannose receptor activity: a marker of alternative immunologic macrophage activation. *Journal of Experimental Medicine, 176*, 287–292. . doi:doi:10.1084/jem.176.1.287

Stoll, G., Griffin, J. W., Li, C. Y., & Trapp, B. D. (1989). Wallerian degeneration in the peripheral nervous system: participation of both Schwann cells and macrophages in myelin degradation. *J Neurocytol, 18*(5), 671-683. doi:10.1007/BF01187086

Stucky, C. L., Dubin, A. E., Jeske, N. A., Malin, S. A., McKemy, D. D., & Story, G. M. (2009). Roles of transient receptor potential channels in pain. *Brain Res Rev, 60*(1), 2-23. doi:10.1016/j.brainresrev.2008.12.018

Sullivan, J. M., Badimon, A., Schaefer, U., Ayata, P., Gray, J., Chung, C. W., . . . Schaefer, A. (2015). Autism-like syndrome is induced by pharmacological suppression of BET proteins in young mice. *J Exp Med, 212*(11), 1771-1781. doi:10.1084/jem.20151271

Sullivan, K. E., Reddy, A. B., Dietzmann, K., Suriano, A. R., Kocieda, V. P., Stewart, M., & Bhatia, M. (2007). Epigenetic regulation of tumor necrosis factor alpha. *Mol Cell Biol, 27*(14), 5147-5160. doi:10.1128/MCB.02429-06

Sun, T., Yu, E., Yu, L., Luo, J., Li, H., & Fu, Z. (2012). LipoxinA(4) induced antinociception and decreased expression of NF-kappaB and pro-inflammatory cytokines after chronic dorsal root ganglia compression in rats. *Eur J Pain, 16*(1), 18-27. doi:10.1016/j.ejpain.2011.05.005

Sun, Z., Zhang, Y., Jia, J., Fang, Y., Tang, Y., Wu, H., & Fang, D. (2020). H3K36me3, message from chromatin to DNA damage repair. *Cell Biosci, 10*, 9. doi:10.1186/s13578-020-0374-z

Sunderland. (1951). A classification of peripheral nerve injuries producing loss of function. *Brain, 74*(4), 491-516. doi:10.1093/brain/74.4.491

Takahashi, K., Yi, H., Liu, C. H., Liu, S., Kashiwagi, Y., Patin, D. J., & Hao, S. (2018). Spinal bromodomain-containing protein 4 contributes to neuropathic pain induced by HIV glycoprotein 120 with morphine in rats. *Neuroreport, 29*(6), 441-446. doi:10.1097/WNR.0000000000000992

Taylor, G. C., Eskeland, R., Hekimoglu-Balkan, B., Pradeepa, M. M., & Bickmore, W. A. (2013). H4K16 acetylation marks active genes and enhancers of embryonic stem cells, but does not alter chromatin compaction. *Genome Res, 23*(12), 2053-2065. doi:10.1101/gr.155028.113

Tiscornia, G., Singer, O., Ikawa, M., & Verma, I. M. (2003). A general method for gene knockdown in mice by using lentiviral vectors expressing small interfering RNA. *Proc Natl Acad Sci U S A, 100*(4), 1844-1848. doi:10.1073/pnas.0437912100

Toffolo, E., Rusconi, F., Paganini, L., Tortorici, M., Pilotto, S., Heise, C., . . . Battaglioli, E. (2014). Phosphorylation of neuronal Lysine-Specific Demethylase 1LSD1/KDM1A impairs transcriptional repression by regulating interaction with CoREST and histone deacetylases HDAC1/2. *J Neurochem, 128*(5), 603-616. doi:10.1111/jnc.12457

Torrance, N., Smith, B. H., Bennett, M. I., & Lee, A. J. (2006). The epidemiology of chronic pain of predominantly neuropathic origin. Results from a general population survey. *J Pain, 7*(4), 281-289. doi:10.1016/j.jpain.2005.11.008

Torres-Espin, A., Santos, D., Gonzalez-Perez, F., del Valle, J., & Navarro, X. (2014). Neurite-J: an image-J plug-in for axonal growth analysis in organotypic cultures. *J Neurosci Methods, 236*, 26-39. doi:10.1016/j.jneumeth.2014.08.005

Toth, C. (2013). Peripheral and central sensitization. In *Neuropathic Pain* (pp. 51-64).

Toyoda, H., Zhao, M. G., Ulzhofer, B., Wu, L. J., Xu, H., Seeburg, P. H., . . . Zhuo, M. (2009). Roles of the AMPA receptor subunit GluA1 but not GluA2 in synaptic potentiation and activation of ERK in the anterior cingulate cortex. *Mol Pain, 5*, 46. doi:10.1186/1744-8069-5-46

Tsai, M. C., Manor, O., Wan, Y., Mosammaparast, N., Wang, J. K., Lan, F., . . . Chang, H. Y. (2010). Long noncoding RNA as modular scaffold of histone modification complexes. *Science, 329*(5992), 689-693. doi:10.1126/science.1192002

Tsutsumi, T., Iwao, K., Hayashi, H., Kirihara, T., Kawaji, T., Inoue, T., . . . Tanihara, H. (2016). Potential Neuroprotective Effects of an LSD1 Inhibitor in Retinal Ganglion Cells via p38 MAPK Activity. *Invest Ophthalmol Vis Sci, 57*(14), 6461-6473. doi:10.1167/iovs.16-19494

Uceyler, N., Tscharke, A., & Sommer, C. (2007). Early cytokine expression in mouse sciatic nerve after chronic constriction nerve injury depends on calpain. *Brain Behav Immun, 21*(5), 553-560. doi:10.1016/j.bbi.2006.10.003

Uchida, H., Ma, L., & Ueda, H. (2010). Epigenetic gene silencing underlies C-fiber dysfunctions in neuropathic pain. *J Neurosci, 30*(13), 4806-4814. doi:10.1523/JNEUROSCI.5541-09.2010

Uchida, H., Sasaki, K., Ma, L., & Ueda, H. (2010). Neuron-restrictive silencer factor causes epigenetic silencing of Kv4.3 gene after peripheral nerve injury. *Neuroscience, 166*(1), 1-4. doi:10.1016/j.neuroscience.2009.12.021

Vacca, V., Marinelli, S., Pieroni, L., Urbani, A., Luvisetto, S., & Pavone, F. (2014). Higher pain perception and lack of recovery from neuropathic pain in females: a behavioural, immunohistochemical, and proteomic investigation on sex-related differences in mice. *Pain, 155*(2), 388-402. doi:10.1016/j.pain.2013.10.027

Van Broeckhoven, J., Erens, C., Sommer, D., Scheijen, E., Sanchez, S., Vidal, P. M., . . . Lemmens, S. (2022). Macrophage-based delivery of interleukin-13 improves functional and histopathological outcomes following spinal cord injury. *J Neuroinflammation, 19*(1), 102. doi:10.1186/s12974-022-02458-2

Vangeel, L., & Voets, T. (2019). Transient Receptor Potential Channels and Calcium Signaling. *Cold Spring Harb Perspect Biol, 11*(6). doi:10.1101/cshperspect.a035048

Vasavda, C., Xu, R., Liew, J., Kothari, R., Dhindsa, R. S., Semenza, E. R., . . . Snyder, S. H. (2022). Identification of the NRF2 transcriptional network as a therapeutic target for trigeminal neuropathic pain. *Sci Adv, 8*(31), eabo5633. doi:10.1126/sciadv.abo5633

Vidal, P. M., Lemmens, E., Dooley, D., & Hendrix, S. (2013). The role of "anti-inflammatory" cytokines in axon regeneration. *Cytokine Growth Factor Rev, 24*(1), 1-12. doi:10.1016/j.cytogfr.2012.08.008

Wagner, R., & Myers, R. R. (1996). Endoneurial injection of TNF-alpha produces neuropathic pain behaviors. *Neuroreport, 7*(18), 2897-2901. doi:10.1097/00001756-199611250-00018

Wahane, S., Halawani, D., Zhou, X., & Zou, H. (2019). Epigenetic Regulation Of Axon Regeneration and Glial Activation in Injury Responses. *Front Genet, 10*, 640. doi:10.3389/fgene.2019.00640

Wale Sulaiman, & Gordon, T. (2013). Neurobiology of Peripheral Nerve Injury, Regeneration,

and Functional Recovery: From Bench Top Research to

Bedside Application. *The Ochsner Journal, 13*, 100-108.

Wang, B. B., Guo, C., Sun, S. Q., Zhang, X. N., Li, Z., Li, W. J., . . . Liu, S. (2023). Comparison of the Nerve Regeneration Capacity and Characteristics between Sciatic Nerve Crush and Transection Injury Models in Rats. *Biomed Environ Sci, 36*(2), 160-173. doi:10.3967/bes2023.001

Wang, J., Telese, F., Tan, Y., Li, W., Jin, C., He, X., . . . Rosenfeld, M. G. (2015). LSD1n is an H4K20 demethylase regulating memory formation via transcriptional elongation control. *Nat Neurosci, 18*(9), 1256-1264. doi:10.1038/nn.4069

Wang, K., Yang, C., Li, H., Liu, X., Zheng, M., Xuan, Z., . . . Wang, H. (2022). Role of the Epigenetic Modifier JMJD6 in Tumor Development and Regulation of Immune Response. *Front Immunol, 13*, 859893. doi:10.3389/fimmu.2022.859893

Wang, N., Wu, R., Tang, D., & Kang, R. (2021). The BET family in immunity and disease. *Signal Transduct Target Ther, 6*(1), 23. doi:10.1038/s41392-020-00384-4

Wang, Z., Zang, C., Rosenfeld, J. A., Schones, D. E., Barski, A., Cuddapah, S., . . . Zhao, K. (2008). Combinatorial patterns of histone acetylations and methylations in the human genome. *Nat Genet, 40*(7), 897-903. doi:10.1038/ng.154

Wilson, S. G., Smith, S. B., Chesler, E. J., Melton, K. A., Haas, J. J., Mitton, B., . . . Mogil, J. S. (2003). The heritability of antinociception: common pharmacogenetic mediation of five neurochemically distinct analgesics. *J Pharmacol Exp Ther, 304*(2), 547-559. doi:10.1124/jpet.102.041889

Witzel, C., Rohde, C., & Brushart, T. M. (2005). Pathway sampling by regenerating peripheral axons. *J Comp Neurol, 485*(3), 183-190. doi:10.1002/cne.20436

Wolf, G., Gabay, E., Tal, M., Yirmiya, R., & Shavit, Y. (2006). Genetic impairment of interleukin-1 signaling attenuates neuropathic pain, autotomy, and spontaneous ectopic neuronal activity, following nerve injury in mice. *Pain, 120*(3), 315-324. doi:10.1016/j.pain.2005.11.011

Wolff, M., Czorlich, P., Nagaraj, C., Schnobel-Ehehalt, R., Li, Y., Kwapiszewska, G., . . . Olschewski, A. (2016). Amitriptyline and carbamazepine utilize voltage-gated ion channel suppression to impair excitability of sensory dorsal horn neurons in thin tissue slice: An in vitro study. *Neurosci Res, 109*, 16-27. doi:10.1016/j.neures.2016.02.006

Wong, C. P., Magnusson, K. R., & Ho, E. (2013). Increased inflammatory response in aged mice is associated with age-related zinc deficiency and zinc transporter dysregulation. *J Nutr Biochem, 24*(1), 353-359. doi:10.1016/j.jnutbio.2012.07.005

Wu, C., Li, A., Hu, J., & Kang, J. (2019). Histone deacetylase 2 is essential for LPS-induced inflammatory responses in macrophages. *Immunol Cell Biol, 97*(1), 72-84. doi:10.1111/imcb.12203

Xiang, Y., Tanaka, Y., Patterson, B., Hwang, S. M., Hysolli, E., Cakir, B., . . . Park, I. H. (2020). Dysregulation of BRD4 Function Underlies the Functional Abnormalities of MeCP2 Mutant Neurons. *Mol Cell, 79*(1), 84-98 e89. doi:10.1016/j.molcel.2020.05.016

Yamashita, T., Yamamoto, S., Zhang, J., Kometani, M., Tomiyama, D., Kohno, K., . . . Tsuda, M. (2016). Duloxetine Inhibits Microglial P2X4 Receptor Function and Alleviates Neuropathic Pain after Peripheral Nerve Injury. *PLoS One, 11*(10), e0165189. doi:10.1371/journal.pone.0165189

Yang, L., Bailey, L., Baltimore, D., & Wang, P. (2006). Targeting lentiviral vectors to specific cell types in vivo. *Proc Natl Acad Sci U S A, 103*(31), 11479-11484. doi:10.1073/pnas.0604993103

Yonekawa, T., & Thorburn, A. (2013). Autophagy and cell death. *Essays Biochem, 55*, 105-117. doi:10.1042/bse0550105

Yoshida, T., Hazan, I., Zhang, J., Ng, S. Y., Naito, T., Snippert, H. J., . . . Georgopoulos, K. (2008). The role of the chromatin remodeler Mi-2beta in hematopoietic stem cell self-renewal and multilineage differentiation. *Genes Dev, 22*(9), 1174-1189. doi:10.1101/gad.1642808

Zhang, F., Rein, B., Zhong, P., Shwani, T., Conrow-Graham, M., Wang, Z. J., & Yan, Z. (2021). Synergistic inhibition of histone modifiers produces therapeutic effects in adult Shank3-deficient mice. *Transl Psychiatry, 11*(1), 99. doi:10.1038/s41398-021-01233-w

Zhao, L., Wang, Y., Jaganathan, A., Sun, Y., Ma, N., Li, N., . . . Cheung, K. L. (2023). BRD4-PRC2 represses transcription of T-helper 2-specific negative regulators during T-cell differentiation. *EMBO J, 42*(6), e111473. doi:10.15252/embj.2022111473

Zhong, Y., Paudel, B. P., Ryan, D. P., Low, J. K. K., Franck, C., Patel, K., . . . Mackay, J. P. (2020). CHD4 slides nucleosomes by decoupling entry- and exit-side DNA translocation. *Nat Commun, 11*(1), 1519. doi:10.1038/s41467-020-15183-2

Zibetti, C., Adamo, A., Binda, C., Forneris, F., Toffolo, E., Verpelli, C., . . . Battaglioli, E. (2010). Alternative splicing of the histone demethylase LSD1/KDM1 contributes to the modulation of neurite morphogenesis in the mammalian nervous system. *J Neurosci, 30*(7), 2521-2532. doi:10.1523/JNEUROSCI.5500-09.2010

Zigmond, R. E., & Echevarria, F. D. (2019). Macrophage biology in the peripheral nervous system after injury. *Prog Neurobiol, 173*, 102-121. doi:10.1016/j.pneurobio.2018.12.001

Zou, Z. K., Huang, Y. Q., Zou, Y., Zheng, X. K., & Ma, X. D. (2017). Silencing of LSD1 gene modulates histone methylation and acetylation and induces the apoptosis of JeKo-1 and MOLT-4 cells. *Int J Mol Med, 40*(2), 319-328. doi:10.3892/ijmm.2017.3032

Acknowledgements

Tenia ganes d'escriure aquesta darrera pàgina, ja que significa que la Tesi està conclosa. Personalment, el dipòsit no només suposa el tancament de la pressió de la escriptura de la tesi i dels quatre anys d'experimentació, sinó també la conclusió d'un darrer any personal especialment dur. Per aquest motiu vull agrair el suport a totes les persones que m'han acompanyat durant aquesta etapa.

Vull començar agraint tota l'ajuda als membres del grup de Neuroplasticitat i Regeneració, un equip de recerca format per persones excepcionals a les quals admiro i tinc gran estima. Primer de tot, vull agrair el suport dels meus directors de tesi en Xavi i la Clara, que són un exemple de dedicació i vocació científica. Gràcies Xavi, per confiar en mi, donar-me l'oportunitat de treballar en aquest gran equip i animar-me a no deixar-me vèncer pels nervis. Moltes gràcies Clara, per tot el que m'has arribat a ensenyar. Pensant en retrospectiva, veig que no només he après de tu a com treballar, sinó a com pensar més críticament.

En segon lloc, volia donar també les gràcies al gran equip d'IPs i de postdocs: a l'Esther, en Rubèn, la Natàlia, la Mireia i en Quino. Sempre que ho he necessitat m'heu donat consells molt valuosos. Vull agrair el suport tècnic de la Jèssica, Mònica, Neus, Marina, Jonathan i la col·laboració de la Cristina Gutiérrez, que ens ha cedit l'Amaxa per als experiments de silenciament. Aquesta tesi no s'hauria pogut concloure sense la vostra ajuda.

A més a més, entregar aquesta memòria no hauria estat viable sense el suport dels actuals doctors i pre-docs amb els que he compartit despatx i vivències. Vull començar dedicant a la Vera i a la Carla les primeres paraules. Fa 5 anys que estàvem juntes estudiant a la pissarra de la biblioteca durant el màster. Sembla mentida com ha passat el temps! Vera, sempre recordaré la conversa que vam tenir a l'Ovella Negra del centre fa tants anys. Tot i que en aparença som molt diferents, hem aconseguit confiar plenament la una amb la altra i dur-nos de meravella. Molta sort en aquesta nova etapa a EEUU. Carla, ets una persona increïble. No només sempre m'has ajudat quan més ho he necessitat, sinó que sempre has aconseguit fer-me riure amb les teves observacions. Espero que celebrem aviat el final de les nostres tesis anant al petit Bangkok o a qualsevol altre restaurant que tingui bona pinta. Que les dues ja ens ho mereixem!

A la Maria, li vull donar les gràcies per dir les coses tal qual les sent i ser sempre tant expressiva. A la Sara M per iniciar la gran tradició de les cases rurals. A l' Aina, que a part

d'ajudar-me a treure endavant les MTT, ha dut sempre molt bon rotllo al laboratori amb el seu amor pel *karaoke*. A la Núria, que té un valors de treball i familiars admirables. Gràcies per ajudar-me quan no sabia com funcionaven les coses quan vaig trepitjar el laboratori i per ser tant atenta amb les persones del teu voltant.

A la Sara B, que és brillant en tot (des de la ciència al ball) i no hi ha res que la pari. M'encanta la confiança que transmets i la teva capacitat de cohesionar a tot el grup de doctorands. A la Judith, que és molt versàtil i amb uns dots de comunicació espectaculars. A Bruno, que siempre nos ha invitado a todos mil veces a su casa y con quien he compartido tantísimos ratos quedándonos hasta última hora en el despacho. A l'Andrea que m'ha salvat més d'un *look* de Carnaval amb el seu talent pel maquillatge. A en Diego, tant treballador i sociable. No sé com, però tens contactes en comú amb quasi totes les persones del despatx. A la Joana, que té una paraula amable per aquell qui ho necessita i una capacitat organitzativa espectacular. Tant fa els experiments més punters, com organitza un festival d'èxit. A Raquel, que trae buen rollo allí donde va. ¡Anda que no nos hemos reído hasta la saciedad cuando éramos compis de mesa! A en Néstor, que ha aconseguit que tots siguem experts en banderes. Gràcies per ser un raig de llum i optimisme quan més cal. A la Bea, que sempre m'ha donat consells molt savis i m'ha transmès una gran tranquil·litat. A la Sònia que té una paciència enorme i sempre una gran quantitat d'anècdotes a explicar-nos. Gràcies a la nova generació de NFIS: Marc, Joan i José pel vostre suport en aquesta etapa final de la meva tesi. Tot i que no hem compartit despatx, vull agrair per la seva amabilitat i bon fer a l'Estefania, Sergi i Rubèn.

També vull dedicar un reconeixement a les persones de fora del laboratori, que m'han donat molts moments especials. Aquests anys no haurien sigut el mateix sense els meus amics del grupet de Secret H, les meves amigues de Súnion, la Jana i el Joanan.

En especial, quiero dar las gracias a una persona que ha aparecido en mi vida a mitad de esta tesis y que ha cambiado mi mundo. Muchas gracias David, por hacer que todo parezca más fácil, aguantarme en los momentos más difíciles y por apoyarme incondicionalmente.

Finalment, vull agrair l'ajuda de la Ina, dels "titos" i especialment dels meus pares. Gràcies per creure sempre en mi, per donar-me totes les oportunitats del món, per estimar-me i animar-me en els moments més difícils.